

Contractile functions of Piezo1 channels in murine arteries

Naima Eltuhami M. Endesh

Submitted in accordance with the requirements for the degree of Doctor of
Philosophy

The University of Leeds Faculty of Medicine and Health

March 2018

The candidate confirms that the work submitted is her own, except where work which has formed part of jointly authored publications has been included. The contribution of the candidate and the other authors to this work has been explicitly indicated below. The candidate confirms that appropriate credit has been given within the thesis where reference has been made to the work of others.

Chapter 4 and 5 contain work from a jointly authored publication:

Baptiste Rode (joint first author), Jian Shi (joint first author), Naima Endesh (joint first author), Mark J. Drinkhill, Peter J. Webster, Sabine J. Lotteau, Marc A. Bailey, Nadira Y. Yuldasheva, Melanie J. Ludlow, Richard M. Cubbon, Jing Li, T.Simon Futers, Lara Morley, Hannah J. Gaunt, Katarzyna Marszalek, Hema Viswambharan, Kevin Cuthbertson, Paul D. Baxter, Richard Foster, Piruthivi Sukumar, Andrew Weightman, Sarah C. Calaghan, Stephen B. Wheatcroft, Mark T. Kearney & David J. Beech. Piezo1 channels sense whole body physical activity to reset cardiovascular homeostasis and enhance performance. *Nature Communications*. 2017, Aug 24;8(1):350. doi: 10.1038/s41467-017-00429-3.

Author contributions are as follows: B.R. coordinated experimental work and data analysis, generated and validated mice, performed experimental studies, generated the HEKT-REx-293-Piezo1 cell line, proposed ideas for experiments and wrote parts of the manuscript. J.S. generated and analysed electrophysiology and pressure myography data. N.E. generated contraction data and analysed the data with B.R. M.J.D. performed telemetry studies and analysed the data with B.R. P.J.W. and H.J.G. isolated and analysed endothelial cells. S.J.L. performed and analysed physical performance studies with B.R. and S.C.C. M.A.B. performed and analysed ultrasound studies with B.R. N.Y.Y. performed the arterial injury studies and analysed the data with B.R. M.J.L. performed and analysed the thallium flux assays. R.M.C. performed and analysed the retinal vasculature studies with B.R. J.L. generated the initial cross of Piezo1flox mice with mice expressing Cadh5-cre. K.M. and T.S.F. maintained mouse colonies and assisted with ethical compliance. H.V. provided technical advice for myography studies. K.C. and R.F. synthesised Yoda1. P.D.B. advised on statistical analysis. A.W. developed hardware for acquiring data and software for analysis of physical performance data. L.M., S.C.C., P.S.,

S.B.W. and M.T.K. provided intellectual input. All authors commented on the manuscript. D.J.B. initiated the project, generated research funds and ideas, led and coordinated the project, interpreted data and wrote most of the paper.

Chapter 3 contains work from a jointly authored publication:

Elizabeth L Evans (joint first author), Kevin Cuthbertson (joint first author), Naima Endesh (joint first author), Baptiste Rode, Nicola M Blythe, Adam J Hyman, Sally J Hall, Hannah J Gaunt, Melanie J Ludlow, Richard Foster and David J Beech. Yoda1 analogue (Dooku1) which antagonises Yoda1-evoked activation of Piezo1 and aortic relaxation. *British Journal of Pharmacology*. 2018 Mar 2. doi: 10.1111/bph.14188.

Author contributions are as follows: E.L.E., K.C., N.E., B.R., N.M.B., A.J.H., S.J.H., H.J.G., and M.J.L. performed experiments and data analysis. E.L.E., K.C., D.J.B. and R.F. designed the research. D.J.B. and R.F. raised funds to support the work. E.L.E., K.C., R.F., and D.J.B. co-wrote the paper.

The right of Naima Eltuhami Endesh to be identified as Author of this work has been asserted by her in accordance with the Copyright, Designs and Patents Act 1988.

© 2018 The University of Leeds and Naima Eltuhami Endesh.

Acknowledgement

I would like to express my sincere gratitude to my main supervisor Prof. David Beech, who provided me with an opportunity to join his team, who gave access to the laboratory and research facilities, and who responded to my questions and queries so promptly for the continuous support of my PhD study, for his motivation, immense knowledge, and patience as English is my second language. His guidance helped me in all the time of research and writing of this thesis. I could not have imagined having a better advisor and mentor for my PhD study.

Besides, I would like to thank my co-supervisor Dr. Neil Turner, for all his assistance throughout my PhD.

I would also like to thank Dr Melanie Ludlow, for her insightful comments and for the suggestions she made in this work.

My sincere thanks also go to Dr Nadira Yuldasheva, Dr Baptiste Rode, Dr Marc Bailey, Dr Jian Shi, Kevin Cuthbertson, Rene Hummel and David Myers for their general help and support.

Additional thanks to all of my colleagues in my group who I had the pleasure of working with. Their constant support and guidance was invaluable.

I would like to express my gratitude to my husband who looked after my daughters and who helped me settle into motherhood while attempting to finish my studies, for his continued support and encouragement without him, this thesis would never have materialised. Huge thanks, to my two beautiful, smart and wonderful girls, Nour Alhouda and mais Alreem for bringing me so much happiness and make it all worthwhile.

Special thanks to my family for their unwavering support and willingness to help in whatever ways they could.

I would like to thank the Libyan government, the Medical Research Council and Wellcome Trust for funding this project which allowed me to undertake this research.

Abstract

Piezo1 proteins are Na⁺ and Ca²⁺ permeable mechanosensitive ion channels. Expressed on endothelial cell membranes, where they sense the shear stress forces created by blood flow, Piezo1 channels are essential for vascular development. The functional significance of vascular Piezo1 channels in adult physiology and pathology, however, remains largely unexplored. Therefore, using an inducible, endothelial-specific Piezo1 knock-out mouse line this study sought to identify and investigate the functional role of this channel in adult arterial vessels. Four morphologically and physiologically distinct arteries, the aorta, mesenteric, saphenous and carotid arteries, were selected and their responses to the vasoconstrictor phenylephrine (PE) and the vasorelaxant acetylcholine (ACh) were assessed using wire myography. While loss of endothelial Piezo1 did not alter or had only a small effect on the overall sensitivity or responsiveness of these vessels to either PE or ACh, further investigation revealed a significant increase in the endothelium-derived hyperpolarizing factor (EDHF) component of ACh-induced relaxation in mesenteric arteries. This anti-EDHF effect of Piezo1 was vascular bed specific, no difference between control or knock-out mice being observed in saphenous or carotid arteries. This finding led to the identification of a flow-stimulated vasoconstriction response in mesenteric vessels and furthermore provided an explanation for the reduced elevation in blood pressure detected in endothelial Piezo1 knock-out mice during exercise. Mesenteric arteries contract during exercise, enabling blood to be directed to tissues actively involved in physical movement. The data support the hypothesis that Piezo1 channels have specific importance in whole body physical exercise, sensing increased blood flow at the endothelium to elevate tone in the underlying vascular smooth muscle cells of visceral arteries, thus redirecting blood to the muscles.

Table of Contents

Acknowledgement	iv
Abstract	vi
Table of Contents	vii
List of Tables	xii
List of Figures	xiii
List of Publications and Communications	xviii
Abbreviations	xix
Chapter 1 Introduction	1
1.1 The Mammalian Cardiovascular System.....	1
1.1.1 Introduction.....	1
1.1.2 Structure of the cardiovascular system	1
1.1.3 Blood pressure	6
1.1.4 Vascular smooth muscle cells.....	13
1.1.5 The endothelium.....	21
1.1.6 Mechanical modulation of arterial tone.....	28
1.2 Arterial Remodelling and Hypertension.....	32
1.2.1 Pharmacological treatment	36
1.2.2 Non-pharmacological treatment.....	36
1.3 Piezo1 channels and their vascular roles.....	37
1.4 Yoda1	40
1.5 Aims and Objectives	43
Chapter 2 General Methods	44
2.1 Materials and Solutions.....	44
2.2 Mouse.....	50
2.2.1 Mouse housing conditions and diet.....	50
2.2.2 Genetic disruption of the Piezo1 gene	50
2.2.3 Patch-clamp electrophysiology	56
2.2.4 Monitoring mouse activity / Running wheel analysis	56
2.2.5 Tissue staining.....	56
2.2.6 Echocardiography.....	57
2.3 Dissection of blood vessels.....	57
2.3.1 Thoracic aorta.....	58

2.3.2	Mesenteric artery	58
2.3.3	Saphenous artery	58
2.3.4	Carotid artery	59
2.4	Vascular myography	64
2.4.1	Wire Myography.....	64
2.4.2	Pressure Myography.....	71
Chapter 3 Vasoactive properties of the Piezo1 channel agonist Yoda1 on the mouse thoracic aorta		77
3.1	Abstract	77
3.1.1	Rationale	77
3.1.2	Aim	77
3.1.3	Method	77
3.1.4	Results	78
3.1.5	Conclusions	78
3.2	Introduction.....	78
3.3	Results	82
3.3.1	Yoda1-induced relaxation in isolated mouse thoracic aorta segments 82	
3.3.2	Cumulative concentration-response of Yoda1.....	82
3.3.3	EC involvement	85
3.3.4	Effects of nitric oxide synthase inhibitor (L-NAME) on Yoda1- induced relaxation.....	85
3.3.5	Inhibitors of Piezo1 involvement	88
3.3.6	Yoda1 inhibition with Dooku1.....	88
3.3.7	Yoda1 inhibition by other Yoda1 analogues.....	91
3.3.8	Specificity of Dooku1	91
3.3.9	Yoda1 does not induce relaxation in control and endothelial Piezo1 ^{ΔEC} thoracic aorta.....	98
3.4	Discussion	104
3.4.1	The Yoda-1 effect depends on endothelial cells.....	104
3.4.2	Yoda-1 depends on NO generation by NOS	104
3.4.3	Piezo1 EC knockout mice	106
3.5	Conclusion.....	106
Chapter 4 Role of endothelial Piezo1 in second-order mesenteric arteries of mice.....		109
4.1	Abstract	109

4.1.1	Background	109
4.1.2	Methods.....	109
4.1.3	Results	109
4.1.4	Conclusion.....	110
4.2	Introduction.....	110
4.3	Results	111
4.3.1	Deletion of endothelial cell Piezo1 affects high potassium-induced contraction	111
4.3.2	Deletion of endothelial cell Piezo1 does not affect phenylephrine-induced contraction.....	112
4.3.3	Deletion of endothelial cell Piezo1 potentiates ACh-induced vasorelaxation	116
4.3.4	Deletion of endothelial cell Piezo1 affected EDHF-mediated-vasorelaxation	116
4.3.5	Deletion of endothelial cell Piezo1 does not affect NO-mediated-vasorelaxation	124
4.3.6	The effect of removal of endothelial cells on ACh-induced relaxation 129	
4.3.7	Measurements of blood pressure.....	134
4.3.8	Flow-induced vasoconstriction	134
4.3.9	Constitutive and flow-induced Piezo1 in mesenteric artery	135
4.3.10	Yoda1 induced relaxation in the mesenteric arteries of control and Piezo1 ^{ΔEC} mice	139
4.3.11	The effect of Piezo1 antagonists on Yoda1-induced relaxation in mesenteric arteries from control and Piezo1 ^{ΔEC} mice	139
4.3.12	The effect of removal of endothelial cells on Yoda1-induced relaxation	146
4.3.13	The contribution of EDHF to Yoda1-induced relaxation.....	150
4.3.14	The contribution of NO to Yoda1-induced relaxation.....	150
4.3.15	The contribution of NO to Yoda1-induced relaxation in denuded ECs.....	151
4.4	Discussion	157
4.4.1	Deletion of endothelial cell Piezo1 affects high potassium-induced contraction	157
4.4.2	Deletion of endothelial cell Piezo1 potentiates ACh-induced vasorelaxation	157
4.4.3	Deletion of endothelial cell Piezo1 affected EDHF-mediated vasorelaxation but does not affect NO-mediated-vasorelaxation.	158

4.4.4	The effect of removal of endothelial cells on ACh-induced relaxation	159
4.4.5	Piezo1 channels role in whole body physical activity	160
4.4.6	Relaxation induced by Yoda1 in control, compared with Piezo1 ^{ΔEC} mice mesenteric arteries.....	160
4.4.7	Contribution of Piezo1 in Yoda1-induced relaxation.....	161
4.4.8	The effect of removal of endothelial cells on Yoda1-induced relaxation.....	161
4.4.9	The contribution of EDHF and NO to Yoda1-induced relaxation .	162
4.5	Conclusion.....	163
Chapter 5 Lack of role of endothelial Piezo1 in saphenous and carotid arteries of mice		165
5.1	Introduction.....	165
5.2	Results	167
5.2.1	Deletion of endothelial cell Piezo1 does not affect high potassium-induced contraction.....	167
5.2.2	Deletion of endothelial cell Piezo1 does not affect phenylephrine-induced contraction.....	167
5.2.3	Deletion of endothelial cell Piezo1 does not affect ACh-induced vasorelaxation	168
5.2.4	Deletion of endothelial cell Piezo1 does not affect EDHF-mediated-vasorelaxation	177
5.2.5	Deletion of endothelial cell Piezo1 does not affect NO-mediated-vasorelaxation	182
5.2.6	The effect of removal of endothelial cells on ACh-induced relaxation	183
5.2.7	Yoda1 induced relaxation in the saphenous and carotid arteries of control and Piezo1 ^{ΔEC} mice	195
5.2.8	The effect of removal of endothelial cells on Yoda1-induced relaxation in saphenous and carotid arteries from control and Piezo1 ^{ΔEC} mice	198
5.3	Discussion	203
5.3.1	Deletion of endothelial cell Piezo1 does not affect high potassium or phenylephrine-induced contraction in saphenous or carotid arteries from control and Piezo1 ^{ΔEC} mice.....	203
5.3.2	Deletion of endothelial cell Piezo1 does not affect ACh-induced vasorelaxation in saphenous or carotid arteries from control and Piezo1 ^{ΔEC} mice.....	203

5.3.3	Deletion of endothelial cell Piezo1 does not affect EDHF or NO-mediated vasorelaxation in saphenous or carotid arteries from control and Piezo1 ^{ΔEC} mice.	204
5.3.4	The effect of removal of endothelial cells on ACh-induced relaxation in saphenous or carotid arteries from control and Piezo1 ^{ΔEC} mice.	206
5.3.5	Endothelial-dependent relaxation induced by Yoda1 in saphenous or carotid arteries from control and Piezo1 ^{ΔEC} mice.....	207
5.3.6	The effect of removal of endothelial cells on Yoda1-induced relaxation in saphenous or carotid arteries from control and Piezo1 ^{ΔEC} mice.	207
5.4	Conclusion.....	208
Chapter 6 Final summary and Future Directions		209
List of References		215

List of Tables

Table 2-1: Composition of solutions used in this study	45
Table 2-2: Drugs/compounds	46
Table 2-3: PCR primer sequences.....	55
Table 4-1: Gd³⁺ and RR inhibitors effects on basal tension and phenylephrine (PE) responses in mouse mesenteric arteries.....	141
Table 6-1: Summarised data for effects of vasoconstriction and vasodilation agonists on mouse mesenteric, saphenous and carotid arteries.....	213
Table 6-2: Summarised data for effects induced by Yoda1 on mouse aorta, mesenteric, saphenous and carotid arteries from control and Piezo1^{ΔEC} mouse.....	214

List of Figures

Figure 1-1: Vessel wall cross-section	4
Figure 1-2: Diagram demonstrating how the structure of blood vessels differs throughout the cardiovascular system.....	5
Figure 1-3: Systemic Blood Pressure	10
Figure 1-4: Explanation of how baroreceptor and the autonomic nervous system control blood pressure (BP).	11
Figure 1-5: Summary of the regulation of blood pressure by the renin-angiotensin system	12
Figure 1-6: Schematic diagram showing contraction mechanisms in vascular smooth muscle cell.	20
Figure 1-7: (a). Diagram showing the endothelial cells and vascular smooth muscle cells in an artery. (b) Endothelium-mediated relaxation through nitric oxide (NO) and prostacyclin (PGI ₂)	25
Figure 1-8: A representative Cryo-EM structure of Piezo1	41
Figure 1-9: Chemical structure of Yoda1	42
Figure 2-1: Synthesis and chemical structure of Dooku1	48
Figure 2-2: Chemical structures of 2e, 7b, 11 and 2g Yoda1 analogues	49
Figure 2-3: Diagram showing insertion of loxP sequences into the mouse Piezo1 gene in the introns between exons 17 and 18 and 21 and 22.....	53
Figure 2-4: Endothelial-specific Piezo1 modification	54
Figure 2-5: Diagram of the aorta dissection	60
Figure 2-6: Schematic diagram of the organisation of the mesenteric vascular bed.....	61
Figure 2-7: Location of the saphenous artery in the rodent hind limb	62
Figure 2-8: Diagram depicting the location of the left and right common carotid arteries in relation to the heart and aorta.....	63
Figure 2-9: The wire myograph	66
Figure 2-10: The mounting procedure	67
Figure 2-11: Standard start protocol was carried out to validate artery segments	74
Figure 2-12: Schematic of the mechanical test system with optional accessories.....	75
Figure 2-13: Artery from a mouse mounted in a pressure myograph	76
Figure 3-1: Picture of mouse thoracic aorta and associated blood vessels. ...	80
Figure 3-2: Regulation of the contractile mechanism in smooth muscle cells.	81

Figure 3-3: Yoda1-induced relaxation in mouse thoracic aorta segments.....	83
Figure 3-4: Cumulative concentration response curves of Yoda1 in mouse thoracic aorta.....	84
Figure 3-5: Effects of Yoda1-induced relaxation mediated by endothelial cells in mouse thoracic aorta segments.....	86
Figure 3-6: Yoda1-induced relaxation mediated by nitric oxide (NO) in mouse thoracic aorta segments.	87
Figure 3-7: Effect of gadolinium (Gd ³⁺) on Yoda1-induced relaxation in mouse thoracic aorta segments.	89
Figure 3-8: Effect of Dooku1, a Yoda1 analogue, on Yoda1-induced relaxation in mouse thoracic aorta segments.....	90
Figure 3-9: Effect of 7b, a Yoda1 analogue, on Yoda1-induced relaxation in mouse thoracic aorta segments.....	92
Figure 3-10: Effect of 2g, a Yoda1 analogue, on Yoda1-induced relaxation in mouse thoracic aorta segments.....	93
Figure 3-11: Effect of 11, a Yoda1 analogue, on Yoda1-induced relaxation in mouse thoracic aorta segments.....	94
Figure 3-12: Effect of 2e, a Yoda1 analogue, on Yoda1-induced relaxation in mouse thoracic aorta segments.....	95
Figure 3-13: Mechanisms involved in the thromboxane mimetic U46619-induced contraction.	96
Figure 3-14: Dooku1 has minimal effect on thromboxane A ₂ mediated contraction and does not affect other vasodilators.....	97
Figure 3-15: Mice with disruption of the endothelial Piezo1 appeared phenotypically normal.....	100
Figure 3-16: Typical responses of control and Piezo1 ^{ΔEC} thoracic aorta.....	101
Figure 3-17: Vascular viability in control compared with Piezo1 ^{ΔEC} thoracic aorta	102
Figure 3-18: Yoda1 responses in control and Piezo1 ^{ΔEC} thoracic aorta	103
Figure 3-19: Mechanism of the relaxation effect by Yoda1	108
Figure 4-1: Vascular reactivity to high potassium (60 mM K ⁺) in control compared with endothelial Piezo1 ^{ΔEC} mesenteric arteries.....	113
Figure 4-2: Mechanisms of contraction in a vascular smooth muscle cell ...	114
Figure 4-3: Vascular reactivity to phenylephrine in control compared with endothelial Piezo1 ^{ΔEC} mesenteric arteries	115
Figure 4-4: The nitric oxide (NO) and endothelial derived hyperpolarization factor (EDHF) pathway in the vascular smooth muscle cells leading to cell relaxation	118
Figure 4-5: Vascular reactivity to ACh in control compared with endothelial Piezo1 ^{ΔEC} mesenteric arteries.....	119

Figure 4-6: Inhibition of endothelial derived hyperpolarisation factor (EDHF)	120
Figure 4-7: EDHF-mediated-vasorelaxation in control mice	121
Figure 4-8: EDHF-mediated-vasorelaxation in endothelial Piezo1^{ΔEC} mice	122
Figure 4-9: Comparison of EDHF-mediated-vasorelaxation in control and endothelial Piezo1^{ΔEC} mice	123
Figure 4-10: The nitric oxide (NO) inhibition	125
Figure 4-11: NO-mediated-vasorelaxation in control mice	126
Figure 4-12: NO-mediated-vasorelaxation in endothelial Piezo1^{ΔEC} mice	127
Figure 4-13: Comparison of NO-mediated-vasorelaxation in control and endothelial Piezo1^{ΔEC} mice	128
Figure 4-14: The effect of removal of endothelial cells on ACh induced-relaxation in control mice	130
Figure 4-15: NO-donor, Linsidomine (SIN-1)	131
Figure 4-16: The effect of removal of endothelial cells on ACh induced-relaxation in Piezo1^{ΔEC} mice	132
Figure 4-17: Comparison of effects of removing the endothelial cells in control and endothelial Piezo1^{ΔEC} mice	133
Figure 4-18: Measurements of blood pressure during whole body physical activity	136
Figure 4-19: Flow-induced vasoconstriction in mesenteric artery. Isobaric external diameter recordings from second-order mesenteric artery	137
Figure 4-20: Piezo1 channels work as flow sensors in the endothelium of mesenteric artery	138
Figure 4-21: Endothelial-dependent relaxation induced by Yoda1 in control compared with endothelial Piezo1^{ΔEC} mesenteric arteries	140
Figure 4-22: The effect of Piezo1 antagonists on Yoda1-induced relaxation in mesenteric arteries from control mice	142
Figure 4-23: The effect of Piezo1 antagonists on Yoda1-induced relaxation in mesenteric arteries from Piezo1^{ΔEC} mice	143
Figure 4-24: The effect of Piezo1 antagonists on Yoda1-induced relaxation in mesenteric arteries from control mice	144
Figure 4-25: The effect of Piezo1 antagonists on Yoda1-induced relaxation in mesenteric arteries from Piezo1^{ΔEC} mice	145
Figure 4-26: The effect of the endothelium removal on Yoda1-induced relaxation in mesenteric arteries from control mice	147
Figure 4-27: The effect of the endothelium removal on Yoda1-induced relaxation in mesenteric arteries from Piezo1^{ΔEC} mice	148

Figure 4-28: NO-donor, Linsidomine (SIN-1)-induced relaxation in mesenteric arteries from control and Piezo1 ^{ΔEC} mice.....	149
Figure 4-29: The contribution of EDHF to Yoda1-induced relaxation in control mesenteric arteries.....	152
Figure 4-30: The contribution of EDHF to Yoda1-induced relaxation in Piezo1 ^{ΔEC} mesenteric arteries	153
Figure 4-31: The contribution of NO to Yoda1-induced relaxation in endothelium-intact control mesenteric arteries	154
Figure 4-32: The contribution of NO to Yoda1-induced relaxation in endothelium-intact Piezo1 ^{ΔEC} mesenteric arteries	155
Figure 4-33: The contribution of NO to Yoda1-induced relaxation in endothelium-denuded mesenteric arteries isolated from wild type mice	156
Figure 4-34: Ischaemic diagram presenting the effects of Piezo1 channel activity in the endothelial cells	164
Figure 5-1: Schematic representation of arterial vessels topography and preparation of mouse arteries.	166
Figure 5-2: Vascular reactivity to high potassium (60 mM K ⁺) in control compared with endothelial Piezo1 ^{ΔEC} saphenous arteries.....	170
Figure 5-3: Vascular reactivity to high potassium (60 mM K ⁺) in control compared with endothelial Piezo1 ^{ΔEC} carotid arteries	171
Figure 5-4: Vascular reactivity to phenylephrine in control compared with endothelial Piezo1 ^{ΔEC} saphenous arteries	172
Figure 5-5: Vascular reactivity to phenylephrine in control compared with endothelial Piezo1 ^{ΔEC} carotid arteries	173
Figure 5-6: EDCF cell-signalling activity	174
Figure 5-7: Vascular reactivity to ACh in control compared with endothelial Piezo1 ^{ΔEC} saphenous arteries	175
Figure 5-8: Vascular reactivity to ACh in control, compared with endothelial Piezo1 ^{ΔEC} carotid arteries.....	176
Figure 5-9: EDHF-mediated-vasorelaxation in control mice saphenous arteries	178
Figure 5-10: EDHF-mediated-vasorelaxation in endothelial Piezo1 ^{ΔEC} mice saphenous arteries.....	179
Figure 5-11: EDHF-mediated-vasorelaxation in control mice carotid arteries.....	180
Figure 5-12: EDHF-mediated-vasorelaxation in endothelial Piezo1 ^{ΔEC} mice carotid arteries	181
Figure 5-13: NO-mediated-vasorelaxation in control mice saphenous arteries	185

Figure 5-14: NO-mediated-vasorelaxation in Piezo1^{ΔEC} mice saphenous arteries	186
Figure 5-15: NO-mediated-vasorelaxation in control mice carotid arteries ..	187
Figure 5-16: NO-mediated-vasorelaxation in Piezo1^{ΔEC} mice carotid arteries	188
Figure 5-17: The effect of removal of endothelial cells on ACh induced-relaxation in control mice saphenous arteries	189
Figure 5-18: The effect of removal of endothelial cells on ACh induced-relaxation in Piezo1^{ΔEC} mice saphenous arteries	190
Figure 5-19: The effect of removal of endothelial cells on ACh induced-relaxation in control mice carotid arteries.....	191
Figure 5-20: The effect of removal of endothelial cells on ACh induced-relaxation in Piezo1^{ΔEC} mice carotid arteries	192
Figure 5-21: Comparison of effects of removing the endothelial cells in control and endothelial Piezo1^{ΔEC} mice saphenous arteries.	193
Figure 5-22: Comparison of effects of removing the endothelial cells in control and endothelial Piezo1^{ΔEC} mice carotid arteries.	194
Figure 5-23: Endothelial-dependent relaxation induced by Yoda1 in control compared with endothelial Piezo1^{ΔEC} saphenous arteries.....	196
Figure 5-24: Endothelial-dependent relaxation induced by Yoda1 in control compared with endothelial Piezo1^{ΔEC} carotid arteries	197
Figure 5-25: The effect of the endothelium removal on Yoda1-induced relaxation in saphenous arteries from control mice	199
Figure 5-26 The effect of the endothelium removal on Yoda1-induced relaxation in saphenous arteries from Piezo1^{ΔEC} mice	200
Figure 5-27: The effect of the endothelium removal on Yoda1-induced relaxation in carotid arteries from control mice	201
Figure 5-28: The effect of the endothelium removal on Yoda1-induced relaxation in carotid arteries from Piezo1^{ΔEC} mice	202

List of Publications and Communications

Publications

Baptiste Rode[†], Jian Shi[†], **Naima Endesh**[†], Mark J. Drinkhill, Peter J. Webster, Sabine J. Lotteau, Marc A. Bailey, Nadira Y. Yuldasheva, Melanie J. Ludlow, Richard M. Cubbon, Jing Li, T.Simon Futers, Lara Morley, Hannah J. Gaunt, Katarzyna Marszalek, Hema Viswambharan, Kevin Cuthbertson, Paul D. Baxter, Richard Foster, Piruthivi Sukumar, Andrew Weightman, Sarah C. Calaghan, Stephen B. Wheatcroft, Mark T. Kearney & David J. Beech. Piezo1 channels sense whole body physical activity to reset cardiovascular homeostasis and enhance performance. *Nature Communications*. 2017, Aug 24;8(1):350. doi: 10.1038/s41467-017-00429-3. († equal contributors).

Elizabeth L Evans[†], Kevin Cuthbertson[†], **Naima Endesh**[†], Baptiste Rode, Nicola M Blythe, Adam J Hyman, Sally J Hall, Hannah J Gaunt, Melanie J Ludlow, Richard Foster and David J Beech. Yoda1 analogue (Dooku1) which antagonises Yoda1-evoked activation of Piezo1 and aortic relaxation. *British Journal of Pharmacology*. 2018 Mar 2. doi: 10.1111/bph.14188. († equal contributors).

Oral Presentations

Piezo1 channels in endothelium-dependent relaxation in adult murine arteries. Endothelial Retreat, Lake District. 2017.

Abbreviations

[Ca ²⁺] _i	Intracellular Calcium
4-OHT	4-hydroxytamoxifen
ACh	Acetylcholine
ANG II	Angiotensin II
ANS	Autonomic Nervous System
ATP	Adenosine-5'-Triphosphate
AUC	Area Under the Curve
BK _{Ca} ²⁺	Big conductance Ca ²⁺ -sensitive K ⁺ channels
BP	Blood Pressure
Ca ²⁺	Calcium
CaM	Calmodulin
cAMP	Cyclic Adenosine Monophosphate
cGMP	Cyclic Guanosine Monophosphate
DAG	1,2-Diacylglycerol
DMSO	Dimethyl sulfoxide
EC ₅₀	50 % effective concentration
ECM	Extracellular Matrix
ECs	Endothelial Cells
EDHF	Endothelial-Derived Hyperpolarisation Factor
Epac	Exchange Protein Activated by cAMP
ER	Endoplasm Reticulum
GPCRs	G-Protein Coupled Receptors
HEK293	Human Embryonic Kidney
IK _{Ca} ²⁺	Intermediate-conductance calcium-activated potassium channels
IP ₃	Inositol-1,4,5-trisphosphate
IP ₃ R	Inositol-1,4,5-trisphosphate Receptors
K _{Ca} ²⁺	Calcium-dependent K ⁺
K ⁺	potassium
Kir	inward-rectifying K ⁺
LECs	Liver Endothelial Cells
LTCCs	L-type calcium channels
MLC	Myosin Light Chain

mN	milliNewtons
MMP	Matrix Metalloprotease
NCX	Na ⁺ /Ca ²⁺ Exchanger
NE	Norepinephrine
NO	Nitric Oxide
NOS	Nitric Oxide Synthase
P	Probability
PE	Phenylephrine
PIP ₂	Phosphatidylinositol-4,5-biphosphate
PKC	Protein Kinase C
PLC	Phospholipase C
K ⁺	Potassium
RyRs	Ryanodine Receptors
SEM	Standard Error of the Mean
sGC	Soluble Guanylate Cyclase
SIN-1	NO-donator, Linsidomine
SK _{Ca} ²⁺	Small-conductance calcium-activated potassium channels
SMCs	Smooth Muscle Cells
SOCE	Store-Operated Ca ²⁺ Entry
STIM1	Stromal Interacting Molecule 1 (STIM1)
TAM	Tamoxifen
TP	Thromboxane receptor
TRPs	Transient Receptor Potential Channels
VEGF	Vascular Endothelial Growth Factor
VGCCs	Voltage-Gated Calcium Channels
VSMCs	Vascular Smooth Muscle Cells

Chapter 1 Introduction

1.1 The Mammalian Cardiovascular System

1.1.1 Introduction

The cardiovascular system is comprised of the heart and a complex network of blood vessels. Together they enable the transport of O₂ and nutrients to tissues and CO₂ and waste products away from tissues. The heart consists of four chambers, two atria and two ventricles. Oxygenated blood is distributed through the body via the strong muscular contraction of the left ventricle. Upon leaving the heart, blood enters elastic conduits named arteries. From there, arteries divide into smaller conduits named arterioles and ever smaller vessels until they contain only a single layer of cells: the capillaries, the major sites of nutrient and gaseous transfer. The deoxygenated blood is collected from the capillary bed by the venous circulation, composed of venules and veins, eventually returning blood towards the heart. Therefore the maintenance and regulation of the cardiovascular system is essential to life (Marieb and Hoehn, 2007).

1.1.2 Structure of the cardiovascular system

Most vessels, arterial and venous, are formed by three layers; the tunica intima, tunica media and tunica adventitia (Fig. 1.1). The thickness of these three layers depends upon the vessel size and type.

The innermost tunica intima comprises a monolayer of endothelial cells (ECs), sealed to each other through tight junctions, supported by a basal lamina consisting of collagen and elastin fibres, smooth muscle cells (SMCs) and occasional fibroblasts. The internal elastic lamina delineates the border of the tunica intima.

The tunica media is the thickest layer of the three layers and, under normal circumstances, is composed solely of SMCs. These cells are orientated in spirals around the long axis of the vessel and linked to each other by gap junctions, thus their coordinated contraction decreases the diameter of the vessel lumen. The SMCs can also synthesize and secrete all fundamental elements, including collagen and proteoglycans that are required for the extracellular matrix and for the formation of the external elastic lamellae. As a consequence they play an important role in the maintenance and remodelling of the medial architecture.

The outermost tunica adventitia contains connective tissues, mostly comprising of collagen fibres, and functions to both support the vessel and to anchor it to adjacent tissues. It is mainly composed of fibroblasts, with some macrophages present.

The adventitia and outer media are supplied by small penetrating blood vessels (the vasa vasorum), while the inner layer is supplied by pinocytic transport from the lumen.

1.1.2.1 Arteries

Receiving blood directly from the heart, elastic or conduit arteries are the thickest arteries (25 - 10 mm in diameter), followed by the medium or muscular arteries (10 - 0.3 mm in diameter) and finally small arteries and arterioles (0.3 mm - 0.01 mm in diameter). All these vessels are connected with one another (Fig. 1.2).

Elastic arteries, such as the aorta and its major branches (brachiocephalic, subclavian, pulmonary, the beginning of common carotid, and iliac), are characterized by their high elasticity, allowing them to absorb the pressure waves produced by contraction and then relaxation of the heart. They serve as an elastic reservoir, storing the stroke volume during systole and then recoiling elastically to force this volume to the downstream part of the vessels during diastole. This phenomenon is called the Windkessel effect, which enables a steady blood flow throughout the cardiac cycle and reduces the workload of the heart (Shadwick, 1999, Wagenseil and Mecham, 2009). The arterial wall components, which provide these elastic properties are collagen and elastin, deposited amongst SMCs in the intermediate layer of the artery (Wagenseil and Mecham, 2009).

The slightly smaller muscular arteries, including the mesenteric and renal arteries, function mainly to control the distribution of blood flow around the body. This is achieved through the presence of large numbers of SMCs in the tunica media, with constriction or relaxation of those cells helping to determine the volume of blood flow through a particular vessel.

The small arteries (lumen <500 μm) and arterioles are positioned immediately prior to the capillaries and are responsible for ensuring that the volume and pressure of blood entering those vessels is correct. They are very similar in composition to muscular arteries, only smaller tunica layers and with loss of the elastic membranes. As with the muscular arteries they rely on SMCs to regulate their blood flow by altering the size of their lumen. In comparison with larger arteries they are much greater in number and consequently in total have a much greater cross sectional area. This makes them a primary determinant of vascular resistance.

1.1.2.2 Veins

Veins serve as a significant reservoir of blood, with around 64% of the circulating blood is located within them. Greater veins, which carry blood back to the heart, gradually merge into bigger muscular venules. The SMC-layer in these vessels is much thinner than that of the arterioles. This is because the lower blood pressure (BP) in venules offers less resistance to vessel contraction. The muscular venules drain blood from the post-capillary venules, which collect the deoxygenated blood from capillaries (Hall, 2015).

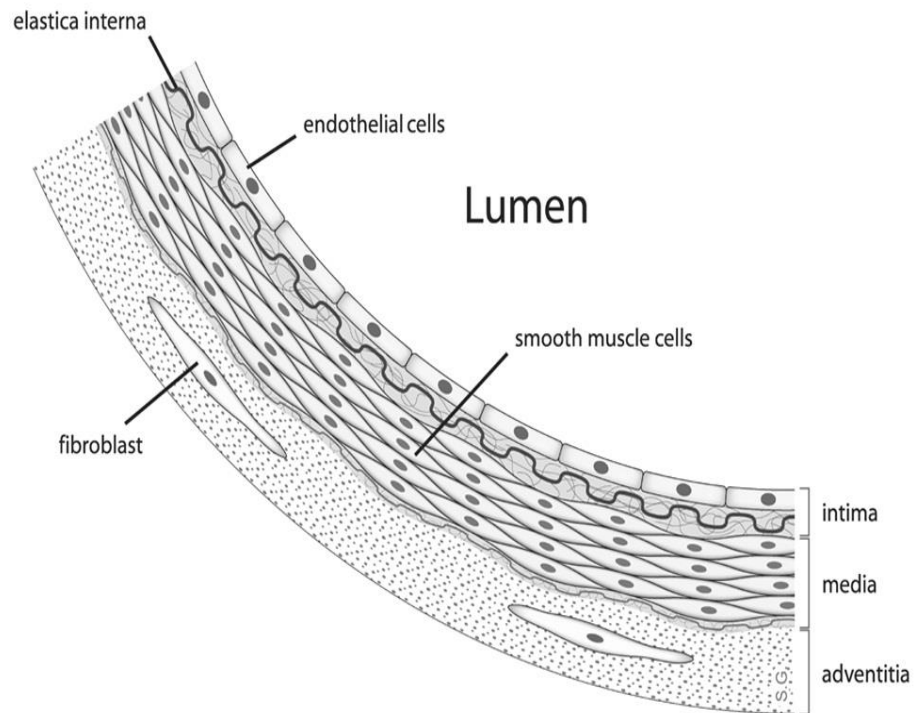


Figure 1-1: Vessel wall cross-section

(Günthner et al., 2009)

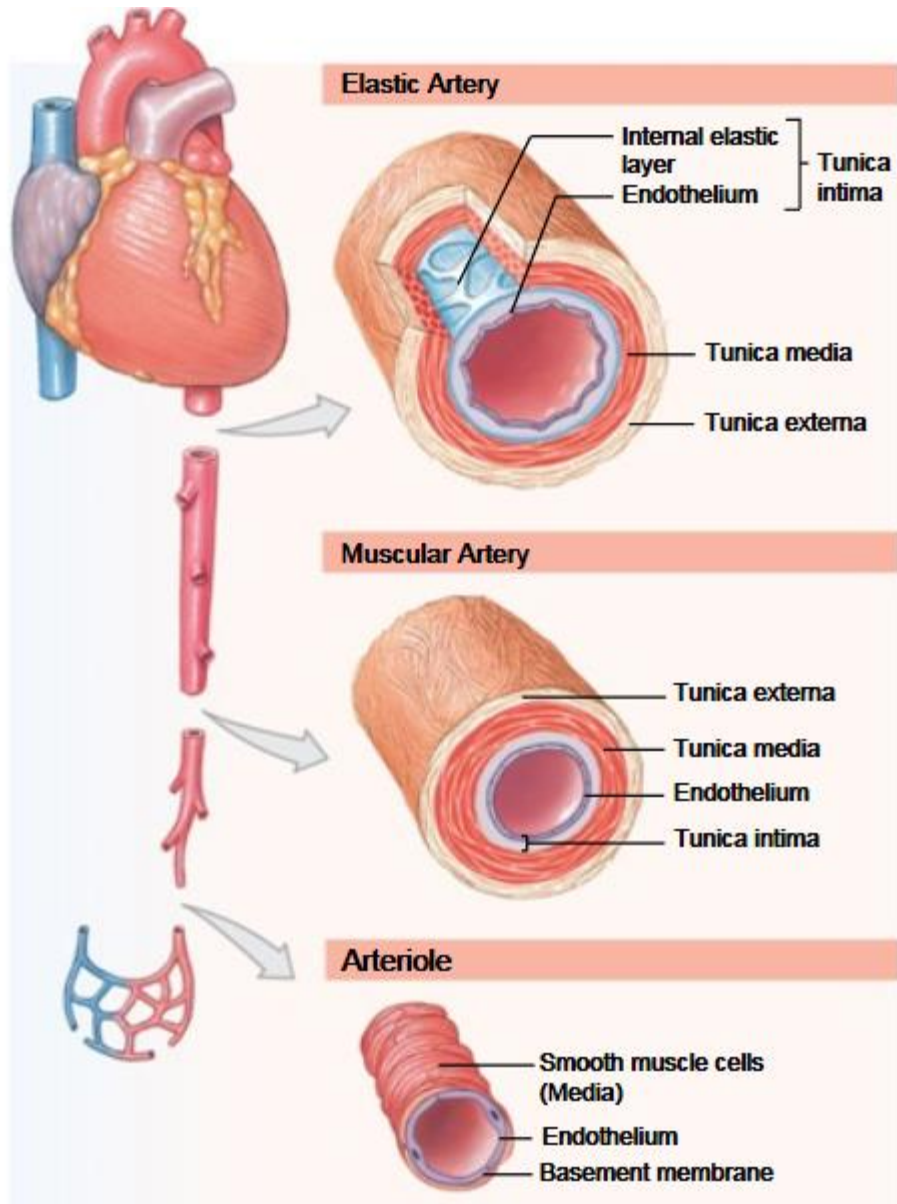


Figure 1-2: Diagram demonstrating how the structure of blood vessels differs throughout the cardiovascular system

(Martini and Nath, 2012).

1.1.3 Blood pressure

BP is the force that the circulating blood volume exerts on the walls of the vascular system. It is mainly determined by cardiac output (the product of heart rate and stroke volume) and peripheral vascular resistance (the resistance of blood vessels to blood flow which is determined by the blood vessels diameter). It is usually expressed as systolic and diastolic BP. Systolic BP is defined as the highest force during a heartbeat (contraction, ventricular systole), while diastolic BP is the lowest force between heart beats (relaxation, ventricular diastole)) (Barrett et al., 2010). After blood leaves the heart of a healthy human, its pressure is maintained at approximately 120/80 mmHg through the elastic and larger muscular arteries, however, as blood flows further from the heart BP progressively decreases in force and the difference between systolic and diastolic BP narrows. In veins the pressure is much lower, at about 5-10 mmHg. Thus, the forces experienced by an individual vessel will depend upon its sub-type and where it is located within the circulatory system (Fig. 1.3).

1.1.3.1 Blood Pressure Control

BP is regulated by a sophisticated system involving neural, hormonal and local mechanisms that can influence cardiac output and/or peripheral resistance.

1.1.3.1.1 The autonomic nervous system

The autonomic nervous system (ANS) has a significant role in BP control. The ANS branches include the sympathetic and parasympathetic systems which are regulated via the central nervous system through the medulla oblongata in the brain. They act in concert to control BP by modulating the contractility of the heart (cardiac output) and the vascular tone (peripheral vascular resistance). Sympathetic and parasympathetic innervation of the heart can efficiently change heart rate and cardiac output. Sympathetic stimulation leads to norepinephrine (NE) release and consequent increased heart rate and contractility, rising cardiac output and BP. Conversely, parasympathetic stimulation leads to acetylcholine (ACh) release to reduce heart rate and contractility and therefore also reducing cardiac output and BP (Gordan et al., 2015, Robertson et al., 1979) (Fig. 1.3). For example, during a period of physical exercise, the activity of parasympathetic nerves is reduced and the activity of sympathetic nerve is raised, leading to a rise in

heart rate and contractility. However, after the cessation of exercise, autonomic tone and corresponding heart rate gradually return towards baseline levels, due to the combination of sympathetic withdrawal and reactivation of the parasympathetic system (Robinson et al., 1966, Lahiri et al., 2008). Furthermore, it is important to recognise that the influence and relative impacts of flow, blood pressure and vascular bed respond during physical exercise are different. In physical activity, while blood flow to the intestines reduces and subsequently increasing blood pressure (Qamar and Read, 1987), blood flow to skeletal muscle increases, therefore, in resistance arteries of skeletal muscle a vasodilator rather than vasoconstrictor mechanism must dominate. Comparably, during physical activity, blood flow to the brain is maintained or slightly raised to avoid syncope (Joyner and Casey, 2015).

Sympathetic innervation of the peripheral circulation, targeting SMCs of blood vessels with efferent motor fibres, can modify peripheral resistance, and consequently BP. In small arteries and arterioles vasoconstriction in response to sympathetic nerve activity causes rises in the peripheral resistance to blood flow. These alterations in vessel diameter, particularly of arterioles, contributes significantly to change BP and regional blood flow (Davis, 1993).

1.1.3.1.2 The venous return of blood

Since cardiac output is specified via stroke volume and heart rate, a rise in stroke volume can enhance the cardiac output or vice versa. Thus the venous return of blood to the heart is critical to determining cardiac output. An alteration in the venous capacitance can reduce venous return of blood to the heart and therefore, stroke volume. Additionally, when veins dilate they act as reservoirs for blood, efficiently decreasing the circulating blood volume and thus reducing BP.

1.1.3.1.3 Baroreceptors

Central nervous system activity can be altered via inputs from baroreceptors to modify BP, one remarkable feature of the nervous system control of BP. The baroreceptor-mediated variations in heart rate are the fastest-responding arterial pressure control mechanism. Baroreceptors located within the aortic arch and the carotid sinus recognize alterations in the stretch of the vessel wall, secondary to the pressure of blood flow (Fig. 1.4). The baroreceptor is one of the most critical elements in BP regulation, as it ensures minimum BP variability throughout normal daily life (Berdeaux and Giudicelli, 1987, Gordan et al., 2015, Hall, 2015).

If a reduction in BP is identified, such as when shifting position from lying down to standing up, impulses are sent from the baroreceptors to the vasomotor centre as the first part of the reflex arc. Efferent signals are then sent out to the blood vessels, especially the arterioles, prompting them to constrict. This raises the peripheral vascular resistance, thus raising BP back to its average level. Impulses are also sent from the baroreceptors to the cardiac centres, stimulating the cardio acceleratory centre to raise sympathetic activity and reduce parasympathetic activity. This raises the heart rate and force of contraction, and consequently cardiac output, and continues until BP returns to its homeostatic level (Gordan et al., 2015).

1.1.3.1.4 The renin-angiotensin-system

The renin-angiotensin-system is a further key modulator of BP regulation. When arterial pressure drops, the kidneys secrete the enzyme renin. Renin then catalyses the formation and production of angiotensin I, which is further converted into angiotensin II (ANG II) by an angiotensin-converting enzyme. ANG II is a potent arteriolar vasoconstrictor and therefore raises BP via enhancing peripheral resistance (Fig. 1.5) (Gordan et al., 2015).

Furthermore, ANG II stimulates aldosterone secretion from the adrenal gland, which leads to a reduction in salt and water excretion via the kidneys, raising blood volume and BP over the period of hours or days. The fluid intake and excretion balance is fundamental for BP homeostasis and maintenance. The mechanism is a feedback loop,

which identifies alterations in BP and changes salt and water excretion accordingly, hence modifying the volume of extracellular fluid and returning BP to its normal levels. As BP rises, the kidneys excrete higher volumes of urine, to decrease extracellular fluid volume and then BP. The excretion of sodium also rises concurrently. On the contrary, in the case of hypotension, renal tubular reabsorption of salt and water rises to increase extracellular fluid volume and raise BP (Fig. 1.5) (Guyton et al., 1972).

In addition, hypotension leads to sympathetic activation of the adrenal glands, located superior to the kidneys, inducing release of epinephrine and norepinephrine release from the adrenal medulla. These hormones increase BP via raising heart rate and heart muscle contractility and also by mediating vasoconstriction of arterial and venous vessels (Guyton et al., 1972).

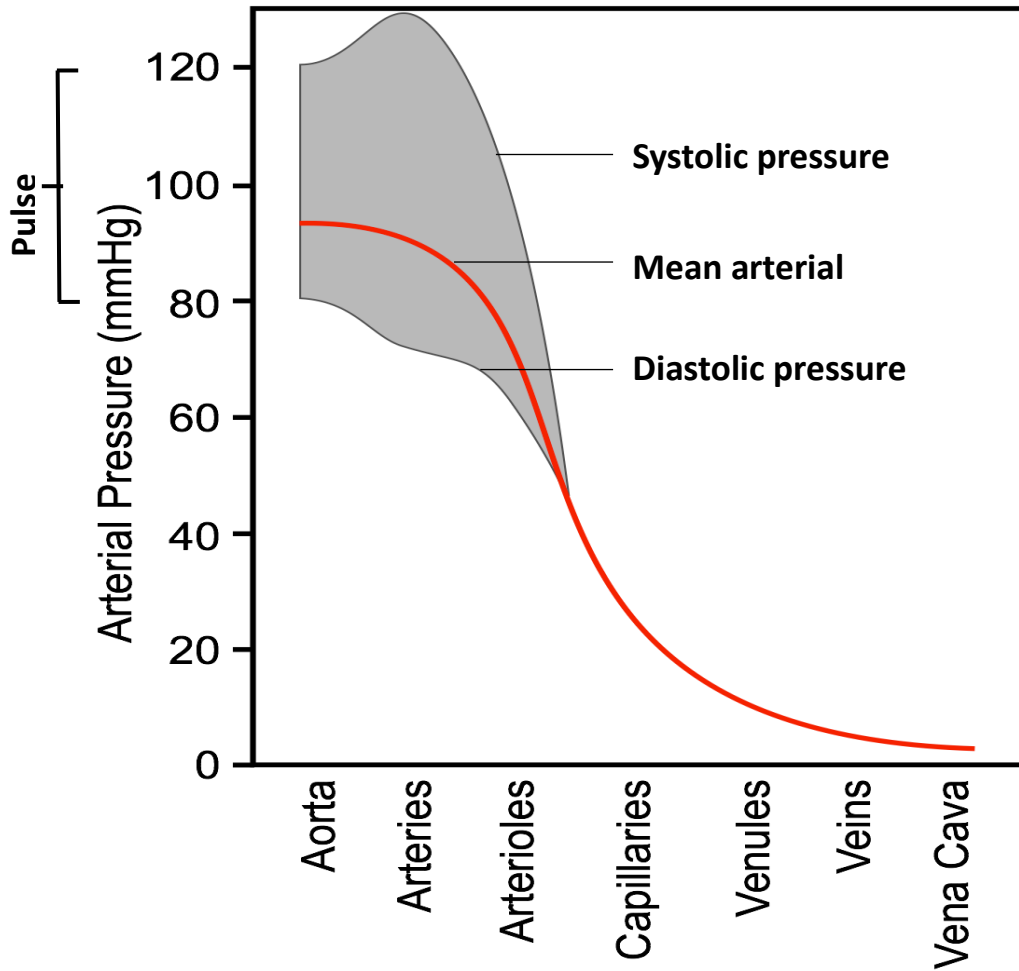


Figure 1-3: Systemic Blood Pressure

The graph shows the components of blood pressure (BP) throughout the blood vessels, including systolic, diastolic, mean arterial, and pulse pressures (Klabunde, 2011).

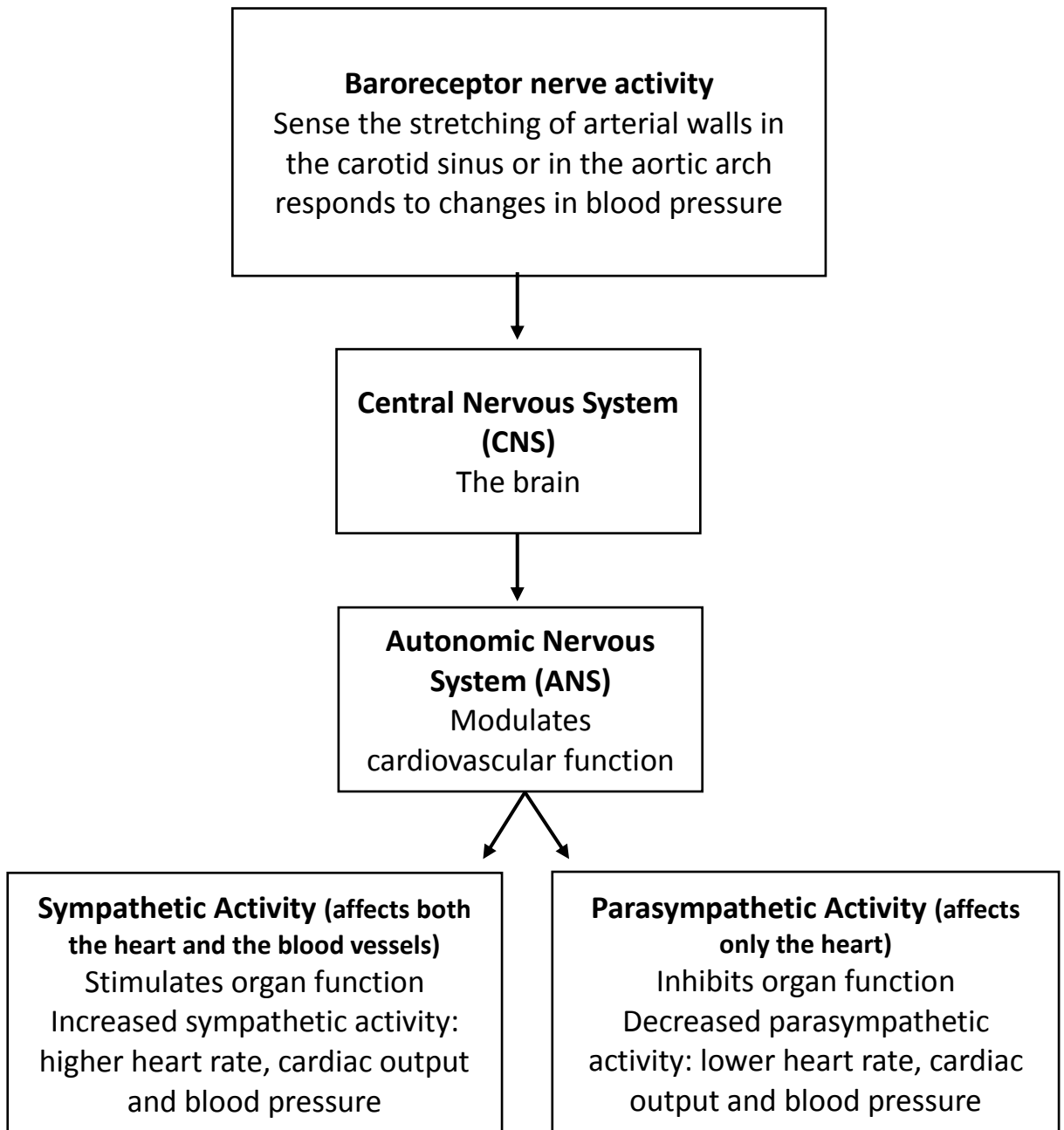


Figure 1-4: Explanation of how baroreceptor and the autonomic nervous system control blood pressure (BP).

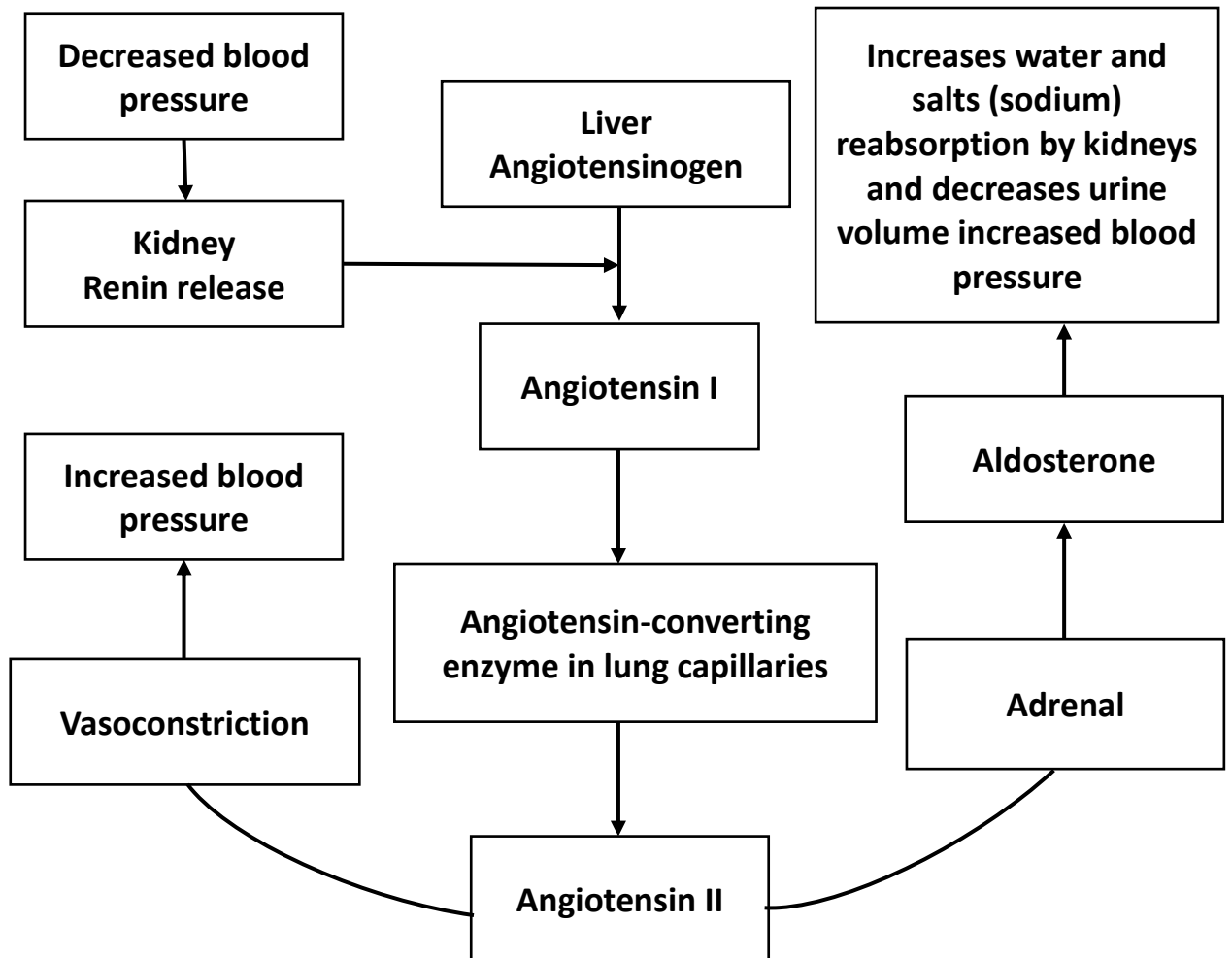


Figure 1-5: Summary of the regulation of blood pressure by the renin-angiotensin system

1.1.4 Vascular smooth muscle cells

Vascular SMCs, which are capable of contracting and relaxing in response to particular stimuli, underlie the principal mechanism of arterial lumen diameter regulation. Force can be generated in SMCs through an increase in the concentration of intracellular calcium ($[Ca^{2+}]_i$). Ca^{2+} can bind to calmodulin (CaM) and then trigger the calmodulin-dependent activation of myosin light chain (MLC) kinase. MLC phosphorylation activates myosin ATPase, enhancing adenosine-5'-triphosphate (ATP) hydrolysis and so production of cross-bridges between the filaments of myosin and actin and force generation (Dillon et al., 1981, Hai and Murphy, 1989). MLC phosphatase dephosphorylates MLC, resulting in the relaxation of SMCs. Consequently, vascular tone control essentially occurs through modulation of the SMCs $[Ca^{2+}]_i$ or via modifying the sensitivity of contractile filaments to Ca^{2+} through regulation of MLC kinase and phosphatase activity (Ratz et al., 2005). Increases in $[Ca^{2+}]_i$ concentration can occur as a consequence of release from intracellular stores, although this source of Ca^{2+} alone appears insufficient to sustain SMC contraction (Lagaud et al., 1999, Berridge, 1995), or influx across the cell membrane. Channels which can mediate this influx include voltage-gated Ca^{2+} channels (VGCCs), transient receptor potential channels (TRPs) and Orai1, along with the Na^+/Ca^{2+} exchanger (NCX). The major vasoconstrictors exert their effects through activation of G-protein coupled receptors (GPCRs), whose downstream signalling cascades can influence the activity of one or more of these Ca^{2+} permeable channels.

1.1.4.1 Gq/11 protein-coupled receptor signalling

The major vasoconstrictors such as epinephrine (and the related synthetic phenylephrine (PE)) and NE exert their effects through activation of particular GPCRs; seven-transmembrane domain receptors coupled to heterotrimeric Gq/11 proteins. Upon stimulation, the receptors serve as a guanine nucleotide exchange factor, increasing exchange of guanosine diphosphate to guanosine triphosphate on the α subunit of the G protein, which results in separation of the α subunit from the $\beta\gamma$ subunits (Clapham and Neer, 1997). Once separated, the α subunit stimulates phospholipase C (PLC) $\beta 1$, which catalyses the hydrolysis of phosphatidylinositol-4,5-bisphosphate (PIP_2) into inositol-1,4,5-trisphosphate (IP_3) and 1,2-diacylglycerol (DAG) (Berridge and Irvine, 1989). IP_3 stimulates IP_3 receptors found on the sarcoplasmic reticulum, resulting in Ca^{2+} efflux from this intracellular store (Grayson et al., 2004) (Fig. 5). This first increase in $[Ca^{2+}]_i$ elicits the additional Ca^{2+} release from the intracellular store following ryanodine

receptor activation (so-called Ca^{2+} -induced Ca^{2+} release) (Boittin et al., 1999). This Ca^{2+} release from intracellular stores can activate Ca^{2+} -sensitive chloride channels (Akata et al., 2003, Piper and Large, 2004), leading to efflux of negatively charged chloride ions from the cell and so membrane depolarisation (Leblanc et al., 2005). The increase in $[\text{Ca}^{2+}]_i$ can also stimulate the sodium-calcium exchanger (NCX), which pumps one Ca^{2+} ion out of the cell in exchange for three Na^+ ions being pumped in (Fig. 1.6) (Berra-Romani et al., 2010, Horiguchi et al., 2001, Weiss et al., 1993). The activity of this exchanger also acts to depolarise the membrane.

DAG, another product of PLC activity, can also contribute to depolarisation and rise of $[\text{Ca}^{2+}]_i$ via stimulation of non-selective cation currents through canonical TRPCs (Fig. 1.6) (Gudermann et al., 2004, Hardie, 2007). TRPC2, TRPC3, TRPC6, and TRPC7 subtypes all exhibit sensitivity to DAG (Gudermann et al., 2004, Hardie, 2007, Large et al., 2009), however, in rat mesenteric arteries it appears to be TRPC6 that is responsible for the effects of DAG on the SMCs (Clapham and Neer, 1997).

1.1.4.2 Voltage-gated Ca^{2+} channels

SMCs in small arteries and arterioles are richly endowed with VGCCs, possessing around 1000 channels per cell. A specific feature of these channels is that their channel open state probability is a constant steep function of the membrane potential; a 10 % variation in membrane potential leads to a three-fold change in channel open state probability.

Ca^{2+} can enter the SMCs through VGCCs upon cell membrane depolarisation. Since there is a large Ca^{2+} gradient across the cell membrane, opening of the VGCCs produces a large influx of extracellular Ca^{2+} resulting in constriction of the arterial vessel. Equally, cell membrane hyperpolarisation leads to VGCCs closure, resulting in decreased $[\text{Ca}^{2+}]_i$ and relaxation of the cell, and so the vessel (Jaggard et al., 1998). Consequently, due to the large quantity of VGCCs, small artery tone heavily relies on membrane potential.

This channel family contains ten members, two of which have been found in the vasculature, the L-type Ca^{2+} channels (LTCCs) (Fig. 1.6) and the T-type voltage-

dependent Ca^{2+} channel. The LTCCs needs high depolarisation to be activated, to between -30 mV and -10 mV depending on LTCCs subtype, while the T-type channel is activated at lower membrane potentials, about -45 mV (Catterall et al., 2005, Smirnov and Aaronson, 1992). While T type channels play a critical role in a number of physiological processes, involving neuronal and cardiac pacemaker activity, LTCCs play a significant role in maintaining BP: mean BP was reduced by a quarter in LTCCs knock-out mice (Moosmang et al., 2003) and comparable changes have been seen in rats treated with a pharmacological blocker of LTCCs channels (Pinterova et al., 2010).

1.1.4.3 Store-operated Ca^{2+} entry

Store-operated Ca^{2+} entry (SOCE) is a cellular response to the depletion of $[\text{Ca}^{2+}]_i$ store, coupling it to the activation of Ca^{2+} permeable channels in the cell membrane (Berridge, 1995). Stimulation of cell surface receptors, such as those for various growth factors, hormones, and neurotransmitters, result in the formation of the IP_3 , stimulation of Ca^{2+} release from the endoplasmic reticulum (ER) by the IP_3 receptor (IP_3R) and consequent store depletion (Smyth et al., 2010). TRPC1, TRPC4, and TRPC5 are suggested to particularly contribute to SOCE in VSMCs (Beech et al., 2004, Xu and Beech, 2001, Xu et al., 2006). Additionally, SOCE in arterial myocytes, involves the transmembrane proteins stromal interacting molecule 1 (STIM1) and Orai1 (Baryshnikov et al., 2009). STIM1 acts as a Ca^{2+} sensor in the ER, which upon translocates Ca^{2+} depletion to the close proximity of the plasma membrane where it can interact with and activate the cell membrane Ca^{2+} permeable Orai1 channel (Fig. 1.6) (Zhang et al., 2005).

Intracellular store depletion can also evoke further Ca^{2+} influx through stimulating NCX to operate in the opposite direction to normal, with Na^+ ions extruded in exchange for entry of one Ca^{2+} ion. NCX is co-expressed with Orai1 in the plasma membrane of human arterial myocytes and shows a functional correlation with SOCE. A functional and spatial relationship between NCX and sarco/endoplasmic reticulum Ca^{2+} pump ATPase was also observed in SMCs of pig coronary arteries (Baryshnikov et al., 2009, Davis et al., 2009). NCX in rat mesenteric arteries was shown to contribute to the Ca^{2+} entry after depletion of the stores (Lagaud et al., 1999).

1.1.4.4 Ca^{2+} sensitization mechanism

In addition to increasing $[\text{Ca}^{2+}]_i$ concentration, vasoconstrictors that activate GPCRs coupled to Gq/11 proteins also increase contractile Ca^{2+} sensitivity (Ca^{2+} -sensitisation) (Bradley and Morgan, 1987, Mulvany et al., 1982). This mechanism involves stimulation of MLC kinase and/or block of MLC phosphatase activity leading to higher Ca^{2+} efficacy (Ratz et al., 2005, Somlyo and Somlyo, 2003).

In rat mesenteric arteries, two important pathways have been recognised, involving either the serine-threonine kinases protein kinase C (PKC) or Rho-kinase respectively. Activation of Gq/11-coupled GPCRs stimulates PLC to cleave PIP_2 into IP_3 and DAG, the latter being an activator of PKC. A target of PKC is calponin, a thin filament-associated protein that interferes with the coupling between actin and myosin by inhibiting the ATPase activity of myosin. When phosphorylated by PKC, calponin changes its structure and its inhibitory effect is lost, thus contraction is enhanced (Budzyn et al., 2006, Gokina et al., 1999, Pohl et al., 1997). α subunits of Gq/11 and G12/13 proteins activate GEF (guanine nucleotide exchange factor) proteins for the small GTPase RhoA, an activator of Rho-kinase. Stimulation of this kinase can downregulate the activity of MLC phosphatase, leading to increased force for a given $[\text{Ca}^{2+}]_i$ (Ratz et al., 2005, Somlyo and Somlyo, 2003). In rat mesenteric arteries and veins, Rho-kinase is involved in the tone creation in response to an elevation of intramural pressure (Enouri et al., 2011, VanBavel et al., 2001). It also contributes to contraction of big arteries, for example the aorta or superior mesenteric artery, in response to α -adrenergic or thromboxane receptor (TP) activation, or high potassium (K^+). (Budzyn et al., 2006).

1.1.4.5 G_s and G_i/o protein-coupled receptors

Receptors coupled to G_s or G_i/o proteins respond to stimuli such as light, gustatory compounds, odorants, neurotransmitters, neuropeptides, hormones, and glycoproteins. All adrenergic and muscarinic receptors are coupled to these proteins (Hollmann et al., 2005). Receptors coupled to G_s or G_i/o proteins, respectively activate or block adenylyl cyclase, which generates cyclic adenosine monophosphate (cAMP) from ATP. cAMP in the vasculature directly opens cyclic nucleotide-gated ion channels (Leung et al., 2010, Shen et al., 2008), activates PKA (Simonds, 1999) and activates exchange protein activated by cAMP (Epac) (Purves et al., 2009).

Cyclic nucleotide-gated channels are nonselective cation channels which can be opened by the direct binding of cyclic nucleotides cAMP and cGMP (Kaupp and Seifert, 2002). In cultured ECs from bovine aorta, cyclic nucleotide-gated channels are involved in adrenaline-mediated increase in $[Ca^{2+}]_i$ (Shen et al., 2008). These channels are expressed in rat mesenteric artery SMCs (Kruse et al., 2006), and they may participate in contraction evoked by the TP receptor agonist U46619 (a thromboxane A₂ receptor agonist) (Leung et al., 2010).

PKA can influence smooth muscle contraction in several ways. This kinase can phosphorylate and so inactivate MLC kinase (Conti and Adelstein, 1981). In contrast phosphorylation by PKA activates multiple K⁺ channels, including ATP-sensitive K⁺ channels (Quinn et al., 2004, Shi et al., 2007), voltage-gated K⁺ channels (Aiello et al., 1998, Waldron and Cole, 1999), and big conductance Ca²⁺-sensitive K⁺ channels (BK_{Ca}²⁺) (Tian et al., 2004), resulting in hyperpolarisation of the cell. Also, PKA can block store-operated Ca²⁺ channels (Liu et al., 2005) and LTCCs (Liu et al., 1997, Orlov et al., 1996, Xiong et al., 1994), reducing and/or preventing an increase in $[Ca^{2+}]_i$ concentration. All these effects lead to SMC relaxation and so vessel dilation. However, PKA can also activate PKC (Wooten et al., 1996), possibly resulting in Ca²⁺ sensitization in SMCs.

Finally, cAMP signalling is involved in the activation of Epac, a guanine nucleotide exchange factor for the small G protein Rap (Bos, 2006, Bos, 2003, Gloerich and Bos, 2010), which reduces the activity of ATP-sensitive potassium channels (K⁺) in rat aortic SMCs (Purves et al., 2009). In cultured human embryonic kidney cells, Epac is capable of activating PLC (Schmidt et al., 1996), however, this action has not yet been demonstrated in small resistance arteries.

1.1.4.6 Potassium channels in smooth muscle cells

The plasma membrane of SMCs comprises a huge number of K⁺ channels (about 50000 per cell). They mainly participate in the regulation of the membrane potential, thus influencing VGCC open probability. K⁺ channel opening leads to an outward flux of K⁺ ions, due to the electrochemical gradient for K⁺ that decreases the net negative charge. This hyperpolarisation of the cell results in closure of VGCCs. Therefore, K⁺ channels can affect vascular tone and resistance (Bonev et al., 1997).

One of the major K^+ channels responsible for maintaining the SMC membrane potential is the delayed rectifier voltage-gated K^+ channel, which can be activated when depolarisation reaches approximately -40 mV (Ko et al., 2008, Nelson and Quayle, 1995). This channel is regulated by PKA, PKC and PKG (Ko et al., 2010), and is sensitive to the magnesium intracellular concentration (Tammaro et al., 2005).

Calcium-dependent K^+ ($K_{Ca^{2+}}$) channels on SMCs are critical for the control of small artery tone and also the fine-tuning of agonist and pressure-induced constriction (myogenic) (López et al., 2009). $K_{Ca^{2+}}$ channels are activated by $[Ca^{2+}]_i$ and depolarisation. Since opening of $K_{Ca^{2+}}$ channels leads to hyperpolarisation, countering the (agonist/pressure-induced) depolarisation that they were stimulated by, they can exert a stabilising, negative feedback on the membrane potential and can limit the contraction. Numerous studies have shown a role of smooth muscle $K_{Ca^{2+}}$ channels in the myogenic response, describing that active closure of $K_{Ca^{2+}}$ channels participates in the beginning of myogenic depolarisation and constriction (Kauser et al., 1991). Additionally, $K_{Ca^{2+}}$ channels may not only have a role in modulating constriction responses but also can be required to mediate the dilation response by endothelial-derived hyperpolarisation factor (EDHF). EDHF will be discussed in sections 1.2.1 and 1.2.2.

The $BK_{Ca^{2+}}$ channels are abundant in blood vessel SMCs. They are activated by Ca^{2+} concentrations greater than 500 nM and are also activated by depolarisation (Ko et al., 2008, Nelson and Quayle, 1995, Xia et al., 2002). The $BK_{Ca^{2+}}$ channels are coupled to ryanodine receptors (RyRs), which are located in the ER membrane and are responsible for the release of Ca^{2+} from intracellular stores during excitation-contraction coupling in both cardiac and skeletal muscle (Lanner et al., 2010). They are also involved in Ca^{2+} spark-elicited membrane hyperpolarisation in arteries (Jaggar et al., 1998) where $BK_{Ca^{2+}}$ channels are activated by Ca^{2+} release, in the form of Ca^{2+} sparks. Ca^{2+} sparks are transient local Ca^{2+} -signaling events caused by the opening of ryanodine-sensitive Ca^{2+} release channels [referred to as RyRs] in the ER membrane (Herrera et al., 2001).

Less abundant is an inward-rectifying K^+ (K_{ir}) channel, which is distinguished by its conduction of an inward current at membrane potentials negative to the equilibrium potential and smaller outward current at membrane potentials positive to equilibrium

potential (Nelson and Quayle, 1995). Consequently, the activity of K_{ir} channels provides a pathway by which extracellular K^+ can change the membrane potential of SMCs (Quayle et al., 1997). This mechanism plays a significant role in endothelium-derived hyperpolarisation (Dora et al., 2008, Edwards et al., 1998). The sarcoplasmic K_{ATP} channel is a hetero-octamer, comprising of four K_{ir} and four sulphonylurea receptor subunits. In rat vascular SMCs, reduction of intracellular ATP levels enable the K_{ATP} channel to open with a conductance of 50-250 pS (Ko et al., 2008). The K_{ATP} channel is responsible for hyperpolarisation in response to β -adrenoceptor activation (Garland et al., 2011, White et al., 2001). PKC has also been reported to modulate the activity of the channel, blocking K^+ current in response to ANG II (Kubo et al., 1997, Sampson et al., 2007).

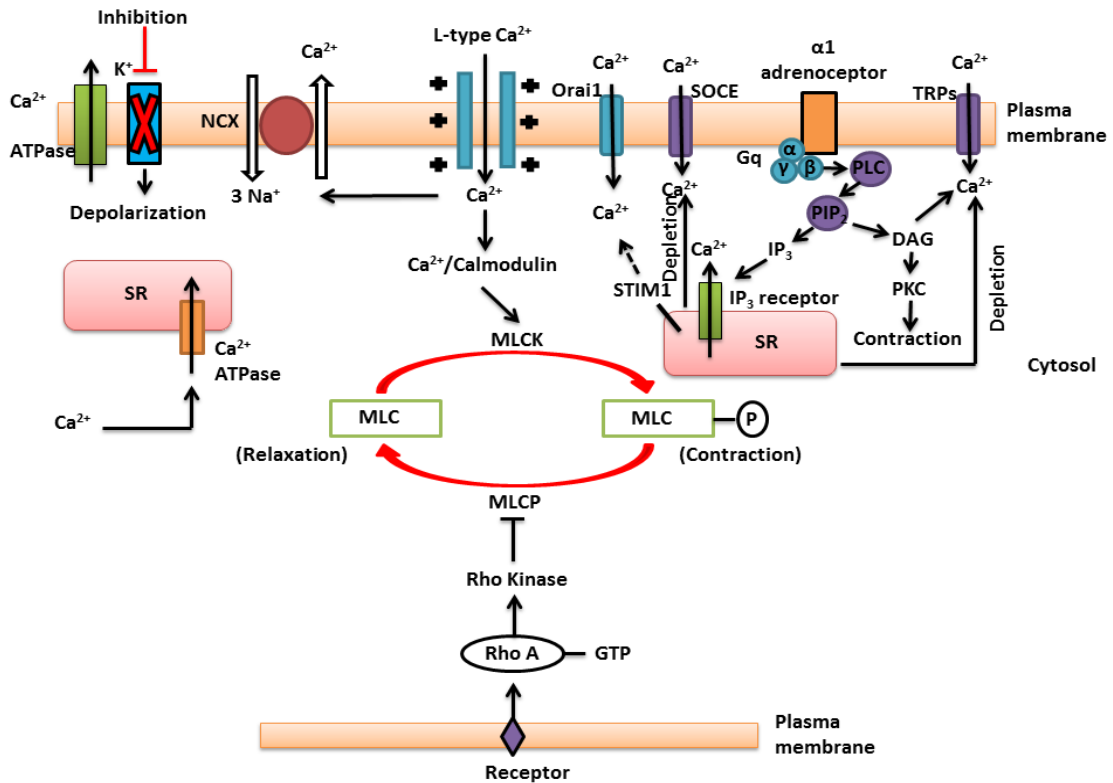


Figure 1-6: Schematic diagram showing contraction mechanisms in vascular smooth muscle cell.

Membrane depolarisation triggers the opening of L-type Ca²⁺ channels (LTCCs), resulting in Ca²⁺ influx into the cells and leading to Ca²⁺/calmodulin dependent myosin light chain kinase (MLCK) activation. MLCK then phosphorylates myosin light chain (MLC), inducing the myocyte to contract. Ca²⁺ is removed from the cytosol by Ca²⁺ ATPase on the plasma membrane and sarcoplasmic reticulum (SR) and also by the Na⁺/Ca²⁺ exchanger (NCX) on the plasma membrane. The myosin light chain phosphatase (MLCP) dephosphorylates MLC, which initiates relaxation of the cells. However, the MLCP activity is blocked via certain agonists by RhoA and Rho-dependent kinase stimulation. The sympathetic nervous system can also increase contraction of myocyte by stimulating α1 adrenoceptors to release the second messengers inositol triphosphate (IP₃) and diacylglycerol (DAG). IP₃ activates IP₃ receptors on the SR to cause Ca²⁺ release from the SR, an intracellular Ca²⁺ store. DAG can activate protein kinase C and so phosphorylation of other proteins. Both mechanisms cause myocyte contraction. Store-operated Orai1 channels are activated by stromal interaction molecule 1 (STIM1) protein, a sensor of depletion of Ca²⁺ in the SR. Store-operate calcium entry (SOCE) is activated by the reduction of SR [Ca²⁺]. Transient receptor potential canonical (TRPC) channels mediated Ca²⁺ influx after the activation by DAG or calcium store depletion.

1.1.5 The endothelium

The internal surface of blood vessels throughout the circulatory system is lined with a single layer of ECs. This layer of ECs is a specialised type of simple squamous endothelium isolated from a basal lamina of the surrounding outer layers (Günthner et al., 2009). ECs usually present a non-thrombogenic surface to which platelets and leukocytes in the circulating blood do not adhere, thus the coagulation system remains inactivated (Félétou, 2011). The endothelium serves as a particular barrier between the blood vessel lumen and surrounding tissue and regulates the entrance of materials such as amino acids and glucose and the transit of white blood cells into and out of the bloodstream. ECs control vessel tone and function by releasing trophic factors, vasodilators and vasoconstrictors that are involved in angiogenesis. These cells also mediate inflammatory responses through the surface expression of chemotactic and adhesion molecules and the release of chemokines and cytokines. Endothelial dysfunction could result in pathophysiological events that contribute to the development of vascular complications resulting from for example atherosclerosis and thrombosis (Cines et al., 1998, Chiu and Chien, 2011).

Focusing on the control of vessel tone, ECs release mediators that influence the contractile state, both positively and negatively, of the neighbouring vascular SMCs (VSMCs). The first mediator to be identified, a vasodilator, was prostacyclin (Moncada et al., 1976). Subsequently, nitric oxide (NO) was identified as a key mediator in the vasorelaxation elicited by the muscarinic receptor agonist ACh (Furchgott and Zawadzki, 1980). A further, incompletely defined, vasodilator is the EDHF, while vasoconstrictors identified include thromboxane and endothelin-1. One or more of these mediators can be released in response to activation of endothelial receptors by agonists such as ACh, bradykinin, ATP, serotonin and substance P, all vasodilators (Vallance and Chan, 2001). Additionally they can be released following activation of mechanoreceptors on ECs, which are able to sense shear stress resulting from blood flow over the cell surface, again inducing vasorelaxation. NO and EDHF, two of the most significant mediators of vasodilation will be discussed further in the following sections.

1.1.5.1 Nitric oxide

Substances such as ACh, bradykinin, or substance P can trigger an increase in $[Ca^{2+}]_i$ in ECs. This Ca^{2+} binds to CaM to create the Ca^{2+} -CaM complex, which has been shown to convert nitric oxide synthase (NOS) into its active form (Busse and Mülsch, 1990). The active enzyme, in the presence of molecular oxygen and NADPH, converts L-arginine into citrulline and NO. The NO generated in the ECs then diffuses to the SMCs, where it activates soluble guanylate cyclase (sGC) leading to the conversion of GTP, guanosine triphosphate, into cGMP (Rapoport and Murad, 1983). Increasing cGMP in SMCs leads to the inhibition of Ca^{2+} entry into the cells, K^+ channel activation, eliciting hyperpolarisation, and activation of the cGMP-dependent protein kinase PKG. Consequently, the decrease in $[Ca^{2+}]_i$ and stimulation of MLC phosphatase reduces the contraction of SMCs (Carvajal et al., 2000) (Fig. 1.7).

1.1.5.2 Endothelium-Derived Hyperpolarising Factor (EDHF)

EDHF is so named because of its hyperpolarising influence on the membrane of ECs, which can be spread to the SMCs, resulting in relaxation (Chen et al., 1988, Taylor and Weston, 1988, Garland and McPherson, 1992).

This factor was first observed in guinea pig mesenteric artery, where the action of the muscarinic agonist carbachol on the ECs resulted in SMC hyperpolarisation and consequently vessel relaxation. After ECs were removed, the inhibitory effect of carbachol was abolished, and the hyperpolarising response to carbachol was changed to a depolarisation, indicating that the hyperpolarisation observed must be derived from the endothelium (Bolton et al., 1984). Further evidence for another endothelium-dependent relaxation factor emerged when it was found that the SMC hyperpolarisation, and relaxation induced by ACh or bradykinin after stimulating ECs, was not affected by pharmacological blocking of NO or prostacyclin (Félétou and Vanhoutte, 2006).

1.1.5.2.1 EDHF relaxation mechanism

It is well known that administration of a muscarinic agonist causes an increase in the concentration of Ca^{2+} within ECs (Peach et al., 1987). Hyperpolarisation occurs as a

result of the ensuing opening of the small and intermediate-conductance calcium-activated potassium channels ($SK_{Ca^{2+}}$ and $IK_{Ca^{2+}}$), triggering positively charged K^+ to efflux (Edwards et al., 1998). EDHF can be inhibited by blockers of endothelial $SK_{Ca^{2+}}$ and $IK_{Ca^{2+}}$, such as apamin or charybdotoxin (Garland and McPherson, 1992).

The mechanism underlying the transmission of the hyperpolarisation to the VSMCs has not been definitively determined (Busse et al., 2002), however, a couple of hypotheses have been put forward;

i) Gap junctions, which allow the movement of small molecules, exist between ECs, between SMCs (both homocellular gap junctions), and between ECs and SMCs (myoendothelial gap junctions). Therefore, the electrical signal may simply be transferred freely between the cells. The coupling between cells will also help to regulate or synchronise a response within a section of the vessel. Ultrastructural evidence showed that ECs can extend cellular protrusions through perforations in the internal elastic lamina to come into close contact with SMCs (myoendothelial gap junctions) in rabbit carotid artery and rat mesenteric artery (Sokoya et al., 2006).

ii) A substance released from the ECs may diffuse into the SMCs.

The evidence supporting each of these pathways for relaxation varies throughout the vasculature.

An *in vivo* study in the hamster cheek pouch microcirculation showed that a small number of ECs stimulated via microiontophoresis of ACh can cause the relaxation of the entire artery length (Duling and Berne, 1970). The rate at which the signal was spread, its spread along the entire length of the vessel far away from the site of ACh stimulation, and the fact that it could be stopped by cutting the vessel all argue against the involvement of a diffusible factor and in support of it being electrical in nature.

It has been suggested that endothelial EDHF-like substances such as the cytochrome P450-derived eicosanoid 11,12 epoxyeicosatrienoic acid (11,12 EET) can diffuse to the neighbouring SMCs, leading to $K_{Ca^{2+}}$ channels opening in the SMCs membrane (Lamping et al., 2000, Fleming, 2001). There is an indication that this can account for the EDHF response in coronary and renal arteries of different species. A

Having been transmitted to VSMCs the hyperpolarisation decreases the open probability of the VGCCs and consequently reduces the levels of cytoplasmic free Ca^{2+} , which leads to SMC relaxation (Nelson et al., 1990).

1.1.5.2.2 EDHF in small arteries

Numerous discoveries have found that communication between cells through gap junctions is most efficient in vessels where the ratio of ECs to SMCs is very high (Berman et al., 2002, Shimokawa et al., 1996); for example, gap junction-mediated dilation is higher in small mesenteric arteries than in the aorta (Chaytor et al., 1998). Therefore, the role EDHF plays in the vasodilatation of small vessels is greater than in big vessels. Given the greater impact that smaller vessels have on BP, EDHF may be critical in BP maintenance. In support of this idea, $SK_{Ca^{2+}}$ and $IK_{Ca^{2+}}$ knockout mice developed hypertension (Taylor et al., 2003, Si et al., 2006) and loss of EDHF function has been observed in hypertensive rats, with the resistance arteries being the most important sites of loss (Goto et al., 2000).

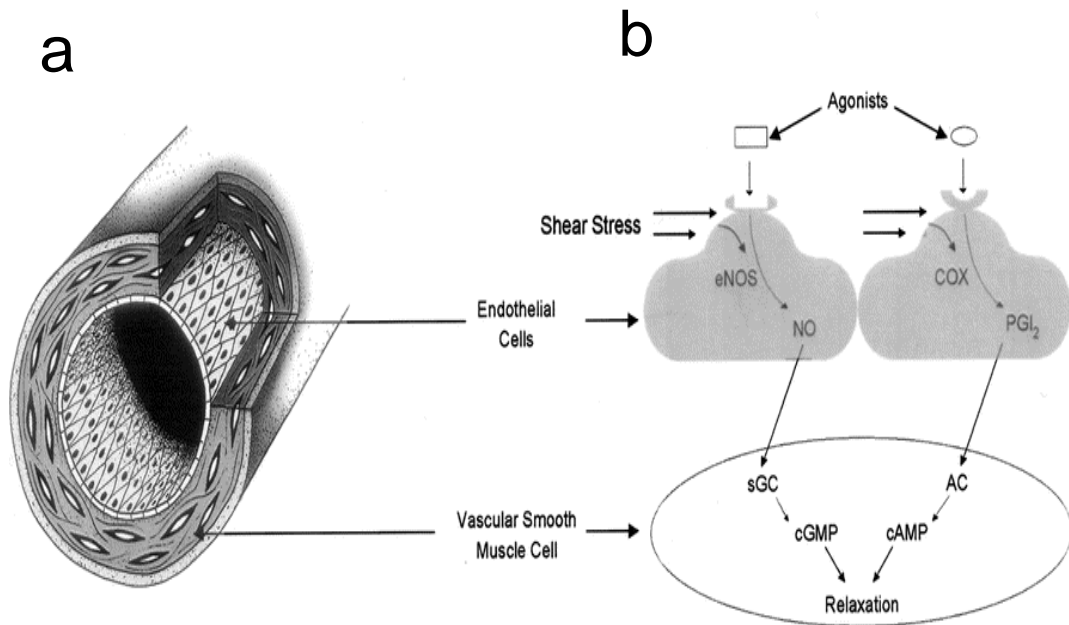


Figure 1-7: (a). Diagram showing the endothelial cells and vascular smooth muscle cells in an artery. (b) Endothelium-mediated relaxation through nitric oxide (NO) and prostacyclin (PGI₂)

AC = adenylyl cyclase; cAMP = cyclic adenosine monophosphate; cGMP = cyclic guanosine monophosphate; COX = cyclooxygenase; eNOS = endothelial nitric oxide synthase; sGC = soluble guanylyl cyclase (Bryan et al., 2005).

1.1.5.3 Endothelium-Derived Contractile Factor (EDCF)

The endothelium is able to exert a relaxation effect on the underlying SMCs by releasing NO and EDHF. Additionally, the endothelium also releases contracting factors in several vascular beds, including in response to thromboxane/endoperoxides, superoxide anions, and endothelin-1 (Vanhoutte and Tang, 2008). The first EDCF observation was made on isolated dog veins, where the ECs induced the surrounding SMCs to constrict in response to arachidonic acid and thrombin (De Mey and Vanhoutte, 1982). Another early observation of EDCF was in the aorta from adult spontaneously hypertensive rats (Lüscher and Vanhoutte, 1986), where ACh induced a concentration-dependent rise in tone. Subsequently the release of EDCF has been observed to be triggered in response to shear stress, muscarinic agonists and serotonin, and as a result of rises in $[Ca^{2+}]_i$.

Although the exact composition of EDCF remains to be determined, it is known to be a result of arachadonic acid metabolism via the cyclooxygenase enzyme which is inhibited via indomethacin, and has been proposed to be mediated via the action of prostaglandin H_2 and prostacyclin on the receptors of TP receptors on the VSMCs (Vanhoutte and Tang, 2008). The balance of EDCF and EDHF is important to endothelial function, as suggested by the hypertension related endothelial dysfunction resulting from their imbalance (rise in EDCF coupled with a decrease in EDHF) (Vanhoutte et al., 2005).

1.1.5.4 Ca^{2+} in the endothelial cell

Stimulation of the vascular endothelium by ACh, bradykinin and histamine is typically correlated with an increase in the EC $[Ca^{2+}]_i$, which occurs as a result of release from $[Ca^{2+}]_i$ stores and/or entry from the extracellular space. The mechanisms that give rise to the changes in $[Ca^{2+}]_i$ are similar to those described in VSMCs (1.1.4). A key difference is that ECs do not express VGCCs. Consequently, in contrast to VSMCs, little Ca^{2+} influx is triggered by increases in membrane potential.

The EC membrane does express $K_{Ca^{2+}}$ channels, which are stimulated by an increase in $[Ca^{2+}]_i$ and depolarisation, however, the channel subtypes appear to be different from VSCM. $K_{Ca^{2+}}$ channels on ECs seem to be lacking the $\beta 1$ subunit, and are consequently less Ca^{2+} sensitive than smooth muscle $K_{Ca^{2+}}$ channels (Katakam et al., 2000). Agonists

such as ACh, which increase $[Ca^{2+}]_i$, can open endothelial $K_{Ca^{2+}}$ channels resulting in K^+ efflux and ECs hyperpolarisation.

In rat mesenteric arteries, activation of Gq/11 protein-coupled receptors by ACh and carbachol increases ECs $[Ca^{2+}]_i$ as a result of phospholipase C-mediated IP_3 generation, IP_3 receptor stimulation and consequently Ca^{2+} efflux from intracellular stores (Mumtaz et al., 2011, McSherry et al., 2005, Oishi et al., 2001, Rodríguez-Rodríguez et al., 2009, Fukao et al., 1997). In human umbilical vein ECs, RyR have been reported to contribute to the rise in $[Ca^{2+}]_i$ in response to ACh and histamine, and spontaneous $[Ca^{2+}]_i$ events (Paltauf-Doburzynska et al., 2000, Kansui et al., 2008). However, rises in $[Ca^{2+}]_i$ in ECs from rat mesenteric arteries responding to muscarinic receptor activation are insensitive to ryanodine (Mumtaz et al., 2011).

In mesenteric arteries, both the amplitude of the $[Ca^{2+}]_i$ increase and the resulting cell hyperpolarisation were diminished by removal of extracellular Ca^{2+} . Demonstrating the additional importance of Ca^{2+} influx (Dora et al., 2008, Fukao et al., 1997, McSherry et al., 2005, Mumtaz et al., 2011).

Attenuation of the mesenteric artery hyperpolarisation was also observed after blocking the sarcoplasmic reticulum Ca^{2+} -ATPase (Fukao et al., 1997). Consequently, it was proposed that store depletion in ECs stimulates SOCE Ca^{2+} entry, probably, through a channel from the TRP family (Mumtaz et al., 2011). All canonical, vanilloid, and melastatin TRP subfamilies are expressed in ECs, with the TRPC subfamily being the main candidate for SOCE (Hill et al., 2006a, Yao and Garland, 2005, Zholos et al., 2011, Tirupathi et al., 2006). It was determined that the TRPC1 and TRPC4 channels can form a complex with IP_3 receptors to optimize signalling of Ca^{2+} (Rath et al., 2009).

Another critical pathway of Ca^{2+} entry can be myoendothelial gap junctions. It has been reported in rat mesenteric arteries that activation of SMCs, with a resulting increase in Ca^{2+} , can lead to an enhanced $[Ca^{2+}]_i$ in the adjacent ECs (Dora et al., 2000, Oishi et al., 2001). This mechanism can function as a negative feedback to decrease vascular tone responding to the sharp rising of SMC $[Ca^{2+}]_i$ by dilators or hyperpolarisation.

Finally, EC cyclic nucleotide-gated channels can play a role in endothelium-dependent vascular relaxation, their activation leading to an influx of Ca^{2+} . These channels are activated following Gs protein – coupled receptor stimulation by neurotransmitters (e.g., noradrenaline, dopamine, serotonin) leading to cAMP production. Irrespective of the source, rises in $[\text{Ca}^{2+}]_i$ can potentially activate endothelial NOS, resulting in release of NO, cyclooxygenase (resulting in production of prostanoids), and/or the intermediate and small conductance Ca^{2+} -sensitive K^+ channels ($\text{IK}_{\text{Ca}^{2+}}$ and $\text{SK}_{\text{Ca}^{2+}}$, respectively), causing K^+ efflux and ECs hyperpolarisation (Chen and Cheung, 1997, Edwards et al., 1998, Zygmunt and Högestätt, 1996). The relative contribution of each differs between different activators in different arteries related to different expression levels.

1.1.6 Mechanical modulation of arterial tone

Mechanical forces correlated with blood flow play a major role in the control of vascular tone. Forces applied to the wall of the vasculature due to blood flow can be categorised into two classes. The first is parallel to the wall to produce shear stress, a frictional force on the ECs surface. The second acts perpendicular to the wall and represents BP (Davies, 1995). While transmural pressure is spread to all vascular layers of the wall (intima, media, and adventitia), shear stress is sensed only by the internal EC layer.

1.1.6.1 Flow-induced responses

Shear stress force is determined by three variables: blood velocity, blood viscosity and the diameter of vascular vessels. Therefore, as these variables alter the degree of shear stress experienced by the cells lining the blood vessels will alter. The major physiological response to shear stress, which was first identified by Schretenmayr in 1933, is vasodilation. This results from the release of NO and prostacyclin. Additionally, laminar shear stress has atheroprotective effects (Davies, 1995), related to anti-thrombotic, anti-inflammatory and anti-adhesive properties. For example, it blocks platelet aggregation (Kramer et al., 1989), leukocyte adhesion and proliferation of SMCs (Berk et al., 2001).

The molecular mechanism underlying the flow-elicited relaxation remains still unclear but presently it is believed to be mediated by the endothelium, the sensor of the force. Shear stress causes mechanical distortion of ECs, initiating mechanotransduction, the

transduction of mechanical force into chemical signalling. Eventually the downstream biochemical signalling results in physiological responses (Li et al., 2005, Lehoux et al., 2006, Davies, 2009).

The role of endothelial-derived agents in flow-elicited responses was not discovered until 50 years after the finding of flow-dependent vasoregulation (Hull Jr et al., 1986). Endothelium-derived NO plays a major role in the control of flow-mediated relaxation in healthy vessels (Joannides et al., 1995, Shiode et al., 1996). After shear stress is applied, NO is generated and sustained for the length of the stimulus (Fleming et al., 2005). NOS, the enzyme responsible for the production of NO, is stimulated by shear-stress in a biphasic manner. One phase is Ca^{2+} dependent, with CaM binding to Ca^{2+} and activating NOS by causing its fast separation from its negative regulator caveolin and its subsequent association with HSP-90. Then NOS is phosphorylated on serine residue (Ser 1177) by protein kinase A (Fleming, 2010), increasing its sensitivity to Ca^{2+} . During the second phase, NOS is stimulated by resting Ca^{2+} . This is named “calcium-independent” NOS stimulation in response to shear stress, which leads to sustained NO production (Balligand et al., 2009).

However, flow-elicited relaxation is not completely dependent upon NO, as responses are still observed in NOS knock-out mice (Huang et al., 2001). PGI_2 , cytochrome P450 metabolites of AA and hydrogen peroxide (H_2O_2) are other mediators of this response (Miura et al., 2001, Sun et al., 2007, Drouin and Thorin, 2009, Kang et al., 2009, Koller et al., 1995). Furthermore, in mesenteric arteries of female rat, the power of EDHF-type control of flow-elicited relaxation has been found (Morton et al., 2011). Thus, flow-induced vasodilatation is a mixed response including the release of various endothelium-derived vasodilators.

1.1.6.2 Pressure response

Arteries continually experience BP and cyclic stretching. A myogenic response of arteries can develop in response to these forces. The myogenic response is an intrinsic constriction state of SMCs, independent of neurohumoral and endothelial influences (Davis and Hill, 1999, Khavandi et al., 2009). Myogenic constriction is a major element of basal vascular tone (Hill and Davis, 2007) from which the contractile machinery can

respond to stimuli, with either gain or loss of contractile force, giving local control of blood flow and pressure in a fast and efficient manner.

A three-phase model of *in vitro* arterial myogenic behaviour has been proposed. The first one is identified as tone development (myogenic tone; 40–60 mmHg). The second one is myogenic reactivity (60 and 140 mmHg), revealing the response to change in transmural pressure. Increased transmural pressure results in myogenic constriction, while decreased pressure leads to myogenic dilatation. The third phase only happens when the vascular wall of the artery is unable to sustain the constriction against the transmural pressure (above 140 mmHg): a total loss of myogenic tone which is known as forced dilatation (Osol et al., 2002).

Small arteries with internal diameter <300µm possess the ability to develop a strong myogenic response (Khavandi et al., 2009) while larger and very small arteries develop only a relatively weak myogenic response. Moreover, the myogenic response differs between species and vascular beds (Osol et al., 1991, Watanabe et al., 1993, Liao and Kuo, 1997, Miller et al., 1997).

Bayliss was the first to report the myogenic response in the beginning of the last century. However, despite intensive investigation into its physiological and pathophysiological significance, so far the cellular mechanisms which translate pressure variations to VSMC contractions are not completely understood. The following series of events are believed to be involved in the myogenic response. Elevated intraluminal pressure is sensed by the ion channels, membrane lipids within the bilayer itself and/or by extracellular matrix-integrin complexes. Stimulation of these pathways results in the opening of non-selective cation channels, membrane depolarisation and activation (opening) of LTCCs. The increased Ca^{2+} level leads to Ca^{2+} /CaM-dependent stimulation of MLC kinase, then phosphorylation of the 20-kDa myosin regulatory light chains and contractile interaction of actin and myosin (Zou et al., 2001, Hill et al., 2006b, Hill et al., 2009).

The consequence of pressure-elicited responses depends upon the duration of the vascular wall exposure to the increased intraluminal pressure. Sustained exposure ultimately leads to structural modifications within the vascular wall, termed 'pressure associated

remodelling' (Mulvany, 2012). For example, in response to increased BP there is a decrease in internal diameter with an increase in wall thickness despite no overall change in cross-sectional diameter of blood vessels, a phenomenon known as 'eutrophic inward remodelling'.

The physiological significance of myogenic constriction is likely to control target organs microcirculation, providing protection from pressure associated damage to exposed organs such as the brain, heart and kidneys. Consequently, the effect of abnormal myogenic responses in the pathogenesis of cardiovascular disease and protection against hypertension-elicited organ damage have been extensively discussed (Davis and Hill, 1999, Hughes and Bund, 2002). Flow and pressure, two mechanical stimuli, have a major role in the local regulation of vascular tone in small arteries.

1.1.6.3 Pharmacological modulation of vascular tone

The manipulation by pharmacological agents of both the myocardium and vasculature at the level of the autonomic nervous system (by α or β adrenoceptors), myocardium (such as Ca^{2+} sensitization by levosimendan), or locally (such as by sympathectomy) is generally accepted in anaesthesia to decrease the effects of critical illness and to control the end-organ perfusion, either by raising vascular tone or cardiac output (Hebbes, 2016).

The pharmacological agents are all vasodilators, targeting SMC and /or the neighbouring vascular EC to reduce vascular tone. The most effective vasodilators work through decreasing the actin-myosin complexes in VSMCs. Vasodilators can be classified into several types (Golan et al., 2011):

- i) NO donors, (for example organic nitrates and sodium nitroprusside), induce vasodilation via stimulating guanylyl cyclase and increasing MLC dephosphorylation.

- ii) Blockers of cGMP phosphodiesterase class V (PDE5) inhibit cGMP hydrolysis and thus enhance dephosphorylation of MLC.

iii) Ca^{2+} channel blockers induce vasodilation through decreasing the concentration of $[\text{Ca}^{2+}]_i$.

iv) K^+ channel openers cause vasodilation via opening ATP-sensitive K^+ channels, thus hyperpolarising the cells and preventing opening of the VGCCs required for the influx of Ca^{2+} and contraction of the VSMCs.

v) Antagonists of endothelin receptors inhibit endothelin-mediated vasoconstriction.

vi) α_1 adrenergic antagonists block the endogenous epinephrine and norepinephrine vasoconstrictive action.

vii) Angiotensin converting enzyme blockers and ANG II receptor subtype 1 (AT1) antagonists block the vasoconstrictive effect of endogenous angiotensin II, either through blocking the formation of the ANG II (ACE inhibitors) or inhibiting its cognate receptor (AT1 antagonists) (Golan et al., 2011).

viii) Hydralazine inhibits Ca^{2+} dependent ATPase and phosphorylation (Jacobs, 1984).

ix) β -adrenergic antagonists competitively inhibit the binding of endogenous catecholamines to β_1 -adrenoceptors in the heart (O'Rourke, 2007).

1.2 Arterial Remodelling and Hypertension

The vascular wall is composed of ECs, SMCs, and fibroblasts which act in concert to form a complicated autocrine-paracrine set of interactions. The vascular wall can detect and sense alterations in the milieu, and integrates these signals via intercellular communication and by the local production of mediators, which affect vascular structure and function. Vascular remodelling is an active process of structural modifications that includes alteration in at least four cellular processes: cell growth, cell death, cell

migration, and the extracellular matrix degradation. Vascular remodelling relies on dynamic interactions among locally created growth factors, vasoactive substances, and hemodynamic stimuli. Furthermore, remodelling is an adaptive process that occurs in response to long-term alterations in hemodynamic conditions; however, it may therefore contribute to the pathophysiology of vascular diseases and circulatory disorders (Gibbons and Dzau, 1994).

In response to raised arterial pressure, the structure of a vessel is changed such that the ratio of the wall width to the lumen width is elevated via either a rise in muscle mass or rearrangements of cellular and noncellular elements. These alterations heighten vascular reactivity, which potentiates the rise in peripheral resistance characteristic of hypertension. Another vascular remodelling form includes alterations primarily in the dimensions of the lumen (Gibbons and Dzau, 1994). Hypertension affects more than 25% of adults in the UK yet, in the majority of cases, the exact mechanisms causing it remain unknown. Hypertension is a long term medical condition in which resting systolic and diastolic BP are persistently elevated greater than 140/90 mmHg, in adults. It is a major risk factor for severe diseases, such as heart attack, stroke, and arterial aneurysms, but can remain undiagnosed since very few symptoms accompany it. It is for this reason that hypertension is termed “a silent killer”. Primary, or idiopathic, hypertension is estimated to be accountable for 90-95% of hypertensive patients, with secondary hypertension, associated with for example kidney disease or an adrenal medulla tumour, only accounting for a small proportion of hypertensive patients.

Although collagen and elastin are both extracellular matrix proteins (ECM), they have different elastic properties. Collagen is the most abundant fibrous protein within the ECM. Collagens, which constitute the main structural element of the ECM, provide tensile strength, regulate cell adhesion, support chemotaxis and migration, and direct tissue development. The bulk of interstitial collagen is transcribed and secreted by fibroblasts that either reside in the stroma or are recruited to it from neighbouring tissues. By exerting tension on the matrix, fibroblasts are able to organize collagen fibrils into sheets and cables and, thus, can dramatically influence the alignment of collagen fibres (Frantz et al., 2010).

Collagen associates with elastin, another major ECM fibre. Elastin fibres provide recoil tension to tissues that undergo repeated stretch due to their mechanical properties. Importantly, elastin stretch is crucially limited by tight association with collagen fibrils. Secreted tropoelastin (the precursor of elastin) molecules assemble into fibers and become highly crosslinked to one another via their lysine residues by members of the lysyl oxidase enzyme family. Elastin fibers are covered by glycoprotein microfibrils, mainly fibrillins, which are also essential for the integrity of the elastin fiber (Frantz et al., 2010).

At low pressure (110 / 70 mmHg in men), elastin is predominantly expressed in the artery wall with collagen contributing less than 10%. However, at higher pressures, collagen expression is enhanced and, as a result, the vessels gradually become stiffer. Thus, hemodynamic forces exert a regulatory effect on the vascular structure and stiffness (Zieman et al., 2005). Any alterations to blood vessel dimension, geometry and/or microstructure that result from changes in haemodynamic forces, such as a persistent rise in BP, are termed 'remodelling' (Humphrey et al., 2009).

It has been proposed that remodelling could be an adaptive response of the arterial wall to control a homeostatic mechanical state (Humphrey, 2008). Stiffening could, for example, help to reduce aortic distension and prevent aortic aneurysm or rupture (Wagenseil and Mecham, 2009, Shadwick, 1999, Rachev et al., 1997, Roach and Burton, 1957). Remodelling, however, can also lead to a number of diseases, such as fibrosis, hyperplasia of the arterial intima and media, modifications in vascular collagen and elastin, endothelial dysfunction, and arterial calcification (Van Varik et al., 2012). Despite the molecular mechanisms underlying vascular remodelling not yet being clear, three types of cells, vascular ECs, VSMCs and adventitial fibroblasts are suggested to be involved in mediating the process, through modulating ECM proteins (Humphrey et al., 2009, Humphrey, 2008).

Hypertension is linked with arterial stiffening and remodelling. Increased BP over time can result in vascular remodelling, hypertrophy, and hyperplasia; structural alterations that contribute to arterial stiffening. Untreated hypertension can lead to a vicious cycle of arterial stiffening, causing further hypertension, which promotes further arterial stiffening and so on (Franklin, 2005). A study by Benetos and colleagues in 2002 demonstrated

that high BP is the main determinant of aortic stiffness (Benetos et al., 2002). However, aortic stiffness in non-hypertensive people is linked with a higher risk of developing hypertension in the future (Dernellis and Panaretou, 2005, Liao et al., 1999, Kaess et al., 2012). Thus, these studies suggest a bi-directional correlation between vascular stiffness and hypertension.

The balance of collagen and elastin in the ECM is frequently controlled by the matrix metalloprotease (MMP) family. The ECM is degraded by MMPs, leading to fragmented and irregular elastin fibers and creating uncoiled, stiffer collagen fibres (Li et al., 1999, Zieman et al., 2005). Since arterial remodelling can be both beneficial and detrimental changes in MMP activity, either increases or decreases could affect cardiovascular function. Deoxycorticosterone acetate-salt hypertensive rats exhibit significantly increased MMP-2 expression and activity (Watts et al., 2007). However, there is a reduction in MMP-1 concentration and a rise in tissue-inhibitor of metalloproteinase-1 (TIMP-1), a blocker of MMPs, in hypertensive patients serum with left ventricular hypertrophy (Laviades et al., 1998).

Mature collagen and elastin contain crosslinks, which can be formed via enzymatic and non-enzymatic pathways. Lysyl oxidase deaminates the side chain of lysine and hydroxylysine residues, leaving highly reactive aldehyde groups that react with each other, or with unmodified lysines (van der Slot et al., 2005, van der Slot et al., 2004, Kagan and Sullivan, 1982). In the non-enzymatic pathway, oxidative reactions between glucose and collagen lead to the formation of so-called advanced glycation end-products (Snedeker and Gautieri, 2014). The crosslinks are essential to the structural integrity of collagen and elastin, however, excess crosslinking can increase their stiffness and reduce their sensitivity to degradation. The numbers of mature crosslinks is increased with hypertension (Hayashi and Naiki, 2009) and lysyl oxidase is upregulated in the vessels of hypertensive rats. Additionally, a study about heart failure in humans revealed that increased lysyl oxidase expression is associated with high collagen crosslinking and possibly collagen-mediated left ventricular stiffness (López et al., 2009).

1.2.1 Pharmacological treatment

The pharmacological treatment of primary hypertension is not very specific, given that so far its main cause remains unclear. Several different therapeutic approaches currently exist. The most commonly used agent is a diuretic (thiazide class), which inhibits renal sodium absorption in the early part of the distal tubule and consequently increases water excretion. This results in a decrease in total blood volume and so BP. Also used are inhibitors of beta-adrenergic receptors; 'beta-blockers'. These inhibit postsynaptic receptors of the noradrenaline system leading to decrease arterial blood pressure by reducing cardiac output (slow down the heart rate) and decrease the force at which blood is pumped round the body. Angiotensin-converting enzyme blockers can lower ANG II levels and aldosterone levels by inhibiting the activity of angiotensin converting enzyme. Angiotensin receptor inhibitors can cause vasodilatation and decrease peripheral resistance by blocking the ANG II receptor. Ca²⁺ channel blockers (dihydropyridine class) can induce vasodilation by inhibiting LTCC activity in vascular cells (Chobanian et al., 2003).

1.2.2 Non-pharmacological treatment

Non-pharmacological interventions have also played an important role in lowering BP. These interventions include low salt consumption, weight reducing diet, regular exercise and moderate alcohol consumption (Ohta et al., 2011). A decrease in salt intake lowers BP persistently. An earlier study (He and MacGregor, 2004) demonstrated that a reduction of 4.6 g in salt intake was associated with a 4.6 mmHg decrease in systolic BP. Losing weight has also been correlated with declines in the levels of BP. Despite following the same exercise recommendation, individuals who lost weight had a bigger reduction in BP than those who did not (Blumenthal et al., 2000). Besides weight loss, exercise itself has the potential to decrease the levels of BP. A study by Cornilisen and colleagues, 2013, showed that any physical activity was linked with a decline of between 1.8 mmHg and 10.9 mmHg in systolic BP, an effect reported in both hypertensive and non-hypertensive individuals (Cornelissen and Smart, 2013). A decline in the alcohol consumption could also lead to decreases in BP. A reduction of 67% in alcohol consumption is correlated with a mean drop of -3.31 mmHg (-2.52 to -4.1 mm Hg) and -2.04 mm Hg (-1.49 to -2.58 mm Hg) in systolic BP and diastolic BP respectively (Xin et al., 2001).

1.3 Piezo1 channels and their vascular roles

Biological mechanosensation forms the basis of many essential physiological functions, such as touch perception, proprioception, organ development, osmotic homeostasis, hearing and equilibrioception, as well as control of BP and arterial remodelling, as discussed earlier. However, very little is known about the mechanosensitive cellular components and their molecular identities.

Ion channels located in the membrane of cells can sense mechanical stimuli, the mechanical force can be transduced via the bilayer tension or the cytoskeleton. Numerous channels have been reported to respond to mechanical stimuli. Two of the best studied are the bacterial mechanosensitive MscS and MscL channels, which seem to be stimulated directly through bilayer tension (Kung et al., 2010). However, in metazoans (animals) homologues of these channels are not present. Other examples include the Shaker K⁺ channels and certain two-pore domain K⁺ channels, though the physiological role of these channels in mechanotransduction is not yet fully clear. Significant roles for members of the DEG/ENac and TRP channel families have been established in *Caenorhabditis elegans* and *Drosophila melanogaster*. However, the function of these channels as mechanotransducers in mammals is not clearly determined.

A significant breakthrough was made in 2010, with the identification of Piezo1 and its homologues, Piezo2 (Coste et al., 2010). Piezo1 was shown to underlie the currents elicited by mechanical activation of the Neuro2A mouse neuroblastoma cell line and Piezo2 was shown to contribute to mechanically activated currents in dorsal root ganglion neurons. Their heterologous expression induced two kinetically distinct mechanically activated currents.

Piezo proteins appear to correspond to an evolutionarily conserved family of ion channels, with homologues identified in species such as the slime mould *D. discoideum* and the rice plant *O. sativa* (Coste et al., 2010). While it remains to be determined whether the homologues form mechanosensitive ion channels in these species the *Drosophila melanogaster* Piezo (DmPiezo, also named CG8486) does mediate

mechanically-stimulated currents, although with distinct pore properties compared with the mammalian channels (Coste et al., 2012).

Characterisation of Piezo1 and Piezo2 as the primary mammalian mechanosensitive ion channels has resulted in a series of studies on their role in physiology and pathophysiology. Although, given the short time since their discovery the roles identified so far likely represent only a small fraction of those that will be found in the future.

Piezo2 has been shown to be required for touch sensing. It is expressed in Merkel cells of mammalian skins and forms the main sensor of mechanical forces in these cells. Furthermore, Piezo2 is expressed in outer hair cells, ECs in the brain, enterochromaffin cells of the gut. It also mediates mechanical transduction in dental primary afferent neurons, particularly in medium- to large-sized neurons that contain nociceptive neuropeptides such as CGRP. Piezo2 has also been shown to sense airway stretch and mediates lung inflation-induced apnoea (Won et al., 2017, Wu et al., 2017b, Wu et al., 2017a, Wang et al., 2017, Ikeda et al., 2014, Maksimovic et al., 2014, Ranade et al., 2014, Nonomura et al., 2017, Beurg and Fettiplace, 2017).

Heterozygous mutations in the PIEZO2 gene affects the function of skeletal muscle and are described to be causative for three phenotypically overlapping conditions termed distal arthrogryposis type 5 (E2727del and I802F), Gordon Syndrome and Marden–Walker Syndrome. These conditions are characterised by cleft palate and congenital contractures of the hands and feet. They are caused by altered amino acids in the highly conserved intracellular C-terminal domain of Piezo2 (Coste et al., 2013, McMillin et al., 2014). Piezo1 is a pore-forming subunit, as confirmed by functional reconstitution into artificial bilayers (Coste et al., 2012). It is permeable to Na^+ , K^+ , Ca^{2+} , and Mg^{2+} , with a slight preference for Ca^{2+} (Coste et al., 2010). The pressure sensitivity of Piezo1 is in the range of ~ -15 to -40 mmHg (Coste et al., 2010, Li et al., 2014).

In 2017, Guo and MacKinnon published a cryo-electron microscopy structure of the mouse Piezo1 channel, revealing that it forms a triskelion with arms consisting of repeated arrays of 4-TM (24 helices arranged as six repeated 4-TM) structural units surrounding a pore. Its shape deforms the membrane locally into a dome (Fig 1.8). It has

been suggested that these structures act as sensors of mechanical force exerted on the channel, thus contributing to mechanical gating of Piezo1 (Guo and MacKinnon, 2017).

Multiple gain- or loss- of function single nucleotide polymorphisms have been linked to human diseases, providing insight into the function of the channels. Piezo1 gain-of-function mutations in humans are associated with a hereditary red blood cell condition termed dehydrated hereditary stomatocytosis. For example R2456H and R2488Q mutations in Piezo1 alter mechanosensitive regulation, leading to increased cation transportation in erythroid cells, which shows a novel role in mechanotransduction in red blood cell biology and pathophysiology (Albuisson et al., 2013, Andolfo et al., 2013, Bae et al., 2013). Piezo1 loss of function mutations cause an autosomal recessive congenital lymphatic dysplasia (Lukacs et al., 2015).

Given the critical role of Piezo1 in mechanotransduction in both red blood cells and bladder urothelium (Miyamoto et al., 2012, Karaki et al., 1997, Zarychanski et al., 2012, Demolombe et al., 2013), it is perhaps not unsurprising that Piezo1 also plays a significant role in ECs. Piezo1 can be activated by shear stress, a frictional force experienced by ECs due to blood flow. This activation is required for the characteristic alignment of ECs with the direction of flow. This phenomenon is also important in vascular development. Global or endothelial-specific disruption of mouse Piezo1 profoundly disturbed the developing vasculature and the remodelling and was embryonic lethal within days of the heart beating. Haplo-insufficiency was not lethal but endothelial abnormalities were detected in mature vessels (Li et al., 2014, Ranade et al., 2014).

Piezo1 is also highly expressed in the myocytes of small diameter arteries. Smooth-muscle-specific deletion of Piezo1 in the mouse fully impairs stretch-activated ion channel activity. Piezo1 is dispensable for the myogenic tone of arterial vessels, but is involved in the remodelling of small arteries in hypertensive conditions ((Retailleau et al., 2015).

1.4 Yoda1

A screen of ~3.25 million compounds identified a synthetic small molecule that can both influence the activation of Piezo1 by mechanical stimuli and activate the channel in the absence of mechanical stimulation (Fig. 1.9) (Syeda et al., 2015). This molecule was named 'Yoda-1'. Yoda-1 was able to activate Piezo1 reconstituted into an artificial cell membrane that did not include any other cellular components, thus suggesting that Yoda-1 interacts with Piezo1 in a manner that does not require any cellular elements or additional signalling apparatus other than a cell membrane. The study also demonstrated the specificity of Yoda-1 for Piezo1 over Piezo2 (Syeda et al., 2015). Yoda1 was successfully used to replicate the effects of mechanical activation of Piezo1 in red blood cells, namely their dehydration (Cahalan et al., 2015), demonstrating that it is a useful tool compound for the investigation of Piezo1 expression and function *in vitro*.

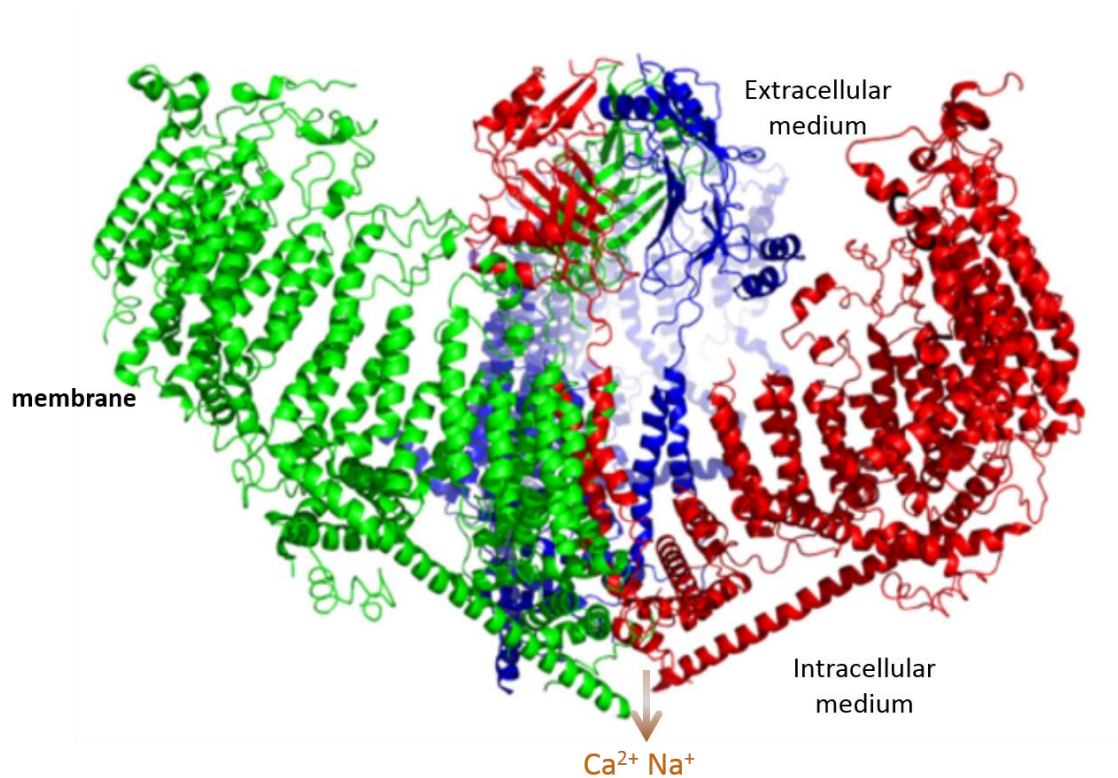


Figure 1-8: A representative Cryo-EM structure of Piezo1

Side view of Piezo1 shows fine features of the trimeric complex with the transmembrane region indicated (Guo and MacKinnon, 2017).

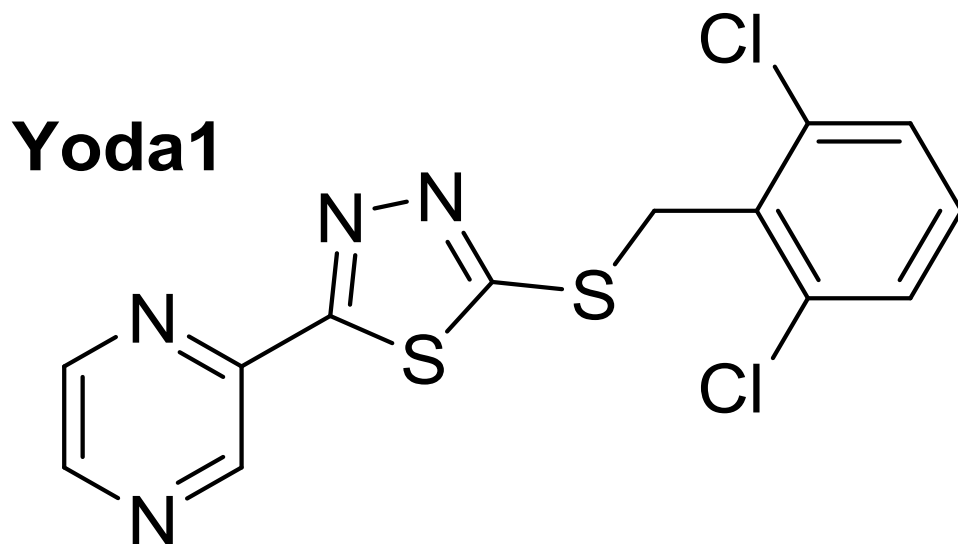


Figure 1-9: Chemical structure of Yoda1
Used as an agonist of Piezo1. (Syeda et al., 2015)

1.5 Aims and Objectives

Endothelial Piezo1 has been shown to be important for vascular development, however, the role of Piezo1 in the maintenance, function and remodelling of mature vessels remains to be determined. The main aims of this thesis relate, therefore, to investigating the relative contribution of Piezo1 channels in the regulation of vascular tone, excitability and contractility. To facilitate this, mice with conditional Cre-Lox-mediated disruption of Piezo1 in the endothelium (Piezo1^{ΔEC} mice) and the Piezo1 channel agonist Yoda1 were utilised.

The objectives of this thesis were:

To increase our understanding of physiological functions of Piezo1 channels in adult mice and to reveal the specific contribution of Piezo1 to vascular function.

To study the role, and underlying mechanisms, of Piezo1 in vasoconstriction and vasorelaxation in intact arteries.

To compare the contractile and vasodilatory responses in intact arteries of control and Piezo1^{ΔEC} mice.

To determine if Yoda1 has vasoactive effects on resistance or conduit arteries and to characterise any effects of Yoda1 in this context.

To identify whether Piezo1 can represent a novel therapeutic target for the treatment of arterial dysfunction.

Chapter 2 General Methods

2.1 Materials and Solutions

The experimental bath solutions, compounds and the solvents in which they were dissolved are shown in Tables 2.1, 2.2 and 2.3. Compounds were diluted in their respective solvent to 1000x the desired working concentration prior to addition to the bath solution. This minimised the solvent concentration that the vessels were exposed to during the experiments.

Yoda1, the recently discovered activator of Piezo1 (Syeda et al., 2015) becomes insoluble in aqueous solutions at concentrations greater than 10 μM , restricting its usage in experiments to this concentration.

Dooku1, a chemical analogue and competitive antagonist of Yoda1, was synthesised by Kevin Cuthbertson within the School of Chemistry at the University of Leeds (Evans et al., 2018). A scaffold (the scaffold is an approach to generate new chemical structures with similar biological activity to the original by changing components of the molecule) was used as starting material and a one-step reaction resulted in production of the compound (Fig. 2.1). Other analogues of Yoda1 were synthesised using three general synthetic approaches: 2e and 2g were synthesised using a one-step procedure (Scheme S1), compounds 7b using a four-step procedure (Scheme S2), and compound 11 using a separate four-step procedure (Scheme S3). All synthesised chemicals were purified by column chromatography and characterised by four methods: ^1H NMR (proton nuclear magnetic resonance), ^{13}C -NMR (carbon-13 nuclear magnetic resonance), IR (infrared spectroscopy) and high-resolution mass spectrometry. Chemical structures of other Yoda1 analogues are shown in Fig 2.2.

Solution	Chemicals	Concentration (mM)
Krebs	Sodium chloride (NaCl)	125
	Potassium chloride (KCl)	3.8
	Magnesium chloride (MgSO ₄ .7H ₂ O)	1.5
	Sodium bicarbonate (NaHCO ₃)	25
	Potassium dihydrogen phosphate (KH ₂ PO ₄)	1.2
	Ethylenediaminetetraacetic acid (C ₁₀ H ₁₆ N ₂ O ₈)	0.02
	Glucose (C ₆ H ₁₂ O ₆)	8
	Calcium chloride (CaCl ₂ .2H ₂ O)	1.2
High potassium Krebs	As with Krebs solution with the following changes	
	Reduced NaCl	68.8
	Increased KCl,	60

Table 2-1: Composition of solutions used in this study

Solutions were made as required. All chemicals listed were supplied by Sigma.

Drug/Compound	Supplier	Solvent for stock	Stock concentration	Storage	Bath concentration
Phenylephrine hydrochloride	Sigma	Distilled water	10 mM	-20°C	0.01-1 μ M
Acetylcholine chloride	Sigma	Distilled water	10 mM	-20°C	0.01-1 μ M
L-NAME (N-nitro-L-arginine methylester)	Sigma	Distilled water	100 mM	-20°C	100 μ M
Linsidomine (SIN-1)	Sigma	DMSO	20 mM	-20°C	0.1-10 μ M
Charybdotoxin	Sigma	Distilled water	10 mM	-20°C	100 nM
Apamin	Tocris	Distilled water	10 mM	-20°C	500 nM
Yoda1	Tocris	DMSO	10 mM	-20°C	0.1-10 μ M
Nifedibine	Sigma	DMSO	1 mM	R.T.	1 μ M
Gadolinium (Gd³⁺)	Sigma	Distilled water	10 mM	R.T.	10 μ M
Ruthenium (RR)	Sigma	Distilled water	30 mM	-20°C	30 μ M

Table 2-2: Drugs/compounds

Suppliers and solvents used to dissolve with stock concentration, storage and further dilution from stock (R.T.; room temperature).

Chemical	Source	Stock concentration	Working concentration	Additional information
Dooku1	—	10 mM in DMSO	10 μ M	30 minutes pre-incubation
7b	—	10 mM in DMSO	10 μ M	30 minutes pre-incubation
2g	—	10 mM in DMSO	10 μ M	30 minutes pre-incubation
11	—	10 mM in DMSO	10 μ M	30 minutes pre-incubation
2e	—	10 mM in DMSO	10 μ M	30 minutes pre-incubation

Table 2 3: Inhibitors applied to thoracic aortic segments.

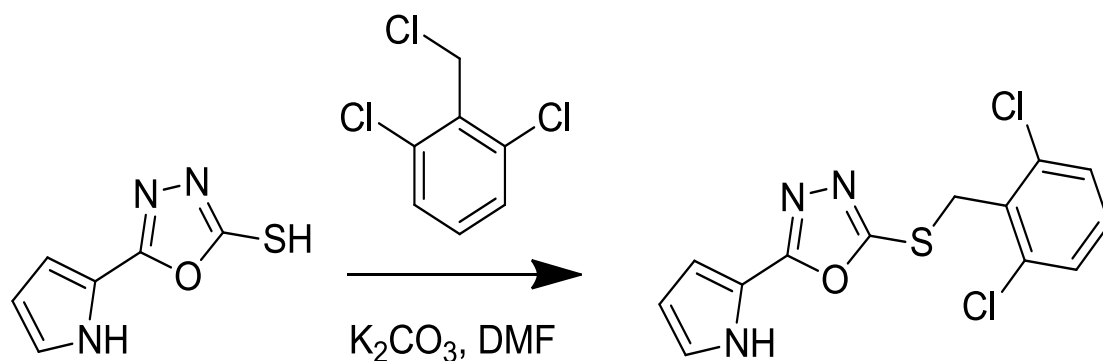


Figure 2-1: Synthesis and chemical structure of Dooku1

Synthesis pathway showing the starting scaffold (on the left-hand side), reagents used (middle arrow) and final compound structure (right-hand side). Product produced via an S_N2 (nucleophilic substitution) reaction. Dooku1 used as an antagonist of Yoda1.

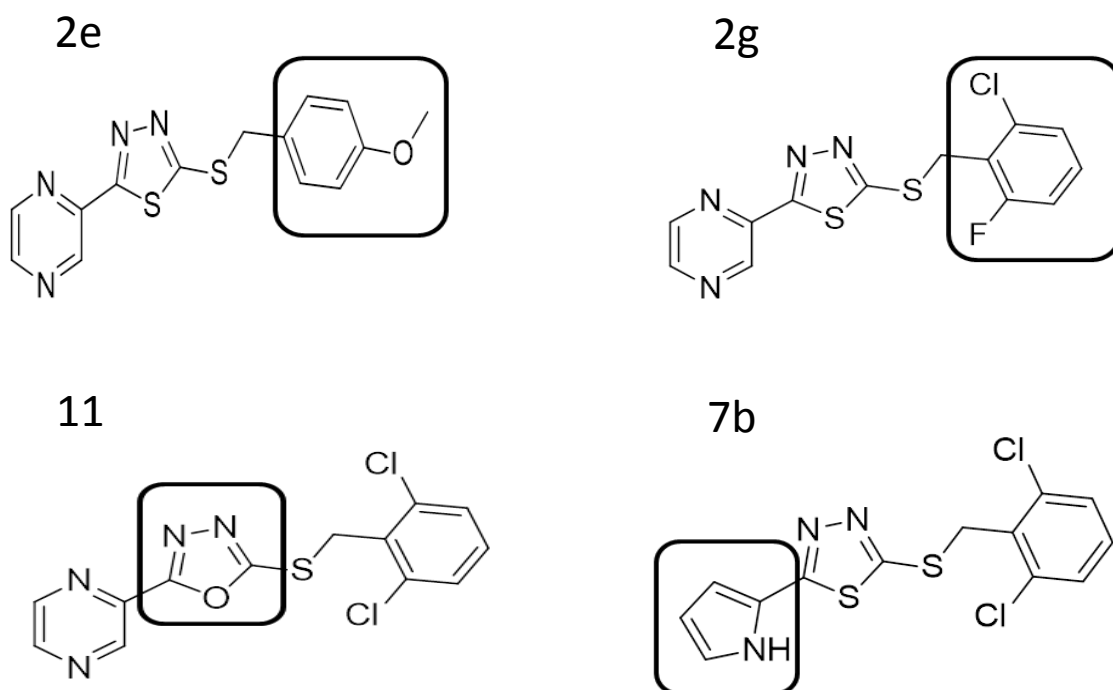


Figure 2-2: Chemical structures of 2e, 7b, 11 and 2g Yoda1 analogues

Structural variation to Yoda1 is highlighted by the box outline.

2.2 Mouse

Mouse models are progressively used in essential scientific research due to their advantages regarding small size, relative inexpensiveness and the capability to manipulate specific genes either via modification, addition or deletion.

2.2.1 Mouse housing conditions and diet

All work with mice was performed by Dr B Rode and Dr S Futers (University of Leeds) and approved by the University of Leeds Animal Welfare Ethics Research Board and by The Home Office, UK (Project Refs: 40/3557 and P606320FB)..

Mice were maintained in GM500 individually ventilated cages (Animal Care Systems), at 21°C, 50–70% humidity, light/dark cycle 12/12 hr, on RM1 diet (Special Diet Services, Witham, UK) *ad libitum* and Pure' o Cell bedding (Datesand, Manchester, UK). Mice were housed in a Home Office-licensed animal facility (University of Leeds) and humanely euthanised by cervical dislocation as specified by Schedule 1 of the Animal Scientific Procedures Act (1986). All procedures and the transgenic mouse production were authorised by both the University of Leeds Animal Ethics Committee and the UK Home Office.

2.2.2 Genetic disruption of the Piezo1 gene

To characterize the physiological function of Piezo1 in ECs an inducible, endothelial-specific Piezo1 knock-out mouse line was created (Rode et al., 2017). Mice with C57Bl/6J genetic background were used in this study.

2.2.2.1 Genetic disruption of the Piezo1 strategy

Firstly, flanking loxP sites were inserted between introns 17 and 18 and introns 21 and 22 of the Piezo1 gene (Piezo1^{flox}) (Li et al., 2014) (Fig 2.3). These C57BL/6 Piezo1^{flox} mice (heterozygous for the floxed allele) were then crossed with mice expressing Cre recombinase under the tamoxifen inducible vascular endothelial specific Cadherin5

promoter (Tg(Cdh5-cre/ERT2)1Rha) and subsequently inbred to yield C57BL/6 Piezo1^{flox/flox}/Cdh5-cre mice (homozygous for the floxed allele) (Fig. 2.4) (Rode et al., 2017). Cre recombination resulted in deletion of exons 18–21 encoding amino acids 770 to 2546. Loss of functional protein was confirmed by absence of Yoda1 response in isolated ECs (as shown in supplementary Figure 2 of the Rode et al. paper) (Rode et al., 2017).

Cre-ERT2 is a chimeric protein of Cre fused to the mutated ligand-binding domain of the human estrogen receptor (ERT2). The mutations render the receptor insensitive to physiological concentrations of its natural ligand, 17 β -estradiol, but sensitive to 4-hydroxytamoxifen (4-OHT), a metabolite of tamoxifen (TAM). Thus, the fusion with ERT2 allows temporal control of the activity of Cre. In the absence of TAM the Cre-ERT2 is retained in the cytoplasm, however, in the presence of TAM the chimeric protein is able to translocate into the nucleus, where it can initiate loxP-specific recombination events (Relaix and Zammit, 2012, Monvoisin et al., 2006).

2.2.2.2 Tamoxifen administration

TAM (Sigma-Aldrich) was dissolved in corn oil (Sigma-Aldrich) at 20 mg/mL. All TAM injections were performed by Dr B Rode and Dr S Futers (University of Leeds). Adult male mice (10 to 16 weeks) were injected intra-peritoneally with 75 mg/kg TAM for 5 consecutive days and analysed 10 to 14 days following the last TAM injection. Piezo1^{flox/flox}/Cdh5-cre mice that received TAM injections are referred to as Piezo1 Δ EC. Piezo1^{flox/flox} littermates (lacking Cdh5-cre) that received TAM injections were the controls (control genotype).

2.2.2.3 Genotyping

Ear notches were collected for genotyping at two weeks of age. All genotyping was outsourced to Transnetyx Company (Cordova, TN, USA). They isolated genomic DNA from ear notches taken from mice at two weeks of age and performed real-time PCR analysis with specific probes designed for each gene of interest. This service probed the sample for the presence of a floxed gene, the wild-type Piezo1 gene and the Cre gene under the control of the Cadherin5 promoter. Primers in table 2.3 were used in our

laboratory by Dr B Rode to confirm the genotype and probe for Piezo1 deletion. Piezo1^{fllox} primers probed for the presence or absence of LoxP sites. Piezo1^D primers probed for deletion of exons 18-21. The product appears only if deletion happened. 18S and Piezo1 probes (the last 2 lines of the table) are for qRT-PCR which is used to analyse mRNA expression. In the Piezo1^{fllox}, the PCR primers targeted the endogenous Piezo1 sequence either side of the 3' terminal loxP site (expected products: 155 bp without the loxP site; 189 bp with the loxP site). In Piezo1^D, The forward primer was 5' of the 5' FRT site and the reverse primer was 3' of the 3' loxP site.

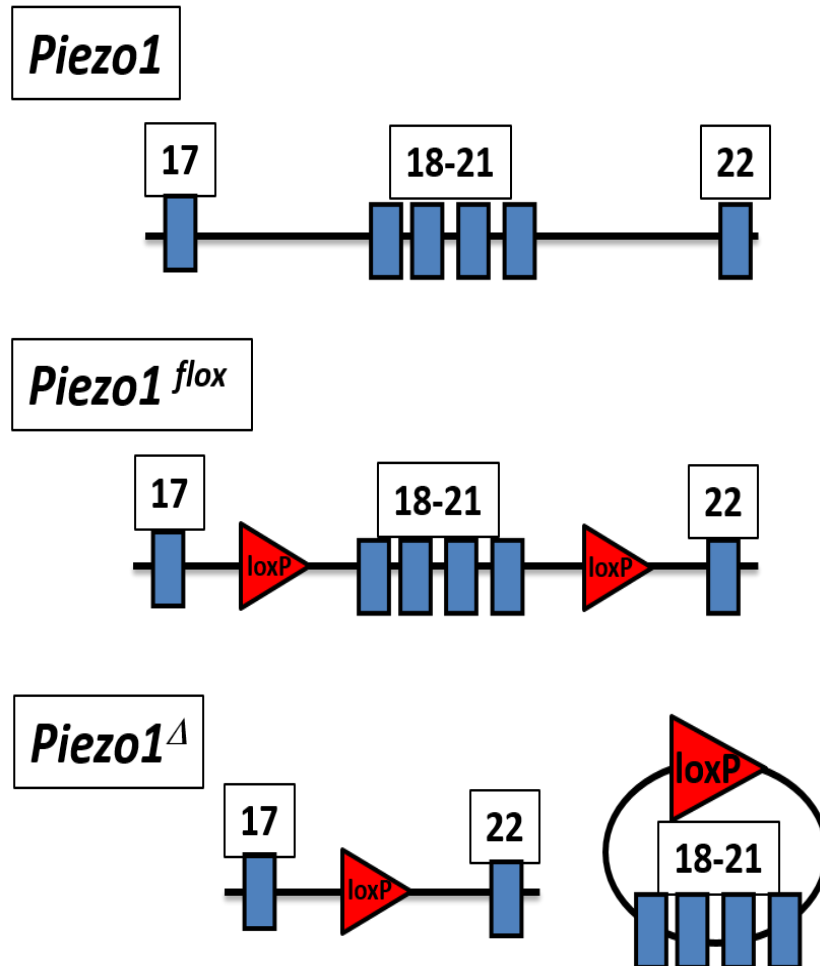


Figure 2-3: Diagram showing insertion of loxP sequences into the mouse *Piezo1* gene in the introns between exons 17 and 18 and 21 and 22

Cre recombination around these two loxP sites results in deletion of exons 18 to 21 from the gene.

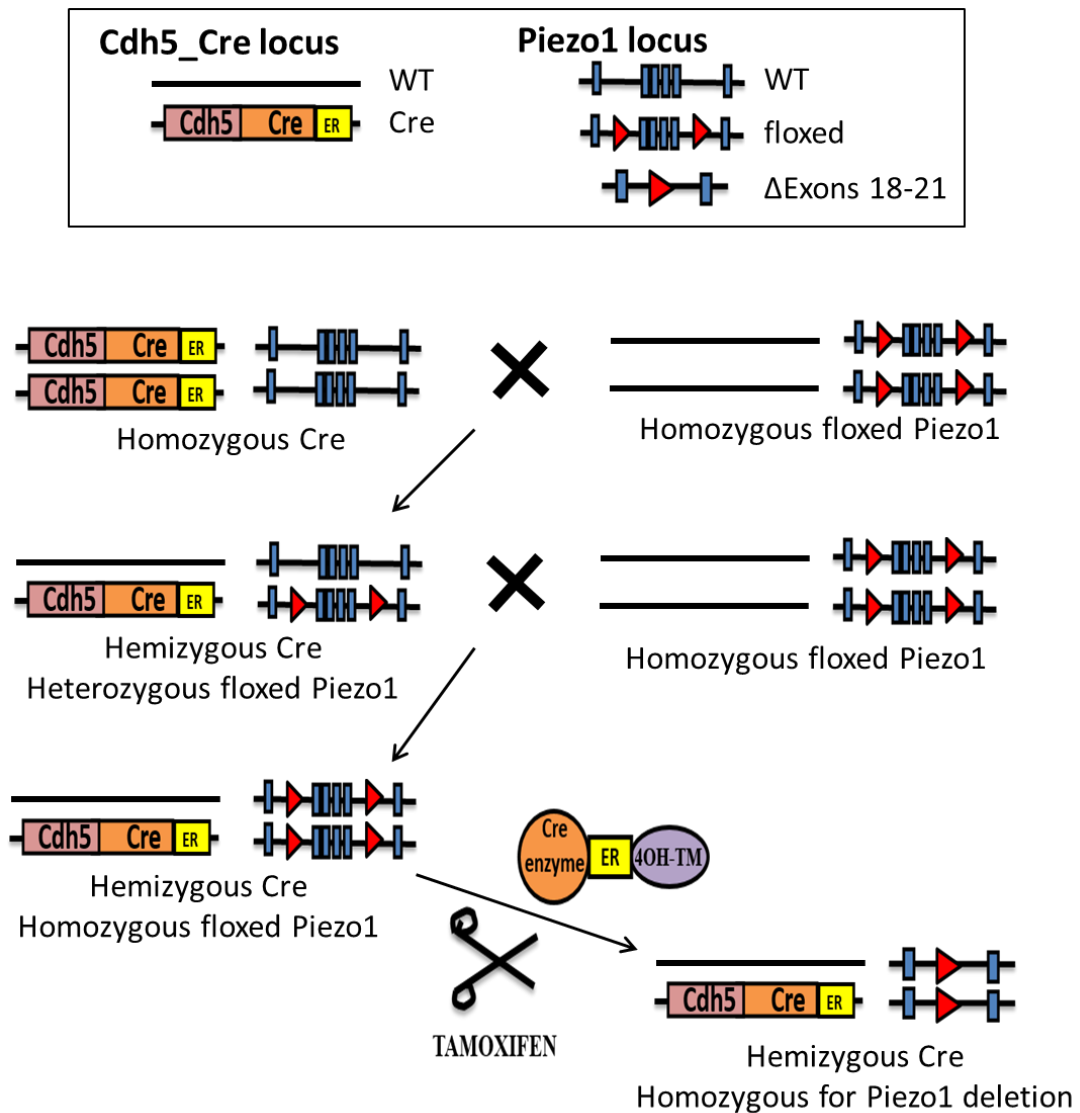


Figure 2-4: Endothelial-specific Piezo1 modification

Transgenic mice containing loxP sites flanking exons 18-21 of the Piezo1 gene (floxed) were crossed with transgenic mice expressing the bacterial Cre enzyme fused to a mutant transgenic mice ligand-binding domain of the human oestrogen receptor (ER) under the control of the endothelial specific *Cdh5* promoter. Resulting offspring that were hemizygous for *Cdh5CreER* and heterozygous for the floxed Piezo1 gene were further crossed with homozygous floxed Piezo1 mice yielding the desired homozygous floxed Piezo1 mice that were hemizygous for *Cdh5CreER*. The Piezo1 gene in ECs of these mice, when exposed to tamoxifen, undergoes Cre-dependent recombination.

Gene	Analysis	Forward primer sequence (5'-3')	Reverse primer sequence (5'-3')	Product size (base pairs)
Cdh5-cre	Genomic DNA	GCATTACCGGTCGATGC AA	AGTGAACGAACCTGGTC GA	408
Piezo1^{fllox}	Genomic DNA	GGAGGGTTGCTTGTTGG ATA	ACTCATCTGGGTGAGGT TGC	155, 189
Piezo1^D (Deletion)	Genomic DNA	ACCACCTGAGAAGTTGT CCC	ACTCATCTGGGTGAGGT TGC	379
18s	cDNA	GATGCTCTTAGCTGAGT GT	GCTCTGGTCCGTCTTG	233
Piezo1	cDNA	CACAAAGTACCGGGCG	AAAGTAAATGCACTTGA CG	370

Table 2-3: PCR primer sequences.

2.2.3 Patch-clamp electrophysiology

Membrane potential was measured using the perforated whole-cell configuration of the patch-clamp technique in current clamp mode with an Axopatch-200A amplifier (Axon Instruments, Inc.) equipped with Digidata 1440 A and pCLAMP 10.6 software (Molecular Devices, Sunnyvale, CA, USA) at room temperature. Outside-out membrane patch recordings were made using the same equipment but in voltage-clamp mode. ECs and endothelium were bathed in a solution consisting of 135 mM NaCl, 4 mM KCl, 2 mM CaCl₂, 1 mM MgCl₂, 10 mM glucose and 10 mM HEPES (pH 7.4). Heat-polished patch pipettes with tip resistances between 3 and 5 MΩ were used. For membrane potential recordings, amphotericin B (Sigma-Aldrich) was used as the perforating agent, added in the pipette solution composed of 145 mM KCl, 1 mM MgCl₂, 0.5 mM EGTA and 10 mM HEPES (pH 7.2). For application of fluid flow, endothelium or membrane patches were manoeuvred to the exit of a capillary tube with tip diameter of 350 μm, out of which ionic (bath) solution flowed at rates specified in the main text and figure legends. Calculation of shear stress (τ_w) was achieved using the Hagen-Poiseuille formula ($\tau_w = 4\mu Q/\pi R^3$) where μ is dynamic viscosity, Q is flow rate and R is radius of the capillary tube.

2.2.4 Monitoring mouse activity / Running wheel analysis

All mice were individually housed with free access to a running wheel. Detailed characteristics of running activity were recorded for each animal using custom-built hardware and software. A mouse was categorised as active when there were ≥ 2 revolutions of the running wheel in each 1 min recording period. This equates to $\approx 10\%$ of the mean dark cycle velocity of running for control animals (0.34 m/s). Continuous activity periods (bouts) were determined as activity showed in 2 or more consecutive minutes. One Piezo1^{ΔEC} mouse exhibiting complete inactivity for the first 3 days was excluded from the analysis along with its control genotype pair.

2.2.5 Tissue staining

Epididymal fat pad and liver tissues were fixed for 48 h in 4% PFA at 4 °C prior to processing on a Leica ASP 200 and embedding in CellWax (Cellpath) on a Leica EG1150H embedding station. Sections of 4 μm were cut on a Leica RM2235 microtome onto Plus Frost slides (Solmedia) and allowed to dry at 37 °C overnight prior to staining.

Slides were de-waxed in xylene and rehydrated in ethanol. H&E was performed by staining in Mayer's Haematoxylin for 2 min and eosin for 2 min. Slides were imaged on an Aperio AT2 (Leica Biosystems) high definition digital pathology slide scanner with a maximal magnification of $\times 20$. Tissue processing and imaging were performed at the Section of Pathology and Tumour Biology, Leeds Institute of Cancer and Pathology.

2.2.6 Echocardiography

Animals were maintained under steady-state isoflurane anaesthesia and placed on a heated platform with ECG and respiration monitoring. Core temperature was measured using a rectal probe (Indus Instruments) and maintained at 37.5 °C throughout recording. Echocardiography was performed using a Vevo2100 high resolution, pre-clinical in vivo ultrasound system (VisualSonics) with the MS-550D transducer at 40 MHz frequency and 100% power. Imaging was performed on a layer of aquasonic gel after the pre-cordial skin had been clipped and de-epilated with cream (Veet). Parasternal long-axis view (PLAX) images were obtained in EKV mode (set at 1000 Hz for recording) over the entire cardiac cycle. The left ventricular area was traced in end-diastole (LVAd) and end-systole (LVAs) and used to derive the ejection fraction (EF) with the Vevo LAB cardiac package software. The investigator performing sonography was blinded to the genotype of the animals. Transverse EKV recordings were also obtained over the abdominal aorta just below the diaphragm using the same settings as described for the heart. These images were evaluated in the VevoVasc software package to determine vessel distensibility. Maximal anteroposterior aortic diameter (from inner wall to inner wall) was measured in the same images in systole and diastole using Vevo LAB general imaging package software.

2.3 Dissection of blood vessels

Animals were killed by CO₂ asphyxiation followed by cervical dislocation. The blood vessels were isolated and rapidly transferred to cold Krebs solution to avoid contact with air. All the dissection was performed by the experimenter (N. Endesh). They were then carefully pinned onto a dissecting dish, coated with a layer of silicone plastic (Sylgard), and placed under a light microscope. During the dissection, surrounding tissue/fat was carefully removed by hand dissection without damaging the blood vessels or stretching the artery. Extreme care was taken to avoid direct contact with the artery by pulling gently

with forceps and cutting through the membrane of the connective tissue because the endothelium is easy to damage by excessive mechanical stretch during the process of isolation, mounting wire, or cannulation. Arteries were stored for a maximum of 30 minutes at 4°C in physiological salt solution, pH 7.4 prior to experiments.

2.3.1 Thoracic aorta

The descending thoracic aorta, which extends from the aortic arch to the diaphragm (Fig 2.5), was accessed by removing the heart and lungs then excised into a Petri dish containing ice-cold oxygenated Krebs solution. It was cleaned off from the surrounding tissue and cut into 1 mm transverse segments. These segments were handled carefully to avoid unintentional damage to the surface of the intima.

2.3.2 Mesenteric artery

The mesenteric arcade (loops of small intestine) was removed after incision of the abdominal cavity to expose and open the overlying peritoneum. Then the mesentery was pinned out on a Petri dish in ice-cold oxygenated Krebs solution as shown in Fig 2.6. The first order arteries were located under a dissection microscope and classified as those branching straight from the superior mesenteric artery. The second-order mesenteric vessels (those that branch from the first order vessels) were carefully dissected from surrounding fat using small scissors and fine forceps (World Precision Instruments, Hertfordshire, England). Second order mesenteric artery was chosen as they are the smallest order branch of the aorta that it was practicable to handle for the experiments. An artery with a small lumen was desirable as they are the most important contributor to the control of vascular tone. Arteries were distinguished from veins due to their thicker muscular walls and an acute angle at the branching site. Arteries were cut into 1 mm segments.

2.3.3 Saphenous artery

The saphenous artery was distinguished as extending distally from the femoral vessels branching towards the knee (Fig 2.7). Arteries were carefully cleaned of all connective

and adipose tissue then the middle part of the saphenous artery was cut into two equal parts (1 mm segments).

2.3.4 Carotid artery

The common carotid artery is a large elastic artery. One carotid artery is positioned on each side of the neck. The right common carotid artery branches from the brachiocephalic artery and extends up the right side of the neck while the left common carotid artery branches from the aorta. These arteries present the main blood supply to the head, neck, and brain.

Beneath a dissecting microscope, the chest was opened to reveal the right and left carotid arteries using dissecting small scissors and fine forceps (Fig 2.8). Both the left and right arteries were used for experimentation. Carefully they were cleaned of fat and surrounding tissue until the full length of both carotids from the aorta to the common carotid bifurcation could be seen (indicated by red lines in Fig 2.8). Once excised the arteries were kept in ice-cold oxygenated Krebs solution. For experimentation the arteries were cut into 1 mm segments.

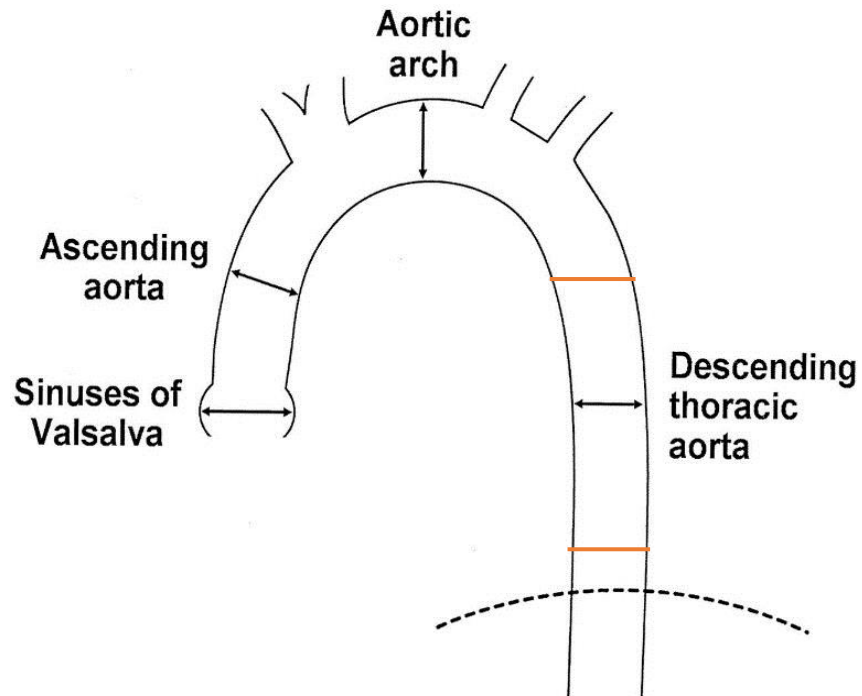


Figure 2-5: Diagram of the aorta dissection

Orange lines indicate the locations at which incisions were made to excise the descending thoracic aorta (Agmon et al., 2003).

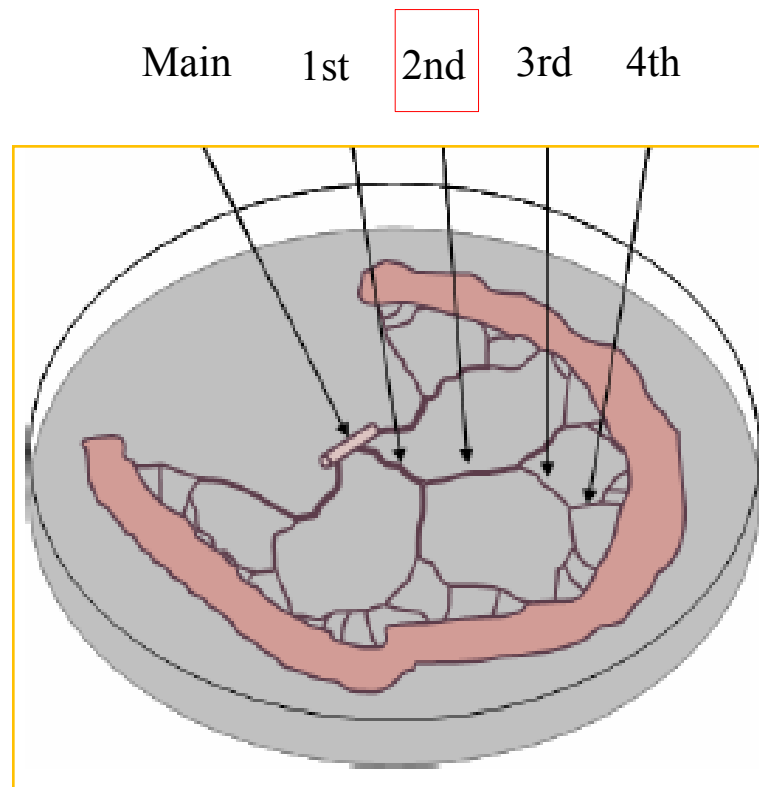


Figure 2-6: Schematic diagram of the organisation of the mesenteric vascular bed

Branching from the main mesenteric artery towards the gut wall are 1st, 2nd, 3rd and 4th order mesenteric arteries sequentially. Second order arteries were excised for use in wire myography experiments. Adapted from DMT website www.dmt.dk.

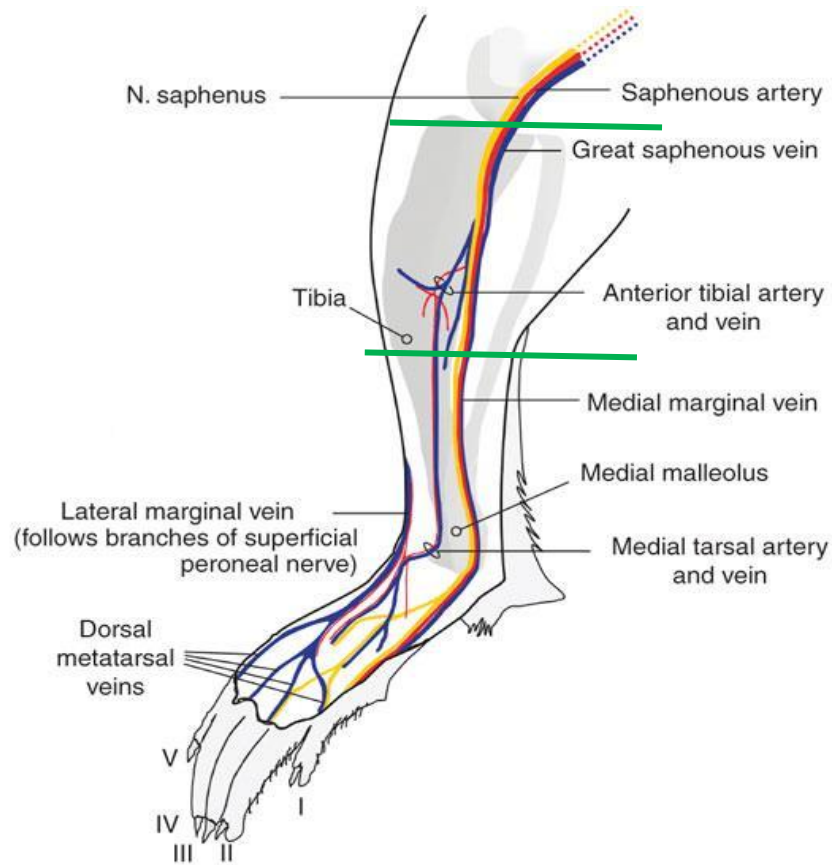


Figure 2-7: Location of the saphenous artery in the rodent hind limb

Green lines indicate the locations at which incisions were made to excise the saphenous artery (Zimmermann et al., 2009).

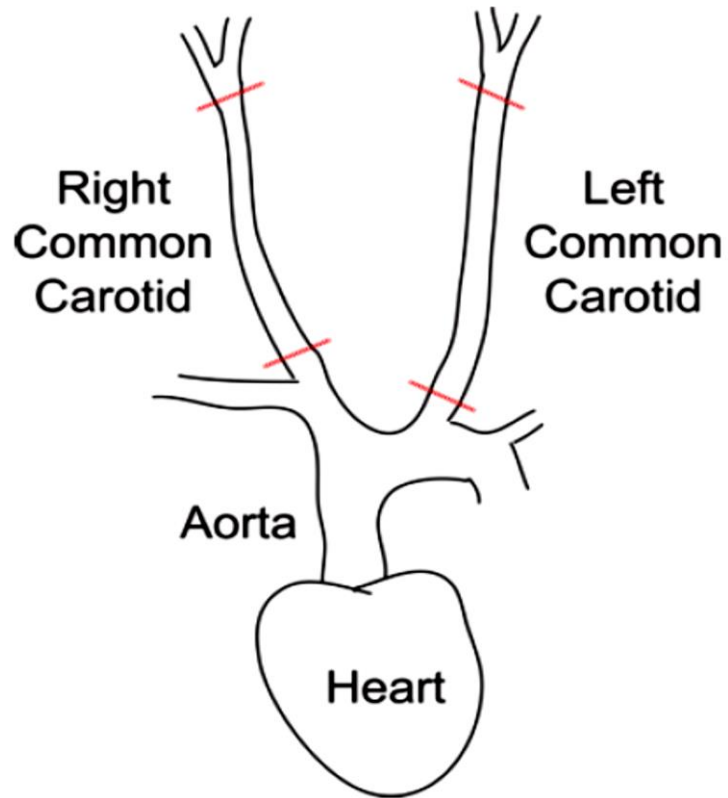


Figure 2-8: Diagram depicting the location of the left and right common carotid arteries in relation to the heart and aorta

The red lines indicate the incision points when dissecting out these vessels. (Monvoisin et al., 2006).

2.4 Vascular myography

Vascular myography is a technique regularly used to evaluate vasomotor responses of isolated blood vessels to vasoactive agents in the context of a controlled environment; for example in the absence of multiple vasoactive influences experienced in vivo such as mechanical forces or neural input. This method allows clear dissection of the vasomotor pathways and the mechanisms by which pharmacological agents manipulate the signalling systems of interest. Furthermore, it affords the possibility to perform experiments where the endothelium has been removed from the lining of the vessel lumen, and thus the ability to identify between responses originating from the endothelium versus those mediated via the smooth muscle cell (endothelium-independent).

2.4.1 Wire Myography

Wire myography was first introduced by Mulvany & Halpern in 1976. The wire myograph is a kind of organ bath that is made of a horizontal stainless steel chamber comprising two opposing stainless steel 'jaws' (Fig 2.9). Each jaw has a pair of teeth between which the arterial segments are placed with the support of two pieces of wire. The jaw on the right side is joined to a micrometer for adjusting the distance between the two jaws. The jaw on the left is joined to a force transducer through a steel rod which passes through a hole in the side of the chamber, enabling the experimenter to assess alterations in isometric tension as the vascular segments dilate or constrict. The hole that the rod passes through is sealed with vacuum grease (Danish Myotechnology, Aarhus, Denmark). In this study, the contractility of four different vessels (mouse thoracic aorta, mesenteric arteries, saphenous and carotid arteries) was studied with the DMT wire myograph (DMT 620 myograph system, Aarhus, Denmark) (Fig 2.9). The chambers were connected to a vacuum pump, enabling wash out and so exchange of the bath solution. A gas inflow ensures the preparations in all four chambers are maintained under physiological conditions (37°C, and bubbled with a gas mixture of 95% O₂:5% CO₂ - this gas mixture was preferred to provide a more physiological oxygen tension than obtained when applying oxygen only). Myographs were washed daily and calibrated on a bi-monthly basis as per the manufacturers' guidelines.

2.4.1.1 Vessel mounting

Following dissection of the vessel, but prior to beginning the mounting procedure, the myograph chamber(s) were filled with 5 ml Krebs solution at room temperature; chamber and solutions were continuously gassed with 95% O₂/5% CO₂ mixture and, to minimize vessel variability, for control and Piezo1 deletion arteries, two branches of the same artery were used in parallel. Pieces of 40 µm stainless steel wires were used for aorta and carotid arteries and 15 µm tungsten wires for mesenteric and saphenous arteries that fit the lumina of small arteries. Segments were freshly cut ready to be used for mounting the vessel. The first wire was secured under a mounting screw with the unsecured end clamped in position by the myograph jaws. Artery segments of approximately 1 mm in length were carefully positioned at the end of the wire and, with great care to prevent any damage to the lumen wall, the artery was pulled over the wire and into the gap between the myograph jaws (Fig 2.10a and b). The remaining free end of the wire was secured under the second screw as shown in Fig 2.10c. Once the first wire was secured the jaws were opened and a second piece of wire was passed through the artery (Fig 2.10d). Once the second wire had been passed through the artery ring such that the artery sat roughly in the middle of it, the jaws were re-closed in order to clamp onto the second wire and render it immobile. Then the two ends of the second wire were secured under the two screws of the second jaw (Fig 2.10e). The first end was secured with the jaw closed; tightening the screw over the wire such that the wire was pulled tight as the screw was tightened. The jaws were then re-opened just enough to loosen the hold over the second wire, and as with the first wire, the free end was held tightly with forceps and pulled taut to take up all slack as it was passed under the remaining screw and as the screw was tightened. Initially the jaws were set slightly apart to prevent the two wires from touching, but not enough to begin stretching the arterial ring. The mount was assessed to ensure the wires were tight, parallel and that the artery sat in the middle of the jaws free of tension or obstruction. All of the above procedures were carried out using a microscope (Nikon). Warm and oxygenated Krebs solution was provided to maintain the physiological properties of the vessels.

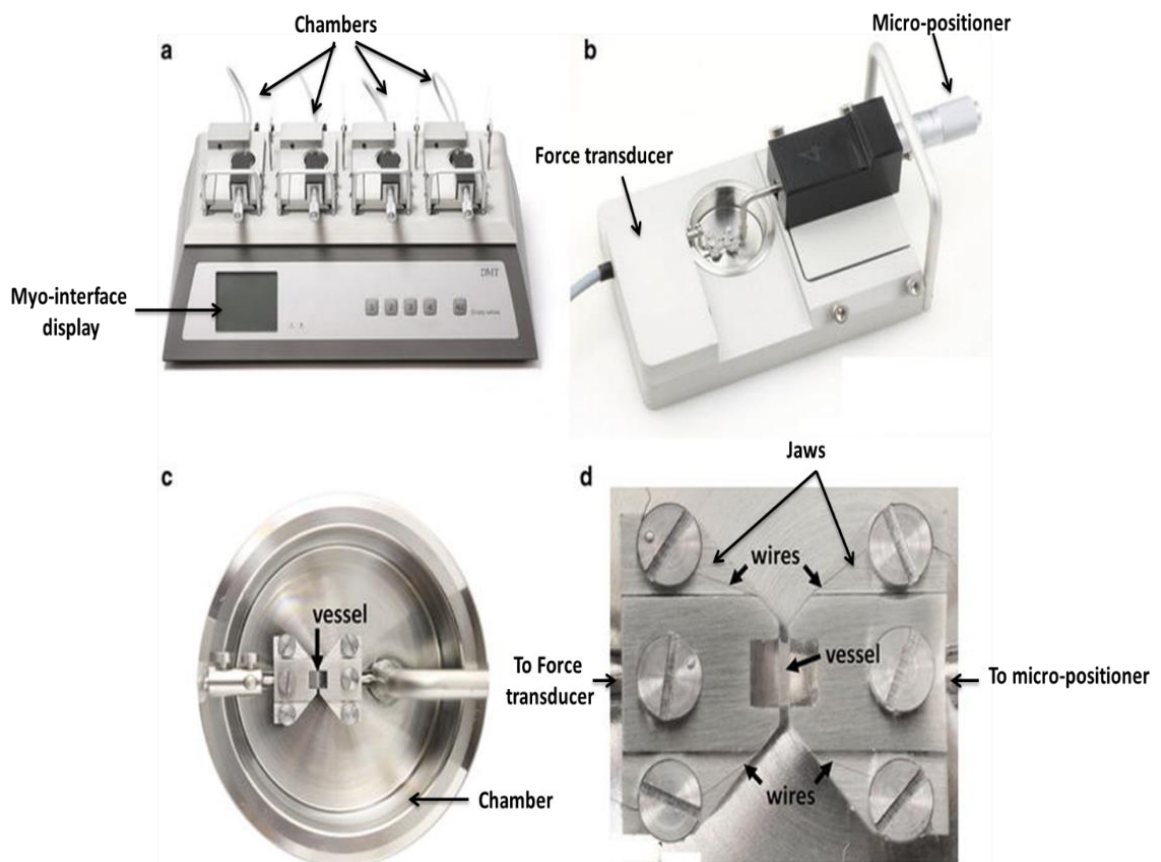


Figure 2-9: The wire myograph

(a) DMT multi-chamber 620M Wire Myograph where the wire myograph interface contains four myograph units. (b) Each myograph unit holds a force transducer (left) and a micrometre (right), and both of them attached to corresponding jaws to maintain the vessel within the chamber. (c) The chamber with the jaws and a mounted vessel segment. Both the upper and lower jaws are attached to the micrometre screw and to the force transducer, respectively. (d) The jaws, wires, screws and a mounted vessel segment. Adapted from DMT website www.dmt.dk.

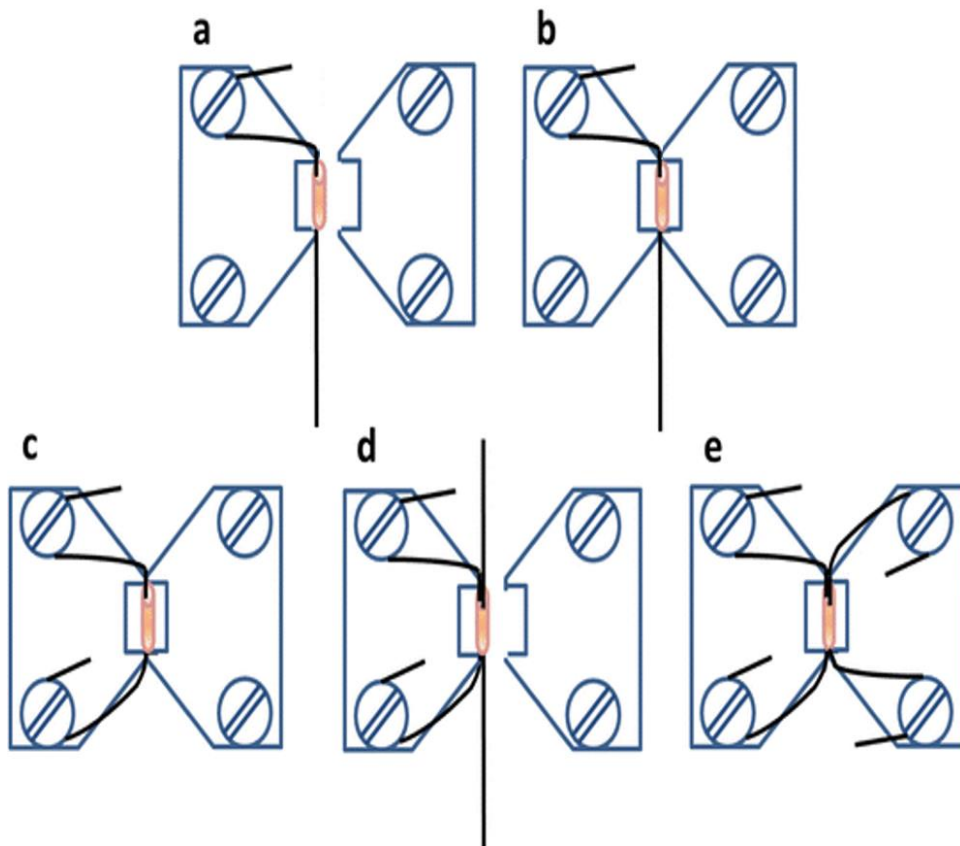


Figure 2-10: The mounting procedure

(a and b) artery segments of 1 mm length were carefully positioned at the end of the wire with great care to avoid any damage to the lumen wall, the artery was pulled over the wire and into the gap between the myograph jaws. (c) The wire was wrapped clockwise around the screws of the jaw and clamped by closing the screws. (d) The jaws were separated and carefully insert another 2-cm-long wire through the lumen of the artery minimising contact with the wall and the second wire was clamped by moving jaws together again. (e) The second wire was wrapped clockwise and clamped to the screws of the second jaw and the wires were moved away so that they were as close to each other as possible without touching. Adapted from DMT website www.dmt.dk.

2.4.1.2 Normalization of the vessels

Artery drug sensitivity and active force are both at their maximum when the artery internal circumference is 90% of that *in vivo* (Moyes et al., 2016). Thus, the normalisation process aims to standardise the tension of the mounted arteries by stretching their internal diameter to 90% of that the vessel would have if relaxed and under a transmural pressure of 100 mmHg/13.3 kPa. After mounting, the artery segments were stabilised in Krebs solution with continuous bubbling with a gas mixture of 95% O₂ and 5% CO₂. During this time, the chambers were heated and twenty minutes after reaching 37°C the normalisation protocol was started. The first step involved determining the length of the vessel segments (in mm) by using an eyepiece reticule. This was the position at which the artery had the smallest diameter, i.e. it had not yet developed any tension, the 'zero' position. It was obtained by adjusting the jaws slowly until the wires touched without pushing against each other. Then, the tension in the arteries was increased in a stepwise manner using the micrometre screw to increase the distance between the two myograph jaws, leaving enough time after every stretch for the artery to reach a steady state tension (5 minutes at least). The wall force and micrometre reading were recorded at each step. The level of stretch was re-adjusted by small increments to the diameter at which the segments contractile response to 60 mM KCl and 0.3 μM PE were maximal. By this the internal diameter was then set to 90% of that value.

2.4.1.3 Wire Myography Protocols

During the functional measurements, the distance between the two wires was kept constant, with changes in vessel contractility being measured through the force transducer (Fig 2.9).

Following the normalisation procedure, arteries were equilibrated under tension for 30 minutes. After this period had elapsed the arteries were initially contracted twice with 60 mM high K⁺, which causes membrane depolarisation and consequently calcium influx through voltage-operated calcium channels (Karaki et al., 1997). This allowed the maximal contraction of the artery to be determined and confirmed that the contractile ability in the arterial smooth muscle was intact. Each high potassium stimulus was maintained for 10 minutes, after which new Krebs solution was added to the bath and the vessels allowed to relax. Any artery segments that were unresponsive to high

potassium were rejected, unresponsiveness being indicative of compromised vascular smooth muscle integrity (Fig 2.11).

Arterial SMCs contain α 1-adrenergic receptors that, when activated, lead to release of calcium from intracellular stores and consequently contraction (Hall et al., 2006). The resting or baseline tension set at the beginning of the protocol is passive and theoretically does not contain any active vessel tone. Therefore, in order to observe vasodilatory responses, vessels must first be pre-contracted to generate a state of active tone from which the vessels can relax. Within this study, PE, an α 1 receptor agonist, was used as a vasoconstrictor for this purpose; arteries were treated with 0.3 μ M final concentrations PE to obtain 60-80% of the maximal reference contraction to high K^+ prior to application of known/potential vasodilators (Fig 2.11).

Activation of ACh receptors present on ECs leads to NO production and consequently vaso-relaxation (Chadha et al., 2011). Therefore, pre-contracted arteries were stimulated with ACh to test for the presence and the functional integrity of the endothelium (Fig 2.11).

Cumulative concentration-response curves of PE (0.01–1 microMolar final concentrations in distilled water) (μ M) (Sigma-Aldrich) were then constructed and the PE concentration that produced 80% of the maximal response (EC_{80}) was determined (0.3 μ M). This concentration was then used to constrict the arteries, followed by ACh concentration-response curves (0.01–1 μ M final concentrations in distilled water; Sigma-Aldrich). (The endothelium was considered intact if ACh caused more than 60% relaxation of arteries pre-constricted with PE). Cumulative dose-response curves were achieved for PE, ACh and Yoda1 by adding concentrations of agonist to the bath in half-log molar increments. This was used to evaluate the response to an agonist as a maximal response can be obtained from these data. It was also possible to calculate the EC_{50} , which indicates the tissue sensitivity to the agonist, from these data.

L-NAME is a competitive inhibitor of NOS, an enzyme involved in the formation of NO. It was used to determine the contribution of NO to endothelium-dependent vasodilatation by incubating artery segments with 100 μ M L-NAME (final concentration) for 20 minutes

prior to contracting the arteries with PE and applying the test vasodilator, this concentration is commonly found in similar studies in published literature (Leo et al., 2014, Cooke and Davidge, 2003) or a combination of apamin (0.5 μM ; final concentration in distilled water) and charybdotoxin (0.1 μM ; final concentration in distilled water) inhibitors of $\text{IK}_{\text{Ca}^{2+}}$ and $\text{SK}_{\text{Ca}^{2+}}$; (Tocris) these concentrations have previously been shown to inhibit $\text{IK}_{\text{Ca}^{2+}}$ and $\text{SK}_{\text{Ca}^{2+}}$ in rat mesenteric arteries (Stankevičius et al., 2006, O'Sullivan et al., 2004).

To investigate the contribution of Piezo1 to Yoda1-induced relaxation, 10 μM Gd^{3+} or 30 μM RR, inhibitors of mechanosensitive channels was applied 20 minutes prior to the pre-constriction with PE. 10 μM Dooku1, a competitive antagonist of Yoda1, and other Yoda1 analogues also were applied 30 minutes before the pre-constriction with PE

Artery baths were washed at least three times with fresh, warm, and oxygenated Krebs solution between the different functional experiments.

In some experiments, the endothelium was removed by gently rubbing the intimal surface with a wire. Care was taken not to over-stretch the segments during rubbing in order to avoid damaging their muscular layer. Endothelial denudation was considered successful if the endothelium-dependent vasodilator, ACh (1 μM), failed to produce relaxation.

The relaxation response of SIN-1 (Sigma-Aldrich), an NO donor (0.01-1 μM in 100% DMSO), and after pre-constriction with 0.3 μM PE, was carried out to test the function of the VSMCs.

2.4.1.4 Data analysis

The experimenter was blind to the genotype of the animals. The individual measurements from each chamber were combined to calculate the mean and standard error of the mean (SEM) for each data set, where n indicates the number of mice. Results were expressed either in milliNewton tension (mN), which is the value of the myograph

response after the baseline tension subtraction, or as a percentage of a control response; high K⁺ or PE pre-constriction.

In order to normalise for the difference in PE contraction, tension changes to ACh and Yoda1 are expressed as a percentage of the maximal vasoconstriction induced by PE in mN, rather than as a percentage of its own maximum relaxation in mN. This is more informative than just expressing the points on the curve as a percentage of the maximal ACh induced relaxation in mN, (all values subscribed by the smallest number that started with then divided by the biggest number and then multiplied by 100) Tension changes to PE are expressed as a percentage of the maximal constriction to 60 mM K⁺. Data were generated in pairs (control mice and Piezo1^{ΔEC} mice) and data sets compared statistically by paired or unpaired *t*-test. It was paired where both data sets were collected from the same mouse. The data were also analysed using paired or unpaired Student *t*-tests of area under the curve (AUC) to detect overall alterations in concentration response curves. The AUC was defined as the area between the mean response value and the baseline value of 0% relaxation (100% of contractile tone). Concentration–response curves were fitted by sigmoid curves with the Hill equation using Origin Pro software. The minimum level of statistical significance considered in the study was probability (*p*) <0.05 (*<0.05, **<0.01, ***<0.001). Where data comparisons lack an asterisk, they were not significantly different. The number of independent experiments of mice is indicated by *n* (one mouse each experiment). Origin Pro software was used for data analysis and presentation.

2.4.2 Pressure Myography

Pressure myography enables the study of artery responses under isobaric conditions, which may be more physiological than the wire myograph. This method was first developed in 1967 to study arterioles as small as 50 μm in diameter, superfused and pressurised by a single cannula (Uchida et al., 1967). Subsequently the technique was optimised to study microvessels up to 12 μm (Duling et al., 1981). Additional improvements have involved constant vessel imaging and using a second cannula to enable the changing of the luminal solution independently of the abluminal solution (Vanbavel et al., 1990). The importance of longitudinal stretching was emphasised to provide optimal experimental conditions for pharmacological studies (Coats and Hillier, 1999).

2.4.2.1 Pressure myograph vessel mounting

The mesenteric bed was dissected out of the abdomen and placed in a dissection dish that contained Krebs solution at 4°C. Second order mesenteric arteries were carefully dissected out of the bed and the surrounding adipose tissue removed under a dissection microscope (Nikon) using fine forceps and scissors, always ensuring that the vessels were not stretched or damaged. The length of the vessels was usually between 3 and 4 mm. The tissue was kept in Krebs solution at 4°C until vessels were set up in the pressure myograph chamber (MODEL 110p, Danish Myo Technology) (Fig. 2.12). Prior to vessel mounting the pressure lines were filled with 37°C temperature Krebs solution to ensure there were no air bubbles in the tubing. Under a dissection microscope, a small artery segment was transferred into a single vessel chamber containing 10 ml Krebs solution. The vessel was then manoeuvred over the tip of the inflow glass cannula using fine forceps and tied on securely with single strands of fine nylon suture. A flow was applied briefly to the vessel to clear the lumen of any blood before the vessel was tied onto the outflow cannula. One of the cannulae was attached to a micrometer that allowed manipulation of the length of the vessel segment. The chamber was placed onto the microscope (Axiovert 40 CFL), which was connected to a CCD camera (DMX41 AU02, Imaging Source Europe, Bremen, Germany), to allow monitoring of vessel diameter (Fig. 2.13). Data were recorded through a Pico-log (AD Instruments, UK) and PC computer, using Data Logger software (AD Instruments, UK). The tissue was perfused with Krebs solution, gassed with 95% air: 5% CO₂ and maintained at a temperature of 37 °C. When the vessel was securely tied at both ends flow was passed through the system, with the tap at the outflow end open to allow the escape of fluid. The tap at the outflow end was then closed to allow pressure to be applied to the system. Pressure was started at 10 mmHg and was stepped up in 10 mmHg intervals over a period of 20 minutes to 60 mmHg. To avoid buckling with increased pressure, the vessel length was adjusted using the micromanipulators if necessary without any additional stretching. The constant pressure in the system confirmed the absence of arterial leakage; any arteries exhibiting leakage were discarded. Each artery was equilibrated at 60 mmHg, which approximates the mean arterial BP of mouse *in vivo*, for at least 45 minutes. After this equilibration period the vessel was ready for use in the protocol.

2.4.2.2 Pressure myography protocol

Following the mounting procedure, the cannulated artery dimensions (outer diameter) were continuously monitored by a video dimension analyser. Furthermore, the chamber was perfused with 37°C Krebs solution gassed with 5% CO₂ in O₂. Viability testing of the artery segments included examining the vasoconstrictive and endothelium-dependent vasodilatory responses to 1 µM PE, and 10 µM ACh respectively. Each agonist concentration was applied extraluminally, while the alterations in the diameter were continually recorded. For studies of luminal flow in second-order mesenteric artery, vessel segments were mounted on glass cannulae as in a pressure myograph (Model 110p, Danish Myo Technology A/S, Denmark). The intraluminal pressure of the artery was always kept at 60 mmHg. Flow was then generated by increasing the pressure difference (ΔP) between inflow and outflow without changing the absolute intraluminal pressure. The pressure difference comes from the increase of inflow and simultaneous decrease of outflow. The outer diameter was monitored using a CCD camera (DMX41 AU02, Imaging Source Europe, Bremen, Germany) and recorded with MyoView II software. All vessels were equilibrated for at least 30 mins to reach a stable baseline. 100 µM L-NAME was used to pre-treat tissue before the pressure difference was produced. Nicardipine was added to inhibit the activity of VGCCs. These experiments were performed together with Dr J Shi (University of Leeds).

2.4.2.3 Data analysis

Due to a dark internal lumen of the artery during stimulation, the two lines which measure the luminal diameter are unstable and make the measurement difficult to obtain. Thus, external artery diameter was measured. For normalisation of external diameter, the constriction to incremental increases in luminal pressure difference (ΔP) (20, 40, 60, 70, 80, 90 and 100 mmHg) was expressed as a percentage of the PE response. The data are expressed as mean \pm SEM (n = the number of animals). Also the data sets of two groups are compared by unpaired *t*-test. All statistical analyses were performed using Origin software (Version 9). Statistical significance is indicated by **P*<0.05, ***P*<0.01 and ****P*<0.001.

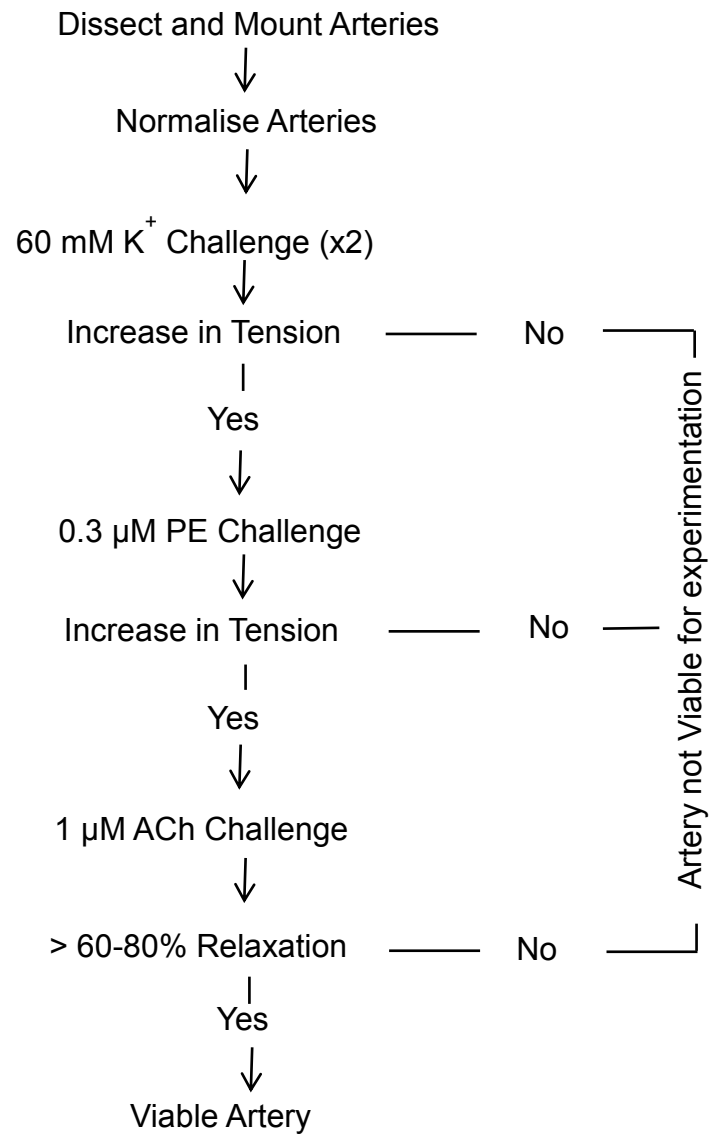


Figure 2-11: Standard start protocol was carried out to validate artery segments

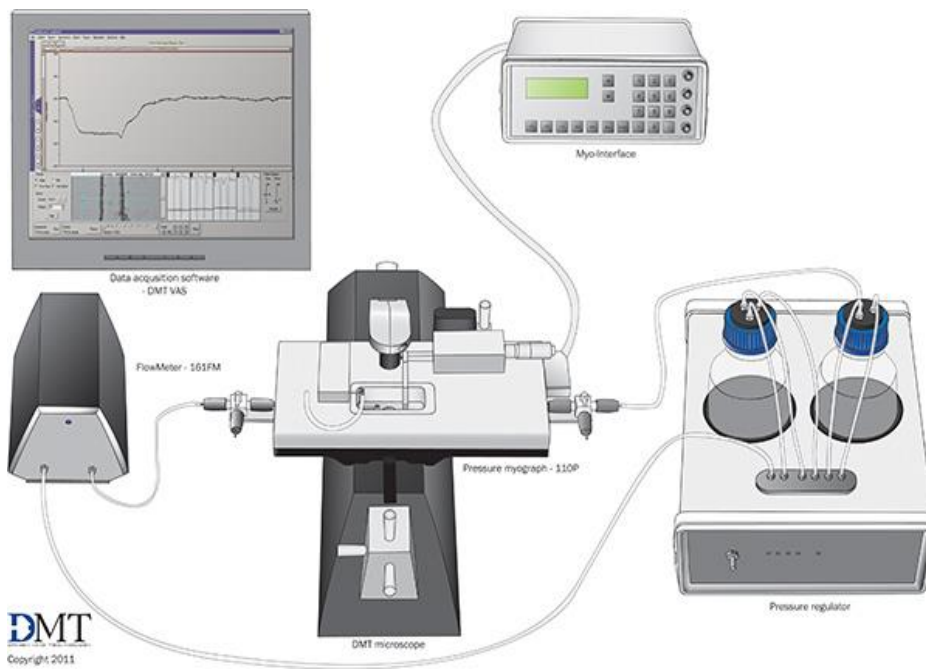


Figure 2-12: Schematic of the mechanical test system with optional accessories

Adapted from DMT website www.dmt.dk.

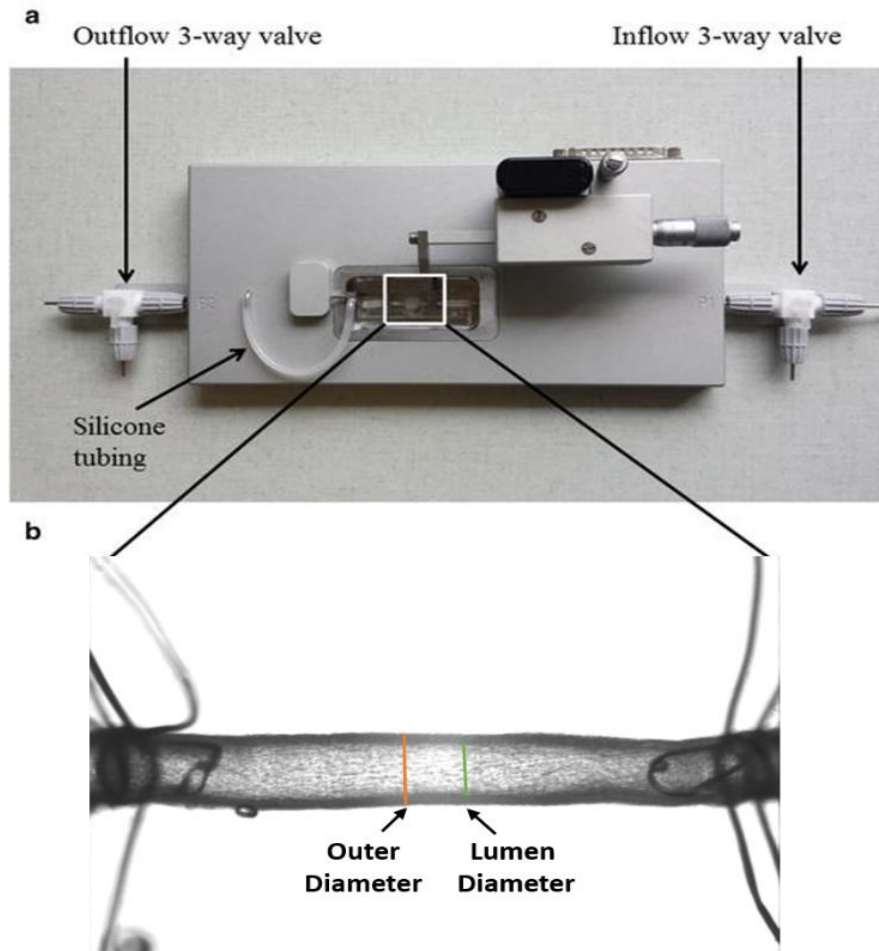


Figure 2-13: Artery from a mouse mounted in a pressure myograph

(a) Pressure myograph chamber showing that the inflow and outflow 3-way valves as well as the silicone tube in between the pressure transducer and the mounting pipette.
 (b) Mouse second-order mesenteric vessel mounted on glass tips of pressure myograph, pressurised at 60mmHg. Bars show outer diameter and inner diameter (lumen diameter).
 Adapted from DMT website www.dmt.dk.

Chapter 3 Vasoactive properties of the Piezo1 channel agonist Yoda1 on the mouse thoracic aorta

3.1 Abstract

3.1.1 Rationale

Recently, Piezo1 has been identified as a protein that integrates vascular architecture with physiological force. Piezo1 has been found to form a critical, mechanical force sensor located to the endothelium which lines the inner walls of blood vessels. Piezo1 can be activated by Yoda1, a synthetic small-molecule activator of Piezo1. Therefore, it is hypothesized that Piezo1 channels are determinants of vascular tone that were previously unrecognised and that chemical modulation of Piezo1 might be an important, novel approach for treating hypertension.

3.1.2 Aim

To investigate whether Piezo1 activation by Yoda1 has vasoactive effects on conduit arteries.

3.1.3 Method

Thoracic aorta segments of adult male mice were prepared and mounted on a wire myograph. Yoda1 effects and the mechanisms of EC-dependent relaxation and role of NO were elucidated by removing the endothelium or using L-NAME, a NOS inhibitor. Furthermore, the Piezo1 channel blocker Gd^{3+} and the Yoda1 competitive antagonist Dooku1 (and other Yoda1 analogues) were used to test dependency on Piezo1.

3.1.4 Results

Yoda1 induced relaxation of mouse thoracic aorta which had been pre-constricted with PE. The relaxation induced by Yoda1 was suppressed by removing the ECs or by the presence of L-NAME. Gd^{3+} or Dooku1 (and other Yoda1 analogues) suppressed the Yoda1 response.

3.1.5 Conclusions

Yoda1 (an activator of Piezo1 channels), relaxed mouse thoracic aorta via an endothelium- and NO-dependent mechanism and this effect is potently reversed by Dooku1.

3.2 Introduction

Piezo1 channels act as mechanical sensors for ECs (Li et al., 2014). They sense shear stress, a frictional force generated by blood flow. Piezo1 is important for alignment of ECs in response to shear stress (Li et al., 2014). EC Piezo1 is required for embryonic development, suggesting a critical role for sensing shear stress in the vascular remodelling required for embryonic growth (Li et al., 2014). While Piezo1 channels open in response to mechanical stimulation, such as shear stress or stretching, they can also be activated in the absence of mechanical stimulation by a synthetic small-molecule activator called Yoda1 (Syeda et al., 2015). Yoda1 was discovered in a screen of 3.25 million compounds in 2015. It lacks activity against the closely related Piezo2 channels and its effect on erythrocytes, in which Piezo1 is functional, was lost upon disruption of the Piezo1 gene (Syeda et al., 2015).

Conduit arteries such as the aorta provide a useful model for studying NO-dependent effects. Vasodilation in these vessels is essentially NO-mediated, in contrast to many resistance arteries where the NO contribution to relaxation is less and other mechanisms often perform a greater role (Chataigneau et al., 1999). The aorta originates from the heart and is the greatest elastic artery in the body and the major trunk of the systemic arterial system. The aortic root originates from the left ventricle and terminates at the aortic bifurcation at the umbilicus, splitting into left and right iliac arteries. The aortic trunk

includes innominate, common carotid and subclavian arteries in the aortic arch of the thoracic aorta, and celiac, mesenteric, renal, and common iliac arteries of the abdominal aorta, and is classified anatomically into the thoracic aorta (superior to the diaphragm) and the abdominal aorta (Mohanta et al., 2016, Dingemans et al., 2000). The mouse thoracic aorta is depicted in Fig. 3. 1.

In this chapter, the role of Piezo1 in the aorta was investigated since it provides a larger vessel on which to perform biochemical investigations compared with small arteries and the mounting procedure is relatively simple. Additionally, dysfunction of large conduit arteries has indications for vascular pathologies like atherosclerosis and coronary artery disease in animals and humans ((Deanfield et al., 2005, Felmeden and Lip, 2005, Heitzer et al., 2001). In the current study, a four chamber wire-myograph was used to investigate whether activation of Piezo1 has any effect on vessel tone in mouse thoracic aorta.

In this study, the SMCs were constricted *in vitro* in two ways: firstly, through membrane depolarization, and secondly, through receptor activation. For the former, increases in cell surface membrane potential to trigger Ca^{2+} influx via VGCCs leading to constriction, while receptor activation stimulates contraction through a complex signalling pathway of second messengers. Stimulation of receptors through agonists at the cell surface leads to Ca^{2+} rise, either via release from intracellular stores or by signalling mechanisms that raise the Ca^{2+} sensitivity of the contractile machinery. In addition, the rise in $[\text{Ca}^{2+}]_i$ can also occur through Ca^{2+} entry from receptor-operated Ca^{2+} channels on plasma membrane, facilitating raised cytosolic Ca^{2+} levels from the extracellular space (Murtada et al., 2012). Ca^{2+} attaches to the protein CaM leading to stimulation of MLC kinase, which phosphorylates the regulatory light chain of myosin. Once myosin has been phosphorylated it is able to form cross bridges with actin, which is required for initiation of SMC contraction as can be seen in Fig. 3.2 (Murtada et al., 2012, Webb, 2003). Therefore, the aim of this chapter was to determine if Yoda1, a Piezo1 activator, has vaso-active effects on murine thoracic aorta, to characterise any effects of Yoda1 and to investigate the mechanisms involved.

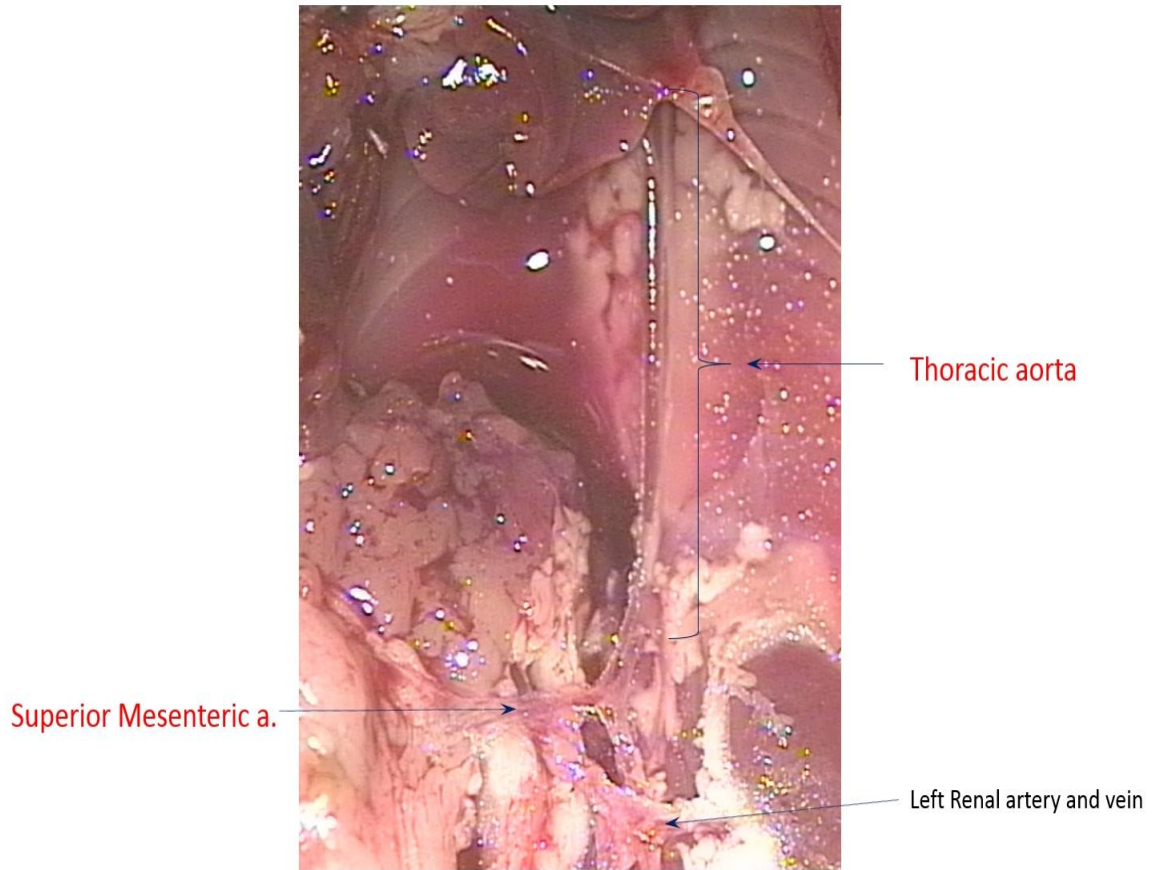


Figure 3-1: Picture of mouse thoracic aorta and associated blood vessels.

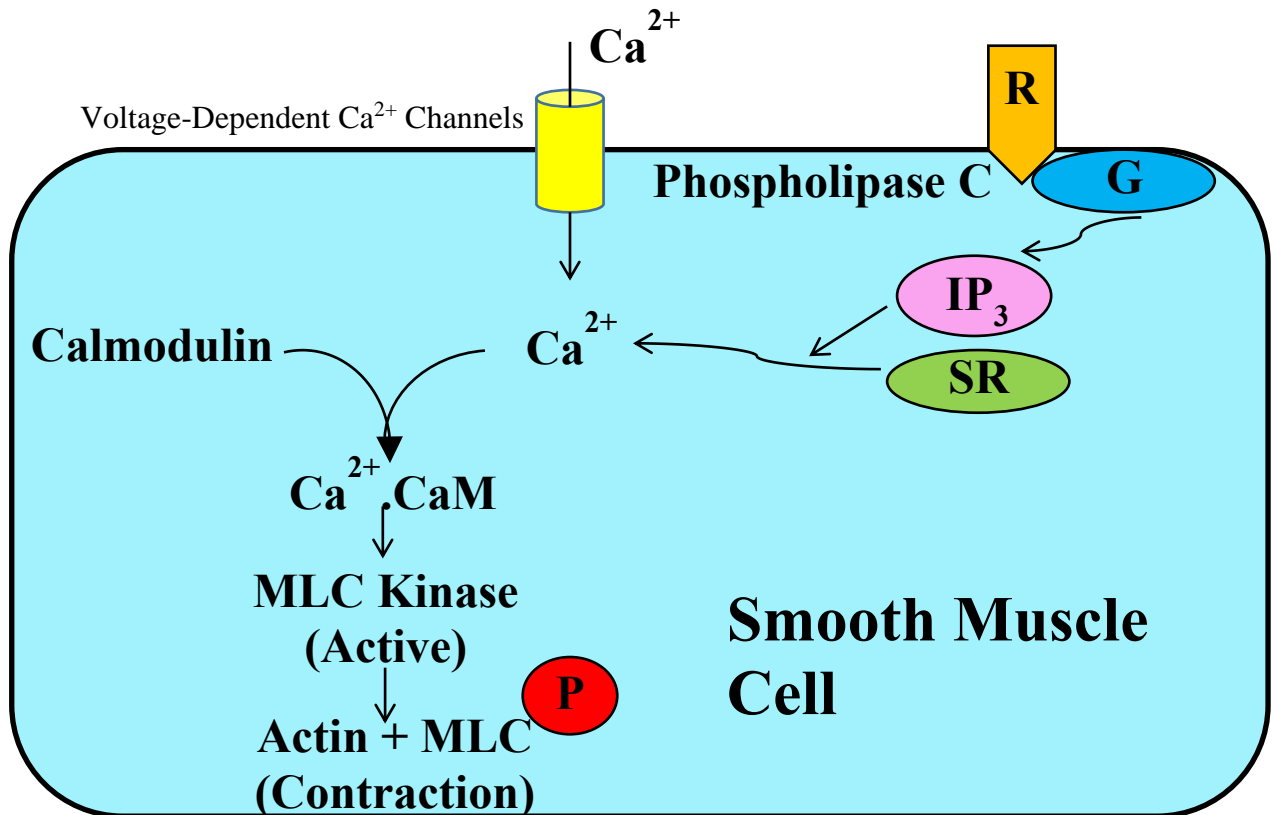


Figure 3-2: Regulation of the contractile mechanism in smooth muscle cells.

Smooth muscle activation via receptor agonists or electrical depolarization typically leads to a rapid rise in $[\text{Ca}^{2+}]_i$ due to the influx of extracellular Ca^{2+} through voltage-gated Ca^{2+} channels and release from the sarcoplasmic reticulum (SR). Agonists bind to specific receptors leading to phospholipase C activity through coupling by a G protein. Phospholipase C produces potent second messengers such as inositol 1, 4, 5-trisphosphate (IP_3) which binds to specific receptors on the sarcoplasmic reticulum. Ca^{2+} binds to calmodulin and stimulates myosin light chain kinase (MLCK), resulting in myosin light chain (MLC) phosphorylation and association with actin. Cross-bridge cycling happens, starting contraction.

3.3 Results

3.3.1 Yoda1-induced relaxation in isolated mouse thoracic aorta segments

To ascertain whether or not Piezo1 has a role in the contractility of the aorta, the Piezo1 activator (Syeda et al., 2015), was applied to segments of mouse thoracic aorta and constriction or relaxation of the vessel measured using wire myography. To ensure contractile integrity, all segments were first challenged with two consecutive exposures to 60 mM K⁺, resulting in vessel contraction as seen in Fig. 3.3a. Application of Yoda-1 alone, tested at concentrations ranging from 0.1 to 10 µM, was without effect (Fig. 3.3b). In contrast, following pre-constriction of the aorta with PE, 5 µM Yoda-1 did cause a change in tension. Comparable to the positive control ACh, it induced relaxation (Fig. 3.3c). In summary, the data reveal that Yoda-1 is able to alter the contractility of the aorta (i.e. cause relaxation) but that the presence of a vasoconstrictor is required to reveal these effects.

3.3.2 Cumulative concentration-response of Yoda1

To determine if the Yoda-1-induced relaxation in thoracic aorta was concentration-dependent, cumulative concentration-effect curves were constructed. In these experiments, aortic segments were pre-contracted using PE (0.3 µM). After stabilisation of PE-induced tone, increasing concentrations of Yoda1 (0.1, 0.3, 1, 3 and 10 µM) were added to the segments without washing out after each concentration. Each successive concentration of Yoda1 was added after relaxation to the preceding concentration had maximised (Fig. 3.4a). The half maximal relaxant effect (EC₅₀) occurred at a Yoda-1 concentration of about 2.3 µM (Fig. 3.4b), lower than the value of 17.1 µM determined for mouse Piezo1 expressed exogenously in human embryonic kidney 293 (HEK293) cell line (Syeda et al., 2015). It should be noted that it was not possible to determine the concentration of Yoda1 required for maximum effect because of solubility limitations of Yoda1 in physiological solution. Therefore the EC₅₀ obtained can only be considered as an estimation.

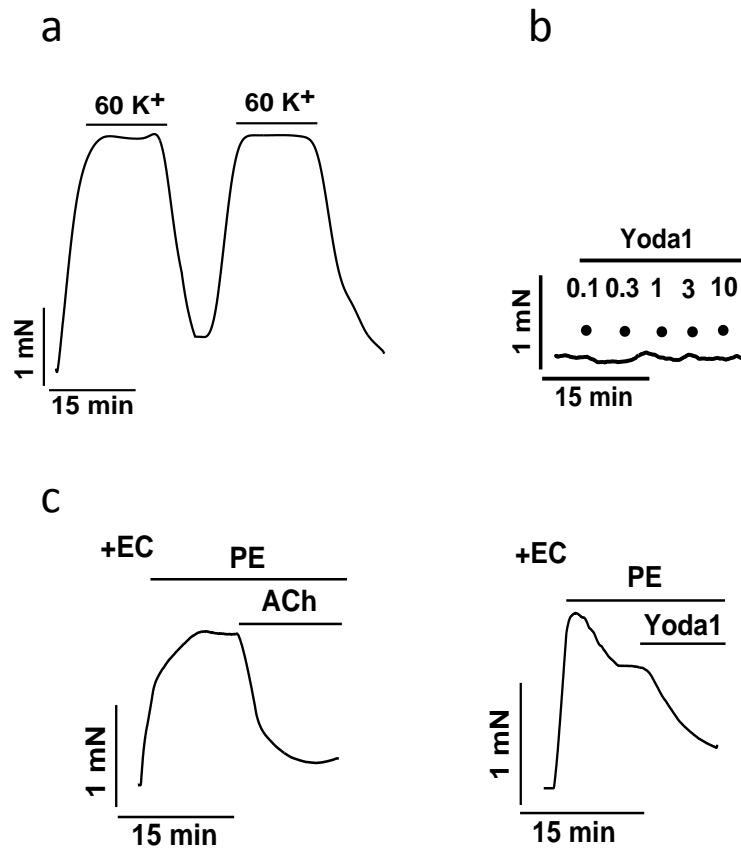


Figure 3-3: Yoda1-induced relaxation in mouse thoracic aorta segments.

Typical tracing obtained from mouse thoracic aorta showing (a) Vasoconstriction in response to high potassium (60 mM K⁺) solution, which validated arterial viability (the control) prior to experimentation. (b) The application of Yoda1 at increasing concentrations as indicated by the dots (0.1, 0.3, 1, 3 and 10 μM) without the addition of phenylephrine (PE). (c) Responses to Yoda1 (5 μM) compared with control acetylcholine (ACh) (1 μM) following PE addition.

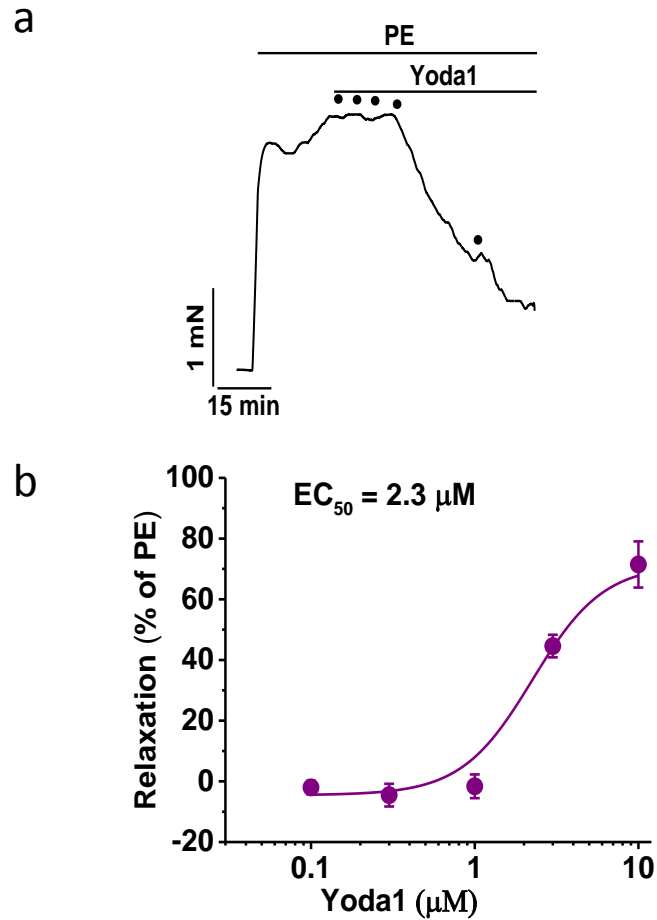


Figure 3-4: Cumulative concentration response curves of Yoda1 in mouse thoracic aorta.

(a) Typical wire myography tracing showing a concentration-dependent relaxation response to Yoda1 as indicated by the dots (0.1, 0.3, 1, 3 and 10 μM) after pre-constriction with 0.3 μM phenylephrine (PE). (b) Concentration response curve indicating the 50 % effective concentration (EC₅₀) (n = 5). Curve was fitted using the Hill1 equation. Data are shown as mean ± SEM.

3.3.3 EC involvement

To ascertain if the Yoda-1-induced relaxation was dependent upon EC, the endothelium was removed from the aortic segments by gently rubbing the intimal surface with a tungsten wire. Care was taken not to over-stretch the rings during rubbing in order to avoid damaging their muscular layer. Endothelial denudation was considered successful if the endothelium-dependent vasodilator ACh (1 μ M) failed to produce relaxation (less than 10%) (Fig. 3.5a).

Similar to ACh, removal of the endothelium resulted in total loss of Yoda1-induced relaxation following pre-constriction with 0.3 μ M PE (Fig. 3.5a and b). These results indicate that the vasorelaxation to Yoda1 was EC-dependent. The contractile response to PE in thoracic aorta following mechanical removal of the endothelium was analysed to investigate the role of basal NO on contraction. No change was observed in PE responses before and after removing the EC (Fig. 3.5c).

3.3.4 Effects of nitric oxide synthase inhibitor (L-NAME) on Yoda1-induced relaxation

ACh-induced relaxation in the aorta is dependent upon NO (Chataigneau et al., 1999). This gaseous molecule is synthesised in ECs by NOS, then NO induces vasorelaxation in VSMCs through inducing activation of the enzyme sGC, resulting in formation of the second messenger cGMP (Rapoport and Murad, 1983). To determine if Yoda-1 induced relaxation is also dependent on NO signalling, aortic segments were pre-incubated for 20 minutes with 100 μ M L-NAME, an inhibitor of NOS. The treated tissues were pre-contracted with 0.3 μ M PE and after stabilisation of the tone, a single dose of 5 μ M Yoda1 or 1 μ M ACh was applied. The relaxation response was abolished as showed in Fig. 3.6a, and as quantified in Fig. 3.6b.

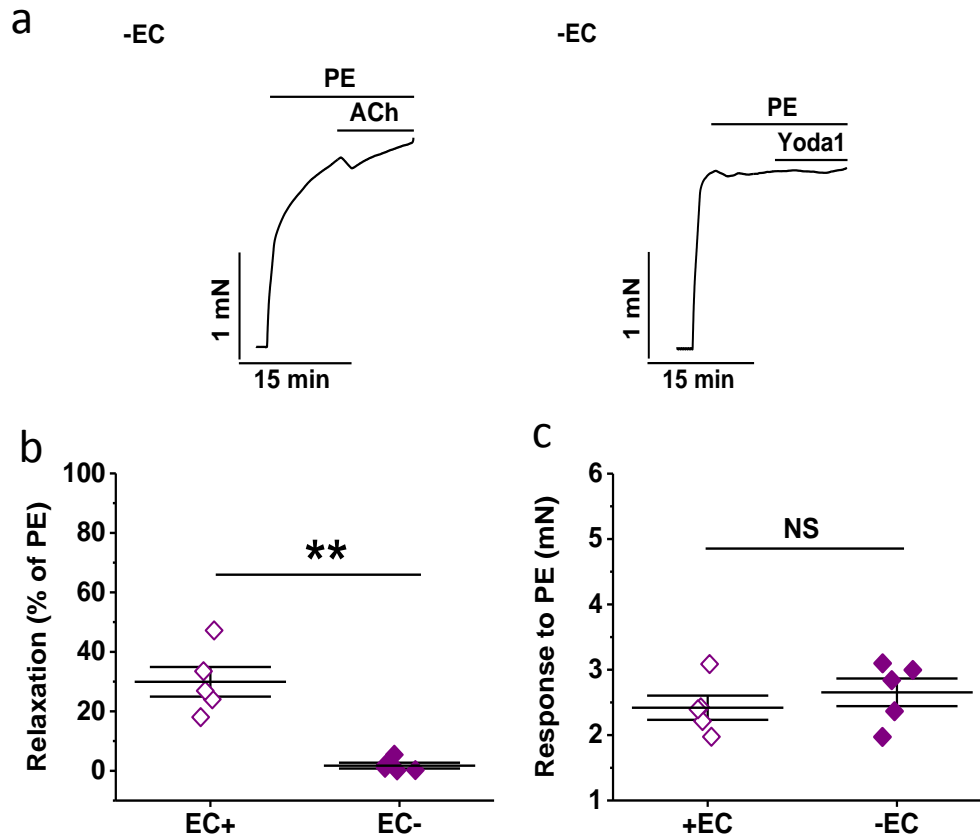


Figure 3-5: Effects of Yoda1-induced relaxation mediated by endothelial cells in mouse thoracic aorta segments.

(a) Typical tracing obtained from mouse thoracic aorta responses to Yoda1 (5 μ M) compared with control acetylcholine (ACh) (1 μ M) after endothelial cells (ECs) were removed. (b) Quantification of the degree of relaxation elicited by Yoda1 before and after removing the EC (-EC) compared with the control. (c) Quantification of the degree of phenylephrine (PE) induced tone before and after removing the EC (n = 5). Data are shown as mean \pm SEM. NS=not significant.

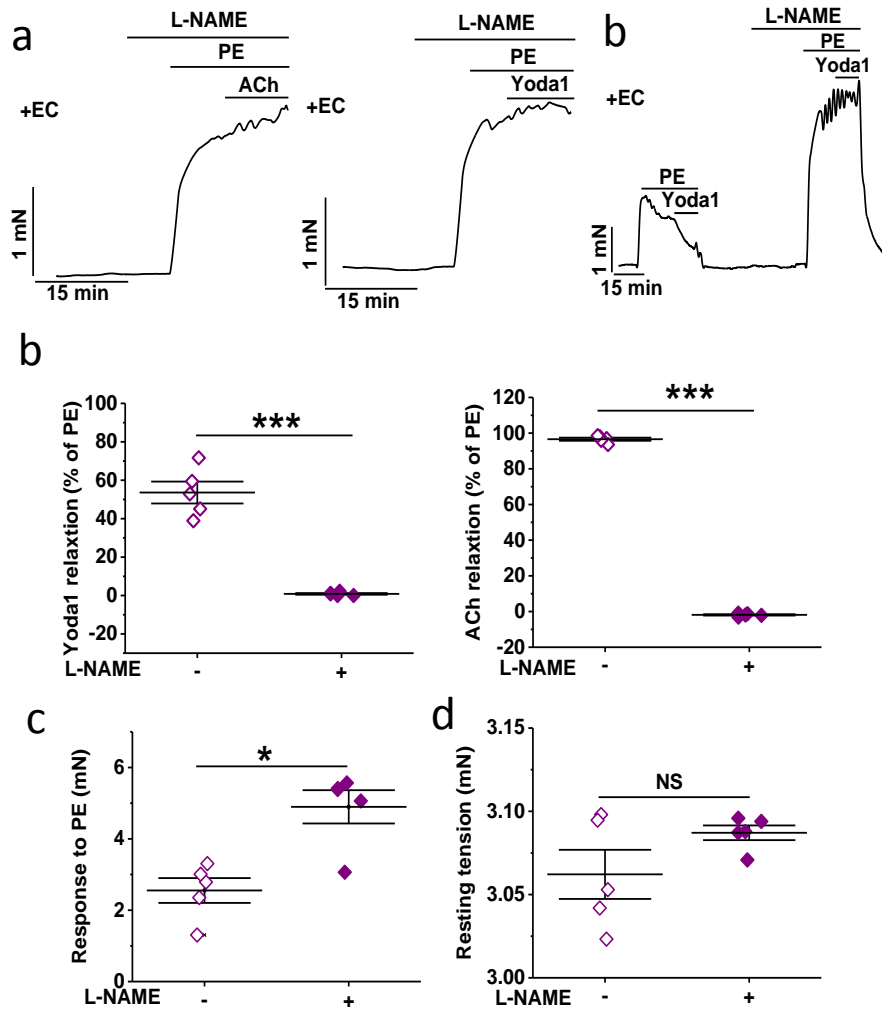


Figure 3-6: Yoda1-induced relaxation mediated by nitric oxide (NO) in mouse thoracic aorta segments.

(a) Typical tracing obtained from mouse thoracic aorta showing responses to Yoda1 (5 μM) compared with control acetylcholine (ACh) (1 μM) after pre-incubation with 100 μM of Nω-nitro-L-arginine methyl ester (L-NAME) with intact ECs. Typical trace also showing the responses to Yoda1 (5 μM) before and after the incubation with (100 μM) L-NAME in endothelium-intact thoracic aorta isolated from control mice. (b) Quantification of the degree of relaxation elicited by Yoda1 or ACh before and after L-NAME treatment. (c) Quantification of the degree of phenylephrine (PE) induced tone before and after pre-incubation with 100 μM L-NAME with intact ECs. (d) Quantification of the L-NAME effects on the basal artery tension. (n = 5). Data are shown as mean ± SEM. NS=not significant.

Basal activity of NO generated by the vascular endothelium exerts a tonic vasodilator effect that suppresses the actions of vasoconstrictor drugs (Moore et al., 1990, Mian and Martin, 1995). Thus, agents that reduce the synthesis or actions of NO produce an enhancement of vasoconstrictor-induced tone by removing this endothelium-dependent suppression of vasoconstriction. This can be seen by L-NAME's enhancement of the vasoconstriction effect of PE (Fig. 3.6c). L-NAME, however, did not significantly increase the basal tone of the aortic segments (Fig. 3.6d).

3.3.5 Inhibitors of Piezo1 involvement

Gd³⁺, an inhibitor of mechanosensitive channels (Ermakov et al., 2010), has been shown to potently block Piezo1 channels (Coste, et al 2010). Gd³⁺ was therefore used to examine if Piezo1 is involved in the Yoda1-evoked relaxation of thoracic aorta. This nonspecific inhibitor of Piezo1 suppressed the Yoda1-evoked relaxation by 85% (Fig. 3.7a-c). In contrast, no differences were observed in the resting tone (Fig. 3.7d) or the PE-induced vascular tone of mouse thoracic aorta when Gd³⁺ was used (Fig. 3.7e). The data support the contribution of Piezo1 to the Yoda1-induced relaxation.

3.3.6 Yoda1 inhibition with Dooku1

Dooku1 is a structural analogue of Yoda-1. It is unable to activate Piezo1 but acts as a competitive antagonist of Yoda-1 at this channel. Pre-treatment of thoracic aortic segments with Dooku1 completely blocked the Yoda1 evoked relaxation (Fig. 3.8a-c). Due to the structural similarity of Dooku1 and Yoda1, Dooku1 likely attaches to the Yoda1-binding site on the Piezo1 channel. No differences were observed in the resting tone of thoracic aorta when Dooku1 was used (Fig. 3.8d). However, a significant reduction (28%) in the level of tone induced by PE was observed (Fig. 3.8e), suggesting that Dooku1 has impact on the PE signalling mechanism.

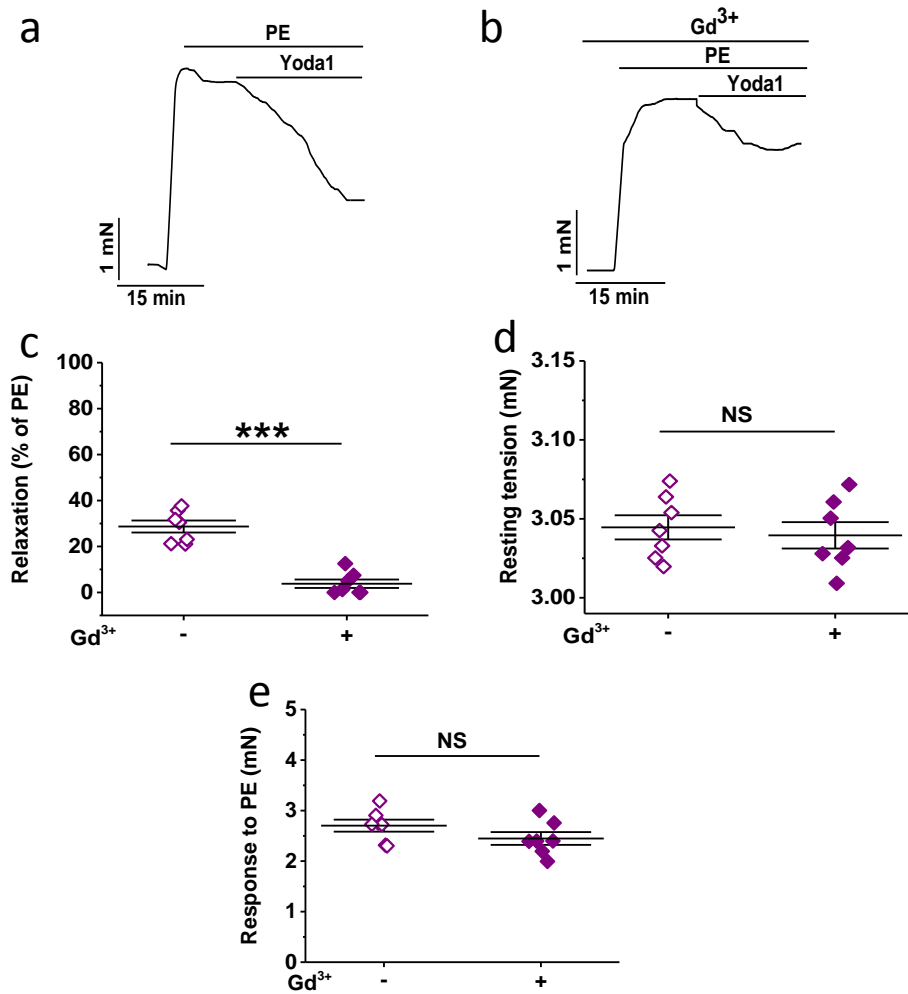


Figure 3-7: Effect of gadolinium (Gd³⁺) on Yoda1-induced relaxation in mouse thoracic aorta segments.

Typical tracing obtained from mouse thoracic aorta (a–b) showing the Yoda1 (5 μM) response before and after pre-incubation for 20 min with gadolinium (Gd³⁺) (10 μM). The aorta was endothelium-intact. (c) Quantification of the degree of relaxation elicited by Yoda1 after Gd³⁺ treatment, compared with the control. (d) Quantification of the Gd³⁺ effects on the basal artery tension. (e) Quantification of the degree of phenylephrine (PE) induced tone before and after pre-incubation with 10 μM Gd³⁺ with intact ECs. (n = 7). Data are shown as mean ± SEM. NS=not significant.

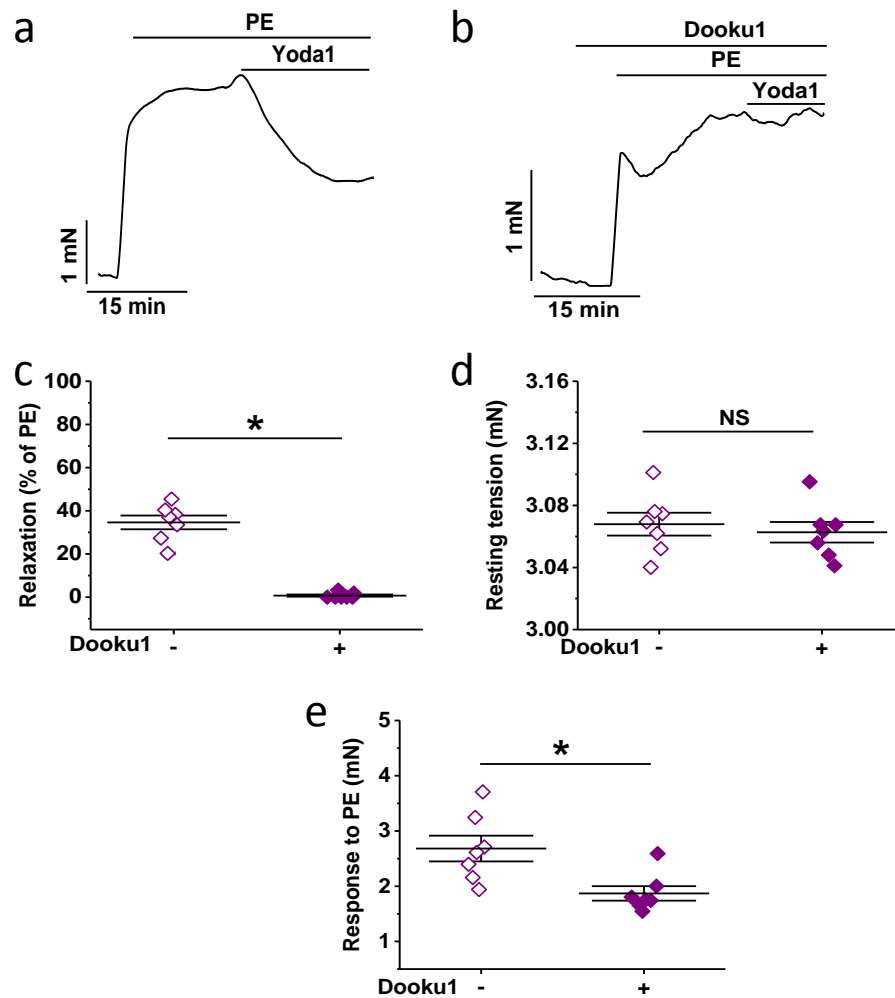


Figure 3-8: Effect of Dooku1, a Yoda1 analogue, on Yoda1-induced relaxation in mouse thoracic aorta segments.

Typical tracing obtained from mouse thoracic aorta (a) showing the Yoda1 (5 μ M) response before and after pre-incubation for 30 min with Dooku1 (10 μ M) in endothelium-intact aorta. (b) Quantification of the degree of relaxation elicited by Yoda1 after Dooku1 treatment, compared with the control. (c) Quantification of the Dooku1 effects on the basal artery tension. (d) Quantification of the degree of phenylephrine (PE) induced tone before and after pre-incubation with 10 μ M Dooku1 with intact ECs (n = 7). Data are shown as mean \pm SEM. NS=not significant.

3.3.7 Yoda1 inhibition by other Yoda1 analogues

7b, 2g, 11 and 2e are other Yoda1 analogues synthesised at the University of Leeds, which have also been tested for inhibition of Yoda1-induced Piezo1 activity and have variable effects *in vitro* on Ca^{2+} entry (experiments performed by Elizabeth Evans, University of Leeds) (Evans et al., 2018). To investigate whether their ability to inhibit Yoda-1 induced Piezo1 activity *in vitro* correlated with their ability to prevent Yoda-1-evoked relaxation of mouse thoracic aorta, the relaxation to Yoda1 was measured in the aortas following pre-treatment with the analogues. Pre-treatment of thoracic aortic segments with 7b, 2g and 11 showed variable inhibition of the Yoda1-evoked relaxation, but this was not observed with 2e (Figs. 3.9a-b, 3.10a-b, 3.11a-b and 3.12a-b). This result correlated well with the *in vitro* intracellular calcium measurements. No difference was observed in the resting tone (Fig. 3.9c, 3.10c, 3.11c and 3.12c) or the PE-induced vascular tone of mouse thoracic aorta when these inhibitors were used (Figs. 3.9d, 3.10d, 3.11d and 3.12d). The data suggest that other Yoda1 analogues, like Dooku1, are able to inhibit Yoda1-induced relaxation on mouse thoracic aorta.

3.3.8 Specificity of Dooku1

Since Dooku1 had an inhibitory effect on the PE-induced contraction of mouse thoracic aorta it was tested for inhibitory activity against another vasoconstrictor which acts through a different mechanism. U46619, a thromboxane A_2 agonist, contracts VSMCs via binding to specific GPCRs (thromboxane receptors) that elevate cytosolic free Ca^{2+} ($[\text{Ca}^{2+}]_i$) via releasing stored Ca^{2+} from the SR leading to contraction (Fig. 3.13) (McKenzie et al., 2009). Similar to PE, U46619-induced constriction were slightly suppressed in the presence of Dooku1 (Fig. 3.14a and c). Dooku1 was also tested for an inhibitory effect on other vasodilators, ACh and SIN-1 were applied after pre-constriction with U46619. Incubation with Dooku1 had no effect on ACh or SIN-1-induced relaxation as quantified in Fig. 14d and e. There was no statistical significance between control relaxation and relaxation in the presence of Dooku1. The data indicate that Dooku1 may have small off target effects against contractile agents through an unknown mechanism, however, it does not seem to block relaxation from other agents.

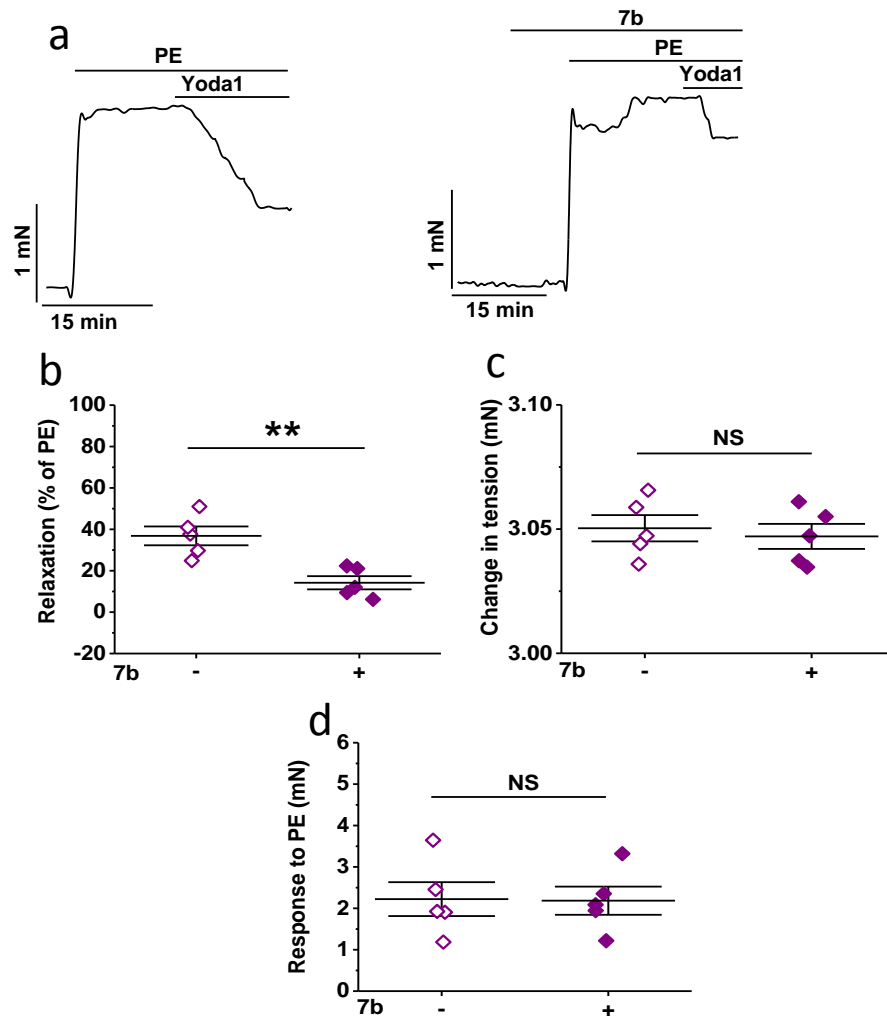


Figure 3-9: Effect of 7b, a Yoda1 analogue, on Yoda1-induced relaxation in mouse thoracic aorta segments.

Typical tracing obtained from mouse thoracic aorta (a) showing Yoda1 (5 μ M) response before and after pre-incubation for 30 min with 7b (10 μ M) in endothelium-intact aorta. (b) Quantification of the degree of relaxation elicited by Yoda1 after 7b treatment, compared with the control. (c) Quantification of the 7b effects on the basal artery tension. (d) Quantification of the degree of phenylephrine (PE) induced tone before and after pre-incubation with 10 μ M 7b with intact ECs (n = 5). Data are shown as mean \pm SEM. NS=not significant.

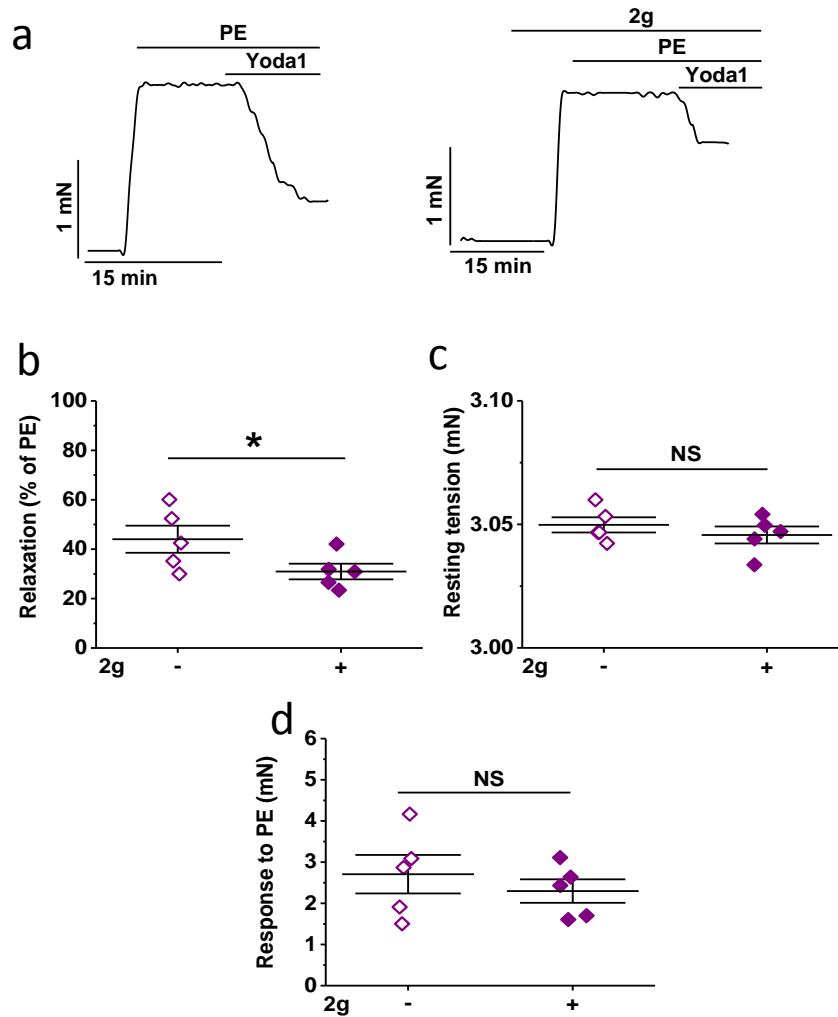


Figure 3-10: Effect of 2g, a Yoda1 analogue, on Yoda1-induced relaxation in mouse thoracic aorta segments.

Typical tracing obtained from mouse thoracic aorta (a) showing Yoda1 (5 μ M) response before and after pre-incubation for 30 min with 2g (10 μ M) in endothelium-intact aorta. (b) Quantification of the degree of relaxation elicited by Yoda1 after 2g treatment, compared with the control. (c) Quantification of the 2g effects on the basal artery tension. (d) Quantification of the degree of phenylephrine (PE) induced tone before and after pre-incubation with 10 μ M 2g with intact ECs (n = 5). Data are shown as mean \pm SEM. NS=not significant.

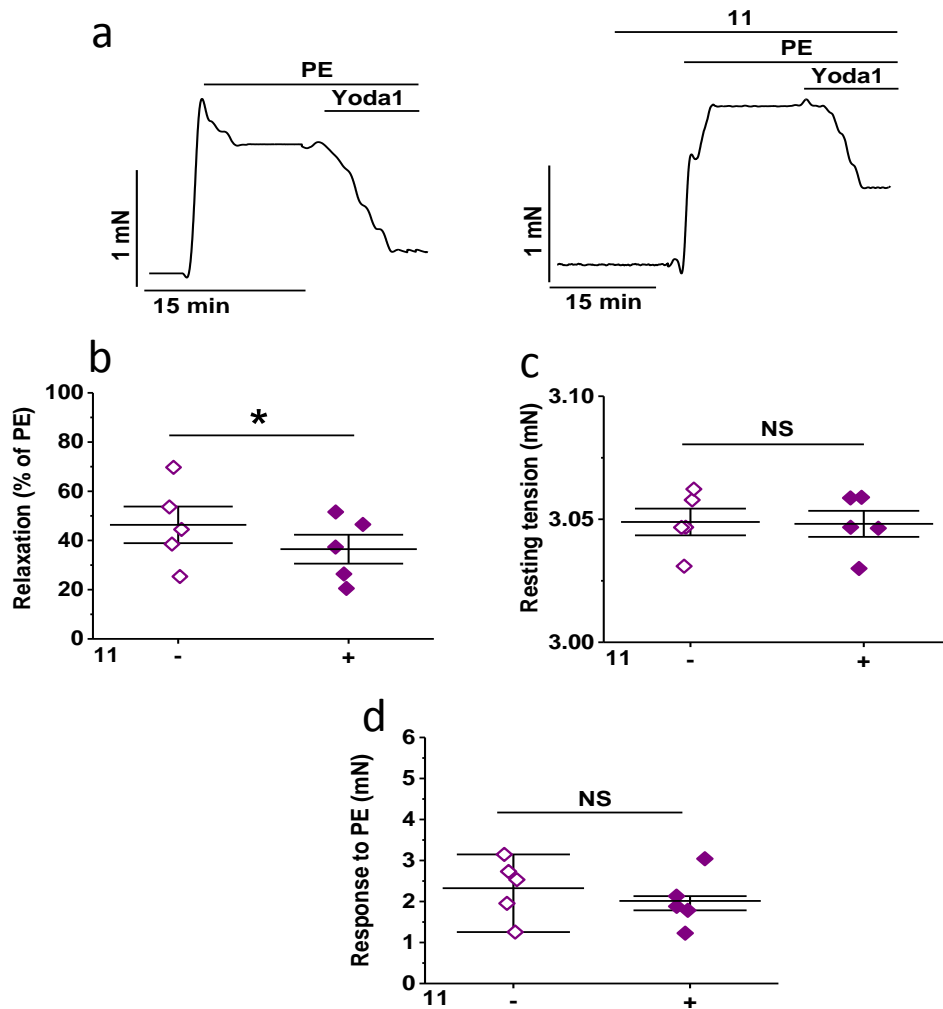


Figure 3-11: Effect of 11, a Yoda1 analogue, on Yoda1-induced relaxation in mouse thoracic aorta segments.

Typical tracing obtained from mouse thoracic aorta (a) showing the Yoda1 (5 μ M) response before and after pre-incubation for 30 min with 11 (10 μ M) in endothelium-intact aorta. (b) Quantification of the degree of relaxation elicited by Yoda1 after 11 treatments, compared with the control. (c) Quantification of the 11 effects on the basal artery tension. (d) Quantification of the degree of phenylephrine (PE) induced tone before and after pre-incubation with 10 μ M 11 with intact ECs (n = 5). Data are shown as mean \pm SEM. NS=not significant.

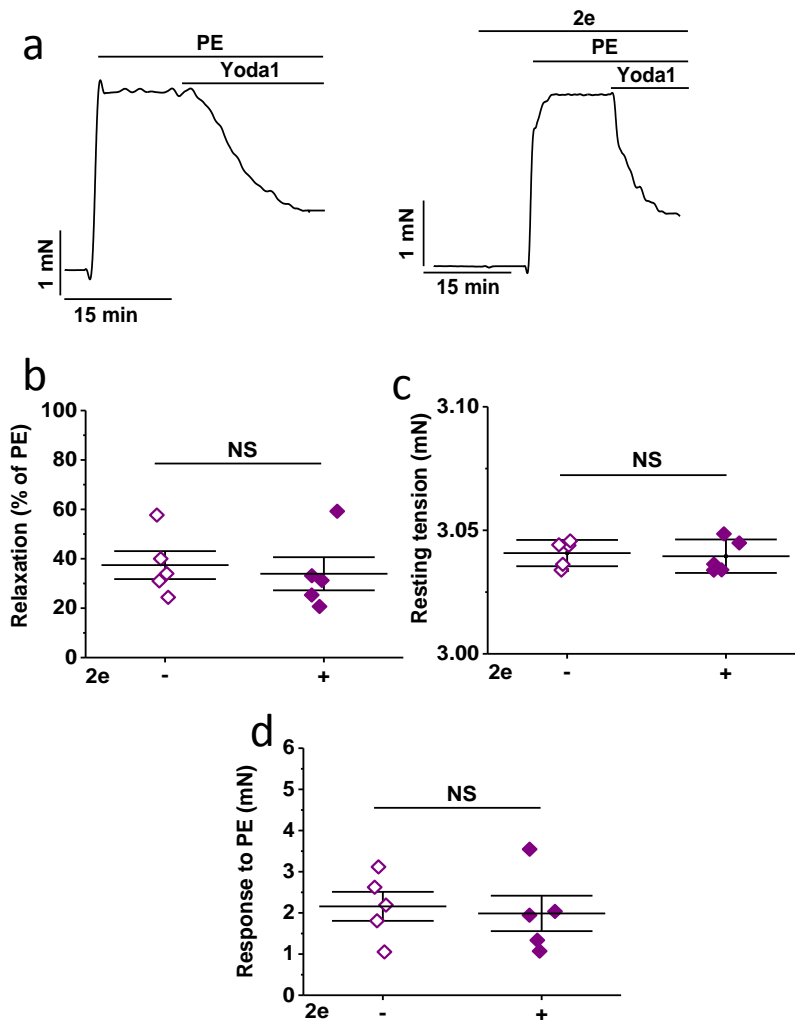


Figure 3-12: Effect of 2e, a Yoda1 analogue, on Yoda1-induced relaxation in mouse thoracic aorta segments.

Typical tracing obtained from mouse thoracic aorta (a) showing the Yoda1 (5 μM) response before and after pre-incubation for 30 min with 2e (10 μM) in endothelium-intact aorta. (b) Quantification of the degree of relaxation elicited by Yoda1 after 2e treatment, compared with the control. (c) Quantification of the 2e effects on the basal artery tension. (d) Quantification of the degree of phenylephrine (PE) induced tone before and after pre-incubation with 10 μM 2e with intact ECs ($n = 5$). Data are shown as mean \pm SEM. NS=not significant.

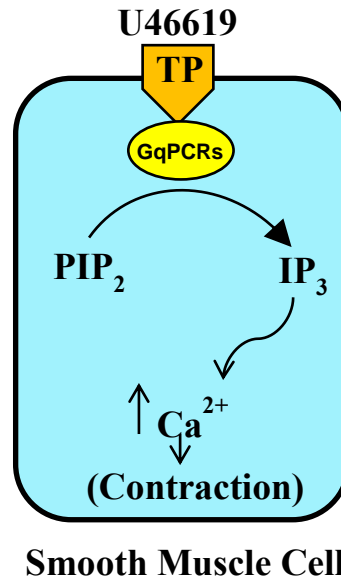


Figure 3-13: Mechanisms involved in the thromboxane mimetic U46619-induced contraction.

The diagram illustrates the common signalling mechanisms of U46619 to mediate contraction. Thromboxane receptor (TP). Gq protein-coupled receptors (GqPCRs). PIP₂, phosphatidylinositol bisphosphate. IP₃, inositol trisphosphate.

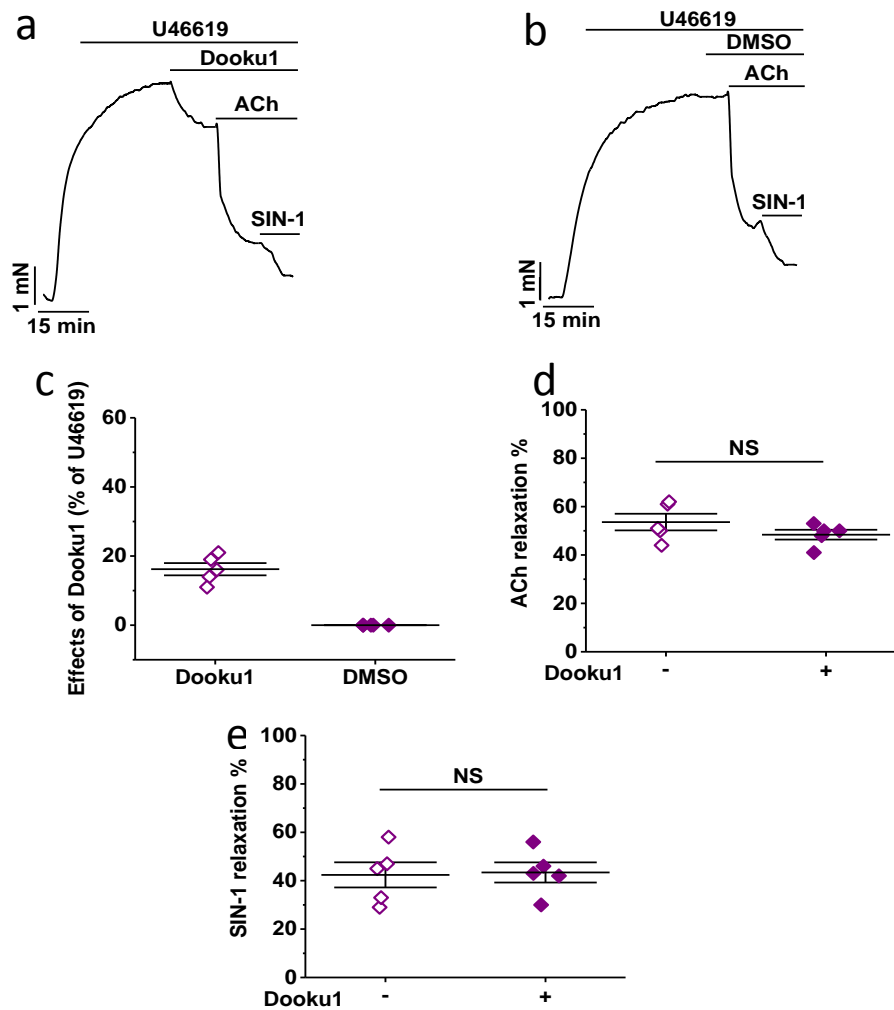


Figure 3-14: Dooku1 has minimal effect on thromboxane A₂ mediated contraction and does not affect other vasodilators

(a) Isometric tension recording of aorta pre-constricted with 0.1 μM U46619, a thromboxane A₂ agonist and exposed to 10 μM Dooku1 followed by the addition of 1 μM acetylcholine (ACh) and then 10 μM NO-donator, Linsidomine (SIN-1). (b) As for (a) except exposed to dimethyl sulfoxide, (DMSO) at concentration of 100% (c-e) Summary data for experiments of the type shown in (a,b) expressed as % of the maximum inhibition of U46619 amplitude by Dooku1 (c), relaxation evoked by ACh (d) or SIN-1 (e) (n=5). Data are shown as mean ± SEM. NS=not significant.

3.3.9 Yoda1 does not induce relaxation in control and endothelial Piezo1^{ΔEC} thoracic aorta

To further investigate the role of Piezo1 in Yoda1 responses of thoracic aortae, myography experiments were performed on vessels from mice with endothelial-specific deletion of Piezo1 (Piezo1^{ΔEC}). Control mice and Piezo1^{ΔEC} mice were injected with TAM. Mice appeared phenotypically normal and the body weight was normal. There were no changes in body weight (gain) and organ weights and serum urea, K⁺ and Na⁺; gross anatomies and functions of the heart and aorta were also normal (Fig 3.15a–m) (all this work was performed by Dr B Rode and Dr M Bailey). Therefore endothelial Piezo1 in the adult is without major phenotype.

As for the previous experiments, traces showing the response to K⁺, PE, ACh and Yoda1 before and after incubation with L-NAME were obtained from control and Piezo1^{ΔEC} thoracic aortae (Fig. 3.16a and b, respectively). In these experiments, addition of high K⁺ (60 mM) induced similar contractions in intact thoracic aorta from control and Piezo1^{ΔEC} littermates (Fig. 3.17a). Following this, PE was added in increasing concentrations (0.01, 0.03, 0.1, 0.3 and 1 μM) to the segments in the wire myograph. The magnitude of the PE-induced arterial contractions was similar in intact thoracic aorta from control and Piezo1^{ΔEC} animals (Fig. 3.17b). Segments of endothelium-intact aorta were pre-contracted with 0.3 μM PE. After tone stabilisation, a cumulative concentration-response curve to ACh (0.01, 0.03, 0.1, 0.3 and 1 μM) was conducted. Both groups of control and Piezo1^{ΔEC} mice also exhibited similar endothelium-dependent relaxation to ACh (Fig. 3.17c). The data suggest that there was no decrease in the viability of tissue preparations from these mice.

Next, a cumulative concentration-response curve to Yoda1 (0.1, 0.3, 1, 3 and 10 μM) was constructed. Unexpectedly, vessels from control and Piezo1^{ΔEC} mice showed no relaxation responses to Yoda1 and actually showed contractile responses (Fig. 3.18a). Furthermore, a cumulative concentration-response curve to Yoda1 was obtained before and after treatment with L-NAME (100 μM, 20 mins). L-NAME did not significantly inhibit the contractile response to Yoda1 in control and Piezo1^{ΔEC} aorta (Fig. 3.18b and c, respectively).

The differences between the 'control mice' used here and the 'wildtype mice' used earlier in this chapter were i) the genotype (Piezo1^{flox/flox}) and ii) being injected with TAM.

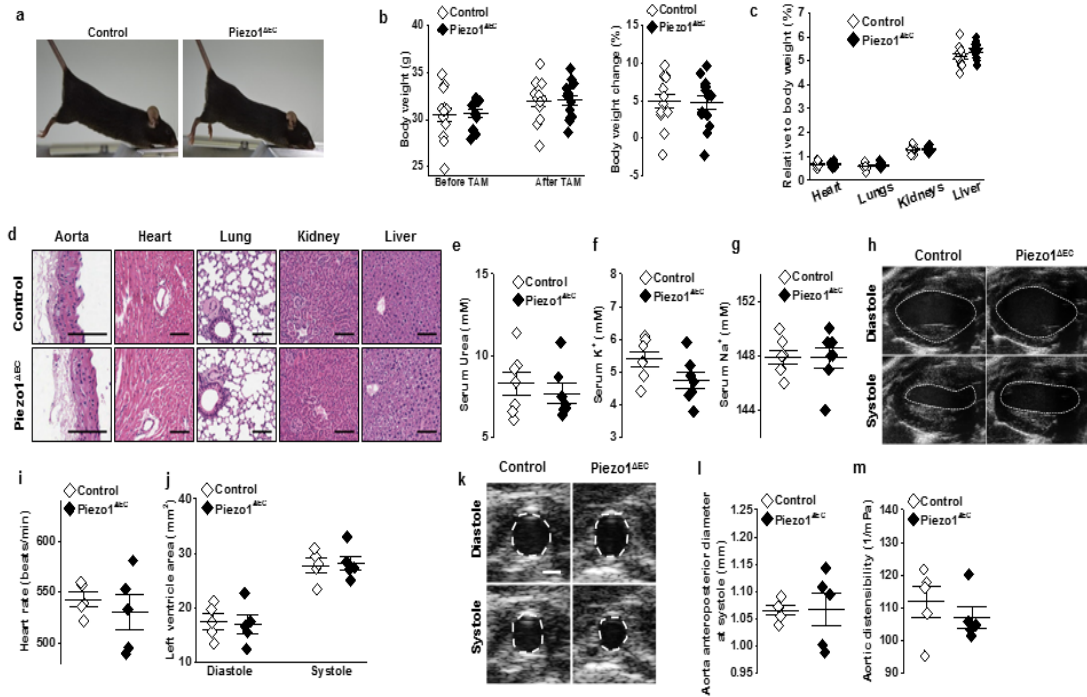


Figure 3-15: Mice with disruption of the endothelial Piezo1 appeared phenotypically normal.

(a) Physical appearance of control and endothelial Piezo1-deleted ($Piezo1^{\Delta EC}$) mice. (b) Body weight and percentage change in body weight of control ($n=13$) and $Piezo1^{\Delta EC}$ ($n=14$) mice before and 10-14 days after tamoxifen (TAM) treatment. (c) As percentages of total body weight, weights of heart, lung, kidney and liver in control ($n=13$) and $Piezo1^{\Delta EC}$ ($n=14$) mice. (d) Histological examples of control (top row) and $Piezo1^{\Delta EC}$ (bottom row) sections of aorta, heart, lung, kidney and liver stained with H&E. Scale bars 100 μm . (e–g) Serum concentrations of urea, K^+ and Na^+ in control ($n=7$) and $Piezo1^{\Delta EC}$ ($n=7$) mice. (h–m) Ultrasound study of the heart (h–j) and aorta (k–m) of control ($n=5$) and $Piezo1^{\Delta EC}$ ($n=5$) mice under anaesthesia. (h) Example of left ventricle images of control and $Piezo1^{\Delta EC}$ at diastole and systole. The left ventricle chamber is circled with a white dashed line. Scale bar 1 mm. (i, j) Cardiac parameters measured by ultrasound. (k) Example of aorta images of control and $Piezo1^{\Delta EC}$ at diastole and systole. The left ventricle chamber is circled with a white dashed line. Scale bar 1 mm. (l) Aorta anteroposterior diameter at systole. (m) Aortic distensibility. Independent data points are displayed with superimposed bars indicating mean \pm SEM. Data sets are compared by t -test. No significant differences were detected. Experiments were performed by Dr B Rode and Dr M Bailey. The figure is from Rode et al, 2017 Nat Comm.

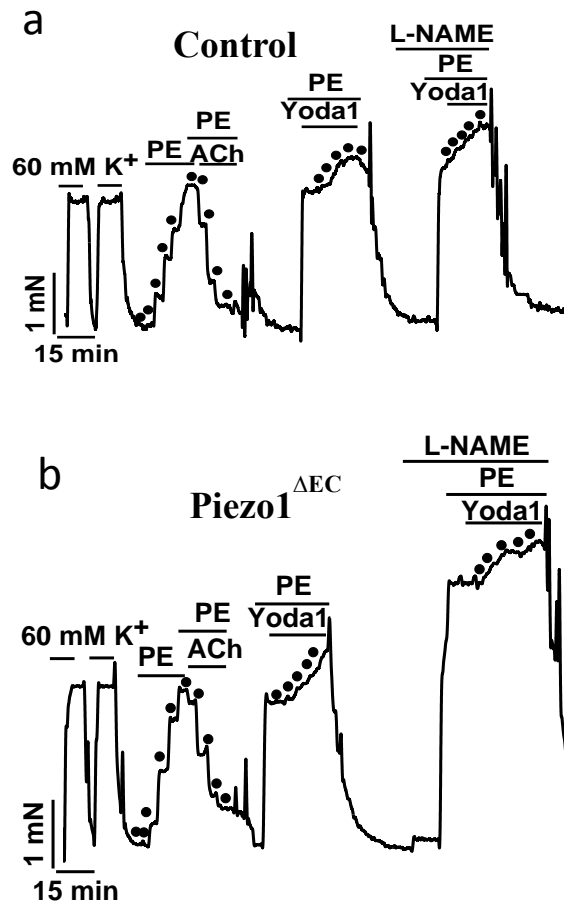


Figure 3-16: Typical responses of control and Piezo1^{ΔEC} thoracic aorta

(a) Typical trace showing vasoconstriction in response to high potassium solution that shows increased tone in response to phenylephrine (PE) as indicated by the dots (0.01, 0.03, 0.1, 0.3 and 1 μ M), a concentration-dependent dilatory response to acetylcholine (ACh) as indicated by the dots (0.01, 0.03, 0.1, 0.3 and 1 μ M) and concentration-response curves (contractions) to Yoda1 as indicated by the dots (0.1, 0.3, 1, 3 and 10 μ M) before and after incubation with (100 μ M) *N*_ω-nitro-L-arginine methyl ester hydrochloride (L-NAME) in endothelium-intact thoracic aorta isolated from control mice. (b) As for (a) except in endothelium-intact thoracic aorta isolated from Piezo1^{ΔEC} mice.

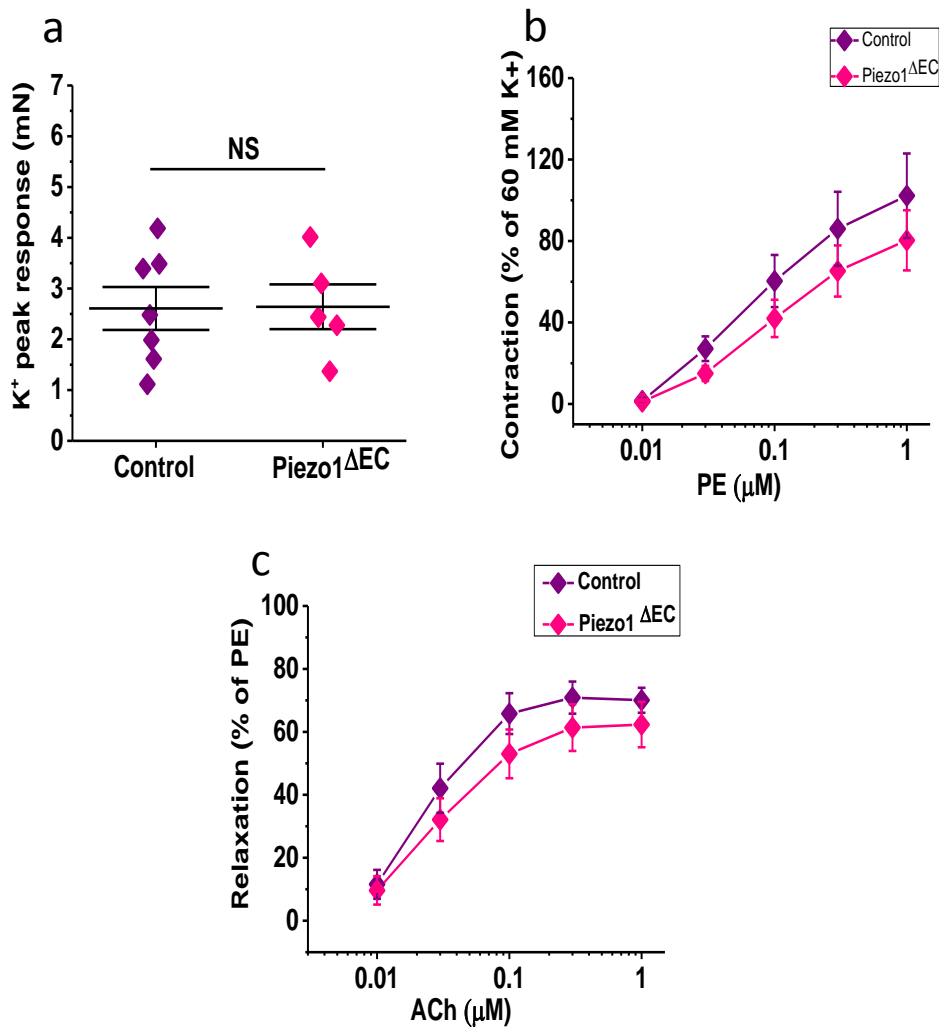


Figure 3-17: Vascular viability in control compared with Piezo1^{ΔEC} thoracic aorta

(a) Comparison of response to high potassium (60 mM K⁺), (b) concentration response curves to phenylephrine (PE) (0.01, 0.03, 0.1, 0.3 and 1 μM), (c) concentration response curves to ACh (0.01, 0.03, 0.1, 0.3 and 1 μM) in thoracic aorta of control ($n=7$) and Piezo1^{ΔEC} mice ($n=5$). For high potassium, responses are expressed by the absolute value of the K⁺-induced contraction. For PE and ACh, responses are expressed as percent constriction of K⁺-induced contraction and as percent relaxation of PE-induced contraction, respectively. Mean ± SEM values are depicted. NS=not significant.

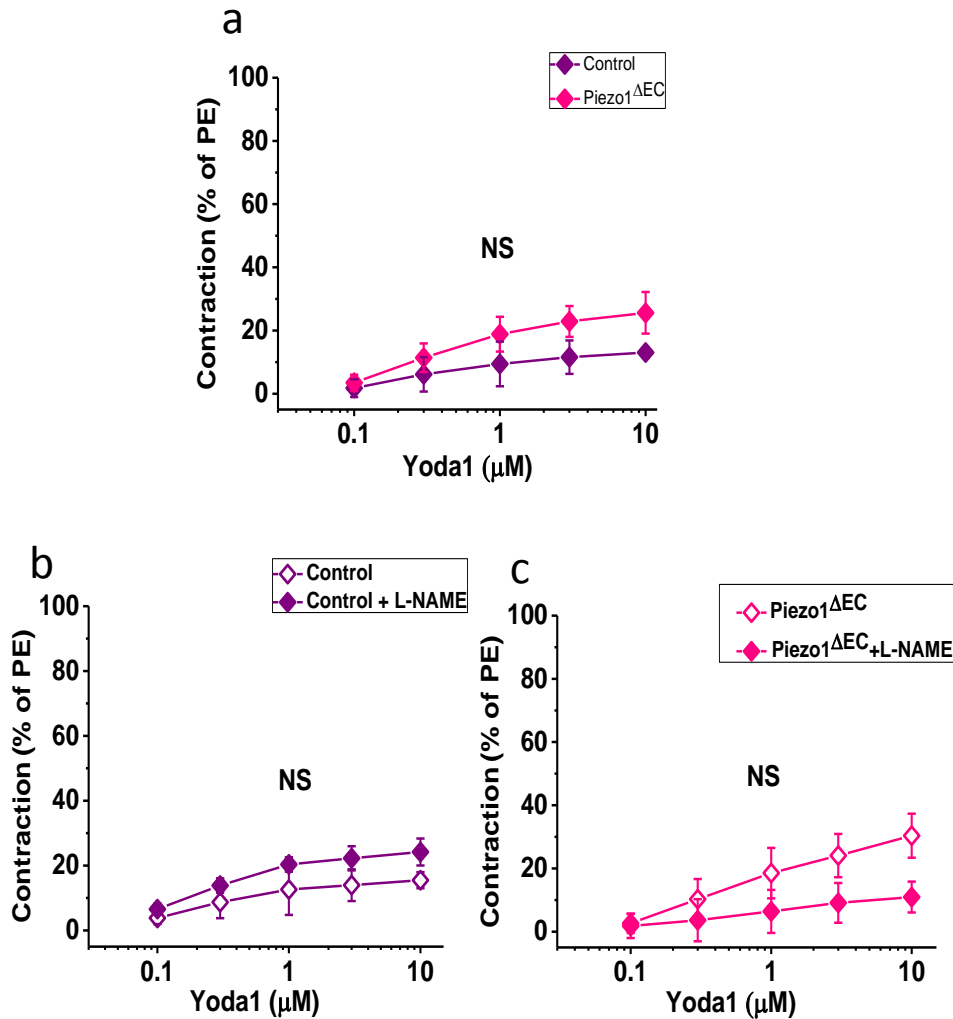


Figure 3-18: Yoda1 responses in control and Piezo1 ΔEC thoracic aorta

(a) Concentration-response curves for Yoda1-induced contraction (0.1, 0.3, 1, 3 and 10 μM) in control ($n=7$) and Piezo1 ΔEC ($n=5$) mice. (b) Concentration-response curves for Yoda1-induced contraction before ($n=3$) and after ($n=3$) L-NAME treatment in control mice. (c) Concentration-response curves for Yoda1-induced contractions before ($n=3$) and after ($n=3$) L-NAME treatment in Piezo1 ΔEC mice. Responses are expressed as percentages of the contraction in response to PE. Mean \pm SEM values are depicted. NS=not significant.

3.4 Discussion

The main finding presented in this chapter is that Yoda1 can induce relaxation in isolated mouse thoracic aorta pre-constricted by PE. Yoda1 relaxed mouse thoracic aorta via an endothelium and NO-dependent mechanism. Furthermore, Dooku1 was a very strong inhibitor of this Yoda1 response.

3.4.1 The Yoda-1 effect depends on endothelial cells

ECs play a critical role in regulating cardiovascular system function and in mediating vasorelaxation by releasing several vasodilating factors, including PGI₂, NO, and EDHF (Sandoo et al., 2010).

The data show that Yoda1 is unable to induce relaxation in vessels which were not PE pre-constricted (Fig. 3.3b), suggesting that Piezo1 may have a role in vasodilation and relaxation only after contraction has been induced by a vasoconstrictor agonist. In mouse thoracic aortae pharmacologically pre-contracted with PE, Yoda1 induced relaxation (Fig. 3.3c). Interestingly, this ability of Yoda1 to relax mouse thoracic aortae was EC dependent as no effect of Yoda1 was observed when the ECs were removed (Fig. 3.5a). These findings are consistent with previous reports (e.g. (Furchgott and Zawadzki, 1980) that the endothelial lining of blood vessels plays a vital role in facilitating vasodilator responses to relaxant agents such as ACh and substance P, due to the production of an endothelium-derived relaxing factor, later shown to be nitric oxide (Palmer et al., 1987).

3.4.2 Yoda-1 depends on NO generation by NOS

L-NAME almost completely blocks the Yoda-1 effect (Fig. 3.6a) suggesting that Yoda1 depends upon NO for its downstream effects. This is consistent with a study from Wang et al, (2016), which found activation of Piezo1 could lead to eNOS activation. They also found that Yoda1 caused relaxation of mouse mesenteric artery in a Piezo1-dependent manner as mice with specific deletion of endothelial-Piezo1 lost the ability to produce NO and relax in response to flow (Wang et al., 2016). Furthermore, Li et al observed that VEGF stimulated eNOS phosphorylation was reduced in aorta from whole body Piezo1 knockout (heterozygous) mice (Li et al., 2014).

No change was observed in the PE responses before and after removing the EC (Fig. 3.5c). These results were unexpected as findings from historical study show that removal of the endothelium from rat aortic rings results in an increase in contraction induced by vasoconstricting agents (Martin et al., 1986). Furthermore, L-NAME had no effect on the resting tension of the thoracic aortae (Fig. 3.6d) suggesting only a small basal release of NO in these arteries, which is in agreement with previous studies (Dora et al., 2000, Inoue et al., 2000). As expected, agents which inhibit NO synthesis produce an enhancement of vasoconstrictor-induced tone by removing this endothelium-dependent suppression of vasoconstriction (Mian and Martin, 1995, Moore et al., 1990). This was observed in the present study, as treatment of endothelial intact thoracic aortae segments with the NO synthase inhibitor, L-NAME, resulted in an increase of PE-induced tone (Fig. 3.5c).

There are only a small number of non-specific blockers available for Piezo1, including RR and Gd^{3+} which irreversibly block Piezo1 (Li et al., 2014). Gd^{3+} is widely used as a blocker of mechanosensitive channels and was thus used in this chapter. The effect of Yoda1 was largely prevented by pre-incubating the aortae with Gd^{3+} (Fig. 3.7a and b) and also by the Yoda1 competitive antagonist Dooku1 (Fig. 3.8a and b) that was found through a screen of Yoda1 analogues synthesised in the School of Chemistry at the University of Leeds in an attempt to find better pharmacological tools for Piezo1 study. The data suggest a specific effect of Dooku1 for Piezo1 channels. The inhibitory effect of Dooku1 against PE and U46619-induced contraction might be related to an unknown mechanism of Piezo1, either on EC or SMCs, or an unknown Piezo1 independent effect. Piezo1 function is not needed for normal myogenic tone, arguing against Retailleau et al, study ((Retailleau et al., 2015).

Together, the data suggest that the activation of Piezo1 by Yoda1 leads to NO formation and to relaxation of vascular tone. As shown in a previous study from our group,, Piezo1 is critical for endothelial cell alignment in response to shear stress and eNOS phosphorylation in the presence of VEGF (Li et al., 2014). Therefore, endothelial Piezo1 is needed for flow-induced formation of NO via eNOS and flow-induced relaxation. These results are novel and add significantly to our understanding of Yoda1-mediated vasomotor function by being the first to investigate the endothelium-dependent functional responses to Yoda1 and the underlying mechanisms, in thoracic aortae of mice. Dooku1, effectively and specifically inhibited Yoda1-induced Piezo1 channel activity.

3.4.3 Piezo1 EC knockout mice

The constrictive effect of Yoda1 was seen in both TAM-treated control and Piezo1^{ΔEC} mice, but was not observed in wild-type mice not treated with TAM. However, all mice exhibited normal responses to both PE and ACh. There is no clear explanation to reconcile the discrepancy between the Yoda1 response in wild-type aortae and vessels from control and Piezo1^{ΔEC} treated with TAM. Finding that Yoda1 could induce contraction was surprising and how one mechanism induced by Yoda1 treatment can be dominant in the Piezo1^{flox} mice, whereas another mechanism can be dominant in the wild-type mice is unclear. The differences could be related to the genotype or to the exposure of the mice to TAM. It would seem unlikely that introduction of loxP sites within intronic regions of the Piezo1 gene would account for the altered phenotype, however, different genetic backgrounds between the wild-type mice and Piezo1^{flox} mice may cause, for example, release of an unknown factor(s)/ mechanisms that might mediate the contractile effect of Yoda1.

Importantly, both Cre⁺ and Cre⁻ mice showed the same phenotype, suggesting that the contraction responses were potentially induced by genotype or TAM injection and could cause developmental effects or compensatory mechanisms contributing to the phenotype of Yoda1-induced contraction, and resulting in failure of Yoda1 to induce relaxation. Alternatively, different genetic strains of mice also may have an impact on the thoracic aorta's response to Yoda1. In this study, mice had a different genetic background, thus there is a possibility that different genetic strains of mice respond differently to Yoda1. Furthermore, the expression of molecules mediating cross-talk between Piezo1 activation and NO production may be different between the strains of mice. More research will be necessary to reconcile the disparity in these findings and to elucidate the consequences of different Yoda1 responses. It would also be useful to determine if this effect is the same in other vascular preparations.

3.5 Conclusion

These results demonstrate that Yoda1, a Piezo1 activator, causes vasodilation via an endothelium-dependent mechanism, mediated by NO in thoracic aortae of wild-type mice which is likely to be Piezo1 dependent. Furthermore, the Yoda1-induced relaxation was inhibited by Dooku1 and other Yoda1 analogues (3. 43). These data suggest that

Piezo1 may be a useful target for improving vasorelaxation in conduit arteries. Activation of Piezo1 by Yoda1 in the vasculature may be a potential strategy for improving the vascular dysfunction that exists in cardiovascular disease states, such as hypertension, or other disease states exhibiting vasomotor dysfunction due to impaired NO-dependent relaxation.

**Schematic representation of the mechanism of Yoda1-induced relaxation
proposed in this chapter**

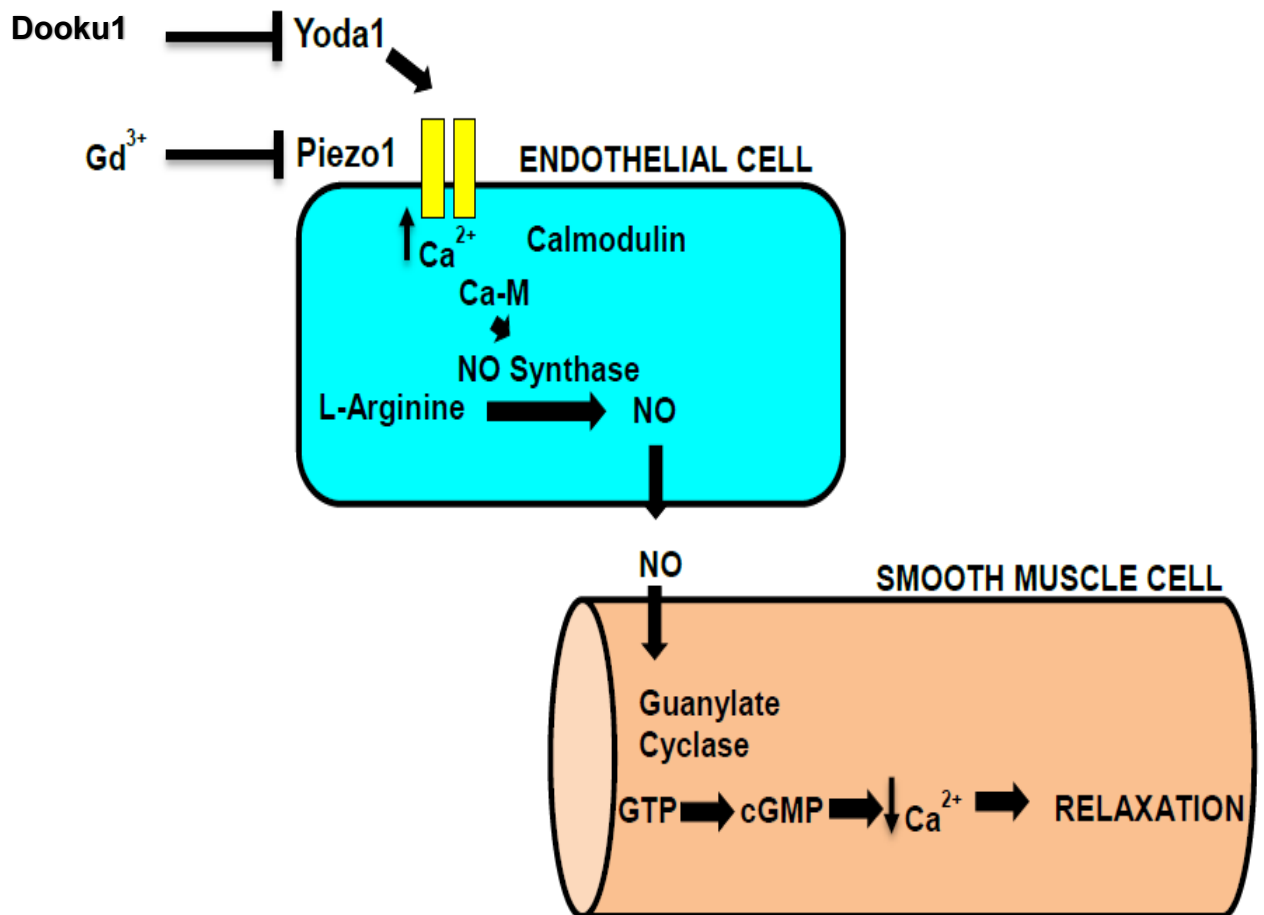


Figure 3-19: Mechanism of the relaxation effect by Yoda1

Chapter 4 Role of endothelial Piezo1 in second-order mesenteric arteries of mice

4.1 Abstract

4.1.1 Background

Resistance arteries, such as mesenteric arteries, provide more than 80% of the resistance to blood flow in the body. Consequently their responses are thought to play an important role in regulation of BP and blood flow. Additionally, many antihypertensive drugs work by reducing peripheral resistance. This study investigates the functional role of Piezo1 channels in modulating blood vessel contractility and relaxation, which sheds light on understanding the function of Piezo1 from a physiological perspective in these arteries.

4.1.2 Methods

Isolated mouse mesenteric arteries were studied using a wire myograph. Endothelial deletion of Piezo1 (Piezo1^{ΔEC}) in adult mice was achieved using a tamoxifen inducible Cre/Lox system.

4.1.3 Results

Second-order mesenteric arteries from wild-type and Piezo1^{ΔEC} mice responded similarly to PE and ACh. Moreover, the inhibition of ACh responses by apamin plus charybdotoxin was strong in arteries from Piezo1^{ΔEC} mice. Yoda1 caused relaxation in mouse mesenteric arteries from control and Piezo1^{ΔEC} mice, was endothelial independent. Furthermore, NO but not the EDHF was involved in Yoda1-induced relaxation. Although Piezo1 blockers inhibited Yoda1-induced relaxation, this relaxation effect of Yoda1 was not affected by removing the ECs.

4.1.4 Conclusion

Endothelial Piezo1 promotes resistance to the ACh-induced relaxation mediated by EDHF. However, activation of the Piezo1 channel by Yoda1 leads to relaxation. Although NO played a role, the relaxation was largely independent of the endothelium.

4.2 Introduction

Isolated ECs have been studied but a role for Piezo1 has yet to be studied in the context of an intact vessel. Functional experiments to assess the vessel's responsiveness to several agonists were administered using a four chamber wire myograph (Danish Myotechnology, Aarhus, Denmark). Wire myography (described in more detail in chapter 2) is a technique which was introduced to study vascular function *in-vitro* (Mulvany & Halpern, 1977). It represented an improvement on the study of vessels in organ baths because the mounting procedure is not compatible with small resistance vessels thus the technique is limited to the study of only larger vessels. Wire myography allowed the functional responsiveness of small resistance vessels *in-vitro* to be measured assessing the interaction of ECs with SMCs. Mesenteric arteries were chosen because they contribute substantially to the regulation of BP. Mechanisms attributed to local blood flow control vary depending on tissue type and can be modulated *in vivo* by central control mechanisms. This is often linked to the cell types involved and the tissue innervation. BP can be altered by changing the total peripheral resistance of the vascular system; where increasing the resistance increases the pressure of the system. Therefore, the vascular tone experienced in large vascular beds, such as mesenteric beds, can easily influence systemic BP.

The mesenteric organs comprise about 5% of body mass, but receive about 30% of blood flow distributed from cardiac output. The mesenteric arteries are composed of "arcades" or branching arteries from the main mesenteric artery. Primary branches are the first branches off of the mesenteric artery. Secondary branches branch off from the primary, and so on, with quaternary branches wrapping around the intestine itself to supply the intestinal tissues directly. Mesenteric arteries with diameters ~100-300 μm in diameter display what is known as a myogenic response which has been well described by many researchers (Bayliss, 1902, Christensen and Mulvany, 2001, Mulvany and Aalkjaer, 1990, Mulvany, 1994, Khavandi et al., 2008). The myogenic response causes

a vessel to constrict in response to an increase in BP. The myogenic response is thought to be a mechanosensor because it senses wall tension, which will induce the constriction of the vessel (Johnson, 1991, VanBavel and Mulvany, 1994). This response, in what are known as small muscular arteries and resistance arterioles, is thought to play an important role in regulation of BP and blood flow (Christensen and Mulvany, 2001).

This study aimed to elucidate the role of Piezo1 channels in modulating blood vessel contractility and relaxation. Vascular responses to vasoconstricting and vasorelaxing factors and Yoda1 were studied in mice with or without endothelial-specific deletion of Piezo1. The dependence of vasorelaxation on NO and EDHF was also investigated.

4.3 Results

The role of Piezo1 in ACh- and Yoda1-induced relaxation was studied by wire myograph on isolated mesenteric arteries of Piezo1^{ΔEC} mice and control mice.

4.3.1 Deletion of endothelial cell Piezo1 affects high potassium-induced contraction

To establish artery viability, high K⁺ is usually used to examine the contractile function of the vessel segments. This disrupts the K⁺ concentration gradient across the cell membrane resulting in depolarisation of SMCs, which consequently leads to Ca²⁺ influx through LTCCs, inducing VSMCs contraction.

Mesenteric arteries from control and Piezo1^{ΔEC} mice displayed typical K⁺-induced contraction (Fig. 4.1a and b, respectively). The magnitude of the K⁺-induced contraction was significantly decreased in mesenteric arteries of Piezo1^{ΔEC} mice by 40% (Fig. 4.1c). These data suggest that in ECs, Piezo1 deletion may reduce K⁺-induced contraction via an unknown mechanism.

4.3.2 Deletion of endothelial cell Piezo1 does not affect phenylephrine-induced contraction

PE is a vasoconstrictor that closely mimics the effects of the endogenous hormones epinephrine and NE. It is an α 1-adrenergic receptor agonist. α 1 receptors are members of the GPCRs family and are coupled to Gq, thus their activation results in a rise in $[Ca^{2+}]_i$. The overall effect is vasoconstriction (a detailed description of the PE mechanisms are provided in Fig. 4.2) (Prewitt et al., 2002, Billington and Penn, 2003). Mesenteric arteries from control and Piezo1 ^{Δ EC} mice displayed typical PE-induced contraction (Fig. 4.3a and b). PE-induced contraction in control and Piezo1 ^{Δ EC} mice had similar responses (Fig. 4.3c) (control mice EC₅₀ value: $0.16 \pm 0.01 \mu\text{M}$, $n=10$, Piezo1 ^{Δ EC} mice EC₅₀ value: $0.18 \pm 0.07 \mu\text{M}$ $n=10$). Fig. 4.3d shows the AUC of the response to PE for each individual curve. These data suggest that endothelial cell Piezo1 has no role in PE-induced contraction.

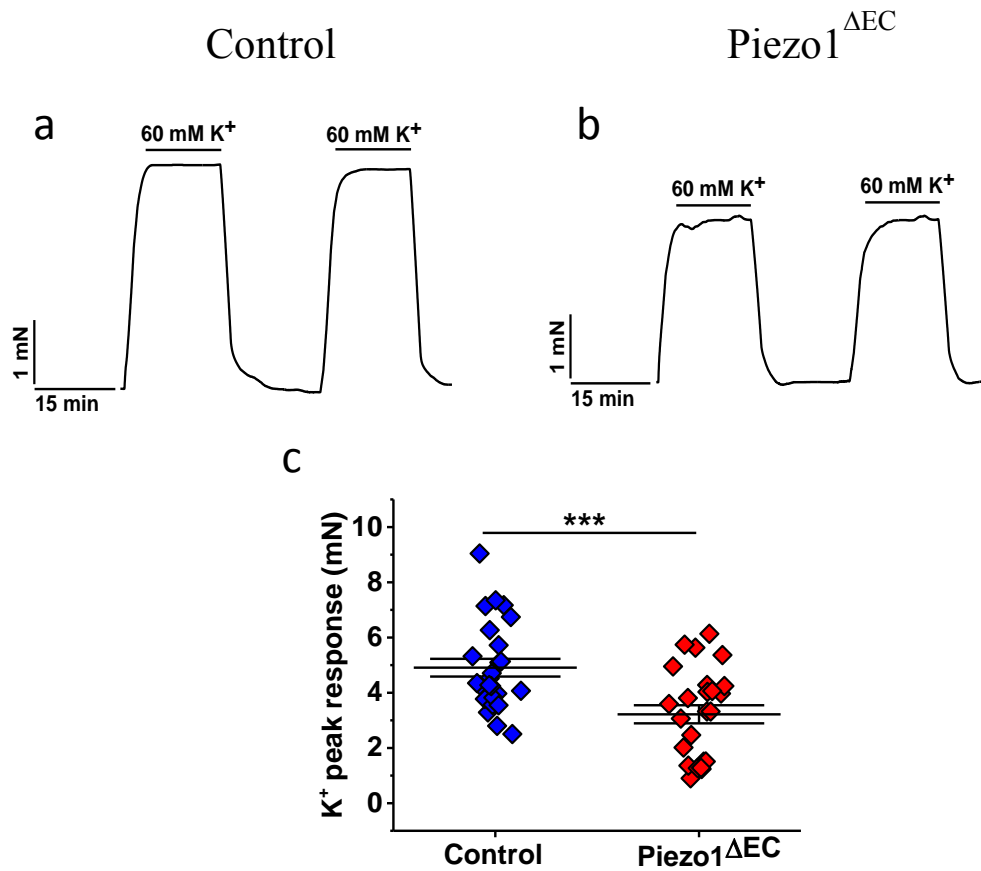
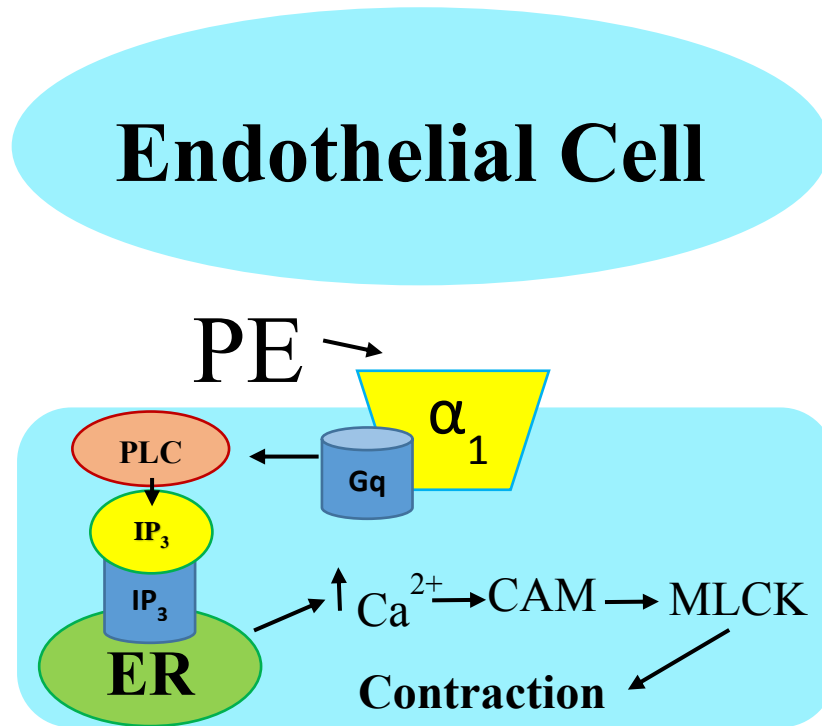


Figure 4-1: Vascular reactivity to high potassium (60 mM K⁺) in control compared with endothelial Piezo1^{ΔEC} mesenteric arteries

(a) Typical wire myograph trace, demonstrating vasoconstriction in response to high potassium solution that validates arterial viability prior to experimentation, in mesenteric arteries isolated from control mice. (b) As for (a) except in mesenteric arteries isolated from Piezo1^{ΔEC} mice. (c) Comparison of response to high potassium (K⁺)-induced contraction in mesenteric arteries of control ($n=25$) and Piezo1^{ΔEC} mice ($n=25$). Responses are expressed by the absolute value of the K⁺-induced contraction. Mean \pm SEM values are depicted. Asterisks indicate statistically significant difference (***, $p < 0.001$).



Vascular Smooth Muscle

Figure 4-2: Mechanisms of contraction in a vascular smooth muscle cell

Phenylephrine (PE) can increase contraction by activating α_1 adrenoceptors which are coupled to stimulate Gq. The resulting activation of PLC leads to the formation of inositol triphosphate (IP_3) from PIP_2 . IP_3 activates IP_3 receptors on the sarcoplasmic reticulum (SR) to cause Ca^{2+} to be released from the SR, an intracellular Ca^{2+} store, thus leading to Ca^{2+} -calmodulin-dependent stimulation of myosin light-chain kinase (MLCK) and subsequent phosphorylation of the myosin regulatory light chain and enhance of actin-myosin interaction (contraction). This mechanism causes contraction.

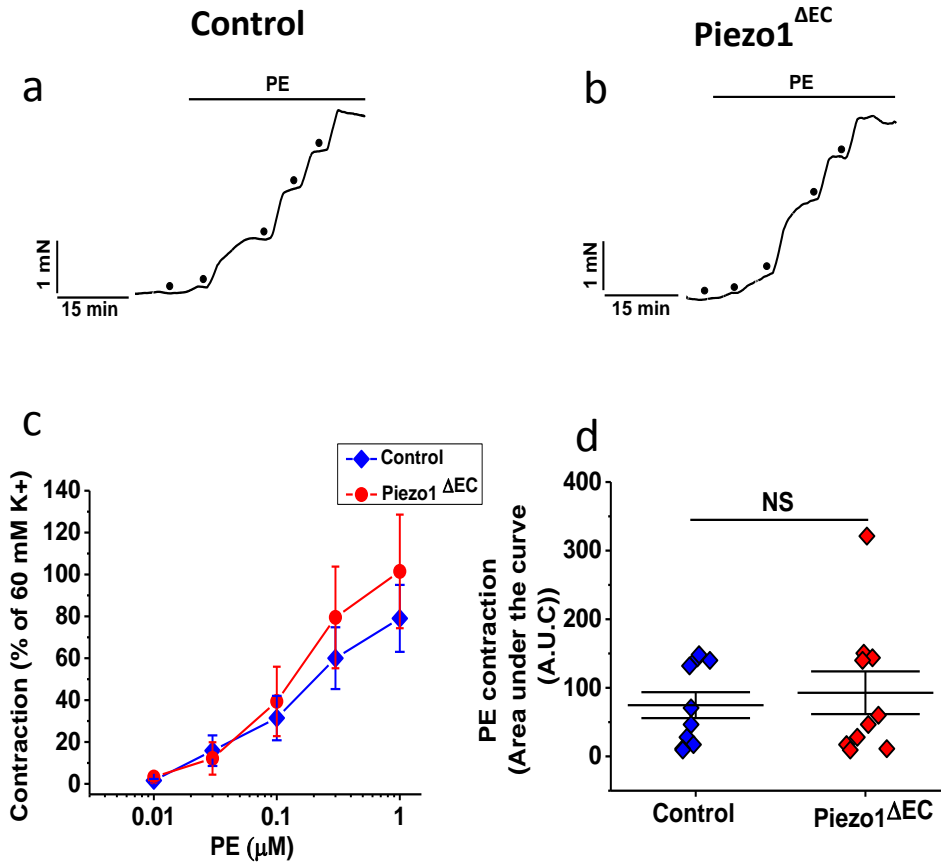


Figure 4-3: Vascular reactivity to phenylephrine in control compared with endothelial *Piezo1*^{ΔEC} mesenteric arteries

(a) Typical wire myograph tracing, demonstrating increased tone in response to phenylephrine (PE) as indicated by the dots (0.01, 0.03, 0.1, 0.3 and 1 μM) in mesenteric arteries isolated from control mice. (b) As for (a) except in mesenteric arteries isolated from *Piezo1*^{ΔEC} mice. (c) Concentration response curves to PE in control; $n=10$) and *Piezo1*^{ΔEC} ($n=10$) mice. (d) The area under the curve (AUC) of the response to PE for each individual curve of mesenteric arteries isolated from control ($n=10$) and *Piezo1*^{ΔEC} mice ($n=10$). Responses are expressed as percent constriction and as the area under the curve (AUC) of the response to PE. Mean \pm SEM values are depicted. NS=not significant.

4.3.3 Deletion of endothelial cell Piezo1 potentiates ACh-induced vasorelaxation

ACh is a neurotransmitter that activates muscarinic receptors in the resistance vessels and is commonly used in vascular research to enhance vasodilation. ACh essentially acts through increasing cellular levels of NO, prostacyclin and EDHF. NO increase sGC activity (Francis et al., 2010), to mediate the GTP conversion to cGMP. This activates PKG (cGMP-dependent protein kinase), the major protein that is responsible for NO relaxation (Hofmann et al., 2006). PKG decreases the concentration of $[Ca^{2+}]_i$ and subsequently reduces Ca^{2+} -dependent activation of MLC kinase, resulting in relaxation (Fig. 4.4). Prostacyclin is an eicosanoid of the cyclooxygenase pathway, induce relaxation of SMCs in most blood vessels. EDHF functions by the activation of $IK_{Ca^{2+}}$ and $SK_{Ca^{2+}}$ thus inducing K^+ efflux. Hyperpolarisation is transmitted from ECs to VSMCs via gap junctions causing hyperpolarisation. These experiments attempted to assess whether deletion of endothelial Piezo1 alters the vasoreactivity in response to ACh.

Mesenteric arteries from control and Piezo1 $^{\Delta EC}$ mice displayed typical ACh-induced relaxation (Fig. 4.5a and b). Vasodilation to ACh was enhanced in Piezo1 $^{\Delta EC}$ compared with control arteries at concentrations of 0.01 and 0.1 μM (Fig. 4.5c), however, no difference was found in the AUC of the response to ACh for each individual curve in both groups (Fig. 4.5d). Overall, this suggests that the response to ACh might have a partial, but fairly small, dependence on endothelial Piezo1.

4.3.4 Deletion of endothelial cell Piezo1 affected EDHF-mediated-vasorelaxation

ACh can induce vessel relaxation by the EDHF pathway (Fig. 4.6). A rise in EC $[Ca^{2+}]_i$ causes stimulation of $IK_{Ca^{2+}}$ and $SK_{Ca^{2+}}$, resulting in endothelial hyperpolarisation (Edwards and Weston, 1998). The endothelial hyperpolarisation can then be transferred to SMCs through EC-SMCs gap junctions to cause hyperpolarisation of SMCs and consequently relaxation (Edwards et al., 1998). The EDHF-mediated response can be inhibited by a combination of charybdotoxin, which blocks $IK_{Ca^{2+}}$, and apamin, which blocks small $SK_{Ca^{2+}}$ then prevent the hyperpolarisation (Kang, 2014). $IK_{Ca^{2+}}$ and $SK_{Ca^{2+}}$ are critical for EDHF where these channels are arranged in endothelial microdomains,

particularly within projections towards the adjacent smooth muscle, which are rich in $IK_{Ca^{2+}}$ channels and close to interendothelial gap junctions where $SK_{Ca^{2+}}$ channels, are prevalent (Garland and Dora, 2016).

Mesenteric arteries from control mice displayed typical trace of ACh-induced relaxation before and after incubation with apamin plus charybdotoxin (Fig. 4.7a). No difference was observed in the resting tone of mouse mesenteric arteries when the combination of apamin plus charybdotoxin inhibitors was used (Fig. 4.7b). However, greater contraction that did not achieve significance was observed in response to PE (Fig. 4.7c).

Incubating mesenteric arteries from control mice with apamin plus charybdotoxin reduced the ACh induced-relaxation at 0.1 and 0.3 μ M concentrations (Fig. 4.7d). However, no significant difference was found in the AUC of the response to ACh before and after the incubation with apamin plus charybdotoxin (Fig. 4.7e). The results suggest that EDHF played a minor role in ACh-induced relaxation.

As for control mice, no differences were observed in either the resting tone (Fig. 4.8b) or the response to PE (Fig. 4.8c) when the combination of the inhibitors apamin and charybdotoxin was used on Piezo1 Δ^{EC} mouse mesenteric arteries. In contrast, however, ACh-induced relaxation was reduced by 80% after incubation with apamin plus charybdotoxin (Fig. 4.8a, 4.8d and 4.8e). The difference in the AUC of the response to ACh before and after the incubation with apamin plus charybdotoxin was compared between control and Piezo1 Δ^{EC} mice and it was significantly different (Fig. 4.9). The results suggest that Piezo1 has an anti-EDHF effect.

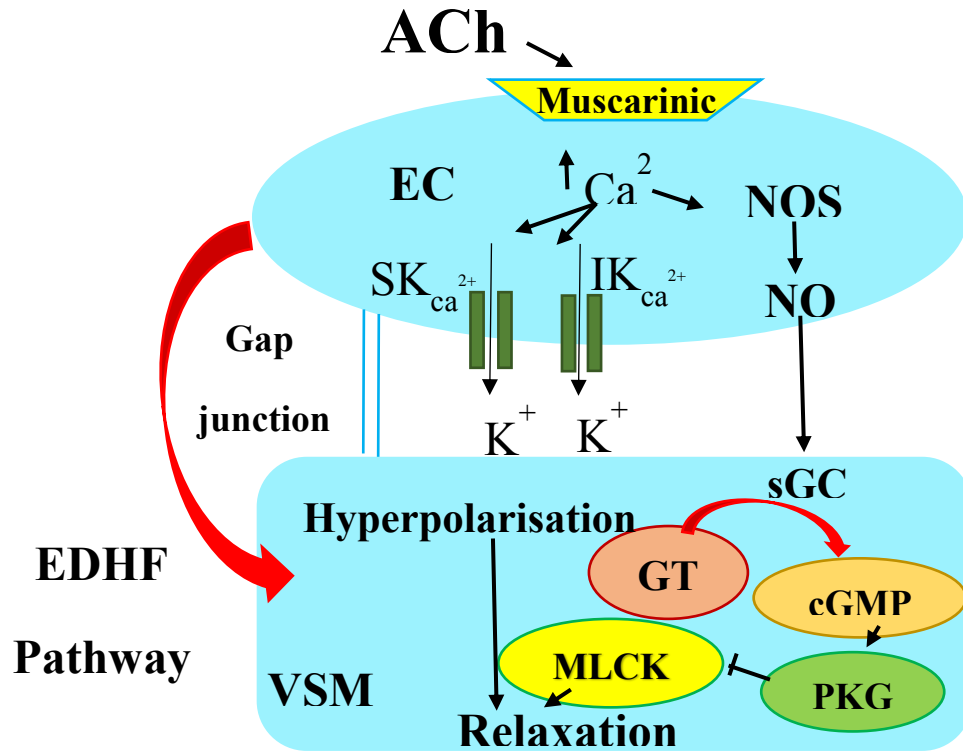


Figure 4-4: The nitric oxide (NO) and endothelial derived hyperpolarization factor (EDHF) pathway in the vascular smooth muscle cells leading to cell relaxation

ACh activates muscarinic receptors increasing cellular levels of NO, prostacyclin and EDHF. In the NO pathway, the endothelial form of NO synthase (NOS) converts L-arginine to NO and citrulline. NO is released and diffuses to the vascular smooth muscle cells to activate soluble guanylate cyclase (sGC), which converts guanosine triphosphate (GTP) to cyclic guanosine monophosphate (cGMP) to activate protein kinase G (PKG) and consequently can block myosin light chain kinase (MLCK), leading to relaxation. In the EDHF pathway, endothelial-dependent agonists activate endothelial cell receptors leading to entry of extracellular and the release of intracellular Ca^{2+} and synthesis of EDHF. Along with the synthesis of EDHF, hyperpolarisation of ECs occurs since the increased Ca^{2+} activates Ca^{2+} -dependent K^+ -channels (KCa^{2+}), intermediate conductance calcium-activated K^+ channels ($IKCa^{2+}$) and small conductance K^+ -channels ($SKCa^{2+}$) thus inducing K^+ efflux. Hyperpolarisation is transmitted from endothelial to vascular smooth muscle cells (VSMCs) via gap junctions. Within the VSMCs it activates $K_{Ca^{2+}}$ channels, causing endothelial-dependent hyperpolarisation and relaxation.

Inhibition. —| Activation. →

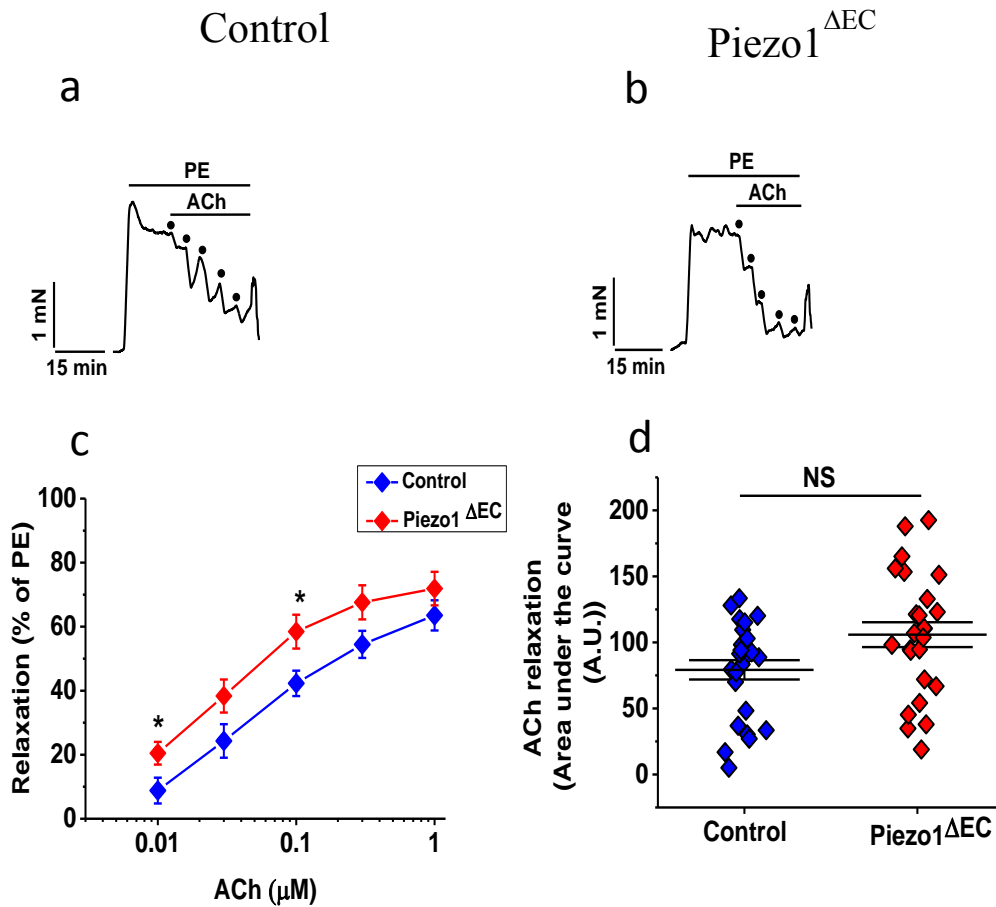


Figure 4-5: Vascular reactivity to ACh in control compared with endothelial $Piezo1^{\Delta EC}$ mesenteric arteries

(a) Typical trace showing a concentration-dependent dilatory response to acetylcholine (ACh) as indicated by the dots (0.01, 0.03, 0.1, 0.3 and 1 μM) in mesenteric arteries isolated from control mice. (b) As for (a) except in mesenteric arteries isolated from $Piezo1^{\Delta EC}$ mice. (c) Concentration response curves to ACh in control (n=25) and $Piezo1^{\Delta EC}$ (n=25) mice. (d) The area under the curve (AUC) of the response to ACh of mesenteric arteries isolated from control (n=25) and $Piezo1^{\Delta EC}$ mice (n=25). Responses are expressed as percent relaxation, and as the area under the curve (AUC) of the response to ACh. Mean \pm SEM values are depicted. Asterisks (*) indicate statistically significant difference in ACh response between control and $Piezo1^{\Delta EC}$ mice ($p < 0.05$). NS=not significant.

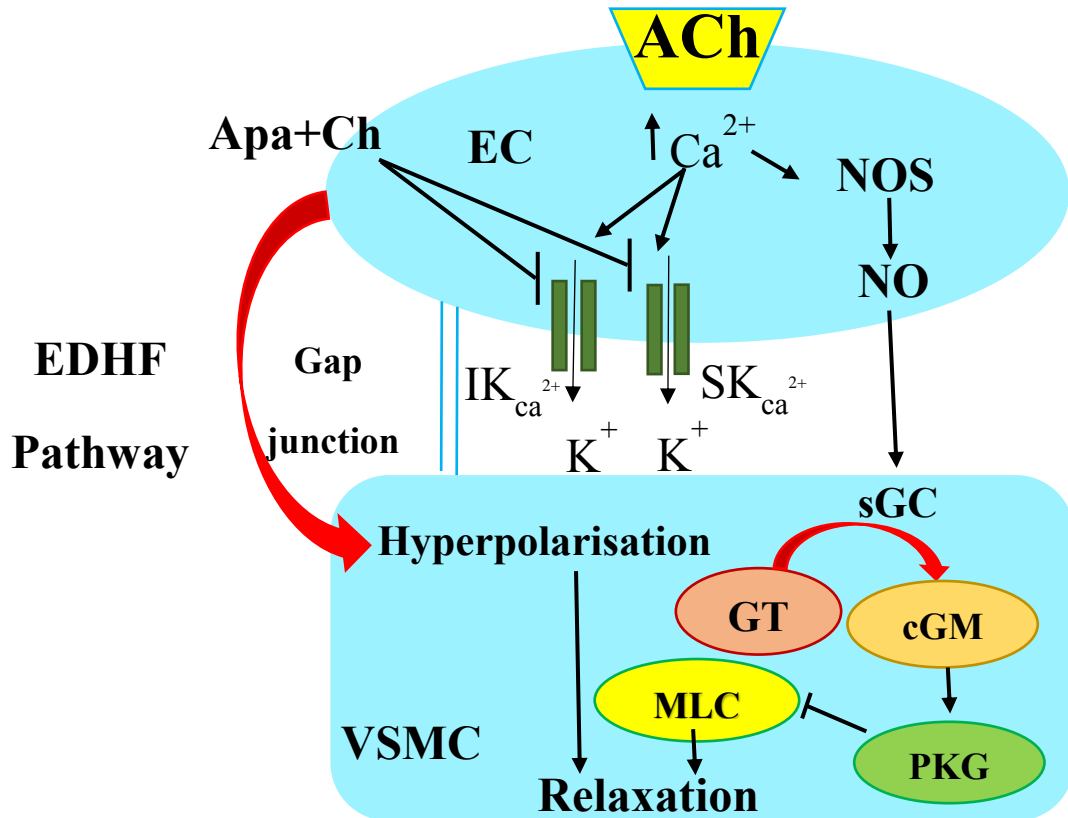


Figure 4-6: Inhibition of endothelial derived hyperpolarisation factor (EDHF)

Endothelial-dependent agonists activate endothelial cell receptors leading to entry of extracellular and the release of intracellular Ca^{2+} and synthesis of EDHF. Along with the synthesis of EDHF, hyperpolarisation of endothelial cells occurs since Ca^{2+} activates Ca^{2+} -dependent K^+ -channels (KCa^{2+}), intermediate conductance calcium-activated K^+ channels ($IKCa^{2+}$) and small conductance K^+ -channels ($SKCa^{2+}$), which all mediate K^+ efflux. EDHF diffuses to vascular smooth muscle cells (VSMCs), activates KCa^{2+} channels and cause endothelial-dependent hyperpolarisation and relaxation. The combination of two toxins, apamin (Apa) that blocks $SKCa^{2+}$ and charybdotoxin (Ch) that inhibits $IKCa^{2+}$, abolishes EDHF-mediated responses. Inhibitors of EDHF do not entirely block the agonist-induced relaxation because the NO pathway remains.

Inhibition $\text{---}\perp$. Activation $\text{---}\rightarrow$.

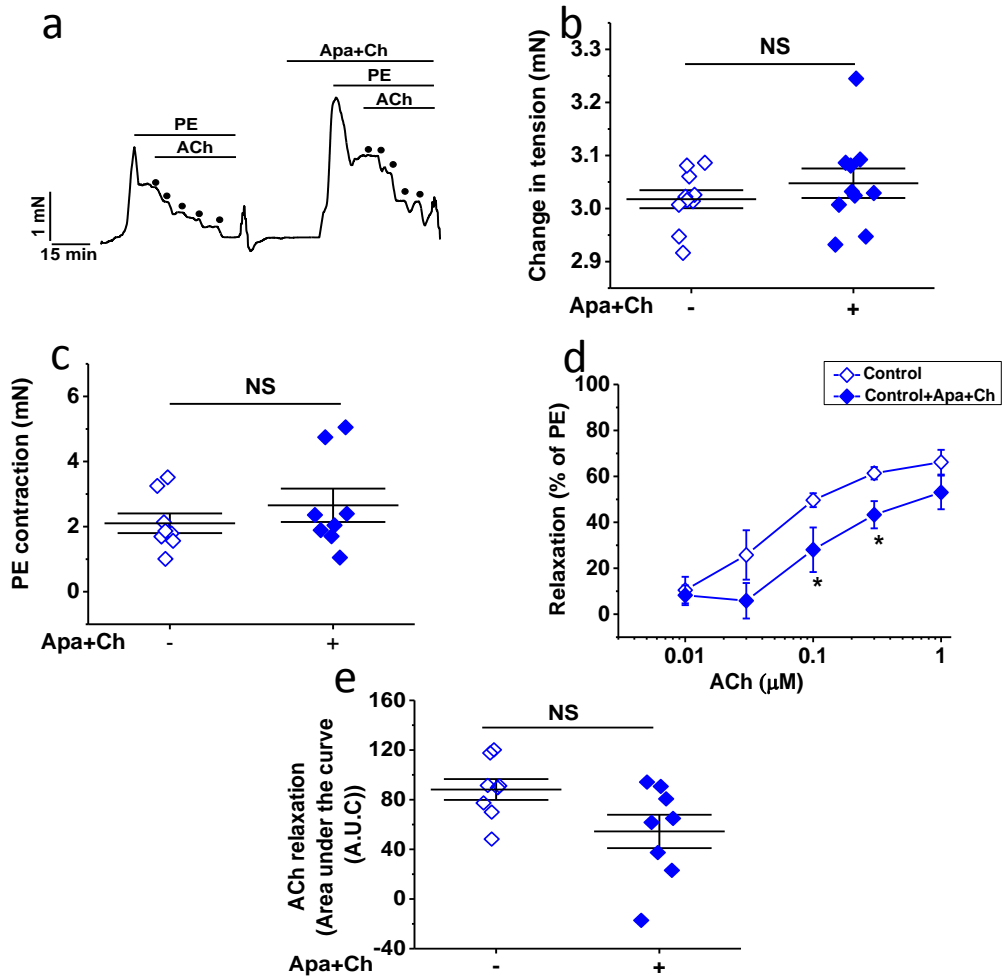


Figure 4-7: EDHF-mediated-vasorelaxation in control mice

(a) Typical trace showing a concentration-dependent dilatory response to acetylcholine (ACh) as indicated by the dots (0.01, 0.03, 0.1, 0.3 and 1 μM) before and after the incubation with apamin (Apa) (500 nM) plus charybdotoxin (Ch) (100 nM) in mesenteric arteries isolated from control mice. (b) Quantification of the Apa+Ch effects on the basal mesenteric artery tension ($n=8$). (c) Quantification of the Apa+Ch effects on phenylephrine (PE)-induced constriction in control mesenteric arteries of mice ($n=8$). (d) Concentration response curves to ACh before and after the application of Apa+Ch in control mesenteric arteries of mice ($n=8$). (e) The area under the curve (AUC) of the response to ACh before and after the incubation with Apa+Ch of mesenteric arteries, isolated from control mice ($n=8$). Responses are expressed as percent constriction and as the area under the curve (AUC) of the response to ACh. Mean \pm SEM values are depicted. Asterisks (*) indicate statistically significant difference in ACh response ($p < 0.05$). NS=not significant.

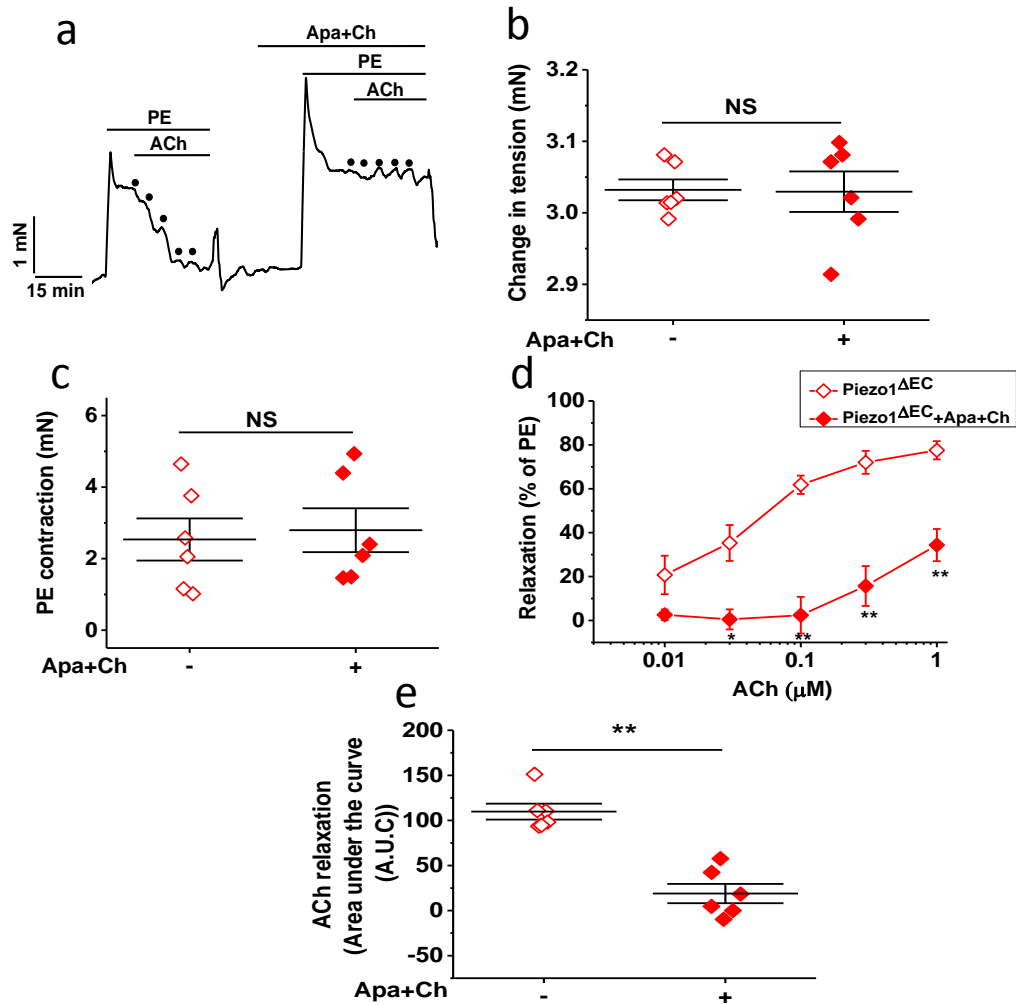


Figure 4-8: EDHF-mediated-vasorelaxation in endothelial Piezo1^{ΔEC} mice

(a) Typical trace showing a concentration-dependent dilatatory response to acetylcholine (ACh) as indicated by the dots (0.01, 0.03, 0.1, 0.3 and 1 μM) before and after the incubation with apamin (Apa) (500 nM) plus charybdotoxin (Ch) (100 nM) in mesenteric arteries isolated from Piezo1^{ΔEC} mice. (b) Quantification of the Apa+Ch effects on the basal artery tension ($n=6$). (c) Quantification of the Apa+Ch effects on phenylephrine (PE)-induced constriction in Piezo1^{ΔEC} mesenteric arteries of mice ($n=6$). (d) Concentration response curves to ACh before and after the application of Apa+Ch in Piezo1^{ΔEC} mesenteric arteries of mice ($n=6$). (e) The area under the curve (AUC) of the response to ACh before and after the incubation with Apa+Ch of mesenteric arteries isolated from Piezo1^{ΔEC} mice ($n=6$). Responses are expressed as percent constriction and as the area under the curve (AUC) of the response to ACh. Mean \pm SEM values are depicted. Asterisks (**) indicate statistically significant difference ($p < 0.01$). NS=not significant.

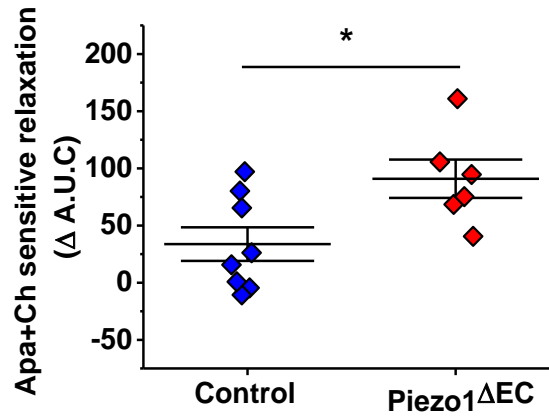


Figure 4-9: Comparison of EDHF-mediated-vasorelaxation in control and endothelial Piezo1 Δ EC mice

The difference in the area under the curve (AUC) of the response to acetylcholine (ACh) before and after incubation with apamin (Apa) (500 nM) plus charybdotoxin (Ch) (100 nM) of mesenteric arteries isolated from control and Piezo1 Δ EC mice ($n=8$ and 6, respectively). Data are expressed as the area under the curve (AUC) of the response to ACh. Mean SEM values are depicted. Asterisks (*) indicate statistically significant difference ($p < 0.05$).

4.3.5 Deletion of endothelial cell Piezo1 does not affect NO-mediated-vasorelaxation

L-NAME is a NOS inhibitor, which tends to be analogue of arginine that features substitutions of the guanidino nitrogen (Fig. 4.10) (Huang et al., 1995). L-NAME was used to study the contribution of NO to ACh-evoked vasodilatation.

Mesenteric arteries from control mice displayed typical trace of ACh-induced relaxation before and after the incubation with L-NAME (Fig. 4.11a). No difference was observed in the resting tone of mice mesenteric arteries in the presence of L-NAME (Fig. 4.11b). However, increased contraction was observed in response to PE by 50% (Fig. 4.11c). L-NAME reduced the ACh-mediated relaxation in mesenteric arteries from control mice by 62% (Fig. 4.11d). A significant difference was found in the AUC of the response to ACh, before and after the incubation with L-NAME (Fig. 4.11e).

Similar to control mice, no differences were observed in the resting tone of mesenteric arteries from Piezo1^{ΔEC} mice when L-NAME was present (Fig. 4.12b). However, in the contractile response to PE was increased by 42% (Fig. 4.12c). L-NAME also had a significant effect on ACh-induced relaxation in mesenteric arteries from Piezo1^{ΔEC} mice (77% reduction) (Fig. 4.12d). A significant difference was found in the AUC of the response to ACh before and after incubation with L-NAME (Fig. 4.12e).

The difference in the AUC of the response to ACh before and after the incubation with L-NAME was compared between control and Piezo1^{ΔEC} mice and no significant difference was observed (Fig. 4.13). These data indicate that Piezo1 deletion did not affect NO mediation of endothelium-dependent relaxation.

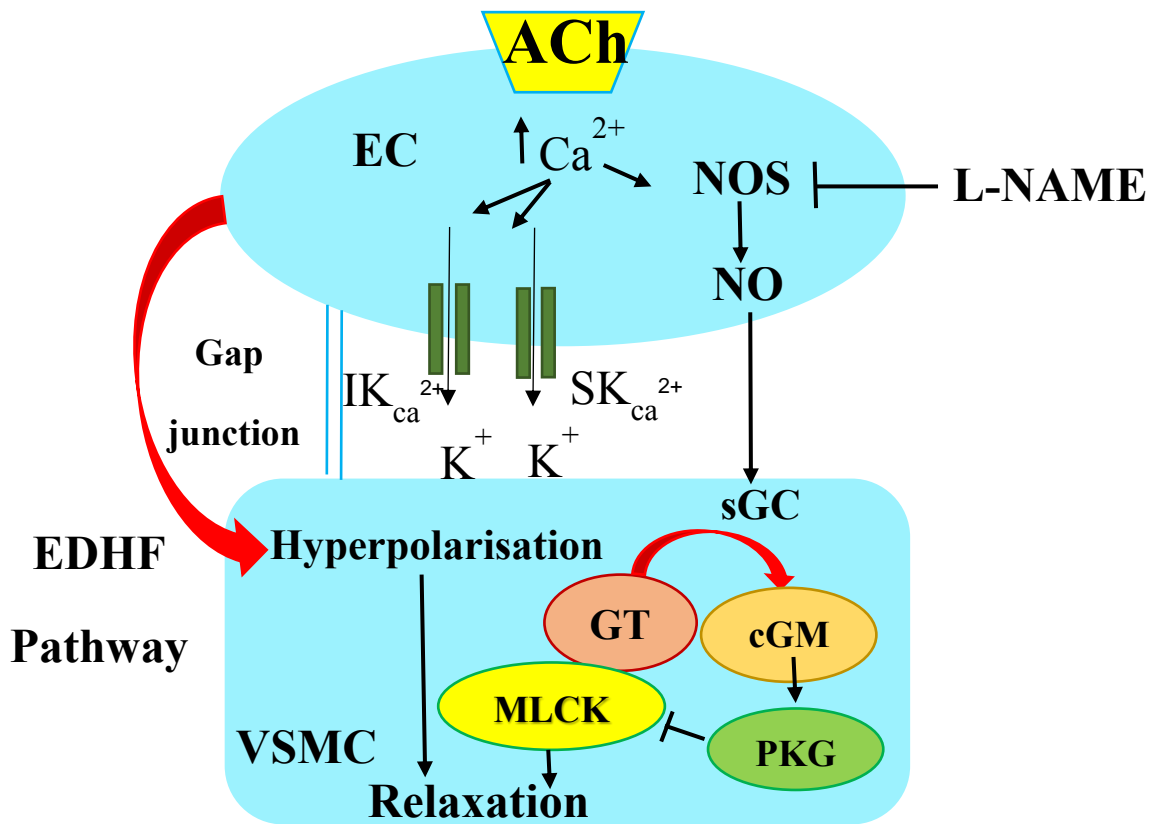


Figure 4-10: The nitric oxide (NO) inhibition

The endothelial form of NO synthase (NOS) is expressed which can convert L-arginine to NO and citrulline. NO is released and diffuses to the vascular smooth cells to activate soluble guanylyl cyclase (sGC), which converts guanosine triphosphate (GTP) to cyclic guanosine monophosphate (cGMP) to activate protein kinase G (PKG) leading to relaxation. NOS could be inhibited by *N* $^{\omega}$ -nitro-L-arginine methyl ester hydrochloride (L-NAME) leads to a reduction in NOS activity and therefore in NO production. However, EDHF mediates relaxation still release.

Inhibition $\text{---}\perp$. Activation $\text{---}\rightarrow$.

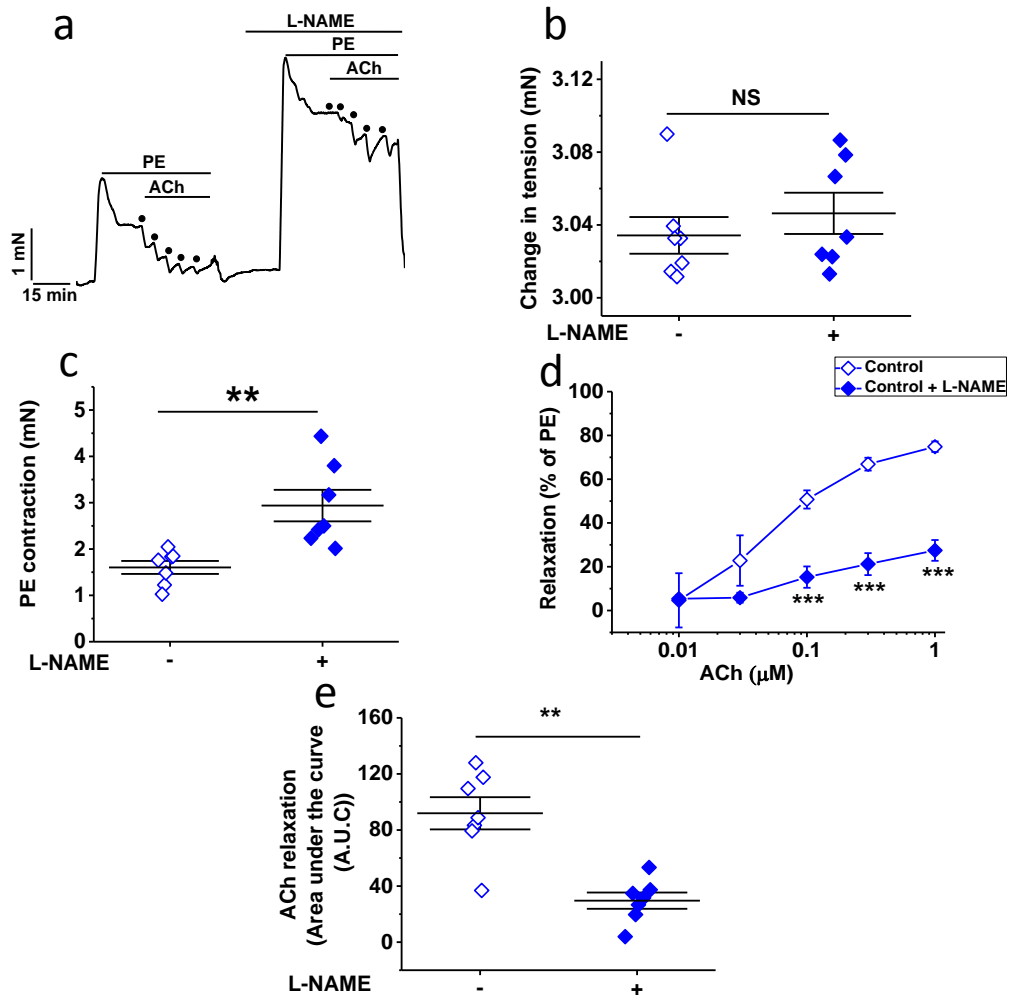


Figure 4-11: NO-mediated-vasorelaxation in control mice

(a) Typical trace showing a concentration-dependent dilatory response to acetylcholine (ACh) as indicated by the dots (0.01, 0.03, 0.1, 0.3 and 1 μM) before and after the incubation with (100 μM) *N_w*-nitro-L-arginine methyl ester hydrochloride (L-NAME) in endothelium-intact mesenteric arteries isolated from control mice. (b) Quantification of the L-NAME effects on the basal mesenteric artery tension ($n=7$). (c) Quantification of the L-NAME effects on phenylephrine (PE)-induced constriction in control mesenteric arteries of mice ($n=7$). (d) Concentration response curves to ACh before and after the application of L-NAME in control mesenteric arteries mice ($n=7$). (e) The area under the curve (AUC) of the response to ACh before and after incubation with L-NAME of mesenteric arteries isolated from control mice ($n=7$). Responses are expressed as percent constriction and as the area under the curve (AUC) of the response to ACh. Mean \pm SEM values are depicted Asterisks (**, ***) indicate statistically significant difference ($p<0.01$ and 0.001). NS=not significant.

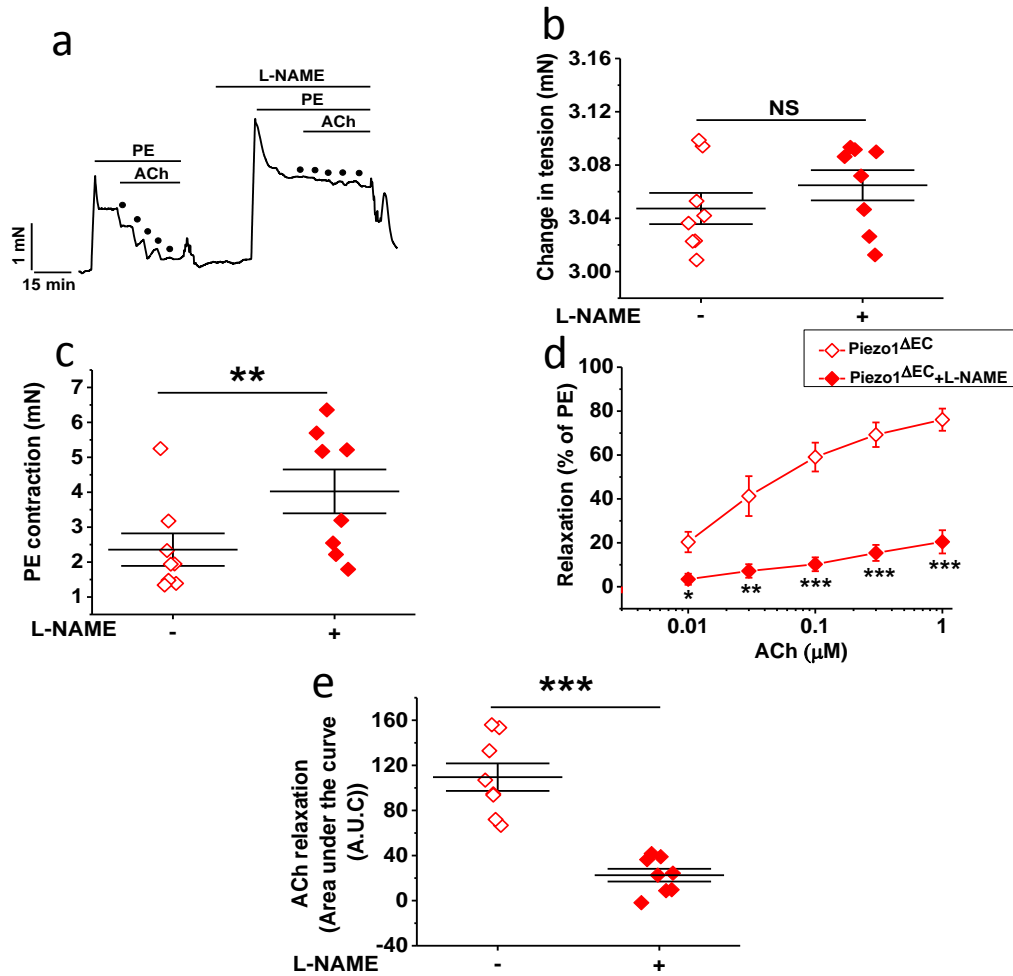


Figure 4-12: NO-mediated-vasorelaxation in endothelial Piezo1 Δ EC mice

(a) Typical trace showing a concentration-dependent dilatatory response to acetylcholine (ACh) as indicated by the dots (0.01, 0.03, 0.1, 0.3 and 1 μ M) before and after incubation with (100 μ M) *N*_ω-nitro-L-arginine methyl ester hydrochloride (L-NAME) in endothelium-intact mesenteric arteries isolated from Piezo1 Δ EC mice. (b) Quantification of the L-NAME effects on the basal mesenteric artery tension ($n=8$). (c) Quantification of the L-NAME effects on phenylephrine (PE)-induced constriction in Piezo1 Δ EC mesenteric arteries of mice ($n=8$). (d) Concentration response curves to ACh before and after the application of L-NAME in Piezo1 Δ EC mesenteric arteries of mice ($n=8$). (e) The area under the curve (AUC) of the response to ACh before and after the incubation with L-NAME of mesenteric arteries isolated from Piezo1 Δ EC mice ($n=8$). Responses are expressed as percent constriction and as the area under the curve (AUC) of the response to ACh. Mean \pm SEM values are depicted. Asterisks (*, **, ***) indicate statistically significant difference ($p < 0.05$, 0.01 and 0.001). NS=not significant.

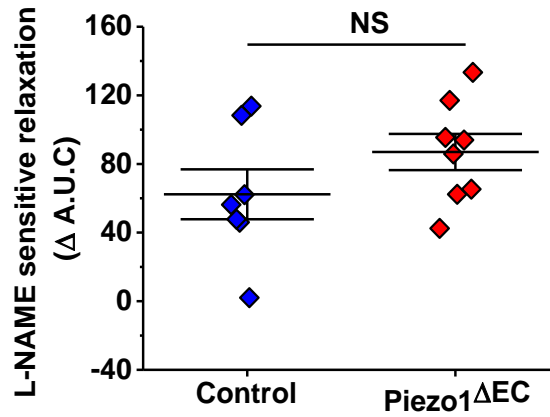


Figure 4-13: Comparison of NO-mediated-vasorelaxation in control and endothelial Piezo1^{ΔEC} mice.

The difference in the area under the curve (AUC) of the response to acetylcholine (ACh) before and after incubation with *N*_ω-nitro-L-arginine methyl ester hydrochloride (L-NAME) in mesenteric arteries isolated from control and Piezo1^{ΔEC} mice (*n*=7 and 8, respectively). Data are expressed as the area under the curve (AUC) of the response to ACh. Mean ± SEM values are depicted. NS=not significant.

4.3.6 The effect of removal of endothelial cells on ACh-induced relaxation

To evaluate whether the relaxation caused by ACh was dependent on the endothelium, the endothelium was removed by introducing into the lumen a wire and rubbing it back and forth various times. Mesenteric arteries from control mice were pre-constricted with 0.3 μM PE, then ACh (0.01–1 μM) was administered in the presence (Fig. 4.14a) or absence of ECs (Fig. 4.14b). PE constriction is dependent on SMCs (as shown in Figs. 4.2 and 4.3). Accordingly, the data show that mesenteric arteries from control mice without functional endothelium are able to produce similar levels of constriction in response to PE (Fig. 4.14c). In contrast, both mechanisms of relaxation, NO and EDHF, are dependent upon ECs (as shown in Fig. 4.6). Therefore, removal of ECs resulted in almost complete elimination of the relaxation response to ACh (94% decrease) (Fig. 4.14d). A significant difference was found in the AUC of the response to ACh before and after removing the ECs (Fig. 4.14e). SIN-1 was used to evaluate an endothelium-independent vasodilatation response. It decomposes in aqueous solutions generating NO without requiring enzymatic bioactivation or other co-factors (Ullrich et al., 1997) (Fig. 4.15), thus is able to elicit vasorelaxation in the absence of endothelial cells (Fig. 4.14b and 4.17b and c).

No difference was observed in the nature or magnitude of the effect of removing the endothelium from Piezo1 ΔEC vessels, compared with control mice. Mesenteric arteries from Piezo1 ΔEC mice without functional endothelium are able to produce similar levels of constriction in response to PE as intact vessels (Fig. 4.16c). Removal of ECs eliminated the relaxation response to ACh by 95% (Fig. 4.16d), a significant difference being found in the AUC of the response to ACh before and after removing the ECs (Fig. 4.16e). The difference in the AUC of the response to ACh before and after removing the ECs was compared between the two groups of mice and no significant difference was observed (Fig. 4.17a). These results are in agreement with the L-NAME experiments. SIN-1 (0.01–1 μM) induced relaxation in both groups was unaffected by the removal of ECs (Fig. 4.17b). No differences were found in the AUC of the response to SIN-1 between the two groups of mice (Fig. 4.17c). These data indicate that both mechanisms of ACh induced relaxation are robustly endothelium-dependent and that the SIN-1 response occurs independently of Piezo1.

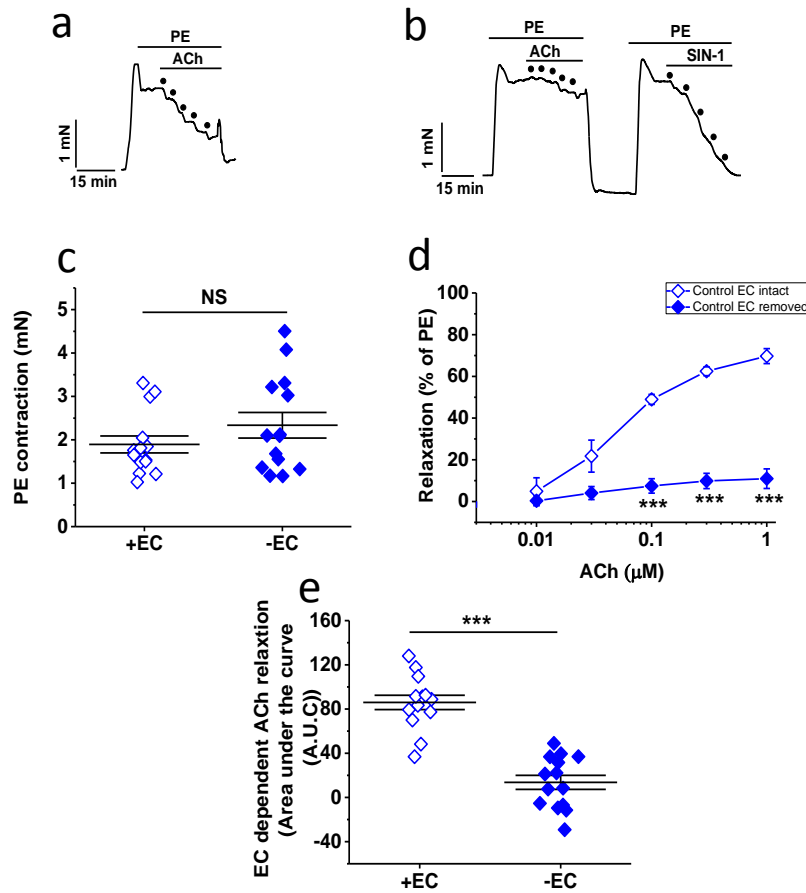


Figure 4-14: The effect of removal of endothelial cells on ACh induced-relaxation in control mice

(a) Typical trace showing a concentration-dependent dilatory response to acetylcholine (ACh) as indicated by the dots (0.01, 0.03, 0.1, 0.3 and 1 μM) before removing the endothelial cells. (b) Typical trace showing a concentration-dependent dilatory response to ACh after removing the endothelial cells (-EC) and the application of NO-donator, Linsidomine (SIN-1) as indicated by the dots (0.01, 0.03, 0.1, 0.3 and 1 μM) (c) Quantification of the effects of removing the endothelial cells on phenylephrine (PE)-induced constriction in control mesenteric arteries of mice (n=14). (d) Concentration response curves to ACh in mesenteric arteries of control mice before and after removing endothelial cells (n=14). (e) The area under the curve (AUC) of the response to ACh before and after removing the endothelial cells of mesenteric arteries isolated from control mice (n=14). Responses are expressed as percent constriction and as the area under the curve (AUC) of the response to ACh. Mean \pm SEM values are depicted. Asterisks indicate statistically significant difference (***, $p < 0.001$). NS=not significant.

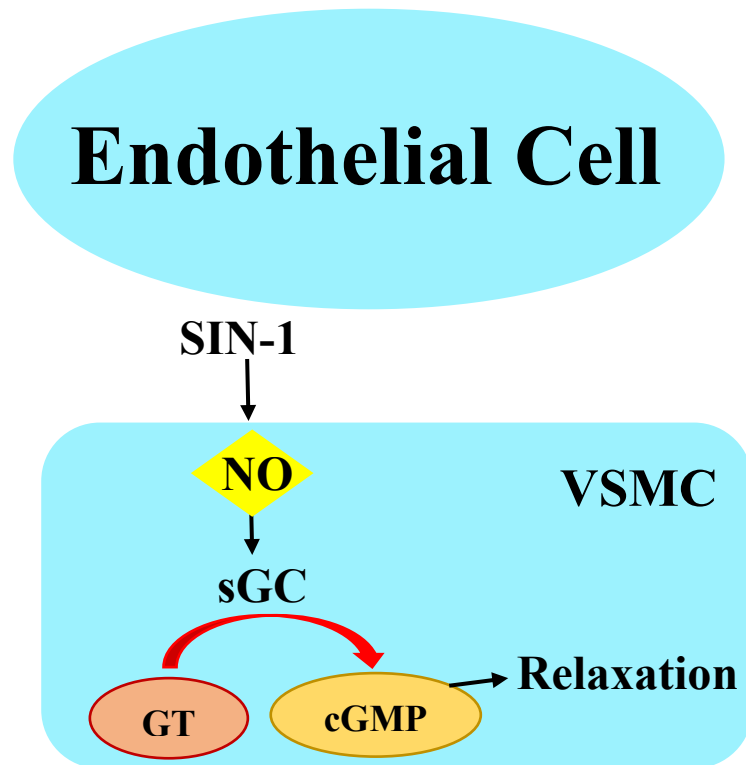


Figure 4-15: NO-donor, Linsidomine (SIN-1)

SIN-1 can be converted into nitric oxide (NO), the common smooth muscle relaxing factor and activates of soluble guanylate cyclase (sGC) and generation of the second messenger cyclic guanosine monophosphate (cGMP), which mediates vasodilation.

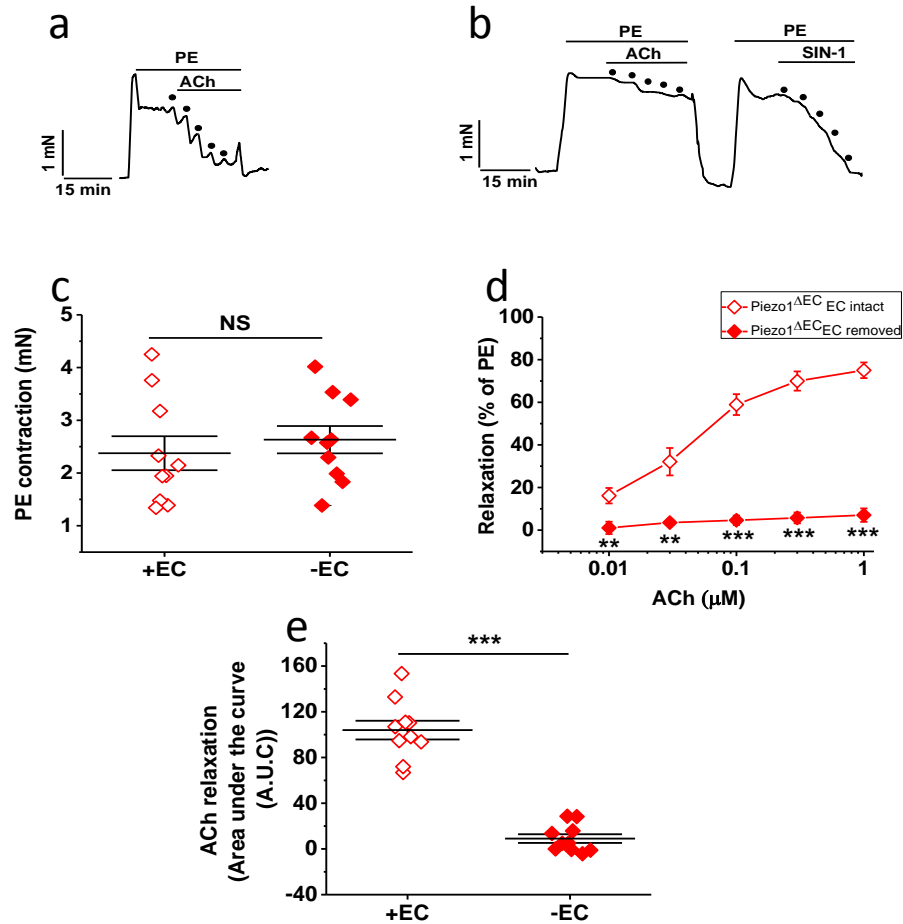


Figure 4-16: The effect of removal of endothelial cells on ACh induced-relaxation in Piezo1^{ΔEC} mice

(a) Typical trace showing a concentration-dependent dilatory response to acetylcholine (ACh) as indicated by the dots (0.01, 0.03, 0.1, 0.3 and 1 μM) before removing the endothelial cells. (b) Typical trace showing a concentration-dependent dilatory response to ACh after removing the endothelial cells (-EC) and the application of SIN-1 as indicated by the dots (0.01, 0.03, 0.1, 0.3 and 1 μM) (c) Quantification of removing the endothelial cells effects on phenylephrine (PE)-induced constriction in Piezo1^{ΔEC} mesenteric arteries of mice ($n=10$). (d) Concentration response curves to ACh in mesenteric arteries of Piezo1^{ΔEC} mice before and after the removal of endothelial cells ($n=10$). (e) The area under the curve (AUC) of the response to ACh before and after removing the endothelial cells of mesenteric arteries isolated from Piezo1^{ΔEC} mice ($n=10$). Responses are expressed as percent constriction and as the area under the curve (AUC) of the response to ACh. Mean \pm SEM values are depicted. Asterisks indicate statistically significant difference (**, $p < 0.01$; ***, $p < 0.001$). NS=not significant.

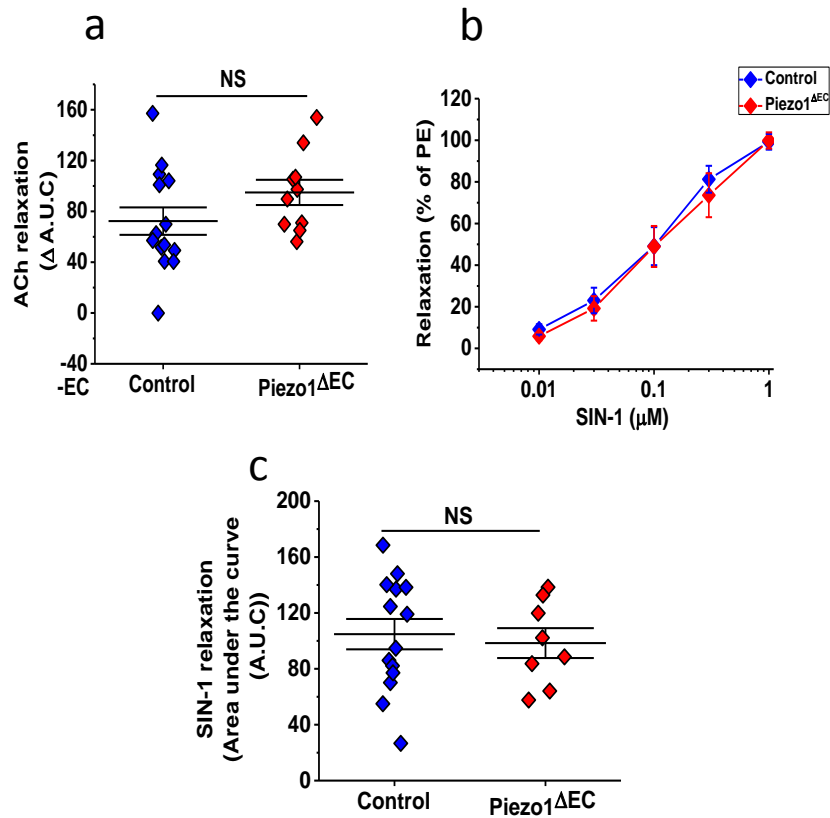


Figure 4-17: Comparison of effects of removing the endothelial cells in control and endothelial Piezo1^{ΔEC} mice

(a) The difference in the area under the curve (AUC) of the response to acetylcholine (ACh) before and after removing the endothelial cells of mesenteric arteries isolated from control and Piezo1^{ΔEC} mice ($n=14$ and 10 , respectively). (b) Concentration response curves to NO-donator, Linsidomine (SIN-1) in mesenteric arteries from control and Piezo1^{ΔEC} mice ($n=14$ and 8 , respectively). (c) The area under the curve (AUC) of the response to SIN-1 in mesenteric arteries isolated from control Piezo1^{ΔEC} mice ($n=14$ and 10 , respectively). Data are expressed as percent constriction and the area under the curve (AUC) of the response to ACh. Mean \pm SEM values are depicted. NS=not significant.

Since the data show that Piezo1 has an anti-EDHF effect (i.e. anti-vasodilatation) in mesenteric arteries, we considered the physiological circumstances in which this regulatory role may be important. Mesenteric arteries contribute substantially to peripheral resistance, therefore, regulation of BP represented an obvious parameter for examination. Studies have shown that exercise reduces mesenteric blood flow in humans, directing it instead to organs/tissues actively required for movement (Qamar and Read, 1987). Therefore, we measured BP in both inactive and active states. The following experiments were performed by Dr B Rode.

4.3.7 Measurements of blood pressure

BP was continuously recorded in mice by implanting telemetry probes. The mice were given unrestricted access to a running wheel placed within their cages. BP did not differ between groups of control and Piezo1^{ΔEC} mice during the periods of physical inactivity (Fig. 4.18a); ~ 108 mmHg in control and ~ 102 mmHg in Piezo1^{ΔEC} mice, and ~ 87 mmHg in control and ~ 83 mmHg in Piezo1^{ΔEC} mice systolic and diastolic values respectively. During periods of physical activity BP increased in both control and Piezo1^{ΔEC} mice, however, this increase was significantly smaller in Piezo1^{ΔEC} mice; ~ 137 mmHg (29 mmHg increase) in control and ~ 119 mmHg (17 mmHg increase) in Piezo1^{ΔEC} mice and ~ 113 mmHg (26 mmHg increase) in control and ~ 97 mmHg (14 mmHg increase) in Piezo1^{ΔEC} mice, systolic and diastolic values respectively. ~ 59% increase in Piezo1^{ΔEC} mice as a proportion/percentage of control mice (Fig. 4.18). These data demonstrate that during whole body physical activity, endothelial Piezo1 plays an important role in regulating BP.

4.3.8 Flow-induced vasoconstriction

We hypothesised that the reduced exercise-induced increase in BP seen in Piezo1^{ΔEC} mice was, at least in part, due to a loss of regulation of mesenteric blood flow in response to activity; Piezo1 is involved in reducing blood flow through mesenteric vessels during exercise (Qamar and Read, 1987). This would suggest the presence of a shear stress induced vasoconstriction mechanism linked to Piezo1 within the mesenteric arteries. To look for such a mechanism, pressure myography studies were performed together with Dr J Shi on isolated intact second-order mesenteric arteries. A pressure myograph can more appropriately model the *in vivo* condition and resistance arteries are more sensitive

to stretch *in vitro* when mounted on a pressure myograph compared with the isometric wire myograph (Halpern and Osol, 1985). In order to focus on the potential Piezo1 vasoconstriction mechanism, the endothelial NOS inhibitor L-NAME was used. Under these conditions, a flow-induced vasoconstriction was seen in vessels from control mice. In contrast, in Piezo1^{ΔEC} mice this vasoconstriction was absent (Fig.4.19d, 4.19e). Interestingly, the vasoconstriction produced in vessels from control mice by the flow was blocked by the LTCCs inhibitor nifedipine (Fig. 4. 19a-c).

4.3.9 Constitutive and flow-induced Piezo1 in mesenteric artery

The presence of functional Piezo1 channels in ECs from second-order mesenteric arteries was confirmed by Dr J Shi using cell-detached outside-out membrane patch-clamp electrophysiology. Piezo1 channels were identified through the size of their unitary current and unitary conductance; the channels had a unitary conductance of about 25 pS, consistent with previous studies (Coste et al., 2010, Coste et al., 2015). Interestingly, constitutive activity of Piezo1 channels was observed (Fig. 4.20a, 4.20b), perhaps explaining the difference in EDHF-mediated vasorelaxation between the control and Piezo1^{ΔEC} mice. Channel activity was enhanced approximately two-fold upon application of flow (Fig. 4.20c). Sensitivity to Gd³⁺, a blocker of Piezo1 channels (Coste et al., 2010), and the absence of a response to fluid flow in Piezo1^{ΔEC} mice (Fig. 4.20d) further confirmed the presence of Piezo1 channels in ECs isolated from mesenteric arteries.

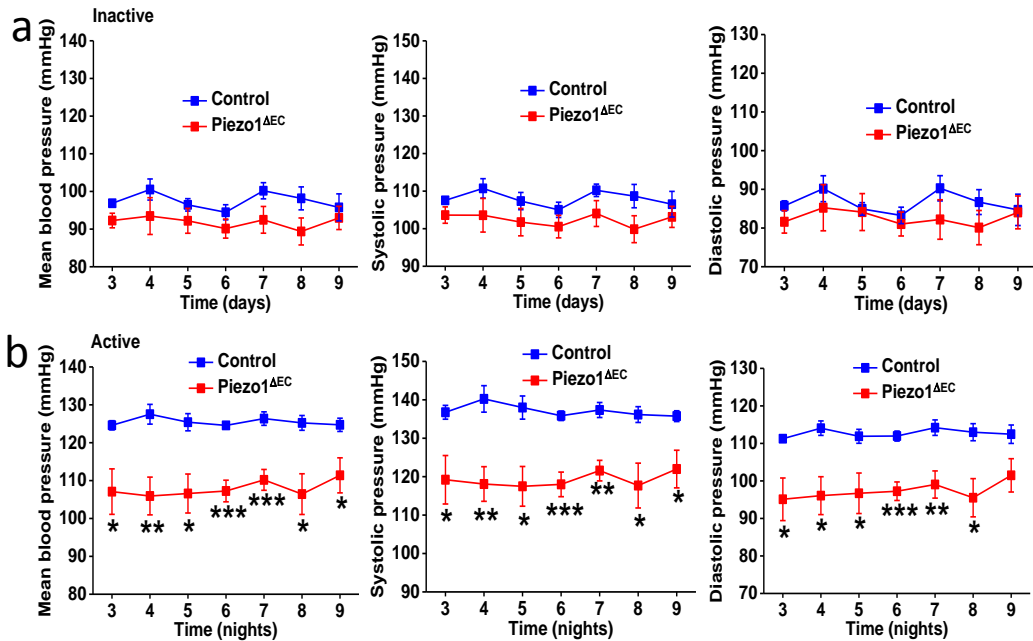


Figure 4-18: Measurements of blood pressure during whole body physical activity

Telemetry measurements of mean, systolic and diastolic BPs in conscious freely-moving control (n=6) and Piezo1^{ΔEC} (n=7) mice. Data were analysed when the mice were inactive during the day (a) and voluntarily active on a running wheel during the night (b). Time zero is when the mouse was introduced to the running wheel cage. Measurements were not made during the first 2 days of acclimatisation. Averaged data are displayed as Mean \pm SEM. Data sets are compared by *t*-test. Statistical significance is indicated by **p*<0.05, ***p*<0.01, ****p*<0.001. Experiments were performed by Dr B Rode.

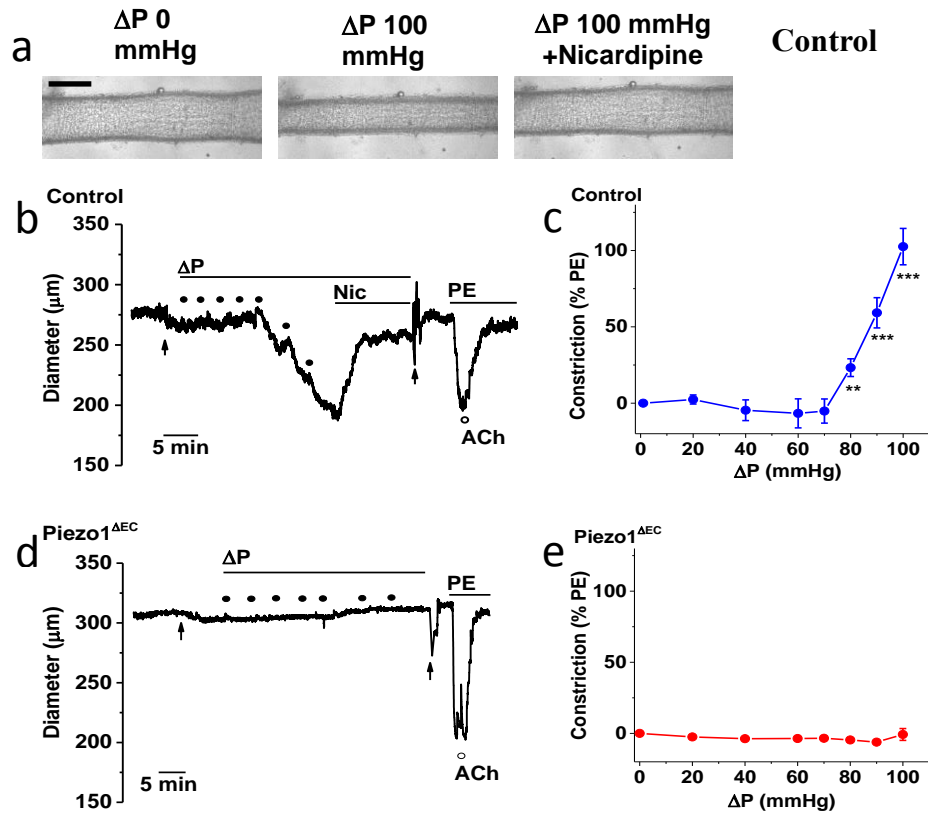


Figure 4-19: Flow-induced vasoconstriction in mesenteric artery. Isobaric external diameter recordings from second-order mesenteric artery

(a) Example images of a cannulated artery before and after luminal pressure difference (ΔP) and then after 10 μM nicardipine was added to the recording chamber. Control genotype mouse. Scale bar, 200 μm . (b) Example diameter recording for a control genotype mouse during incremental increases in ΔP as indicated by the black dots (20, 40, 60, 70, 80, 90 and 100 mmHg). Nicardipine (Nic, 10 μM), phenylephrine (PE, 1 μM) and acetylcholine (ACh, 10 μM) were applied as indicated. The first arrow indicates addition of 100 μM N(ω)-nitro-L-arginine methyl ester (L-NAME) to the recording chamber and the second arrow multiple washes of the chamber to remove nicardipine and L-NAME. (c) Mean data for the type of experiment shown in (b) presented as the constriction to ΔP as a percentage of the PE response (9 arteries from $n=6$ mice). Nicardipine significantly (***) reduced the 100 mmHg ΔP response to $30.7 \pm 3.9\%$ ($n=6$ mice). (d, e) The same as for (b, c) but using Piezo1 $^{\Delta EC}$ genotype mice (8 arteries from $n=3$ mice). Averaged data are displayed as Mean \pm SEM. Data sets are compared by t -test. Statistical significance is indicated by ** $p < 0.01$, *** $p < 0.001$. Experiments were performed in collaboration with Dr J Shi.

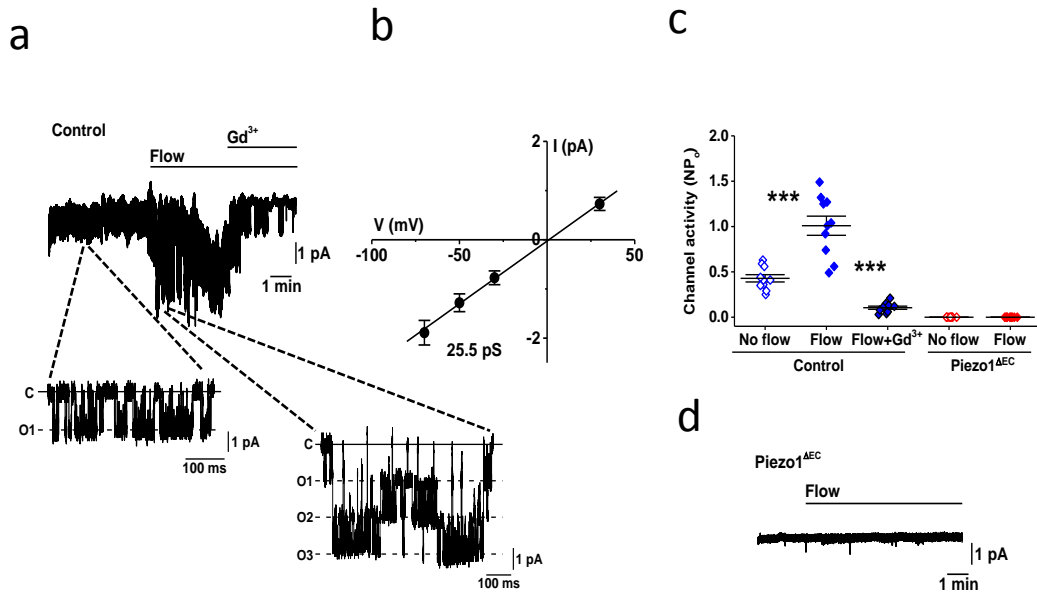


Figure 4-20: Piezo1 channels work as flow sensors in the endothelium of mesenteric artery

Piezo1 channels are flow sensors in endothelium of mesenteric resistance artery. Data are for ionic current recordings from outside-out patches excised from freshly isolated endothelium of second-order mesenteric arteries. (a) Example recording at -70 mV. Two sections are expanded to clarify unitary current events (C: channel closed) (O: 1, 2 or 3 simultaneous channel openings). The patch was placed at the outlet of a capillary from which flowed ionic solution at $20 \mu l s^{-1}$. Gadolinium ion (Gd^{3+} , $10 \mu M$). (b) Mean unitary current amplitudes for channels activated by flow as in a ($n = 10$). (c) Mean channel activity (NP_0 : number \times probability of opening) for experiments of the type exemplified in a for no flow and flow conditions and the two genotypes (Control and $Piezo1^{\Delta EC}$). Individual data points for each independent experiment are shown as *symbols*, superimposed on which are the mean \pm s.e.m. values ($n = 10$ for each group). (d) Example original trace for a patch from $Piezo1^{\Delta EC}$ endothelium exposed to $20 \mu l s^{-1}$ flow. Averaged data are displayed as mean \pm SEM. Data sets are compared by *t*-test. Statistical significance is indicated by *** $p < 0.001$. Experiments were performed by Dr J Shi.

4.3.10 Yoda1 induced relaxation in the mesenteric arteries of control and Piezo1^{ΔEC} mice

Yoda1 is a synthetic small-molecule activator of Piezo1 which was discovered in a screen of 3.25 million compounds (Syeda et al., 2015). Previous data within this chapter considered a modulatory effect of Piezo1 on vasoconstrictor/vasorelaxant compounds. Here the aim was to determine if activation of Piezo1 itself leads to contraction/relaxation of a resistance artery. Mesenteric arteries from control and Piezo1^{ΔEC} mice were pre-constricted with 0.3 μM PE, then Yoda1 (0.1–10 μM) was administered as shown in Fig. 4.21a, and 4.21b respectively. In control segments, Yoda1 caused a concentration-dependent relaxation (~ 80 % relaxation at 10 μM Yoda1). Unexpectedly, this vasorelaxation was not significantly diminished in Piezo1^{ΔEC} segments (Fig. 4.21c). No significant difference was found in the AUC of the response to Yoda1 for each individual curve in both groups (Fig. 4.21d). The data suggest that activation of EC Piezo1 by a pharmacological agonist does not influence vessel tension. However, the activation of Piezo1 in other cell types (e.g. VSMCs) might promote vasorelaxation.

4.3.11 The effect of Piezo1 antagonists on Yoda1-induced relaxation in mesenteric arteries from control and Piezo1^{ΔEC} mice

Two previously identified non-specific inhibitors of Piezo1 are Gd³⁺ and ruthenium red (RR). They were used to determine the contribution of Piezo1 to the relaxation induced by Yoda1 on isolated mesenteric arteries from control and Piezo1^{ΔEC} mice. A typical relaxation response of Yoda1 before and after inhibition with Gd³⁺ or RR was obtained from control and Piezo1^{ΔEC} mesenteric arteries (Fig. 4.21a, 4.22a for Gd³⁺, 4.23a and 4.24a for RR, respectively). There was no significant reduction in PE-induced constriction observed when these inhibitors were used (Table 4.1). Both of these inhibitors significantly reduced Yoda1 induced-relaxation on isolated mesenteric arteries from control (45% and 40% reduction respectively) and Piezo1^{ΔEC} mice (31% and 33% reduction respectively). (Fig. 4.21b, 4.22b, 4.23b and 4.24b). A significant difference was found in the AUC of the response to Yoda1 before and after the incubation with Gd³⁺ or RR (Fig. 4.21c, 4.22c for Gd³⁺, 4.23c and 4.24c for RR, respectively). These data suggest that Piezo1 contributes to Yoda1-induced relaxation.

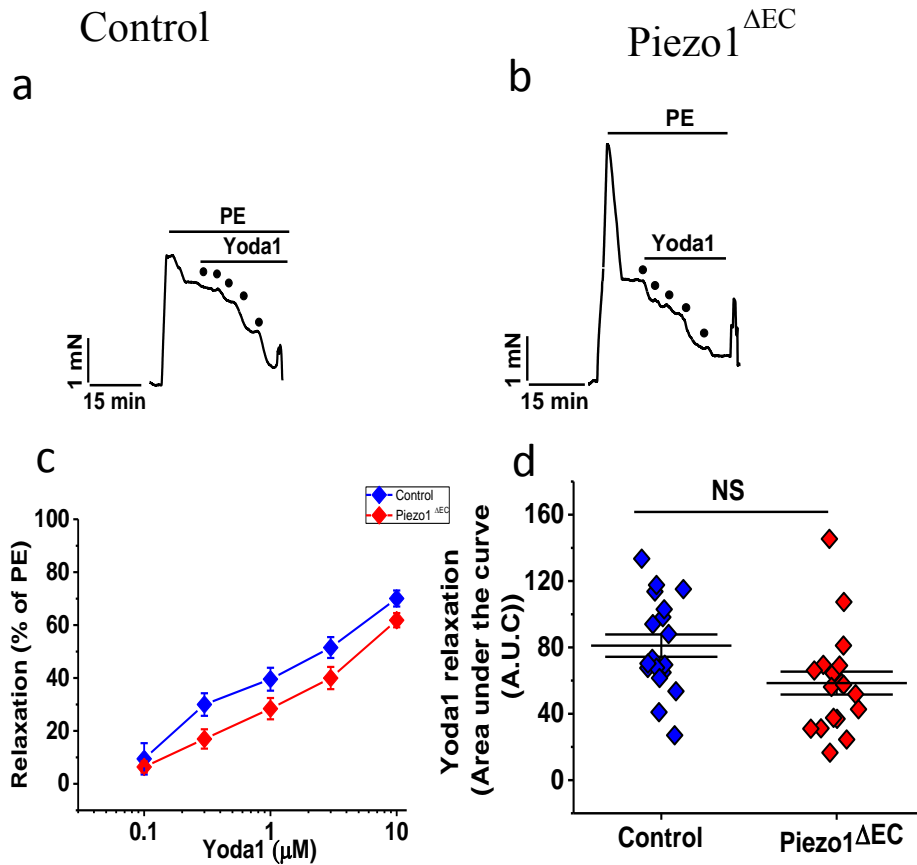


Figure 4-21: Endothelial-dependent relaxation induced by Yoda1 in control compared with endothelial *Piezo1*^{ΔEC} mesenteric arteries

(a) Typical trace showing a concentration-dependent dilatory response to Yoda1 as indicated by the dots (0.1, 0.3, 1, 3 and 10 μM) in endothelium-intact mesenteric arteries isolated from control mice. (b) As for (a) except in endothelium-intact mesenteric arteries isolated from *Piezo1*^{ΔEC} mice. (c) Concentration response curves to Yoda1 in control ($n=18$) and *Piezo1*^{ΔEC} ($n=19$) mice. (d) The area under the curve (AUC) of the response to Yoda1 of mesenteric arteries isolated from control ($n=18$) and *Piezo1*^{ΔEC} mice ($n=19$). Responses are expressed as percent relaxation, and as the area under the curve (AUC) of the response to Yoda1. Mean \pm SEM values are depicted. NS=not significant.

Treatment	Basal tension before PE (mN)	Basal tension after PE (mN)	Maximum tension before PE (mN)	Maximum tension after PE (mN)	N
	Control				
Gd³⁺	3.09±0.01	3.06±0.02	5.15±0.04	3.74±0.01	6
RR	3.02±0.02	3.07±0.01	5.24±0.06	3.19±0.04	3
	Piezo1^{ΔEC}				
Gd³⁺	3.04±0.02	3.08±0.03	5.93±0.06	3.24±0.04	6
RR	3.00±0.01	3.02±0.02	6.35±0.03	3.79±0.03	6

Table 4-1: Gd³⁺ and RR inhibitors effects on basal tension and phenylephrine (PE) responses in mouse mesenteric arteries.

The data are presented as mean ± SEM of the mice number (*n*). There was no significant difference in Gd³⁺ or RR treatments for basal tension (before the application of PE) or for maximum tension (after the application of 0.3 μM PE).

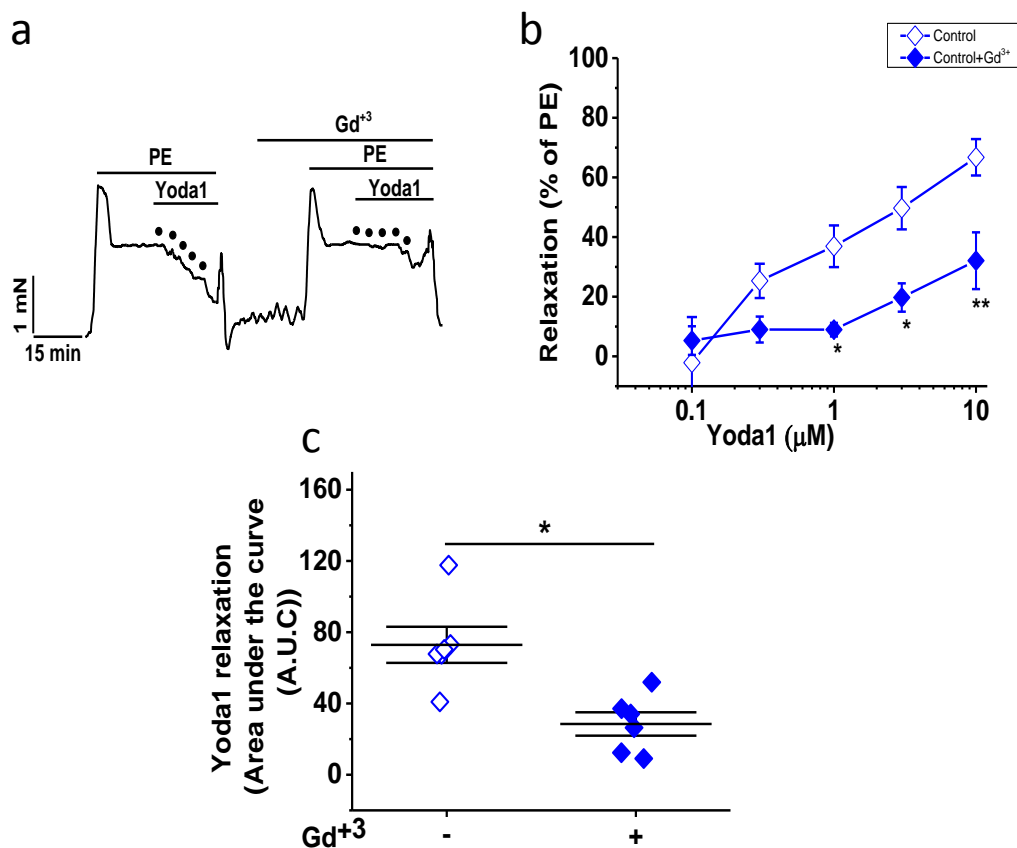


Figure 4-22: The effect of Piezo1 antagonists on Yoda1-induced relaxation in mesenteric arteries from control mice

(a) Typical trace showing a concentration-dependent response to Yoda1 as indicated by the dots (0.1, 0.3, 1, 3 and 10 μM) in the mesenteric arteries isolated from control mice before and after (10 μM) gadolinium ions (Gd^{3+}). (b) Concentration response curves to Yoda1 in the mesenteric arteries from control mice before and after Gd^{3+} ($n=6$). (c) The area under the curve (AUC) of the response to Yoda1 before and after Gd^{3+} in the mesenteric arteries isolated from control mice ($n=6$). Responses are expressed as percent constriction and as the area under the curve (AUC) of the response to Yoda1. Mean \pm SEM values are depicted. Asterisks indicate statistically significant difference ($*p < 0.05$, $**p < 0.01$).

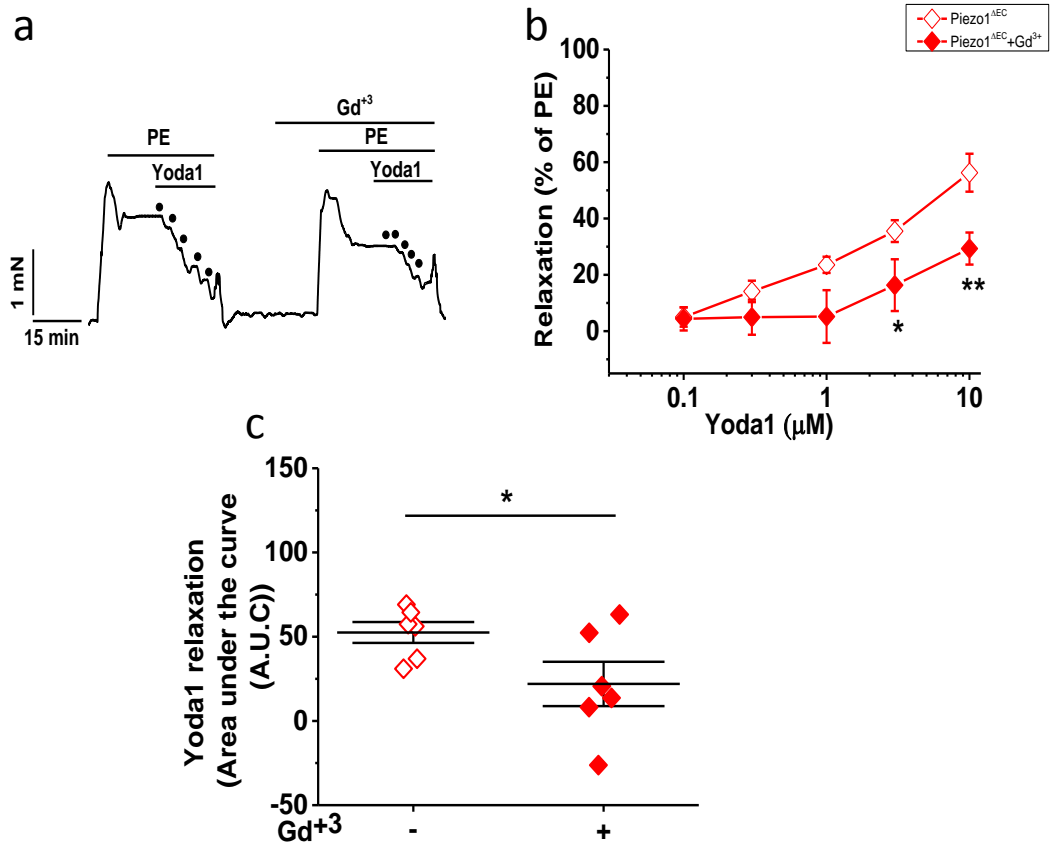


Figure 4-23: The effect of Piezo1 antagonists on Yoda1-induced relaxation in mesenteric arteries from Piezo1 Δ EC mice

(a) Typical trace showing a concentration-dependent response to Yoda1 as indicated by the dots (0.1, 0.3, 1, 3 and 10 μ M) in the mesenteric arteries isolated from Piezo1 Δ EC mice before and after (10 μ M) gadolinium ions (Gd^{3+}). (b) Concentration response curves to Yoda1 in the mesenteric arteries from control mice before and after Gd^{3+} ($n=6$). (c) The area under the curve (AUC) of the response to Yoda1 before and after Gd^{3+} in the mesenteric arteries isolated from Piezo1 Δ EC mice ($n=6$). Responses are expressed as percent constriction and as the area under the curve (AUC) of the response to Yoda1. Mean \pm SEM values are depicted. Asterisks indicate statistically significant difference (* $p < 0.05$, ** $p < 0.01$).

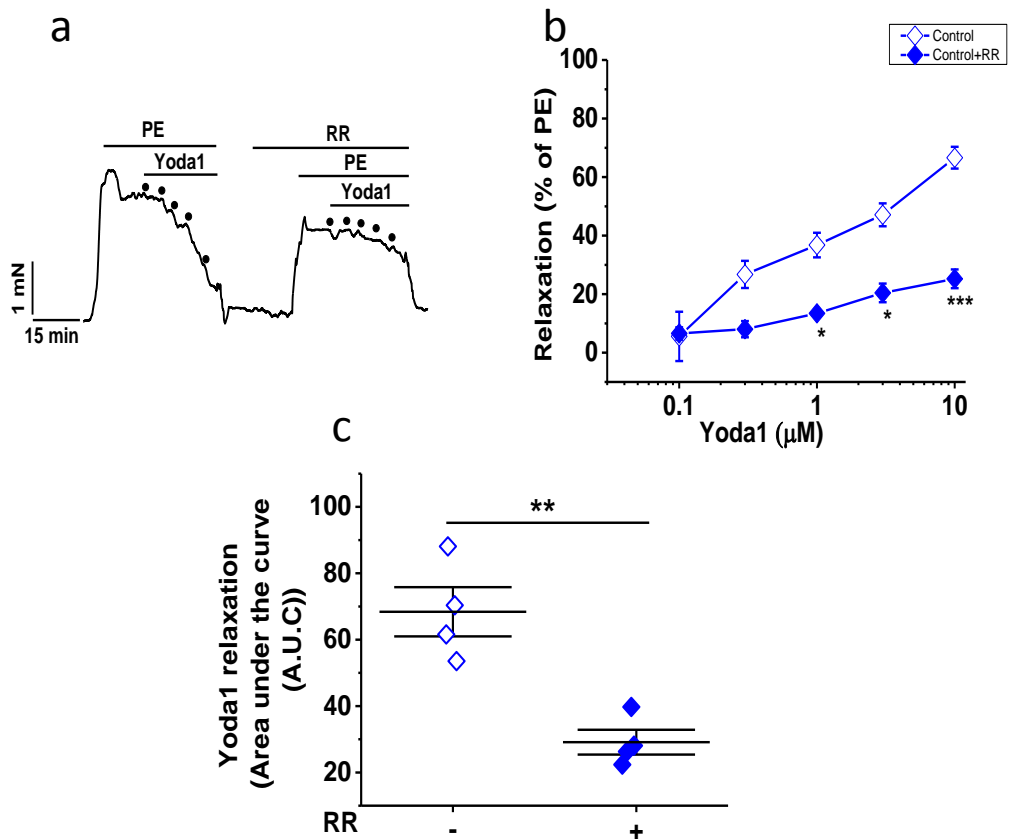


Figure 4-24: The effect of Piezo1 antagonists on Yoda1-induced relaxation in mesenteric arteries from control mice

(a) Typical trace showing a concentration-dependent response to Yoda1 as indicated by the dots (0.1, 0.3, 1, 3 and 10 μM) in the mesenteric arteries isolated from control mice before and after (30 μM) ruthenium red (RR). (b) Concentration response curves to Yoda1 in the mesenteric arteries from control mice before and after RR (n=3). (c) The area under the curve (AUC) of the response to Yoda1 before and after RR in the mesenteric arteries isolated from control mice (n=3). Responses are expressed as percent constriction and as the area under the curve (AUC) of the response to Yoda1. Mean ± SEM values are depicted. Asterisks indicate statistically significant difference (* $p < 0.05$, ** $p < 0.01$, *** $p < 0.001$).

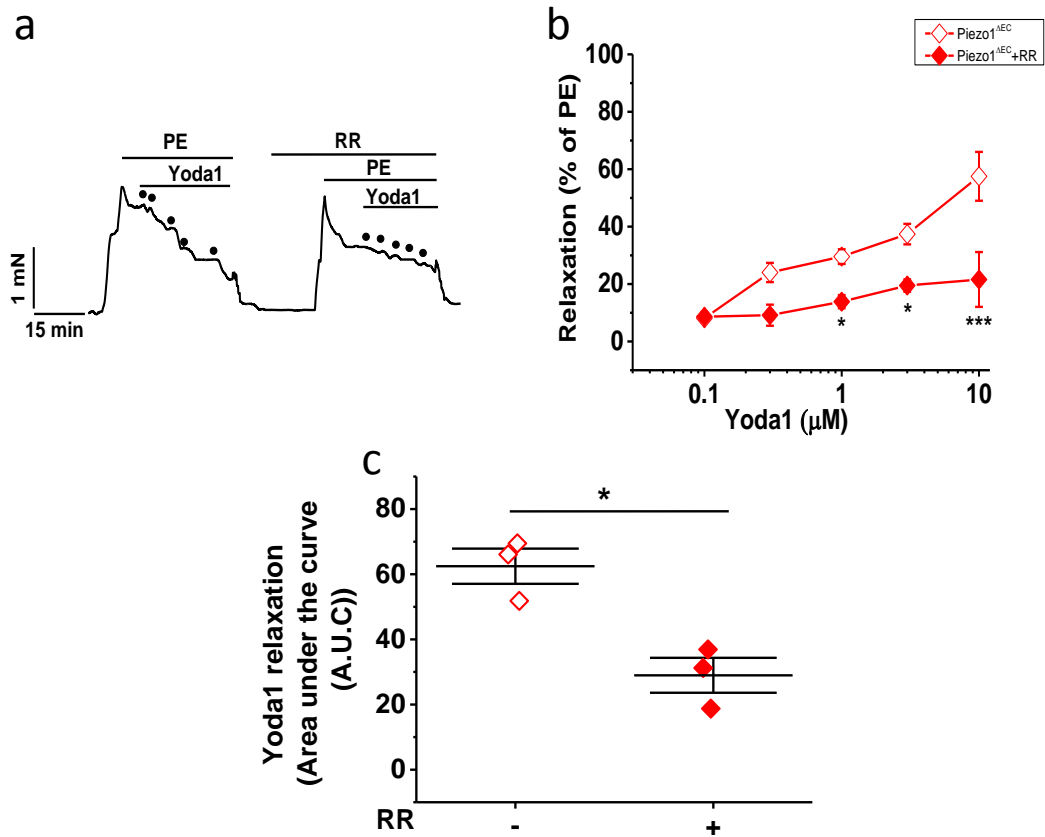


Figure 4-25: The effect of Piezo1 antagonists on Yoda1-induced relaxation in mesenteric arteries from Piezo1 $^{\Delta\text{EC}}$ mice

(a) Typical trace showing a concentration-dependent response to Yoda1 as indicated by the dots (0.1, 0.3, 1, 3 and 10 μM) in the mesenteric arteries isolated from Piezo1 $^{\Delta\text{EC}}$ mice before and after (30 μM) ruthenium red (RR). (b) Concentration response curves to Yoda1 in the mesenteric arteries from control mice before and after RR ($n=3$). (c) The area under the curve (AUC) of the response to Yoda1 before and after RR in the mesenteric arteries isolated from Piezo1 $^{\Delta\text{EC}}$ mice ($n=3$). Responses are expressed as percent constriction and as the area under the curve (AUC) of the response to Yoda1. Mean \pm SEM values are depicted. Asterisks indicate statistically significant difference ($*p < 0.05$).

4.3.12 The effect of removal of endothelial cells on Yoda1-induced relaxation

Yoda1 was used in the mesenteric arteries from control and Piezo1^{ΔEC} mice after pre-constriction with PE, with and without functional endothelium. Endothelium was removed by gently rubbing the lumen of the arteries with a wire to test whether removing the ECs would affect Yoda1-induced relaxation. Endothelial denudation was confirmed via the failure of the arteries to relax in response to ACh.

A typical relaxation response of Yoda1 before and after removing EC was obtained from control and Piezo1^{ΔEC} mesenteric arteries (Fig. 4.26a, 4.27a, respectively). Thus, the vasorelaxant effect of Yoda1 is largely EC-independent which agrees with the Piezo1^{ΔEC} data. Furthermore, neither the maximal relaxation nor concentration-dependent relationship of Yoda1 was significantly altered by removal of the ECs (30% relaxation). Yoda1 caused a concentration-dependent vasorelaxation, and was not significantly influenced by removing the endothelium, although there was a trend towards a rightward shift in the concentration-relaxation curve to Yoda1. (Fig. 4.26b). In Piezo1^{ΔEC} mice (Fig. 4.27b), likewise, no significant difference was found in the AUC of the response to Yoda1 before and after removing the ECs (Fig. 4.26c and 4.27c)

As introduced previously, the NO donor SIN-1 was used as a control to test the ability of the smooth muscle to relax. SIN-1 (0.01–1 μM) elicited concentration-dependent relaxation in endothelium-denuded arteries pre-stimulated with PE (0.3 μM) (Fig. 4.28a). No differences were observed between the relaxant actions in both groups. No significant difference was observed in the AUC of the response to SIN-1 in both groups (Fig. 4.28b). Together with the previous results, this suggests that Piezo1 might be involved in the portion of vasorelaxation mediated by VSMCs.

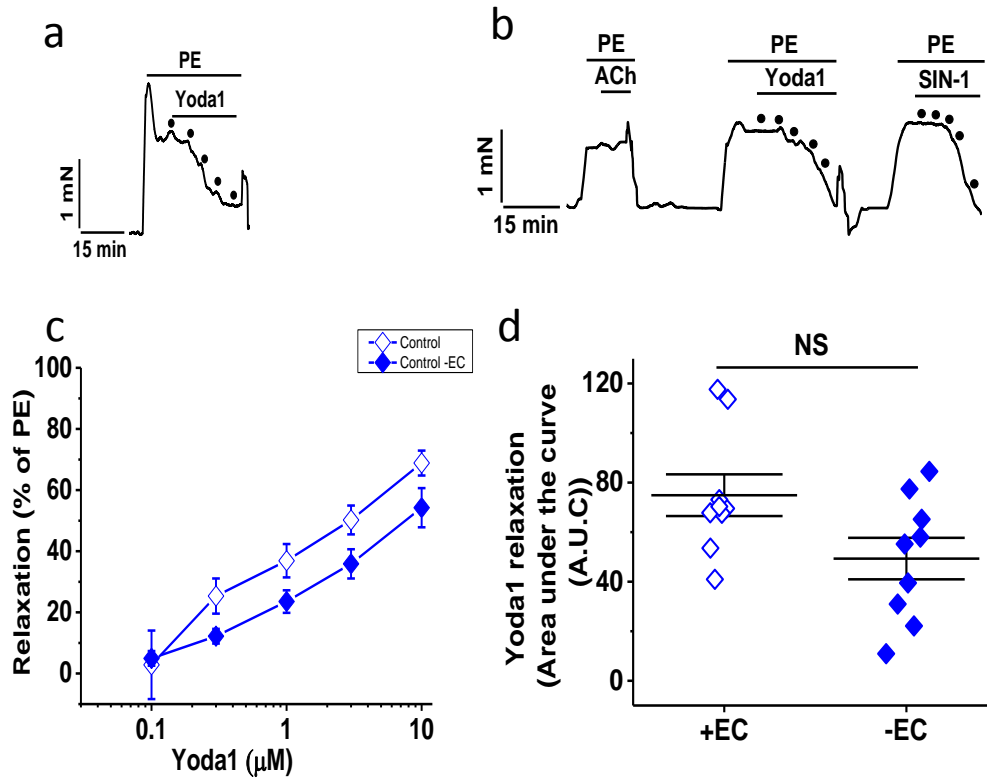


Figure 4-26: The effect of the endothelium removal on Yoda1-induced relaxation in mesenteric arteries from control mice

(a) Typical trace showing a concentration-dependent response to Yoda1 as indicated by the dots (0.1, 0.3, 1, 3 and 10 μM) in the mesenteric arteries isolated from control mice before and after EC removing (-EC). (b) (c) Concentration response curves to Yoda1 in the mesenteric arteries from control mice before and after -EC ($n=9$). (d) The area under the curve (AUC) of the response to Yoda1 before and after -EC in the mesenteric arteries isolated from control mice ($n=9$). Responses are expressed as percent constriction and as the area under the curve (AUC) of the response to Yoda1. Mean \pm SEM values are depicted. NS=not significant.

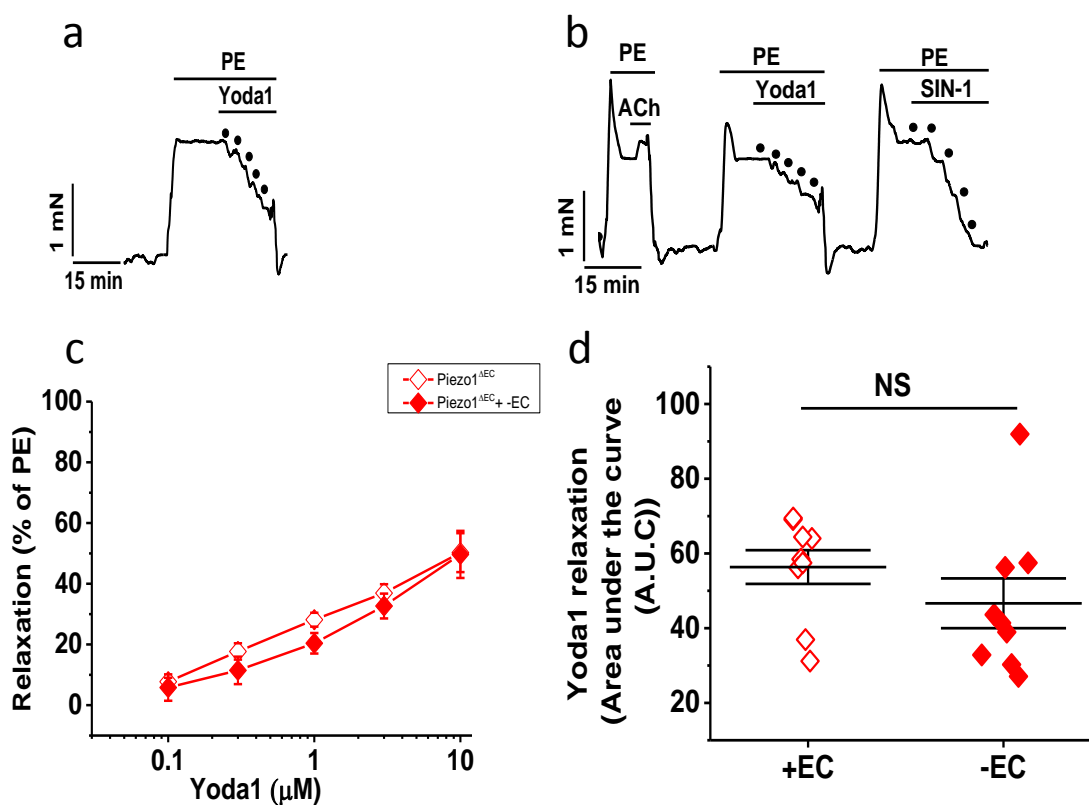


Figure 4-27: The effect of the endothelium removal on Yoda1-induced relaxation in mesenteric arteries from Piezo1 ΔEC mice

(a) Typical trace showing a concentration-dependent response to Yoda1 as indicated by the dots (0.1, 0.3, 1, 3 and 10 μM) in the mesenteric arteries isolated from Piezo1 ΔEC mice before and (b) after EC removing (-EC). (c) Concentration response curves to Yoda1 in the mesenteric arteries from Piezo1 ΔEC mice before and after -EC ($n=6$). (d) The area under the curve (AUC) of the response to Yoda1 before and after -EC in the mesenteric arteries isolated from Piezo1 ΔEC mice ($n=6$). Responses are expressed as percent constriction and as the area under the curve (AUC) of the response to Yoda1. Mean \pm SEM values are depicted. NS=not significant.

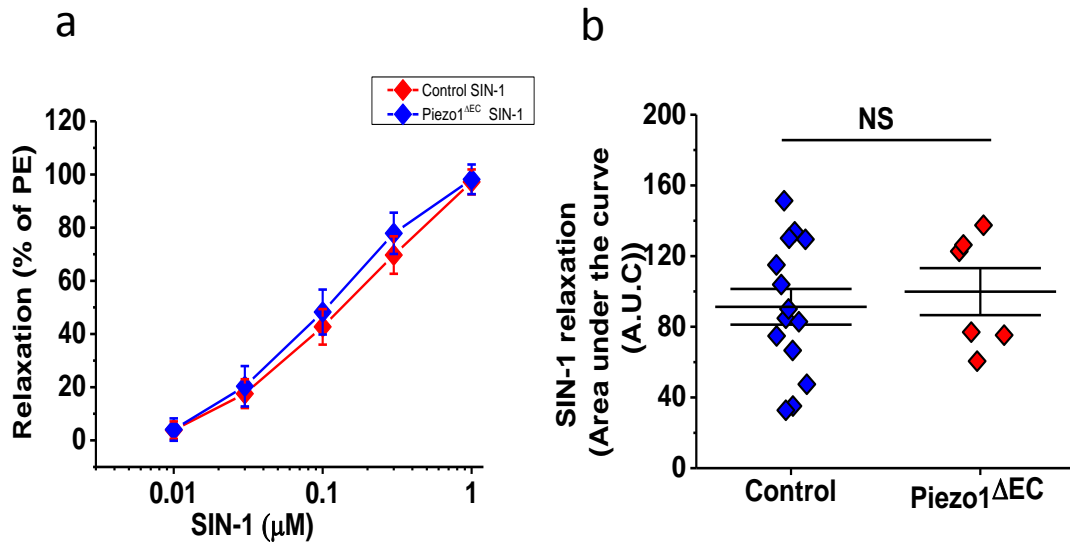


Figure 4-28: NO-donor, Linsidomine (SIN-1)-induced relaxation in mesenteric arteries from control and Piezo1^{ΔEC} mice

(a) Concentration response curves to (0.01, 0.03, 0.1, 0.3 and 1 μM) SIN-1 in the mesenteric arteries from control and Piezo1^{ΔEC} mice after EC removing ($n=14$, 6 respectively). (b) The area under the curve (AUC) of the response to SIN-1 after EC removing in the mesenteric arteries isolated from control and Piezo1^{ΔEC} mice ($n=14$, 6 respectively). Responses are expressed as percent constriction and as the area under the curve (AUC) of the response to SIN-1. Mean \pm SEM values are depicted. NS=not significant.

4.3.13 The contribution of EDHF to Yoda1-induced relaxation

To test if the trend towards a rightward shift in the concentration-relaxation curve to Yoda1 in -EC vessels was associated with the action of EDHF, a combination of apamin plus charybdotoxin against Yoda1 was used.

Relaxation responses of Yoda1 before and after inhibition with apamin plus charybdotoxin were obtained from control and Piezo1^{ΔEC} mesenteric arteries (Fig. 4.29a and 4.30a, respectively). In control mice, the degree of relaxation by Yoda1 was unaffected by the combination of apamin plus charybdotoxin, although there was a trend towards reduced relaxation (Fig. 4.29b). No significant difference was found in the AUC of the response to Yoda-1 before and after the incubation with apamin plus charybdotoxin (Fig. 4.29c). In mesenteric arteries from Piezo1^{ΔEC} mice, the combination of apamin plus charybdotoxin has no significant effect on Yoda1-induced relaxation (Fig. 4.30b). No differences were found in the AUC of the response to Yoda1 before and after the incubation with apamin plus charybdotoxin (Fig. 4.30c). This indicates that EDHF is unlikely to contribute to Yoda1-induced relaxation.

4.3.14 The contribution of NO to Yoda1-induced relaxation

To test if the trend of a rightward shift in the concentration-relaxation curve to Yoda1 was associated with the action of endothelium derived NO, L-NAME against Yoda1 was used.

Relaxation responses to Yoda1 before and after inhibition with L-NAME were obtained from control and Piezo1^{ΔEC} mesenteric arteries (Fig. 4.31a and 32a, respectively). In control mice, incubation with L-NAME resulted in a significant reduction in relaxation induced by Yoda1. (Fig. 4.31b). Also, a significant difference was found in the AUC of the response to Yoda-1 before and after the incubation with L-NAME (Fig. 4.31c). This indicates the involvement of NO in Yoda1 induced relaxation.

Conversely, in mesenteric arteries from Piezo1^{ΔEC} mice, the incubation with L-NAME (Fig. 4.32b) had no significant effect on Yoda1-induced relaxation. No differences were found in the AUC of the response to Yoda1 before and after the incubation with L-NAME

(Fig. 4.32c). These data suggest that NO-mediated vasorelaxation has no role in Yoda1 induced relaxation in Piezo1^{ΔEC} mice.

4.3.15 The contribution of NO to Yoda1-induced relaxation in denuded ECs.

L-NAME was found to be a potent inhibitor of Yoda1-induced relaxation, despite the fact that the activity of Yoda-1 was essentially endothelium-independent.

Therefore, to investigate the role of NO in Yoda1-induced relaxation further mesenteric arteries were incubated with L-NAME following removal of the endothelium. Curiously, incubation with L-NAME did not affect the Yoda1-induced relaxation of mouse mesenteric arteries in the absence of endothelial cells. A similar response was observed before and after 20 min incubation with L-NAME (Fig. 4.33). This potentially suggests a role for the endothelium in modulating the relaxation induced by Yoda1 in mouse mesenteric artery.

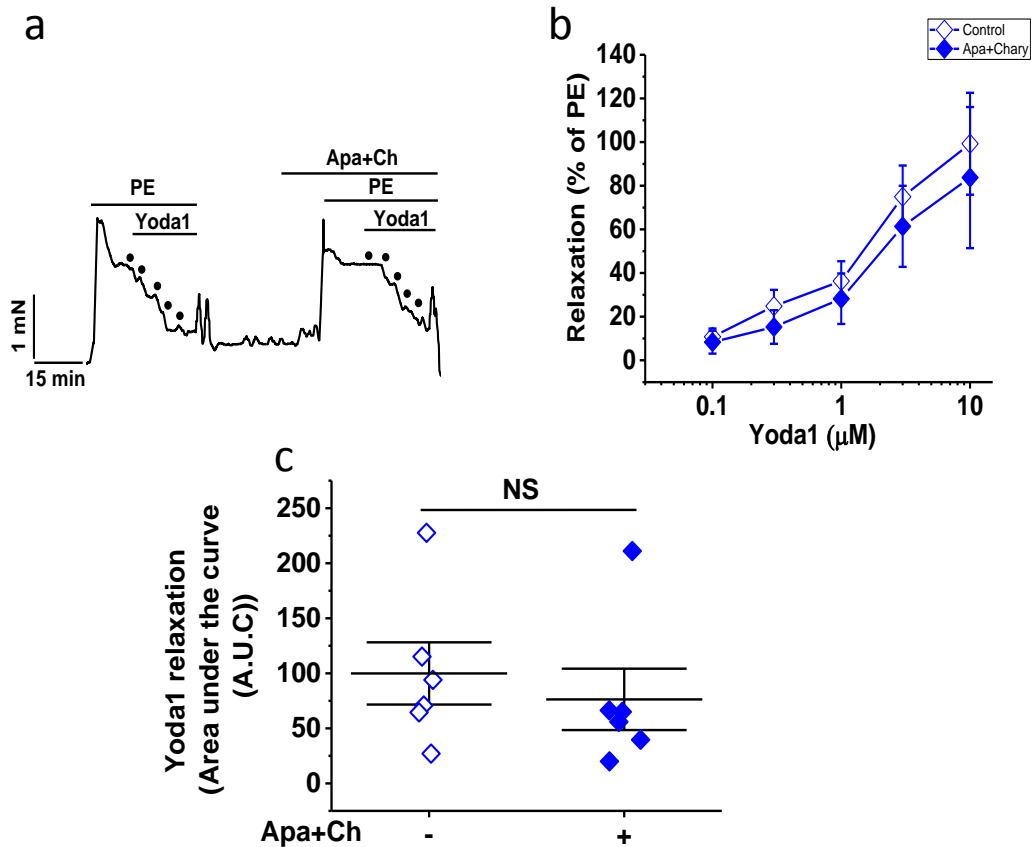


Figure 4-29: The contribution of EDHF to Yoda1-induced relaxation in control mesenteric arteries

(a) Typical tracing showing a concentration-dependent relaxation response to Yoda1 as indicated by the dots (0.1, 0.3, 1, 3 and 10 μM) before and after incubation with apamin (Apa) (500 nM) plus charybdotoxin (Ch) (100 nM) in endothelium-intact mesenteric arteries isolated from control mice. (b) Concentration response curves to Yoda1 before and after the application of Apa+Ch in control mesenteric arteries mice ($n=6$). (c) The area under the curve (AUC) of the response to Yoda1 before and after the incubation with Apa+Ch of mesenteric arteries isolated from control mice ($n=6$). Responses are expressed as percent constriction and as the area under the curve (AUC) of the response to Yoda1. Mean \pm SEM values are depicted. NS=not significant.

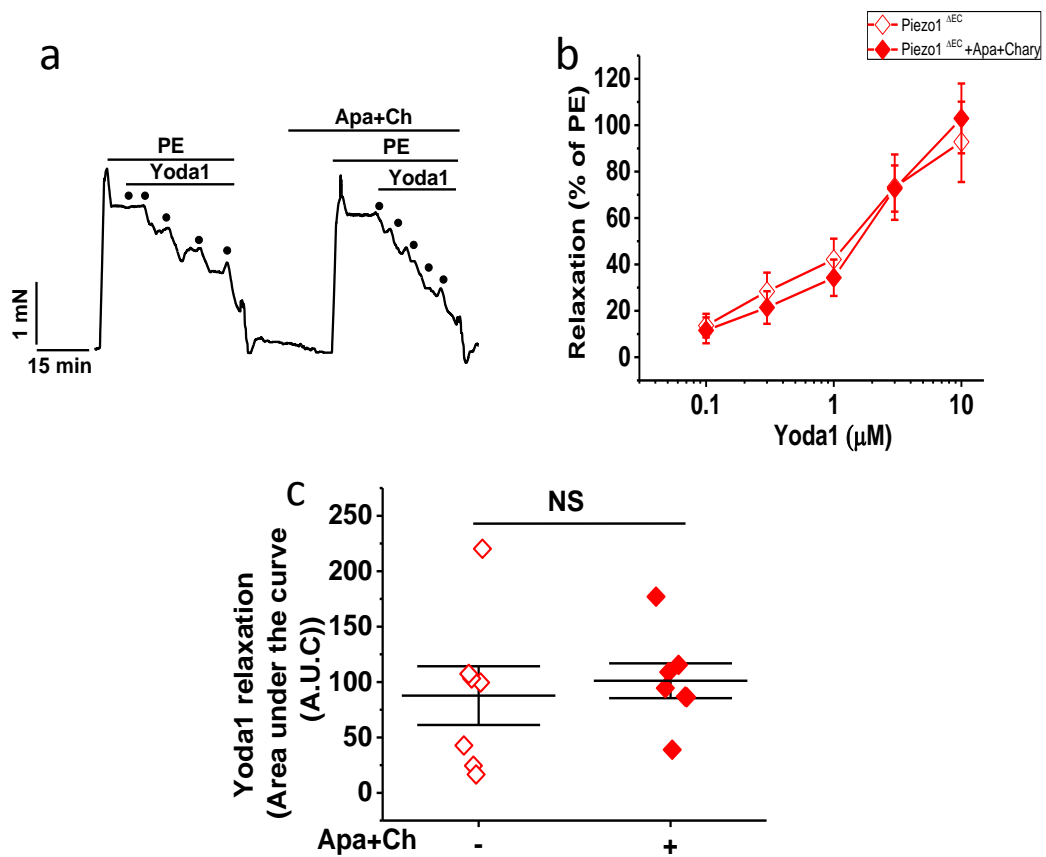


Figure 4-30: The contribution of EDHF to Yoda1-induced relaxation in Piezo1 $^{\Delta\text{EC}}$ mesenteric arteries

(a) Typical trace showing a concentration-dependent relaxation response to Yoda1 as indicated by the dots (0.1, 0.3, 1, 3 and 10 μM) before and after the incubation with apamin (Apa) (500 nM) plus charybdotoxin (Ch) (100 nM) in endothelium-intact mesenteric arteries isolated from Piezo1 $^{\Delta\text{EC}}$ mice. (b) Concentration response curves to Yoda1 before and after the application of Apa+Ch in Piezo1 $^{\Delta\text{EC}}$ mesenteric arteries mice ($n=8$). (c) The area under the curve (AUC) of the response to Yoda1 before and after the incubation with Apa+Ch of mesenteric arteries isolated from Piezo1 $^{\Delta\text{EC}}$ mice ($n=8$). Responses are expressed as percent constriction and as the area under the curve (AUC) of the response to Yoda1. Mean \pm SEM values are depicted. NS=not significant.

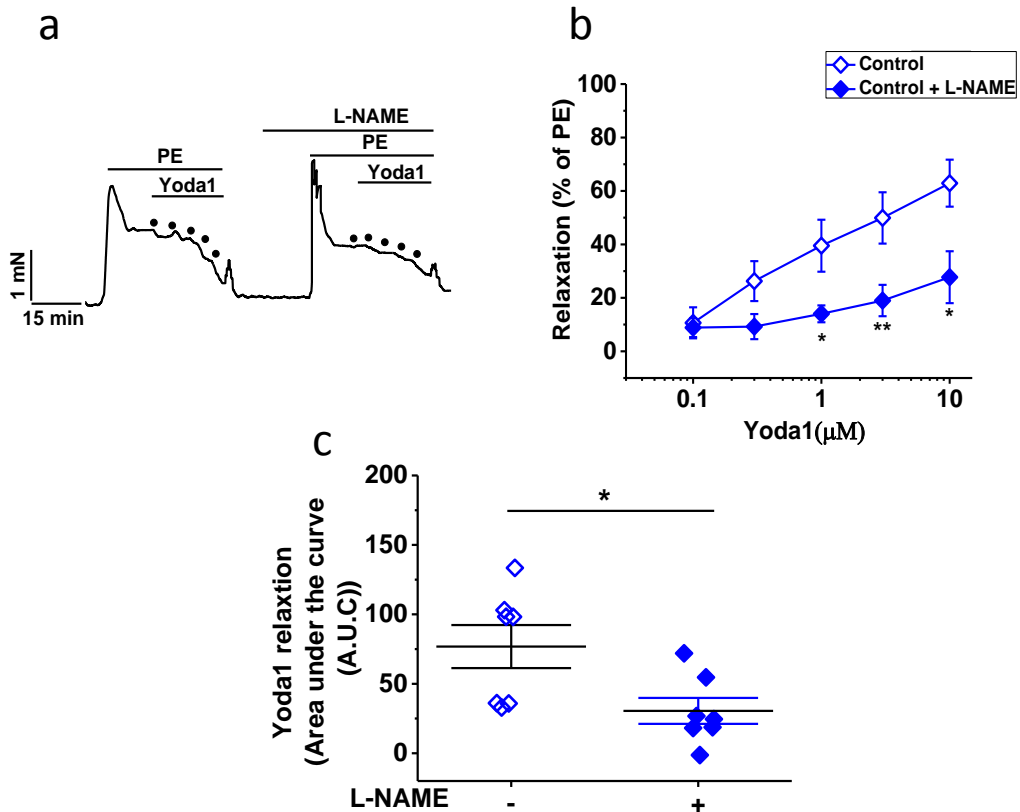


Figure 4-31: The contribution of NO to Yoda1-induced relaxation in endothelium-intact control mesenteric arteries

(a) Typical trace illustrating a concentration-dependent relaxation response to Yoda1 as indicated by the dots (0.1, 0.3, 1, 3 and 10 μM) before and after 20 min of incubation with (100 μM) *N*_ω-nitro-L-arginine methyl ester hydrochloride (L-NAME) in endothelium-intact mesenteric arteries isolated from control mice. (b) Concentration response curves to Yoda1 before ($n=7$) and after ($n=7$) L-NAME treatment. (c) The area under the curve (AUC) of the response to Yoda1 before and after the incubation with L-NAME of mesenteric arteries isolated from control mice ($n=7$). Responses are expressed as percent constriction and as the area under the curve (AUC) of the response to Yoda1. Mean \pm standard error of the mean (SEM) values are depicted. Asterisks indicate statistically significant difference (* $p<0.05$ and ** $p<0.01$).

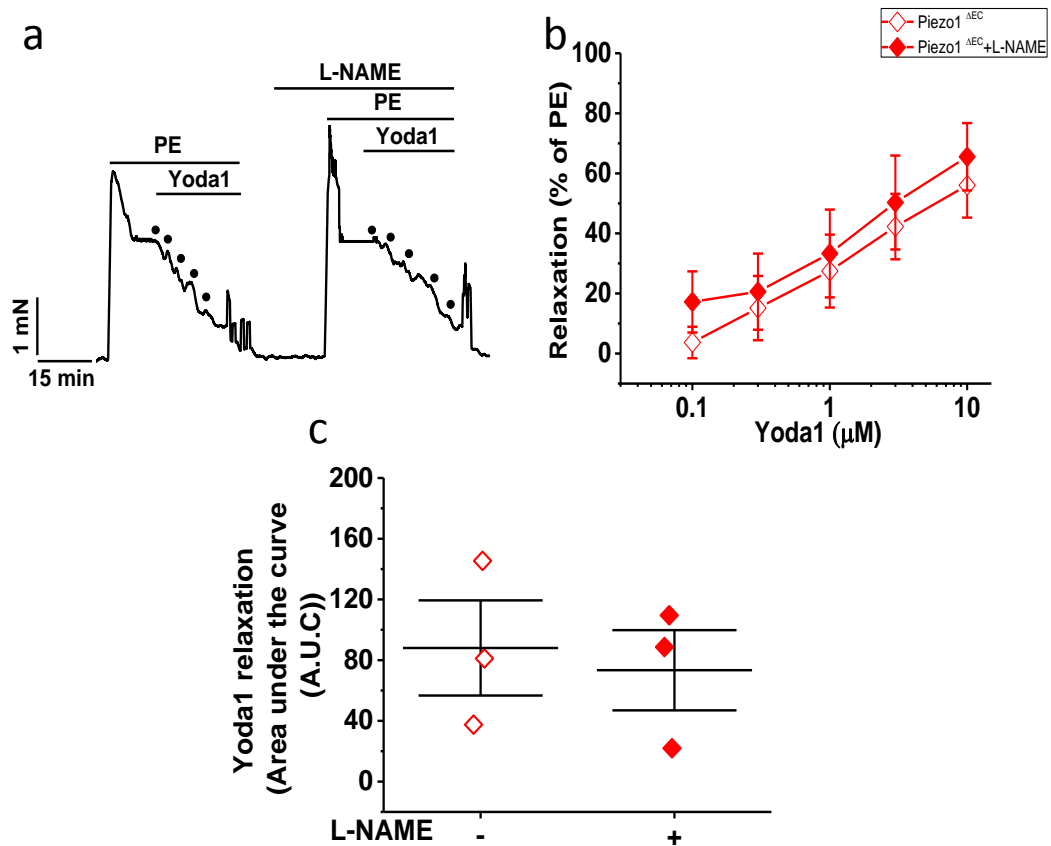


Figure 4-32: The contribution of NO to Yoda1-induced relaxation in endothelium-intact Piezo1 $^{\Delta\text{EC}}$ mesenteric arteries

(a) Typical trace illustrating a concentration-dependent relaxation response to Yoda1 as indicated by the dots (0.1, 0.3, 1, 3 and 10 μM) before and after 20 min of incubation with (100 μM) *N_ω*-nitro-L-arginine methyl ester hydrochloride (L-NAME) in endothelium-intact mesenteric arteries isolated from Piezo1 $^{\Delta\text{EC}}$ mice. (b) Concentration response curves to Yoda1 before ($n=3$) and after ($n=3$) L-NAME treatment. (c) The area under the curve (AUC) of the response to Yoda1 before and after the incubation with L-NAME of mesenteric arteries isolated from Piezo1 $^{\Delta\text{EC}}$ mice ($n=3$). Responses are expressed as percent constriction and as the area under the curve (AUC) of the response to Yoda1. Mean \pm SEM values are depicted.

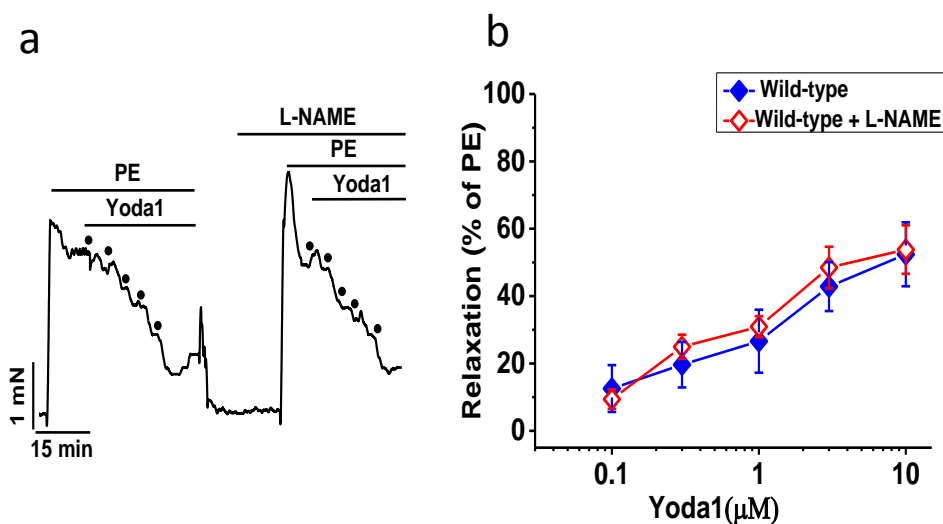


Figure 4-33: The contribution of NO to Yoda1-induced relaxation in endothelium-denuded mesenteric arteries isolated from wild type mice

(a) Typical trace illustrating a concentration-dependent relaxation response to Yoda1 as indicated by the dots (0.1, 0.3, 1, 3 and 10 μM) before and after 20 min of incubation with (100 μM) *N*_ω-nitro-L-arginine methyl ester hydrochloride (L-NAME) in endothelium-denuded mesenteric arteries isolated from wild type mice. (b) Concentration response curves to Yoda1 before (*n*=4) and after (*n*=4) L-NAME treatment. Responses are expressed as percent constriction of the response to Yoda1. Mean ± SEM values are depicted. NS=not significant.

4.4 Discussion

This study used endothelial-specific deletion of Piezo1 to determine the contribution of Piezo1 in endothelium-dependent and -independent relaxation, as well as the effects of Piezo1 on arterial tone and BP. It was found that vasodilation in response to ACh was enhanced in Piezo1^{ΔEC} mice and that Piezo1 activity opposes EDHF. All ACh responses were endothelium-mediated. However, the relaxation due to Yoda1 was not significantly reduced in Piezo1^{ΔEC} mice. Furthermore, Yoda1 vasodilator responses were impaired with L-NAME treatment but not with a combination of apamin plus charybdotoxin. This illustrates an opposing influence of Piezo1 on endothelial function with ACh- and Yoda1-induced relaxation in mouse mesenteric arteries.

4.4.1 Deletion of endothelial cell Piezo1 affects high potassium-induced contraction

High K⁺ solution was used to confirm vessel viability. However, the addition of high potassium solution did not contract the vessels from both control and Piezo1^{ΔEC} mice to a similar level. Without further study it is not possible to know whether the reason for this decrease in contraction in Piezo1^{ΔEC} vessels results directly from loss of Piezo1 activity or some other unknown indirect impact of Piezo1 deletion. Comparing the contractile potential of endothelium-denuded arteries from control and Piezo1^{ΔEC} mice in response to 60mM K⁺ might offer some insight.

4.4.2 Deletion of endothelial cell Piezo1 potentiates ACh-induced vasorelaxation

In addition to their activation by shear stress Piezo1 seems to also function in ECs in the absence of mechanical stimulation (Li et al., 2014, Rode et al., 2017). ACh-induced relaxation was enhanced in Piezo1^{ΔEC} segments, compared to control segments. One possible explanation is that constitutive Piezo1 activity causes depolarisation, which counteracts the hyperpolarisation induced by the activation of muscarinic receptors by ACh. The next experiments investigated the relative importance of NO and EDHF mechanisms in ACh responses of Piezo1^{ΔEC} compared with control mice.

4.4.3 Deletion of endothelial cell Piezo1 affected EDHF-mediated vasorelaxation but does not affect NO-mediated-vasorelaxation

ACh has been reported to promote the release of EDHF and NO from vascular endothelium via the M₂ muscarinic receptor. Additional research has shown that EDHF induces hyperpolarisation of the VSMC membrane through the activation of a K⁺ channel, resulting in VSMC relaxation (Endo et al., 1995). In contrast, NO is synthesized in the endothelium from L-arginine, by the enzyme NO synthase, and causes vasodilation by an increase in cGMP by the activation of guanylate cyclase in VSMCs (Endo et al., 1995). Therefore, a combination of apamin plus charybdotoxin was used to inhibit EDHF while L-NAME was used to inhibit NO synthesis with and without the presence of endothelial Piezo1.

Under basal conditions, the tension in mesenteric arteries from control and Piezo1^{ΔEC} mice was unaffected after the incubation with L-NAME or combination of apamin plus charybdotoxin. This is consistent with the study of Dora, et al (2000) because at this time there was no stimulus for contraction, so simply recording resting tension would not allow an assessment of either NO or EDHF release (Dora, et al, 2000). Further contraction was observed in response to the pre-constriction with PE after incubation with L-NAME or the combination of apamin and charybdotoxin. This is again consistent with Dora, et al (2000) who suggests that EDHF is released together with NO during smooth muscle contraction to PE, as blockade of NO synthesis, or EDHF-release, greatly augmented the contraction to PE. These observations demonstrate that even before the onset of contraction there are already signalling processes occurring between the ECs and SMCs which can significantly modulate the contraction (Dora et al., 2000).

Pre-incubation of the mesenteric arteries from both groups with apamin plus charybdotoxin decreased the level of ACh-induced vasodilation mediated by EDHF. This is consistent with previous findings which illustrate that blocking the Ca²⁺-activated K⁺ channels via apamin and charybdotoxin abolishes the EDHF-mediated relaxation in rat mesenteric arteries (Yang et al., 2010). these results are also consistent with previous studies that showed EDHF-mediated relaxation in small mesenteric arteries (Yang et al., 2010, Yap et al., 2014). In arteries from control mice the toxins caused a slight inhibition

of the ACh response (Fig. 4.7), but they strongly inhibited the ACh response in arteries from Piezo1^{ΔEC} mice (Fig. 4.8). This confirms that the depolarisation induced by Piezo1 channels (a contractile function) was opposing the hyperpolarisation-induced by EDHF (a relaxation mechanism), meaning active Piezo1 channels act as an anti-EDHF modulators. Previous studies suggested that endothelial Piezo1 channels-induce NOS and the NO formation and thus enhance relaxation in response to flow (Li et al. 2014; Wang et al. 2016). These differences indicate a dichotomy for Piezo1 channel activity in endothelial biology. While Ca²⁺ entry leads to activation of the prorelaxant endothelial nitric oxide synthase, entry of cations as a whole (Ca²⁺ and Na⁺) cause membrane potential depolarisation and thus enhance contraction.

Previous research has shown that in rat mesenteric arteries, NO-mediated hyperpolarisation has only a minor role in ACh-induced relaxation (Garland and McPherson, 1992). Within this study, pre-treatment of the mesenteric arteries from both control and Piezo1^{ΔEC} mice with L-NAME resulted in a more major decrease in ACh-induced relaxation (Fig. 4.11 and 4.12). These results suggest that NO is important in ACh-induced vasodilation and that Piezo1 depletion does not affect NO-induced relaxation. Figure 4.12 showed that incubation with L-NAME suppressed ACh induced relaxation. L-NAME itself can significantly increase the PE-induced vasoconstriction. Therefore, NO signal seems involved in the vasoconstriction induced by PE. Then after L-NAME and ACh were added simultaneously to the chamber, it is expected that L-NAME itself can still evoke more contraction by inhibiting No signal in the presence of ACh. ACh-mediated relaxation will be compromised significantly even NO signal plays very limited role in ACh-mediated relaxation. It is not surprising that ACh and L-NAME added together would significantly reduced the PE-induced vasoconstriction.

4.4.4 The effect of removal of endothelial cells on ACh-induced relaxation

ECs play an essential role in maintaining local vascular tone (Lüscher et al., 1990). Removal of the endothelium entirely abolished ACh-induced relaxation (Fig. 4.14 and 4.16), which is consistent with previous studies (Raffetto et al., 2012, Kwon et al., 1999).

SIN-1, a NO donor, causes relaxation by the direct activation of guanylate cyclase, resulting in a rise in cGMP levels in SMCs (Plane, Sampson et al. 2001). Here, data showed that there was no difference in the levels of SIN-1-induced relaxation of the mesenteric arteries among the two groups (Fig. 4.17), suggesting that functional changes in the SMCs due to endothelial Piezo1 deletion are unlikely.

4.4.5 Piezo1 channels role in whole body physical activity

In addition to determining that loss of endothelial Piezo1 channels affects the activity of isolated mesenteric arteries, we observed that endothelial Piezo1 channels have a significant role in controlling BP in vivo in mice. The depolarising, anti-EDHF and so pro-contractile effects of Piezo1 observed in mesenteric arteries might be expected to cause depressed BP levels in the Piezo1^{ΔEC} mice, these mice possessing more dilated blood vessels. Under resting conditions, however, no change in BP was observed. This finding was in contrast to a recent study which reported that deletion of endothelial Piezo1 in mice results in an increase in systolic BP (Wang et al., 2016). They demonstrated in HUAEC, HUVEC and BAECs that Piezo1 was important for shear stress induced eNOS activity, thus proposing that Piezo1 is involved in flow-induced NO-dependent vasodilatation. They did not, however, observe any an increase in diastolic BP (personal communication), which would be expected to accompany any loss of vasodilatation. Intriguingly, while a flow-induced vasodilatation mechanism is present in mesenteric arteries (Wang et al., 2016, Ahn et al., 2017) we have demonstrated that pressure can also activate a vasoconstrictive mechanism, which is also dependent on Piezo1. Under active conditions we propose that the latter is pre-dominant since elevations seen in BP, both systolic and diastolic, during physical activity were reduced in Piezo1^{ΔEC} mice. It has been shown that exercise reduces mesenteric blood flow in humans (Qamar and Read, 1987), with our study suggesting that Piezo1 channels are the dominant source of the vasoconstrictor mechanism responsible.

4.4.6 Relaxation induced by Yoda1 in control, compared with Piezo1^{ΔEC} mice mesenteric arteries

Yoda1, a chemical activator of Piezo1, evoked calcium responses dependent largely on Ca²⁺ influx (Syeda et al., 2015, Cahalan et al., 2015). Yoda1 induced relaxation in mouse

mesenteric artery segments. These data are consistent with other data showing that Yoda1 caused relaxation in mouse mesenteric arteries (Wang et al., 2016). However, Yoda1-induced relaxation was not significantly reduced in Piezo1^{ΔEC}. It was therefore concluded that the ability of Yoda1 to induce relaxation is not influenced by the deletion of Piezo1 in the endothelium and thus that Piezo1 in the endothelium is not essential to the relaxation response mediated by Yoda1. Previously, Wang and colleagues, using equivalent concentrations of Yoda1 as tested here, reported that Yoda1 responses were lost in a knockout of endothelial Piezo1 in mouse mesenteric arteries (Wang et al., 2016). This inconsistency with the results presented here may arise from different strategies to knockout endothelial Piezo1 in mice. Additionally in conflict with their data, results from our lab found that at rest, BP was the same in control and Piezo1^{ΔEC} mice, suggesting endothelial Piezo1 does not affect basal vascular tone. Another previous study suggests that endothelial inwardly rectifying K⁺ channels regulate flow-induced vasodilatation rather than Piezo1 in ECs (Ahn et al., 2016).

The following experiments aim to explore Yoda1-mediated vasorelaxation in the absence or the presence of non-specific Piezo1 inhibitors, EC, EDHF and NO.

4.4.7 Contribution of Piezo1 in Yoda1-induced relaxation

The data show that control and Piezo1^{ΔEC} mesenteric arteries of mice treated with Piezo1 inhibitors, Gd³⁺ and RR (Cinar et al., 2015), have significantly reduced the vasorelaxation response to Yoda1 (Fig. 4.21). These antagonists were able to reduce Yoda1-induced relaxation, indicating that Piezo1 channels are involved in Yoda1-induced relaxation.

4.4.8 The effect of removal of endothelial cells on Yoda1-induced relaxation

The findings reported here show only a small role for the ECs in mediating Yoda1-induced relaxation. Removal of ECs did not alter Yoda1-induced relaxation in either control or Piezo1^{ΔEC} mice. Mesenteric arteries from both groups were still able to respond to Yoda1. It can be concluded that the ability of Yoda1 to provide relaxation is not influenced by removing ECs and is largely endothelial independent, and that Piezo1 present in SMCs might be involved in this relaxation ((Retailleau et al., 2015). These

results are inconsistent with a recent study showing that Yoda1 responses were strongly reduced in a knockout of Piezo1 in mouse mesenteric arteries (Wang et al., 2016). However, the level of SIN-1-induced relaxation was similar in both groups. It appears that SMCs function is protected in both groups.

4.4.9 The contribution of EDHF and NO to Yoda1-induced relaxation

It is well known that EDHF is a mechanism for endothelium-dependent vasodilatation. However, Yoda1-induced vasodilation does not seem to be different from that of mesenteric arteries incubated with apamin plus charybdotoxin, indicating that EDHF does not contribute to Yoda1 responses.

Piezo1 is important for alignment of ECs in response to shear stress and for the phosphorylation of endothelial NOS in the presence of VEGF (Li et al., 2014) and also Yoda1 induced NOS phosphorylation (Wang et al., 2016). Relaxation induced by in control segments treated with the endothelial NOS inhibitor L-NAME was impaired. Yoda1 relaxation appears to act through NO pathways. These results showed the effect of L-NAME on the Yoda1 response which does not match a previous observation that in vessels with denuded endothelium, the relaxation response of Yoda1 can still be observed, suggesting that the endothelium may play a minor role in endothelium-dependent relaxations and a dominant role of endothelial NOS activity. In contrast, mesenteric artery segments from Piezo1^{ΔEC} mice were insensitive to the endothelial NOS inhibitor L-NAME. Furthermore, after denuding the ECs the incubation with L-NAME did not reduce the Yoda1-induced relaxation and the independent relaxation effect of Yoda1 is clear in mesenteric arteries from wild-type mic.

Overall, the Yoda1 response has both endothelium-dependent and independent vasodilation. However, the endothelium-dependent effect did not reach statistical significance, thus without increasing the numbers of these experiments this effect is still difficult to show. This could be related to the fact that Yoda1 has both endothelium dependent vasodilator and vasoconstrictor effects of Yoda1, which makes it difficult to ensure that an endothelium-dependent vasodilator effect of Yoda1 is seen. Moreover, the presence of endothelium and vascular smooth muscle is necessary for endothelial NOS and Yoda1 activation of Piezo1, because the loss of the endothelium means the

loss of the vascular smooth muscle Piezo1 channel dependency on endothelial NOS. However, the reason why they lose this dependence is unknown, but it might relate to a signalling system between ECs and VSMCs, whereby the VSMCs adapt to achieve different properties when the endothelium is damaged. Hence, endothelial damage can lead to change in the mechanisms or the properties of the vascular SMCs.

4.5 Conclusion

The data presented here suggest that constitutive Piezo1 channel activity in the endothelium normally opposes ACh-induced vasorelaxation of mouse mesenteric arteries with Piezo1 deletion and EDHF contributing to this relaxation. A possible mechanism is that Piezo1 channel activity depolarises the membrane, therefore counteracting the effect of ACh (Fig. 4.34). The consequence is that Piezo1 in the endothelium may increase BP. However, activation of Piezo1 channels by Yoda1 leads to relaxation, suggesting the potential to lower BP by enhancing Piezo1 channel activity over and above the constitutive level. Furthermore, endothelial Piezo1 may be a molecular mechanism for sensing whole body physical activity. The channels could sense and transduce fluid-flow into constriction of mesenteric arteries leading to increased BP at the time of physical activity where these arteries contribute to total peripheral resistance.

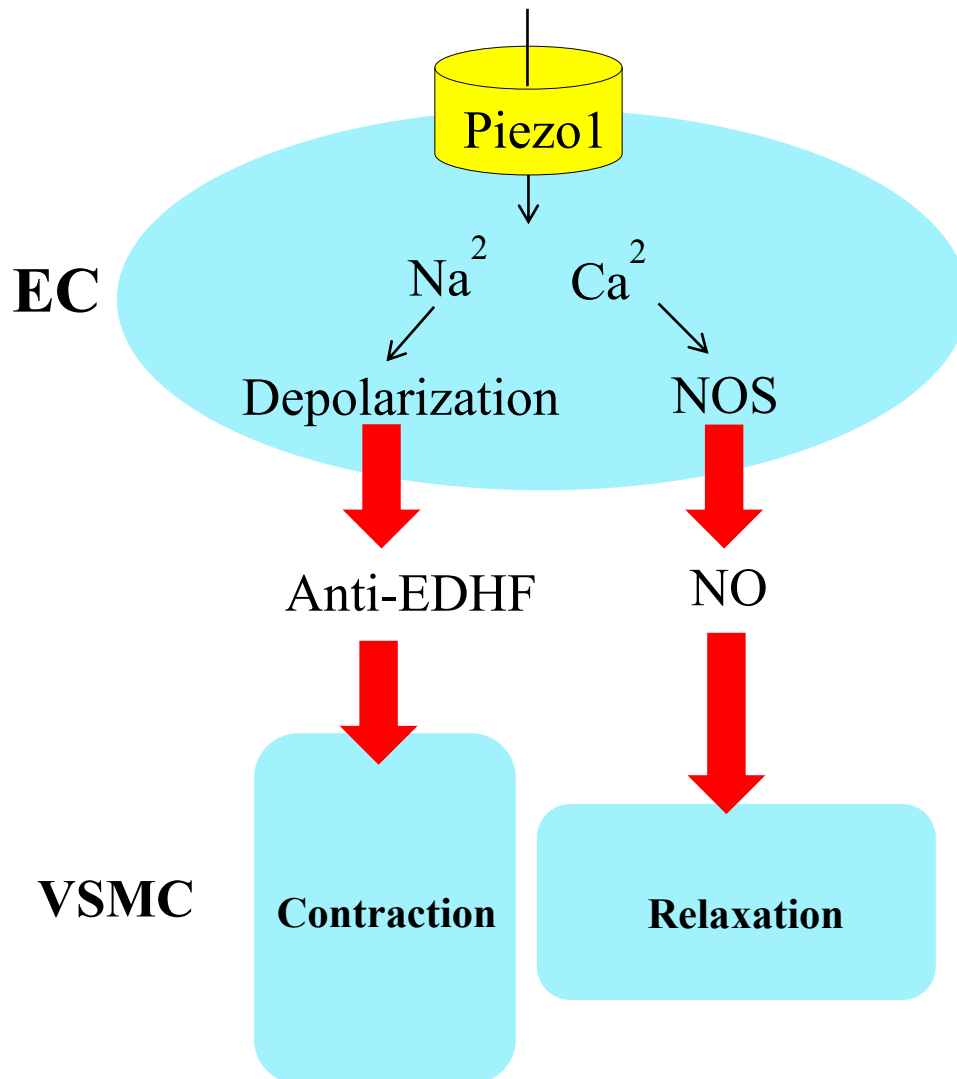


Figure 4-34: Ischaemic diagram presenting the effects of Piezo1 channel activity in the endothelial cells

Chapter 5 Lack of role of endothelial Piezo1 in saphenous and carotid arteries of mice

5.1 Introduction

The arterial system is the network of blood vessels which carries oxygenated blood from the heart to organs. Beginning with the ascending aorta the arterial system undergoes repeated branching, both as asymmetrical bifurcations and also higher order branching. Fig. 5.1 demonstrates the arteries' anatomical layout. It also reveals the reduction in the diameter of the arteries as they advance to the periphery. Diameter variations also happen at the branches, with the daughter branches having smaller diameters than the parent. The descending aorta is also noticeably tapered, narrowing as it spreads away from the heart. It is evident that functional and morphological properties of elastic and muscular arteries vary considerably. Elastic arteries, such as the aorta and the carotid artery, include more elastin per unit area and have significant pulse-smoothing properties of the pressure wave starting in the left ventricle. On the other hand, the muscular arteries, such as femoral or mesenteric arteries, have relatively more smooth muscle and less elastin. They distribute the blood according to moment-to-moment demands and are more able of vasoconstriction and dilation. The structure of the arterial system in humans and in several other mammals is comparable. Several mammalian species illustrate similar pressure and flow waveforms at several sites along the arterial tree (Leloup et al., 2015).

Having established that the functional role of endothelial Piezo1 differs between the aorta (Chapter 3) and mesenteric arteries (Chapter 4), in this chapter two further arteries are studied in order to further our understanding of this channel's involvement in the mammalian arterial system. The saphenous artery, a skeletal muscle vessel that supplies the leg, and the carotid artery, a main blood vessel that supplies the brain, were chosen for comparison. As in the previous chapters, the functional responses of saphenous and carotid arteries from control and Piezo1^{ΔEC} mice were assessed by wire myography. There are currently no reports in the literature relating to Piezo1 function or expression in ECs in these vessels.

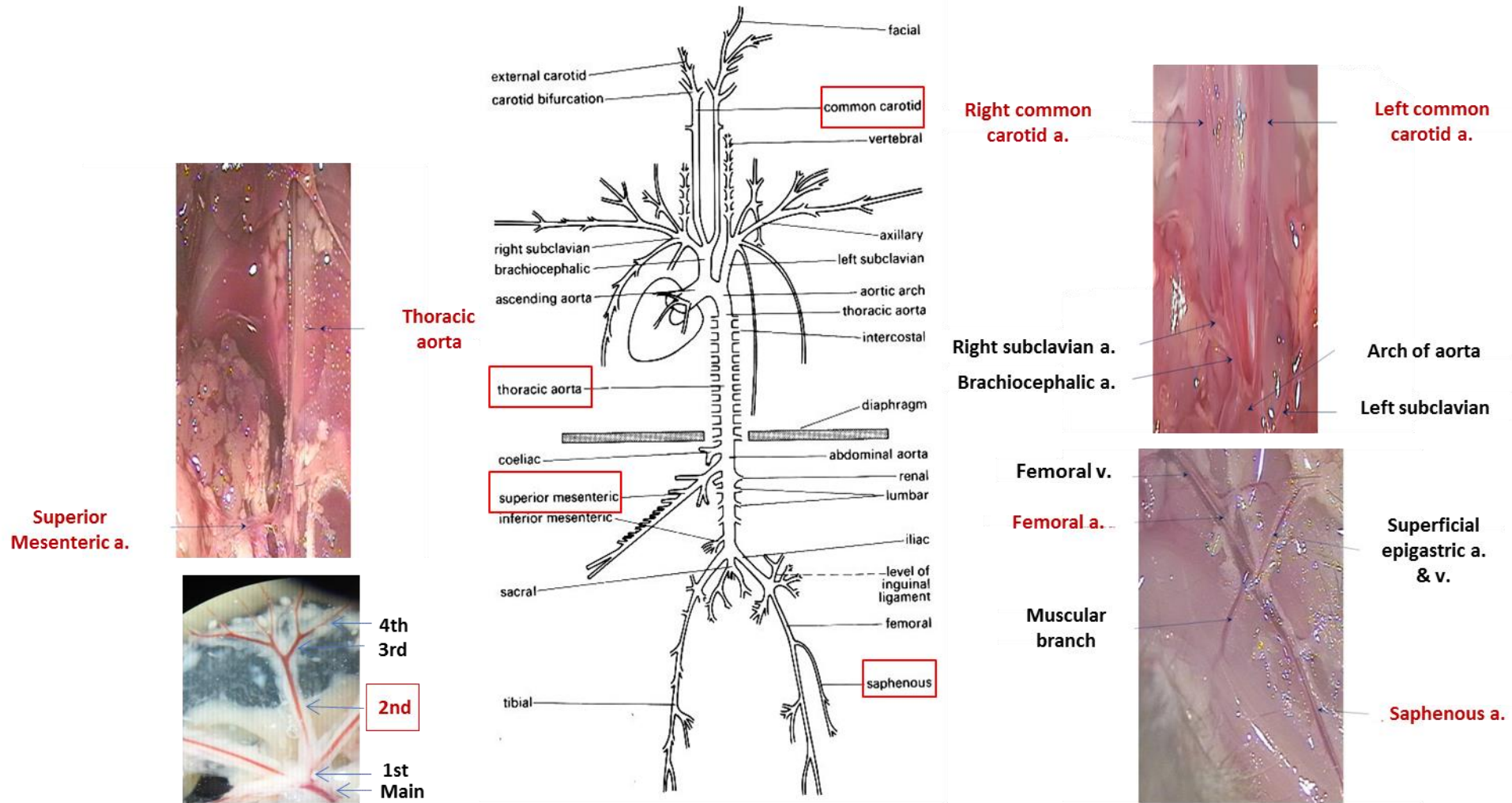


Figure 5-1: Schematic representation of arterial vessels topography and preparation of mouse arteries.

5.2 Results

5.2.1 Deletion of endothelial cell Piezo1 does not affect high potassium-induced contraction

Incubation of saphenous and carotid arteries from control and Piezo1^{ΔEC} mice in high K⁺ (60 mM) over a 10 minute period induced constriction, confirming their viability. Saphenous and carotid arteries from control and Piezo1^{ΔEC} mice displayed typical K⁺-induced contraction as shown in Fig. 5.2a and 5.2b respectively (saphenous artery) and Fig. 5.3a and 5.3b respectively (carotid artery). Similar to previous findings (Golubinskaya et al., 2014), the active tone of saphenous arteries was around ~ 5 mN, and in carotid arteries was about ~1.3 mN. Of the four vessels tested in this thesis carotid arteries were the least contractile in response to high K⁺, this difference possibly relating to size, composition and role of the vessel. K⁺-induced contractions were similar in magnitude for control and Piezo1^{ΔEC} mice in both saphenous and carotid arteries (Fig. 5.2c and 5.3c). These data suggest that in EC Piezo1 deletion does not affect K⁺-induced contraction in either saphenous or carotid arteries.

5.2.2 Deletion of endothelial cell Piezo1 does not affect phenylephrine-induced contraction

After the standard high K⁺ start procedure, contractions to increasing concentrations of PE were measured to further assess the contractile responses of the vessels (similar dose range for PE that used with mouse mesenteric artery). Representative traces of PE-induced tone are provided of saphenous and carotid arteries from control and Piezo1^{ΔEC} mice (Fig. 5.4a and 5.4b, respectively of saphenous artery and Fig. 5.5a and 5.5b, respectively of carotid artery). The two vessels displayed distinct sensitivities and responsiveness.

At 1 μM PE saphenous arteries were ~50% contracted, while carotid arteries were ~130% contracted, the greater than 100% value arising because PE responses are expressed as percentage of the 60 mM of high K⁺-induced contraction. Furthermore, contraction to PE was seen at a slightly lower concentration for carotid than saphenous arteries, 0.1 μM compared with 0.03 μM. For both vessels, however, there was no

difference in the PE-induced tone between control and Piezo1^{ΔEC} mice (Fig. 5.4c, 5.4d and 5.5c, 5.5d). These data suggest that the sensitivity to PE in the saphenous and carotid arteries is not influenced by endothelial Piezo1.

5.2.3 Deletion of endothelial cell Piezo1 does not affect ACh-induced vasorelaxation

Saphenous and carotid arteries were pre-contracted with 0.3 μM PE in order to establish a maintained constriction of the vessel upon which concentration dependent relaxations to ACh could be assessed. When a stable plateau in tension was achieved, each ring was exposed to increasing concentrations of ACh to generate concentration-dependent relaxation responses.

In saphenous arteries relaxation was observed at concentrations equal to or above 0.01 μM ACh (the dose range for ACh was based on prior experiments examining mouse mesenteric arteries). However, in carotid arteries, since transient contraction (rather than relaxation) was observed in response to ACh concentrations above 0.03 μM, the concentration range tested had to be extended down to 1 nM to assess ACh-induced relaxation. The maximal magnitude of relaxation was very similar (~90%) in both arteries, although this occurred at different concentrations. Particular sensitivity of the carotid artery to ACh has been reported previously, as compared with the femoral artery (Crauwels et al., 2000).

In carotid arteries at concentrations of ACh above 0.03 μM, contractions, rather than relaxations were observed. These contractions likely correspond to the EDCF that has been demonstrated in mouse carotid arteries and other blood vessels (Furchgott and Vanhoutte, 1989, Tang et al., 2005). The fundamentals of the EDCF cell-signalling pathway seem to be as follows. In response to receptor activation, an increase in endothelial [Ca²⁺]_i stimulates Ca²⁺-dependent phospholipase A₂, releasing arachidonic acid that is subsequently metabolised via cyclooxygenases resulting in the synthesis and liberation of endoperoxides and/or prostaglandins. These then travel to the VSMCs, stimulating thromboxane prostanoid receptors and leading to calcium influx into the SMCs and so activation of contractile signalling. (Fig. 5.6) (Katusic et al., 1988, Miller and Vanhoutte, 1985, Tang et al., 2005). This phenomenon was not observed in

saphenous arteries, which could be related to differential sensitivity of different types of artery or that the EDCF is not created in saphenous arteries.

Representative traces of ACh concentration response curves in control and Piezo1^{ΔEC} mice saphenous and carotid arteries are provided in Fig 5.7 and 5.8. The control and Piezo1^{ΔEC} mice saphenous arteries showed a steady decrease in tension until a maximal relaxation of near 80% was achieved, thus almost fully reversing the PE induced contraction (Fig. 5.7a and 5.7b, respectively of saphenous artery and Fig. 5.8a and 5.8b, respectively of carotid artery). The response to cumulative concentrations of ACh, for both control and Piezo1^{ΔEC} mice saphenous and carotid arteries, was not different (Fig. 5.7c for saphenous artery and Fig. 5.8c for carotid artery). Furthermore, no difference was found in the AUC of the response to ACh for each individual curve as indicated in Fig. 5.7d and 5.8d of saphenous and carotid arteries from control and Piezo1^{ΔEC} mice respectively. Overall, this suggests that the response to ACh was not modified by deletion of endothelial Piezo1 in saphenous or carotid arteries.

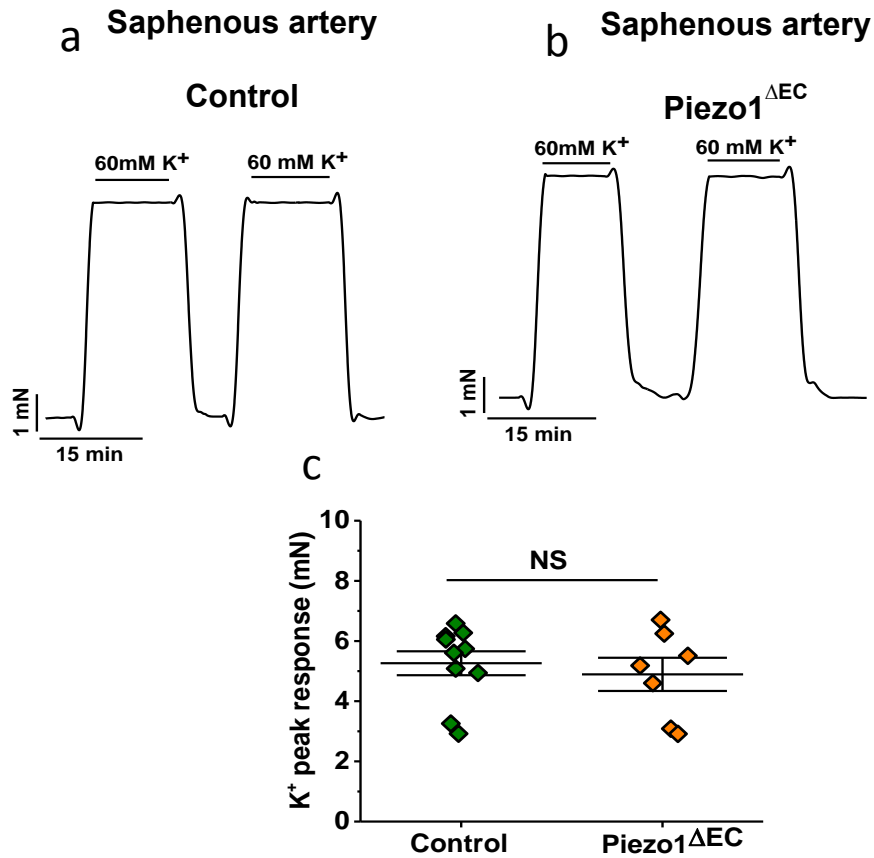


Figure 5-2: Vascular reactivity to high potassium (60 mM K⁺) in control compared with endothelial Piezo1^{ΔEC} saphenous arteries

(a) Typical wire myograph trace, demonstrating vasoconstriction in response to high potassium solution that validates arterial viability prior to experimentation, in saphenous arteries isolated from control mice. (b) As for (a) except in saphenous arteries isolated from Piezo1^{ΔEC} mice. (c) Comparison of response to high potassium (K⁺)-induced contraction in saphenous arteries of control ($n=10$) and Piezo1^{ΔEC} mice ($n=7$). Responses are expressed by the absolute value of the K⁺-induced contraction. Mean \pm SEM values are depicted. NS=not significant.

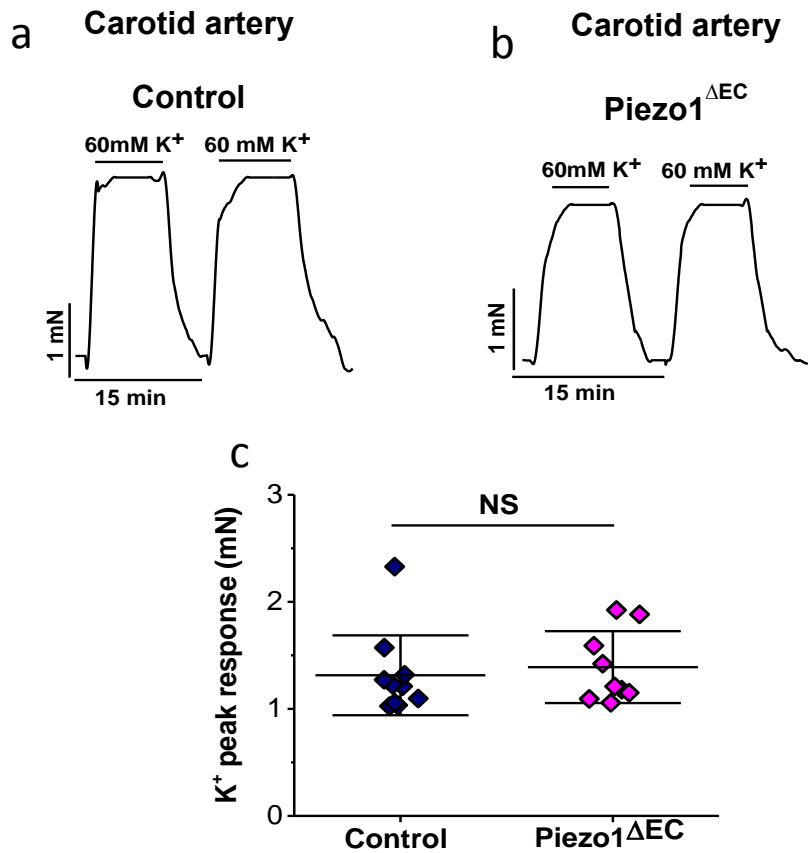


Figure 5-3: Vascular reactivity to high potassium (60 mM K⁺) in control compared with endothelial Piezo1^{ΔEC} carotid arteries

(a) Typical wire myograph trace, demonstrating vasoconstriction in response to high potassium solution that validates arterial viability prior to experimentation, in carotid arteries isolated from control mice. (b) As for (a) except in carotid arteries isolated from Piezo1^{ΔEC} mice. (c) Comparison of response to high potassium (K⁺)-induced contraction in carotid arteries of control ($n=10$) and Piezo1^{ΔEC} mice ($n=9$). Responses are expressed by the absolute value of the K⁺-induced contraction. Mean \pm SEM values are depicted. NS=not significant.

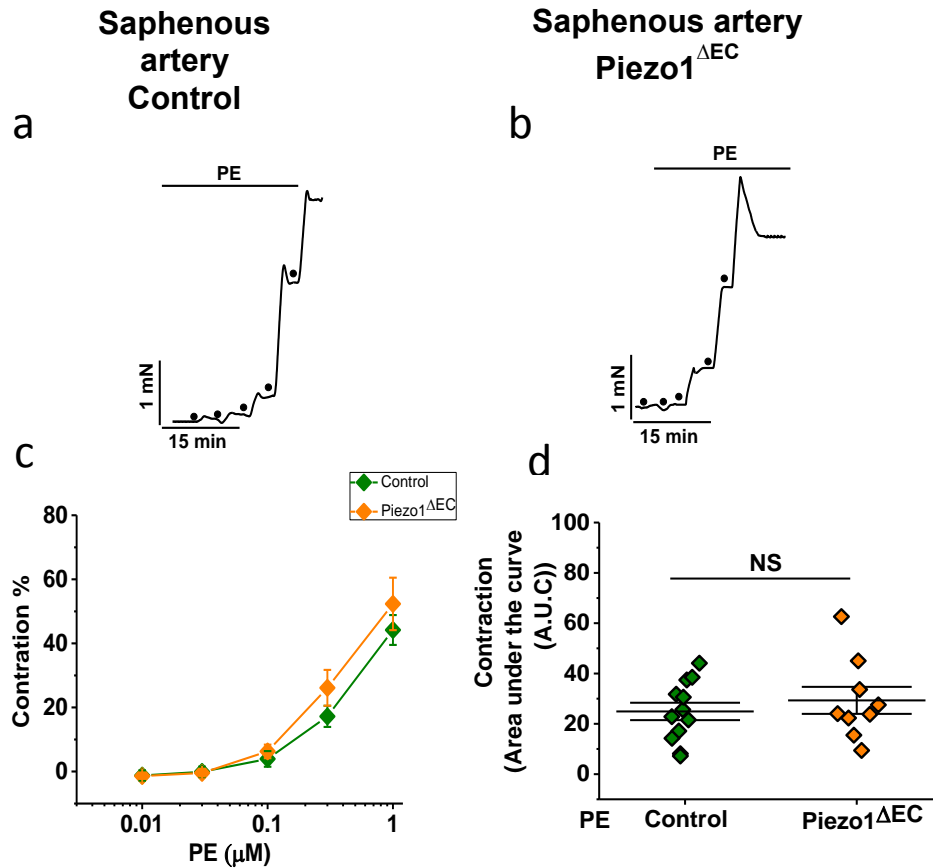


Figure 5-4: Vascular reactivity to phenylephrine in control compared with endothelial Piezo1^{ΔEC} saphenous arteries

(a) Typical wire myograph tracing, demonstrating increased tone in response to phenylephrine (PE) as indicated by the dots (0.01, 0.03, 0.1, 0.3 and 1 μM) in saphenous arteries isolated from control mice. (b) As for (a) except in saphenous arteries isolated from Piezo1^{ΔEC} mice. (c) Concentration response curves to PE in control; $n=11$) and Piezo1^{ΔEC} ($n=9$) mice. (d) The area under the curve (AUC) of the response to PE for each individual curve of saphenous arteries isolated from control ($n=11$) and Piezo1^{ΔEC} mice ($n=9$). Responses are expressed as percent constriction and as the area under the curve (AUC) of the response to PE. Mean \pm SEM values are depicted. NS=not significant.

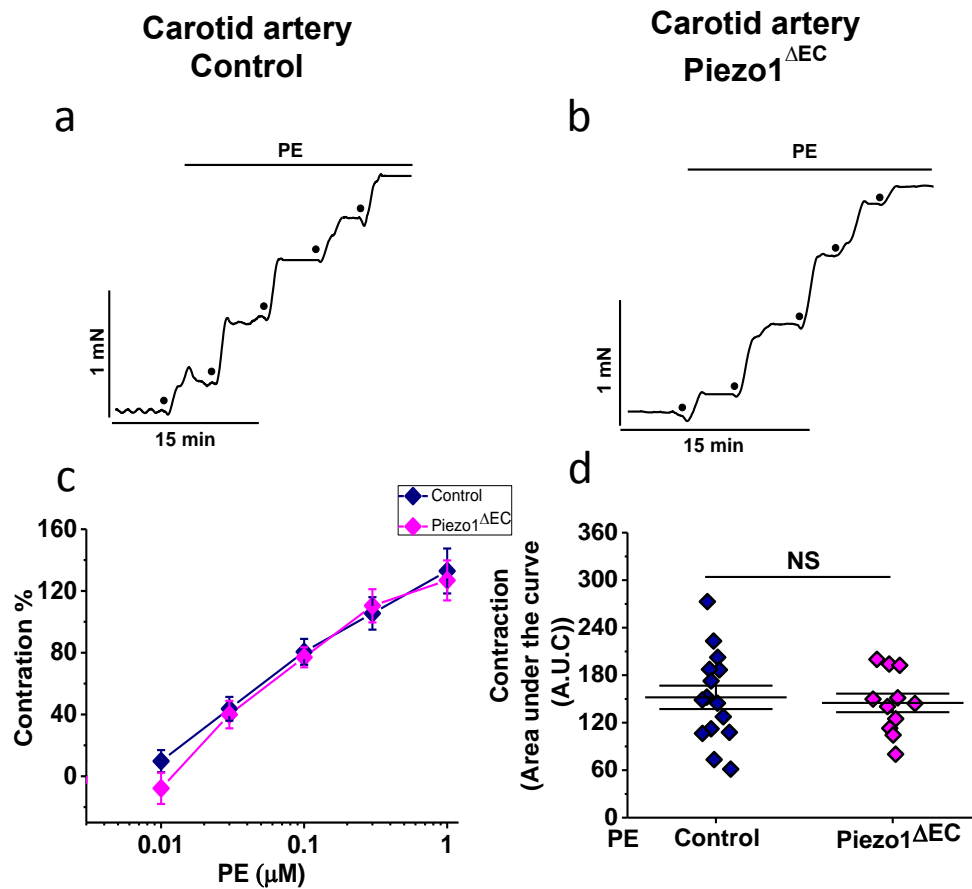


Figure 5-5: Vascular reactivity to phenylephrine in control compared with endothelial Piezo1^{ΔEC} carotid arteries

(a) Typical wire myograph tracing, demonstrating increased tone in response to phenylephrine (PE) as indicated by the dots (0.01, 0.03, 0.1, 0.3 and 1 μ M) in carotid arteries isolated from control mice. (b) As for (a) except in carotid arteries isolated from Piezo1^{ΔEC} mice. (c) Concentration response curves to PE in control; ($n=15$) and Piezo1^{ΔEC} ($n=11$) mice. (d) The area under the curve (AUC) of the response to PE for each individual curve of carotid arteries isolated from control ($n=11$) and Piezo1^{ΔEC} mice ($n=9$). Responses are expressed as percent constriction and as the area under the curve (AUC) of the response to PE. Mean \pm SEM values are depicted. NS=not significant.

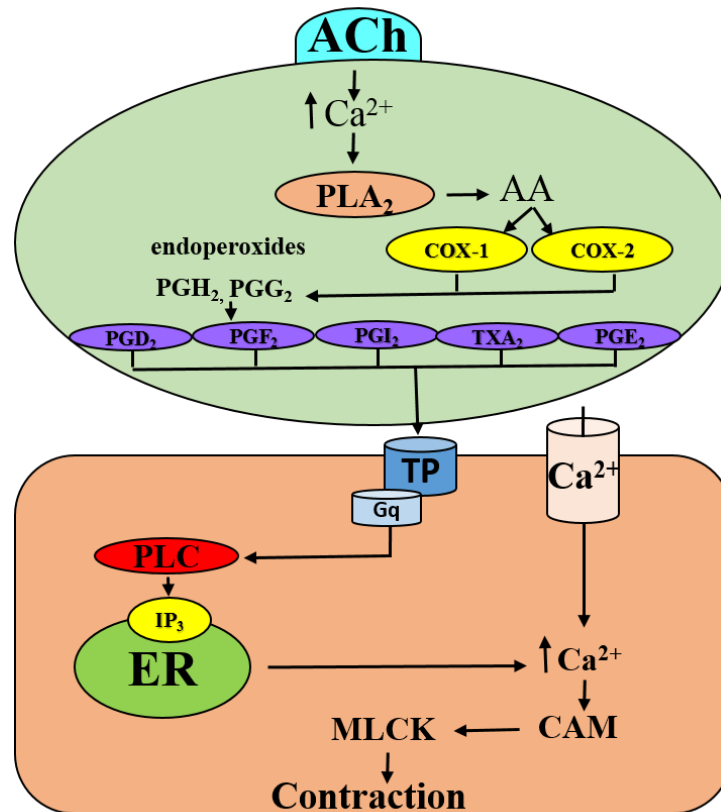


Figure 5-6: EDCF cell-signalling activity

Arachidonic acid (AA) can be metabolised into endoperoxides by cyclooxygenases, which can be additionally broken down through enzymes producing prostaglandin E₂, prostaglandin D₂, prostaglandin F₂, prostacyclin, and also thromboxane A₂. One or several of these prostanoids can diffuse across to the smooth muscle cell (SMC) and activate thromboxane prostanoid (TP) receptors, which leads to calcium (Ca²⁺) influx into the SMC and induces its contraction.

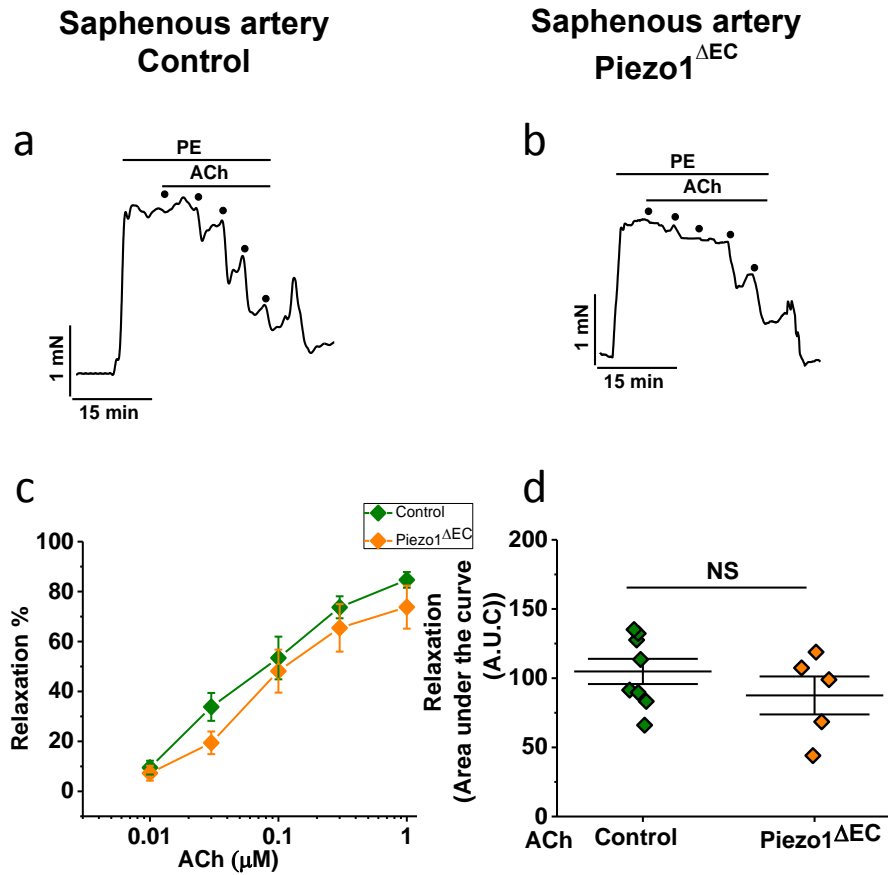


Figure 5-7: Vascular reactivity to ACh in control compared with endothelial Piezo1^{ΔEC} saphenous arteries

(a) Typical trace showing a concentration-dependent dilatory response to acetylcholine (ACh) as indicated by the dots (0.01, 0.03, 0.1, 0.3 and 1 μM) in saphenous arteries isolated from control mice. (b) As for (a) except in saphenous arteries isolated from Piezo1^{ΔEC} mice. (c) Concentration response curves to ACh in control ($n=10$) and Piezo1^{ΔEC} ($n=7$) mice. (d) The area under the curve (AUC) of the response to ACh of saphenous arteries isolated from control ($n=10$) and Piezo1^{ΔEC} mice ($n=7$). Responses are expressed as percent relaxation, and as the area under the curve (AUC) of the response to ACh. Mean \pm SEM values are depicted. NS=not significant.

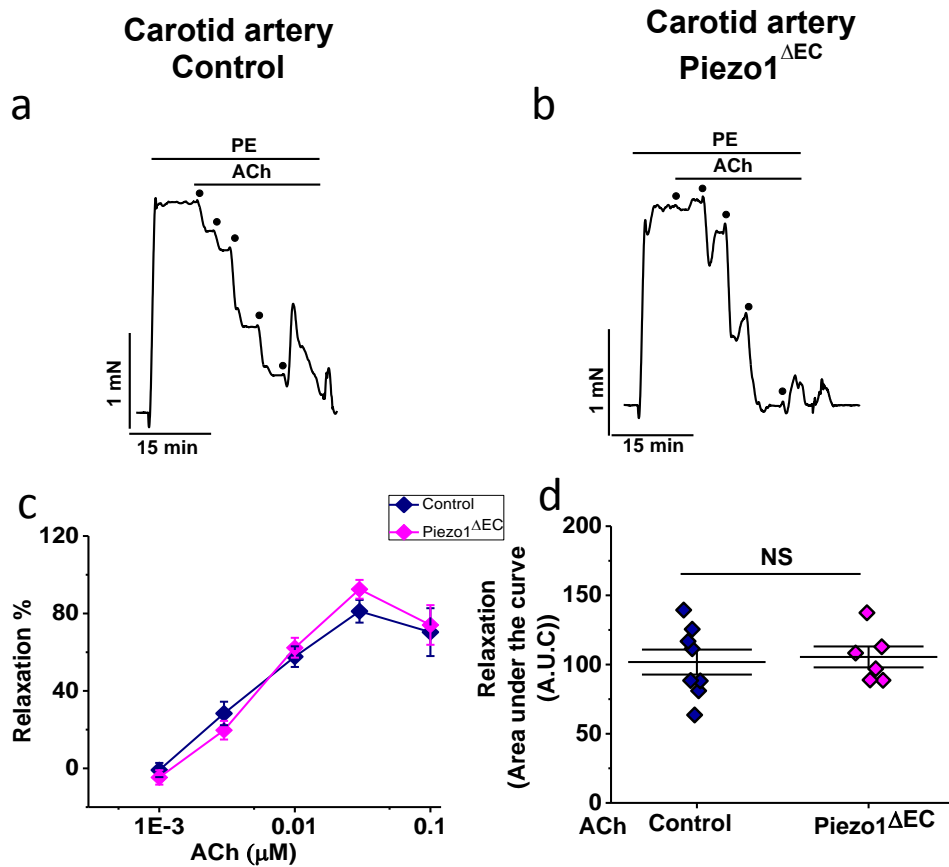


Figure 5-8: Vascular reactivity to ACh in control, compared with endothelial Piezo1^{ΔEC} carotid arteries

(a) Typical trace showing a concentration-dependent dilatory response to acetylcholine (ACh) as indicated by the dots (0.001, 0.003, 0.01, 0.03 and 0.1 μM) in carotid arteries isolated from control mice. (b) As for (a) except in carotid arteries isolated from Piezo1^{ΔEC} mice. (c) Concentration response curves to ACh in control ($n=10$) and Piezo1^{ΔEC} ($n=9$) mice. (d) The area under the curve (AUC) of the response to ACh of carotid arteries isolated from control ($n=10$) and Piezo1^{ΔEC} mice ($n=8$). Responses are expressed as percent relaxation, and as the area under the curve (AUC) of the response to ACh. Mean \pm SEM values are depicted. NS=not significant.

5.2.4 Deletion of endothelial cell Piezo1 does not affect EDHF-mediated-vasorelaxation

As in the previous chapter, the ACh response was analysed in more detail, assessing the contributions of both the EDHF and NO derived mechanisms underlying the relaxation induced. Again apamin and charybdotoxin, blockers of $SK_{Ca^{2+}}$ and $IK_{Ca^{2+}}$ channels respectively located on the endothelium, were employed to prevent hyperpolarisation of the endothelial cell but leave the NO component of relaxation intact. Apamin and charybdotoxin had no effect on either the basal or PE-induced tension in either vessel nor on the ACh-induced relaxation of the carotid artery (Fig. 5.11 and 5.12). The blockers did, however, significantly reduce the magnitude of the ACh-induced relaxation of the saphenous artery (Fig. 5.9 and 5.10).

Saphenous and carotid arteries from control and Piezo1 $^{\Delta EC}$ mice displayed a typical trace of ACh-induced relaxation before and after incubation with apamin plus charybdotoxin (Fig. 5.9a and 5.10a, respectively for the saphenous artery and Fig. 5.11a and 5.12a, respectively for the carotid artery). Comparing control with Piezo1 $^{\Delta EC}$ mice vessels, no differences were observed in the resting tone (Fig. 5.9b and 5.10b, respectively of the saphenous artery and Fig. 5.11b and 5.12b, respectively of the carotid artery) or PE-induced contraction (Fig. 5.9c to 5.12c). Similar significant differences were observed in ACh-induced relaxation of mouse saphenous arteries from both strains of mice when the combination of the apamin plus charybdotoxin inhibitors was used (44% decrease for control and 39% decrease for Piezo1 $^{\Delta EC}$) (Fig. 5.9d-5.10d). As for control mice, apamin plus charybdotoxin had no effect on the ACh-induced relaxation of carotid arteries of Piezo1 $^{\Delta EC}$ mice (Fig. 5.11d-5.12d). The data suggest that endothelial Piezo1 is of no consequence to the EDHF-derived component of the ACh response.

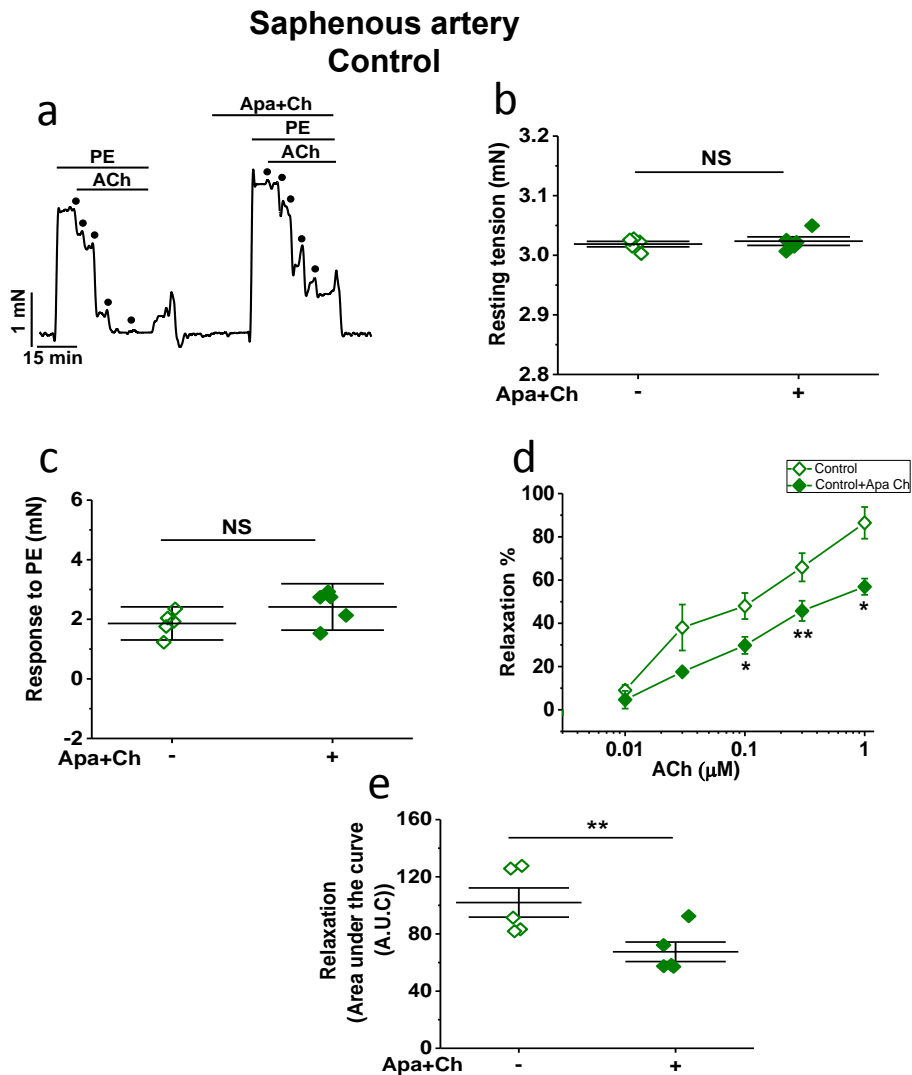


Figure 5-9: EDHF-mediated-vasorelaxation in control mice saphenous arteries

(a) Typical trace showing a concentration-dependent dilatory response to acetylcholine (ACh) as indicated by the dots (0.01, 0.03, 0.1, 0.3 and 1 μM) before and after the incubation with apamin (Apa) (500 nM) plus charybdotoxin (Ch) (100 nM) in saphenous arteries isolated from control mice. (b) Quantification of the Apa+Ch effects on the basal saphenous artery tension ($n=5$). (c) Quantification of the Apa+Ch effects on phenylephrine (PE)-induced constriction in control saphenous arteries of mice ($n=5$). (d) Concentration response curves to ACh before and after the application of Apa+Ch in control saphenous arteries of mice ($n=5$). (e) The area under the curve (AUC) of the response to ACh before and after the incubation with Apa+Ch of saphenous arteries, isolated from control mice ($n=5$). Responses are expressed as percent constriction and as the area under the curve (AUC) of the response to ACh. Mean \pm SEM values are depicted. Asterisks indicate statistically significant difference (* $p<0.05$ and ** $p<0.1$). NS=not significant.

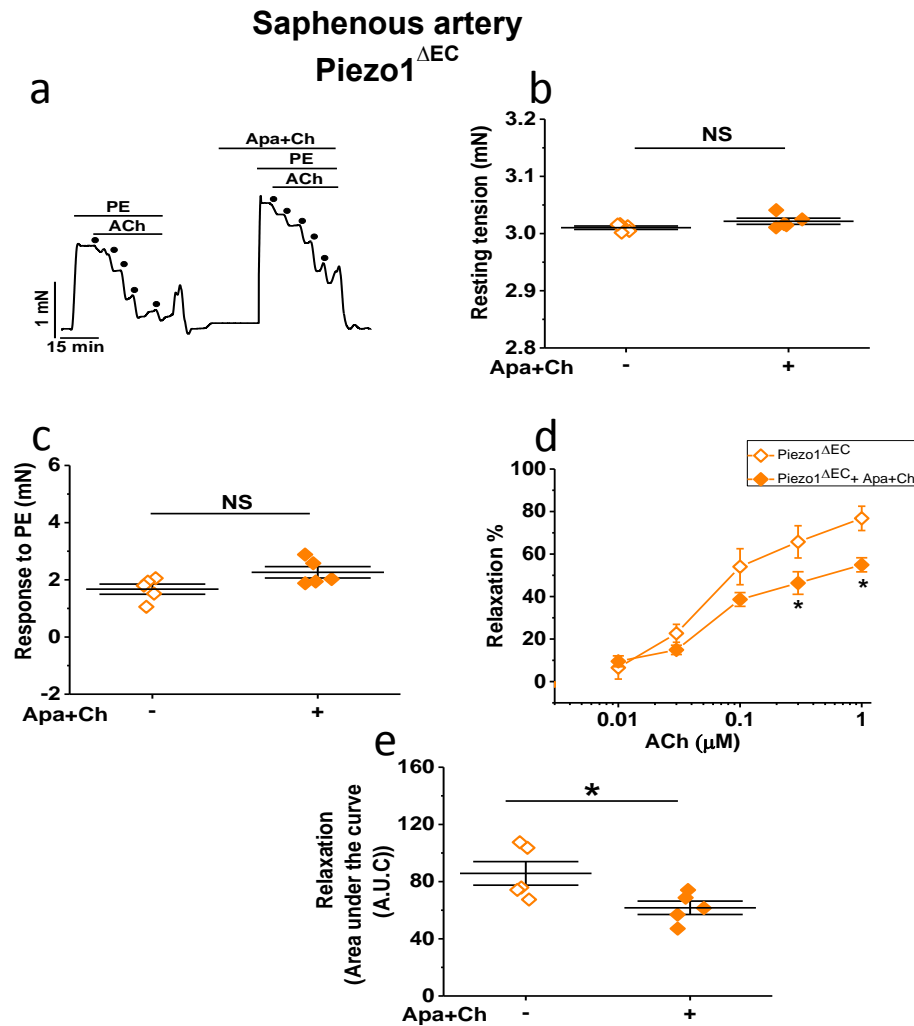


Figure 5-10: EDHF-mediated-vasorelaxation in endothelial Piezo1^{ΔEC} mice saphenous arteries

(a) Typical trace showing a concentration-dependent dilatory response to acetylcholine (ACh) as indicated by the dots (0.01, 0.03, 0.1, 0.3 and 1 μM) before and after the incubation with apamin (Apa) (500 nM) plus charybdotoxin (Ch) (100 nM) in saphenous arteries isolated from Piezo1^{ΔEC} mice. (b) Quantification of the Apa+Ch effects on the basal artery tension ($n=5$). (c) Quantification of the Apa+Ch effects on phenylephrine (PE)-induced constriction in Piezo1^{ΔEC} saphenous arteries of mice ($n=5$). (d) Concentration response curves to ACh before and after the application of Apa+Ch in Piezo1^{ΔEC} saphenous arteries of mice ($n=5$). (e) The area under the curve (AUC) of the response to ACh before and after the incubation with Apa+Ch of saphenous arteries isolated from Piezo1^{ΔEC} mice ($n=5$). Responses are expressed as percent constriction and as the area under the curve (AUC) of the response to ACh. Mean \pm SEM values are depicted. Asterisks indicate statistically significant difference (* $p<0.05$ and ** $p<0.01$). NS=not significant.

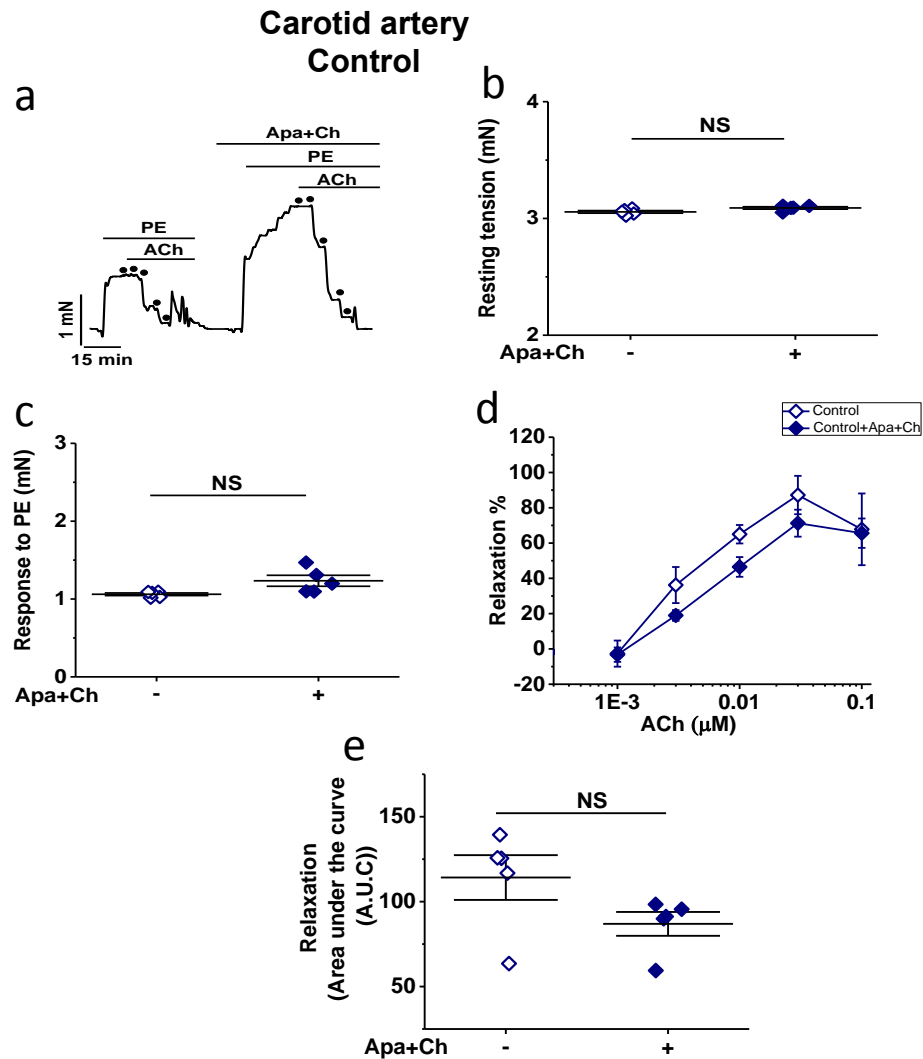


Figure 5-11: EDHF-mediated-vasorelaxation in control mice carotid arteries

(a) Typical trace showing a concentration-dependent dilatory response to acetylcholine (ACh) as indicated by the dots (0.001, 0.003, 0.01, 0.03 and 0.1 μM) before and after the incubation with apamin (Apa) (500 nM) plus charybdotoxin (Ch) (100 nM) in carotid arteries isolated from control mice. (b) Quantification of the Apa+Ch effects on the basal carotid artery tension ($n=5$). (c) Quantification of the Apa+Ch effects on phenylephrine (PE)-induced constriction in control carotid arteries of mice ($n=5$). (d) Concentration response curves to ACh before and after the application of Apa+Ch in control carotid arteries of mice ($n=5$). (e) The area under the curve (AUC) of the response to ACh before and after the incubation with Apa+Ch of carotid arteries, isolated from control mice ($n=4$). Responses are expressed as percent constriction and as the area under the curve (AUC) of the response to ACh. Mean \pm SEM values are depicted. NS=not significant.

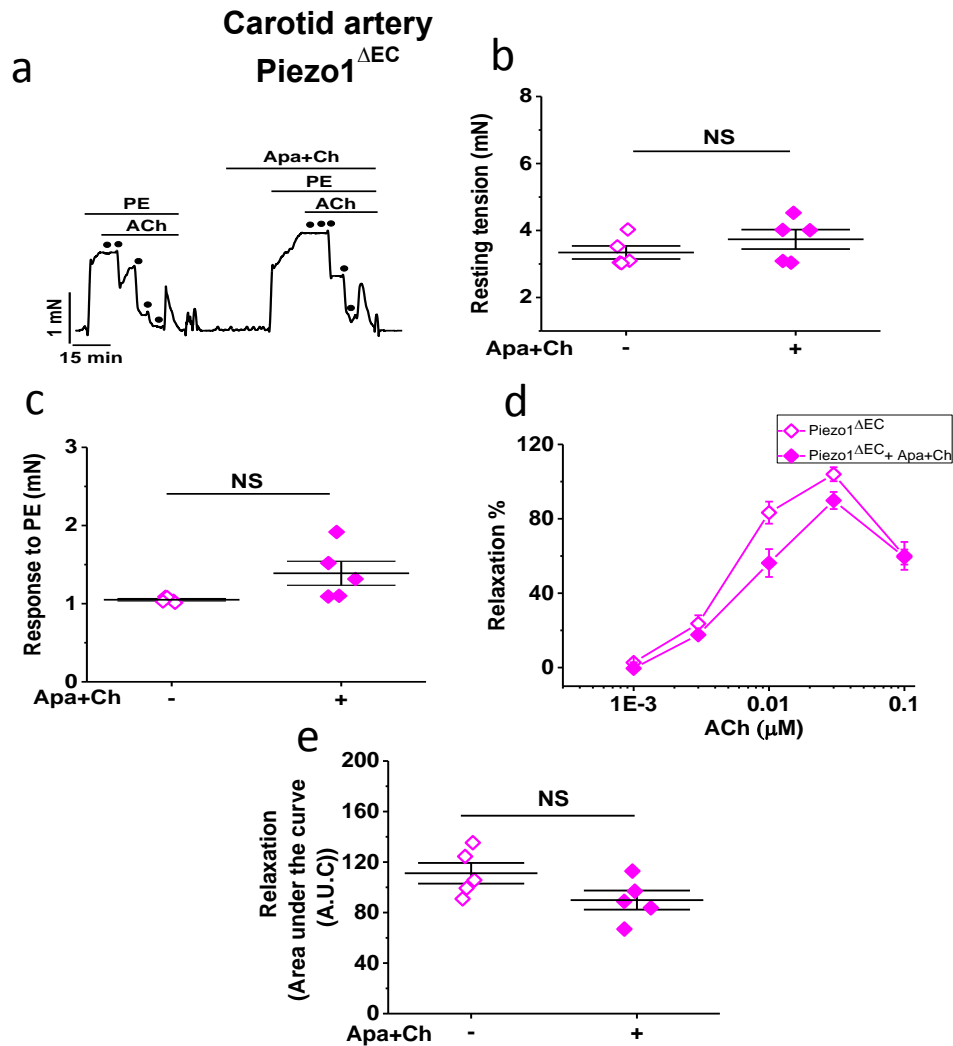


Figure 5-12: EDHF-mediated-vasorelaxation in endothelial Piezo1^{ΔEC} mice carotid arteries

(a) Typical trace showing a concentration-dependent dilatory response to acetylcholine (ACh) as indicated by the dots (0.001, 0.003, 0.01, 0.03 and 0.1 μM) before and after the incubation with apamin (Apa) (500 nM) plus charybdotoxin (Ch) (100 nM) in carotid arteries isolated from Piezo1^{ΔEC} mice. (b) Quantification of the Apa+Ch effects on the basal artery tension ($n=5$). (c) Quantification of the Apa+Ch effects on phenylephrine (PE)-induced constriction in Piezo1^{ΔEC} carotid arteries of mice ($n=5$). (d) Concentration response curves to ACh before and after the application of Apa+Ch in Piezo1^{ΔEC} carotid arteries of mice ($n=5$). (e) The area under the curve (AUC) of the response to ACh before and after the incubation with Apa+Ch of carotid arteries isolated from Piezo1^{ΔEC} mice ($n=5$). Responses are expressed as percent constriction and as the area under the curve (AUC) of the response to ACh. Mean \pm SEM values are depicted. NS=not significant.

5.2.5 Deletion of endothelial cell Piezo1 does not affect NO-mediated-vasorelaxation

L-NAME, a NOS inhibitor, was used to study the NO contribution to this ACh-induced relaxation. Saphenous and carotid arteries from control and Piezo1^{ΔEC} mice showed a typical trace of ACh-induced relaxation before and after the incubation with L-NAME (Fig. 5.13a and 5.14a, respectively of saphenous arteries and Fig. 5.15a and 5.16a, respectively of the carotid artery). After the first concentration-response curves to ACh, the saphenous and carotid arteries from control mice were washed with Krebs solution and the procedure was repeated following incubation with L-NAME to block the production of NO. No difference in resting tone was observed in control saphenous arteries (Fig. 5.13b), but a significant increase was apparent for control carotid arteries (Fig. 5.15b), indicating that the basal NO release is not important for saphenous arteries but is essential for carotid arteries. The magnitude of the PE response increased in both arteries in the presence of L-NAME (30% for the saphenous artery and 51% for the carotid artery) (Fig. 5.13c and 5.15c, respectively). Furthermore, in the saphenous artery L-NAME decreased the ACh-induced relaxation by 77%, the magnitude of this decrease fitting reasonably well with the apamin plus charybdotoxin data (44% reduction). In control carotid arteries, which displayed a minimal EDHF component to the ACh response (Fig. 5.11d), L-NAME almost completely abolished relaxation (95% decrease) (Fig. 5.15d). The contraction element of the ACh response in carotid arteries remained evident over a similar concentration range in the presence of L-NAME (Fig. 5.15d). This suggests, as expected, that the EDCF mechanism is NO-independent.

Similar to saphenous arteries from control, no differences were observed in the resting tone of saphenous arteries from Piezo1^{ΔEC} mice when L-NAME was used (Fig. 5.13b and 5.14b respectively). Moreover, further significant contraction was observed in response to the pre-constriction with PE (30% increase for control and 25% increase for Piezo1^{ΔEC}) (Fig. 5.13c and 14c respectively). As for saphenous arteries from control mice, incubation with L-NAME significantly reduced the ACh-induced relaxation in saphenous arteries from Piezo1^{ΔEC} mice (77% decrease for control and 71% decrease for Piezo1^{ΔEC}) (Fig. 5.13d and 5.14d respectively), and also a significant difference was observed in the AUC of the response to ACh, before and after the incubation with L-NAME in control and Piezo1^{ΔEC} mice saphenous arteries (Fig. 5.13e and 5.14e respectively).

Similar to carotid arteries from control mice, in carotid arteries from Piezo1^{ΔEC} mice, significant differences were found in the resting tone and in response to the pre-contraction with PE (51% increase for control and 42% increase for Piezo1^{ΔEC}) when L-NAME was used (Fig. 5.15b, 5.15c and 5.16b, 5.16c respectively). Furthermore, ACh-mediated relaxation was totally abolished by the NOS inhibitor in both mouse strains (95% decrease for control and 100% decrease for Piezo1^{ΔEC}). However, contraction remained over a similar concentration range in both control and Piezo1^{ΔEC} mice (Fig. 5.15d and 5.16d, respectively). A significant difference was also found in the AUC of the response to ACh before and after incubation with L-NAME in carotid arteries from control and Piezo1^{ΔEC} mice (Fig. 5.15e and 5.16e, respectively). This indicates that the relaxation in these arteries is mediated by NO. Overall, the data suggest that endothelial Piezo1 is of no consequence to the NO-derived ACh response.

5.2.6 The effect of removal of endothelial cells on ACh-induced relaxation

After undergoing the same set-up protocol used prior to the ACh concentration-response curve experiments of saphenous and carotid arteries were also performed on endothelium-denuded arteries. This was used to confirm that the relaxation-induced by ACh was endothelium-dependent and to further investigate the ACh response (Fig. 5.17a and 5.18a, respectively of saphenous arteries and Fig. 5.19a and 5.20a, respectively of the carotid artery). After removal of the endothelium by rubbing the endothelial surface of the artery with a wire, arteries were pre-contracted with PE (0.3 μM), and then exposed to increasing concentrations of ACh (0.1 μM to 1 μM for saphenous arteries and (0.001 μM to 0.1 μM) to generate concentration-response curves (Fig. 5.17b and 5.18b, respectively of saphenous arteries and Fig. 5.19b and 5.20b, respectively of carotid artery). In endothelium-denuded saphenous arteries from control mouse, there was no change in PE response and no response to ACh. However, in endothelium-denuded carotid arteries from control mouse, an increase in PE contraction was seen where removing the ECs prevented NO release, which linked to the L-NAME data. Furthermore, contraction in response to ACh was observed which fits with the L-NAME data. SIN-1-induced relaxation was unaffected by the removal of ECs in saphenous and carotid arteries from both control groups of mice. Further experiments are needed to show if this contractile effect without PE pre-stimulation can be seen.

Similar to control saphenous arteries, the data showed that removing the endothelium did not modify PE-induced contraction in Piezo1^{ΔEC} mice saphenous arteries (2% increase for control and % 10 increase for Piezo1^{ΔEC}) (Fig. 5.17c and 5.18c). In both control carotid arteries and Piezo1^{ΔEC} carotid arteries, removing the endothelium potentiated PE-induced contraction (20% increase for control and 23% increase for Piezo1^{ΔEC}) (Fig. 5.19c and 5.20c) indicating the presence of endothelium-derived relaxing factors. Furthermore, ACh-induced relaxation was abolished in Piezo1^{ΔEC} saphenous arteries and carotid arteries of mice, and compared to endothelium intact arteries, the difference was significant (100% decrease for control and 95% decrease for Piezo1^{ΔEC}, 96% decrease for control and 99% decrease for Piezo1^{ΔEC}, respectively) (Fig. 5.17d and 18d, respectively of saphenous arteries and Fig. 5. 19d and 20d, respectively of carotid artery). A significant difference was found in the AUC of the response to ACh before and after removing the ECs (Fig. 5.17e and 18e, respectively of saphenous arteries and Fig. 5.19e and 20e, respectively of carotid artery). These results are opposite to those obtained with the L-NAME experiments. The endothelial-independent relaxation responses to the NO donor, SIN-1 were also obtained in Piezo1^{ΔEC} mice saphenous and carotid arteries to assess the endothelium-independent relaxation responses and if Piezo1 has a role in SIN-1 response.

SIN-1 (0.01–1 μM) induced relaxation was unaffected by the removal of EC in both groups of Piezo1^{ΔEC} mice saphenous and carotid arteries (Fig. 5.21a for saphenous arteries and Fig. 5. 22a for carotid artery). No differences were found in the AUC of the response to SIN-1 between control and Piezo1^{ΔEC} mice saphenous and carotid arteries (Fig. 5.21b for saphenous arteries and Fig. 5.22b for carotid artery). These data suggest that each of these effects is due to endothelium-dependent effects of ACh in control and Piezo1^{ΔEC} mice saphenous and carotid arteries and that the SIN-1 response is Piezo1 independent.

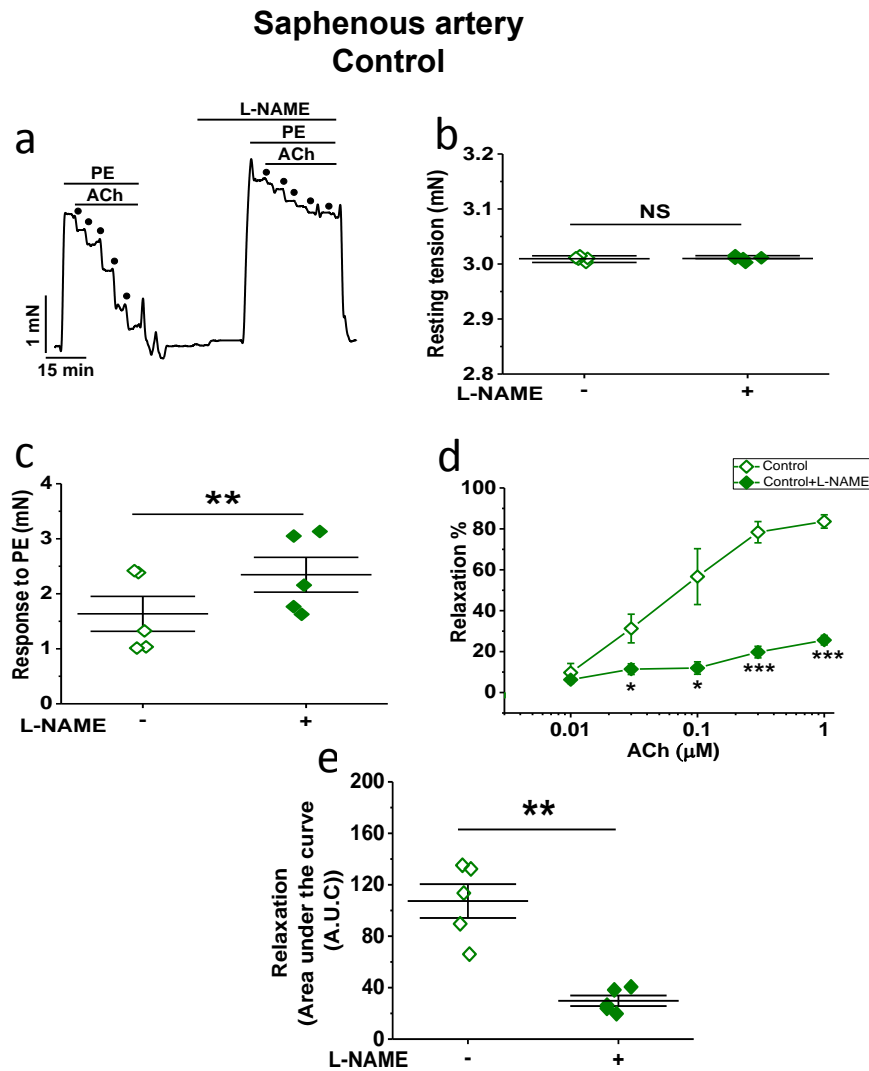


Figure 5-13: NO-mediated-vasorelaxation in control mice saphenous arteries

(a) Typical trace showing a concentration-dependent dilatory response to acetylcholine (ACh) as indicated by the dots (0.01, 0.03, 0.1, 0.3 and 1 μM) before and after the incubation with (100 μM) N_{ω} -nitro-L-arginine methyl ester hydrochloride (L-NAME) in saphenous arteries isolated from control mice. (b) Quantification of the L-NAME effects on the basal saphenous artery tension ($n=5$). (c) Quantification of the L-NAME effects on phenylephrine (PE)-induced constriction in control saphenous arteries of mice ($n=5$). (d) Concentration response curves to ACh before and after the application of L-NAME in control saphenous arteries mice ($n=5$). (e) The area under the curve (AUC) of the response to ACh before and after incubation with L-NAME of saphenous arteries isolated from control mice ($n=5$). Responses are expressed as percent constriction and as the area under the curve (AUC) of the response to ACh. Mean \pm SEM values are depicted. Asterisks indicate statistically significant difference (* $p<0.05$, ** $p<0.01$ and *** $P<0.001$). NS=not significant.

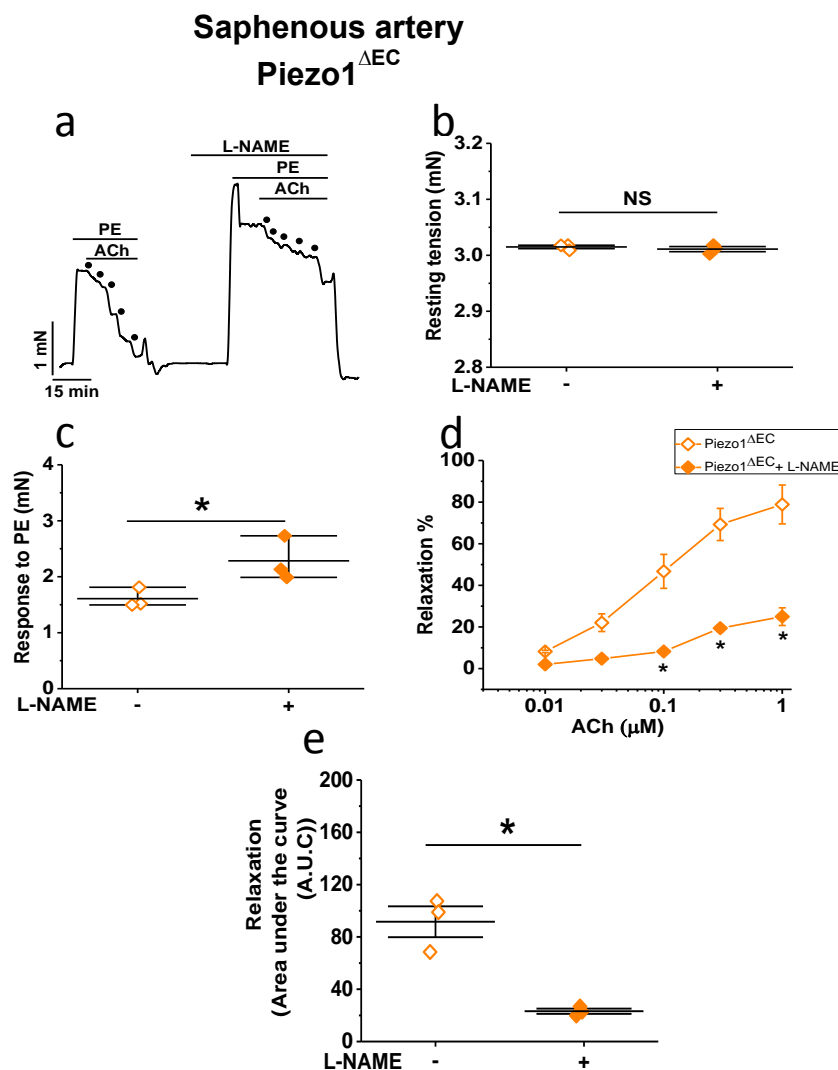


Figure 5-14: NO-mediated-vasorelaxation in Piezo1^{ΔEC} mice saphenous arteries

(a) Typical trace showing a concentration-dependent dilatory response to acetylcholine (ACh) as indicated by the dots (0.01, 0.03, 0.1, 0.3 and 1 μM) before and after the incubation with (100 μM) *N*_ω-nitro-L-arginine methyl ester hydrochloride (L-NAME) in saphenous arteries isolated from control mice. (b) Quantification of the L-NAME effects on the basal saphenous artery tension ($n=3$). (c) Quantification of the L-NAME effects on phenylephrine (PE)-induced constriction in control saphenous arteries of mice ($n=3$). (d) Concentration response curves to ACh before and after the application of L-NAME in control saphenous arteries mice ($n=3$). (e) The area under the curve (AUC) of the response to ACh before and after incubation with L-NAME of saphenous arteries isolated from control mice ($n=3$). Responses are expressed as percent constriction and as the area under the curve (AUC) of the response to ACh. Mean \pm SEM values are depicted. * $p < 0.05$, for ACh in control mice. Asterisks indicate statistically significant difference (* $p < 0.05$). NS=not significant.

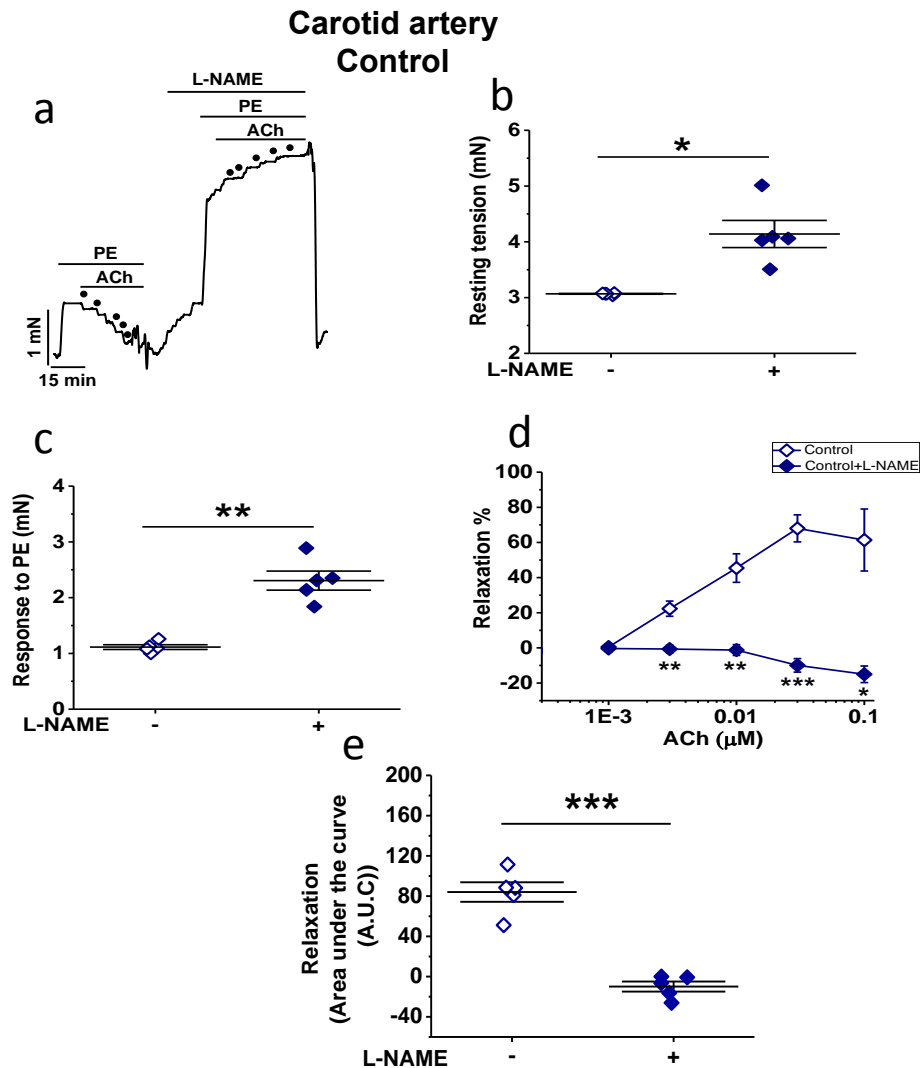


Figure 5-15: NO-mediated-vasorelaxation in control mice carotid arteries

(a) Typical trace showing a concentration-dependent dilatory response to acetylcholine (ACh) as indicated by the dots (0.001, 0.003, 0.01, 0.03 and 0.1 μM) before and after the incubation with (100 μM) N_{ω} -nitro-L-arginine methyl ester hydrochloride (L-NAME) in carotid arteries isolated from control mice. (b) Quantification of the L-NAME effects on the basal carotid artery tension ($n=5$). (c) Quantification of the L-NAME effects on phenylephrine (PE)-induced constriction in control carotid arteries of mice ($n=5$). (d) Concentration response curves to ACh before and after the carotid of L-NAME in control carotid arteries mice ($n=5$). (e) The area under the curve (AUC) of the response to ACh before and after incubation with L-NAME of carotid arteries isolated from control mice ($n=5$). Responses are expressed as percent constriction and as the area under the curve (AUC) of the response to ACh. Mean \pm SEM values are depicted. * $p<0.05$ and 0.001 for ACh in control mice. Asterisks indicate statistically significant difference (* $p<0.05$ and ** $p<0.001$).

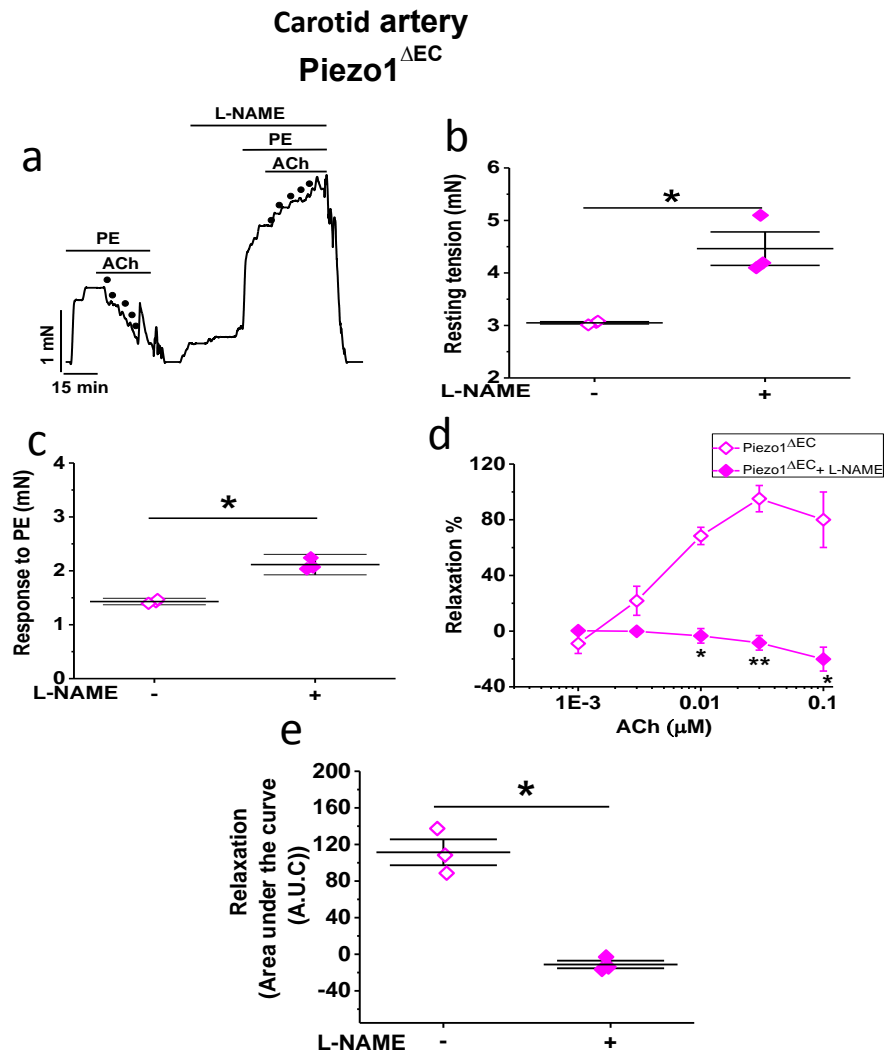


Figure 5-16: NO-mediated-vasorelaxation in Piezo1^{ΔEC} mice carotid arteries

(a) Typical trace showing a concentration-dependent dilatory response to acetylcholine (ACh) as indicated by the dots (0.001, 0.003, 0.01, 0.03 and 0.1 μM) before and after the incubation with (100 μM) *N*_ω-nitro-L-arginine methyl ester hydrochloride (L-NAME) in carotid arteries isolated from control mice. (b) Quantification of the L-NAME effects on the basal carotid artery tension ($n=3$). (c) Quantification of the L-NAME effects on phenylephrine (PE)-induced constriction in control carotid arteries of mice ($n=3$). (d) Concentration response curves to ACh before and after the carotid of L-NAME in control carotid arteries mice ($n=3$). (e) The area under the curve (AUC) of the response to ACh before and after incubation with L-NAME of carotid arteries isolated from control mice ($n=3$). Responses are expressed as percent constriction and as the area under the curve (AUC) of the response to ACh. Mean \pm SEM values are depicted. Asterisks indicate statistically significant difference (* $p<0.05$ and ** $p<0.01$).

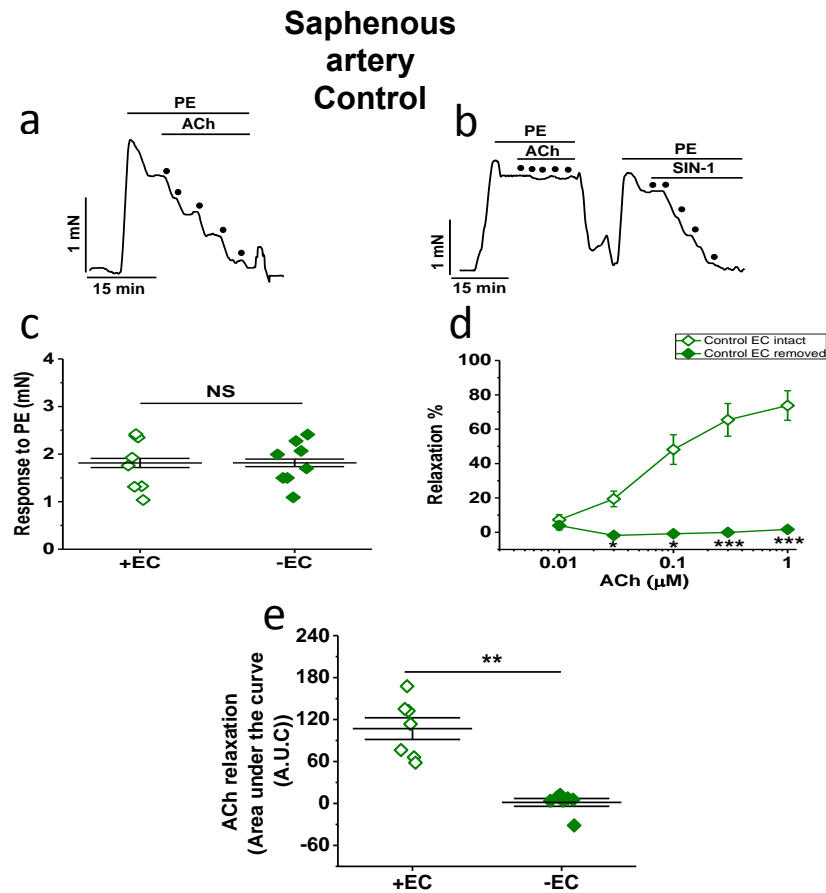


Figure 5-17: The effect of removal of endothelial cells on ACh induced-relaxation in control mice saphenous arteries

(a) Typical trace showing a concentration-dependent dilatory response to acetylcholine (ACh) as indicated by the dots (0.01, 0.03, 0.1, 0.3 and 1 μM) before removing the endothelial cells. (b) Typical trace showing a concentration-dependent dilatory response to ACh after removing the endothelial cells (-EC) and the application of (concentration) amino-3-morpholinyl-1,2,3-oxadiazolium (SIN-1) as indicated by the dots (0.01, 0.03, 0.1, 0.3 and 1 μM). (c) Quantification of the effects of removing the endothelial cells on phenylephrine (PE)-induced constriction in control saphenous arteries of mice ($n=7$). (d) Concentration response curves to ACh in saphenous arteries of control mice before and after endothelial cells removing ($n=7$). (e) The area under the curve (AUC) of the response to ACh before and after removing the endothelial cells of saphenous arteries isolated from control mice ($n=7$). Responses are expressed as percent constriction and as the area under the curve (AUC) of the response to ACh. Mean \pm SEM values are depicted. Asterisks indicate statistically significant difference (* $p < 0.05$, ** $p < 0.01$ and *** $p < 0.001$). NS=not significant.

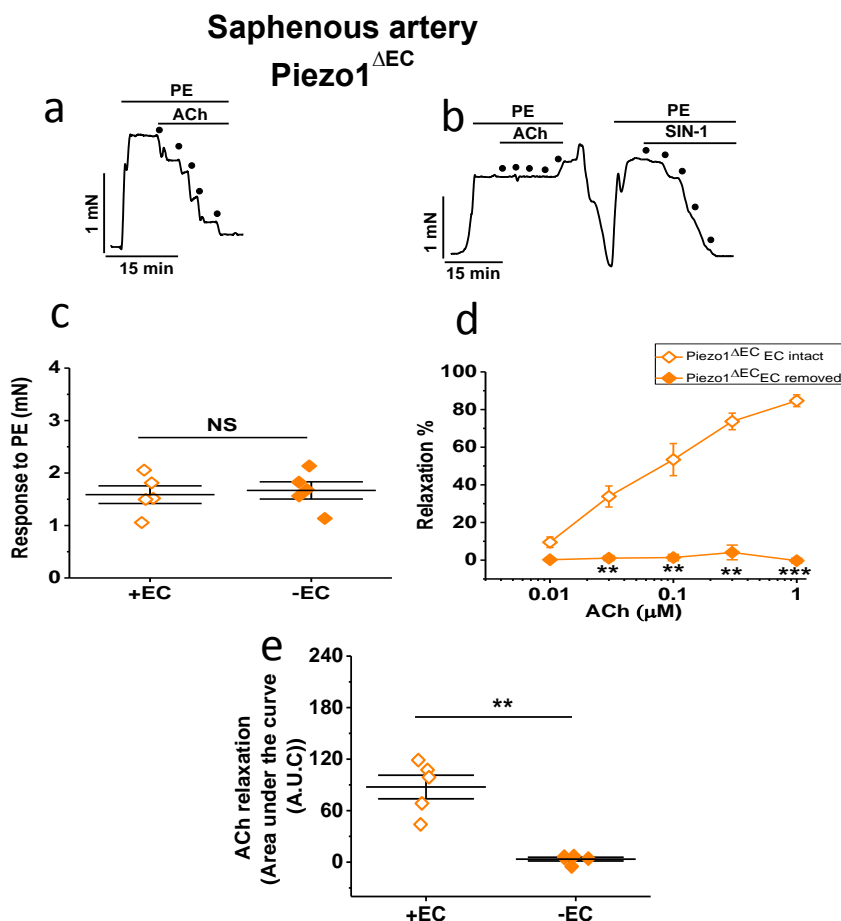


Figure 5-18: The effect of removal of endothelial cells on ACh induced-relaxation in Piezo1^{ΔEC} mice saphenous arteries

(a) Typical trace showing a concentration-dependent dilatory response to acetylcholine (ACh) as indicated by the dots (0.01, 0.03, 0.1, 0.3 and 1 μM) before removing the endothelial cells. (b) Typical trace showing a concentration-dependent dilatory response to ACh after removing the endothelial cells (-EC) and the application of (concentration) amino-3-morpholinyl-1,2,3-oxadiazolium (SIN-1) as indicated by the dots (0.01, 0.03, 0.1, 0.3 and 1 μM). (c) Quantification of the effects of removing the endothelial cells on phenylephrine (PE)-induced constriction in Piezo1^{ΔEC} saphenous arteries of mice ($n=5$). (d) Concentration response curves to ACh in Piezo1^{ΔEC} arteries of control mice before and after endothelial cells removing ($n=5$). (e) The area under the curve (AUC) of the response to ACh before and after removing the endothelial cells of saphenous arteries isolated from Piezo1^{ΔEC} mice ($n=5$). Responses are expressed as percent constriction and as the area under the curve (AUC) of the response to ACh. Mean \pm SEM values are depicted. Asterisks indicate statistically significant difference (** $p < 0.01$ and *** $p < 0.001$). NS=not significant.

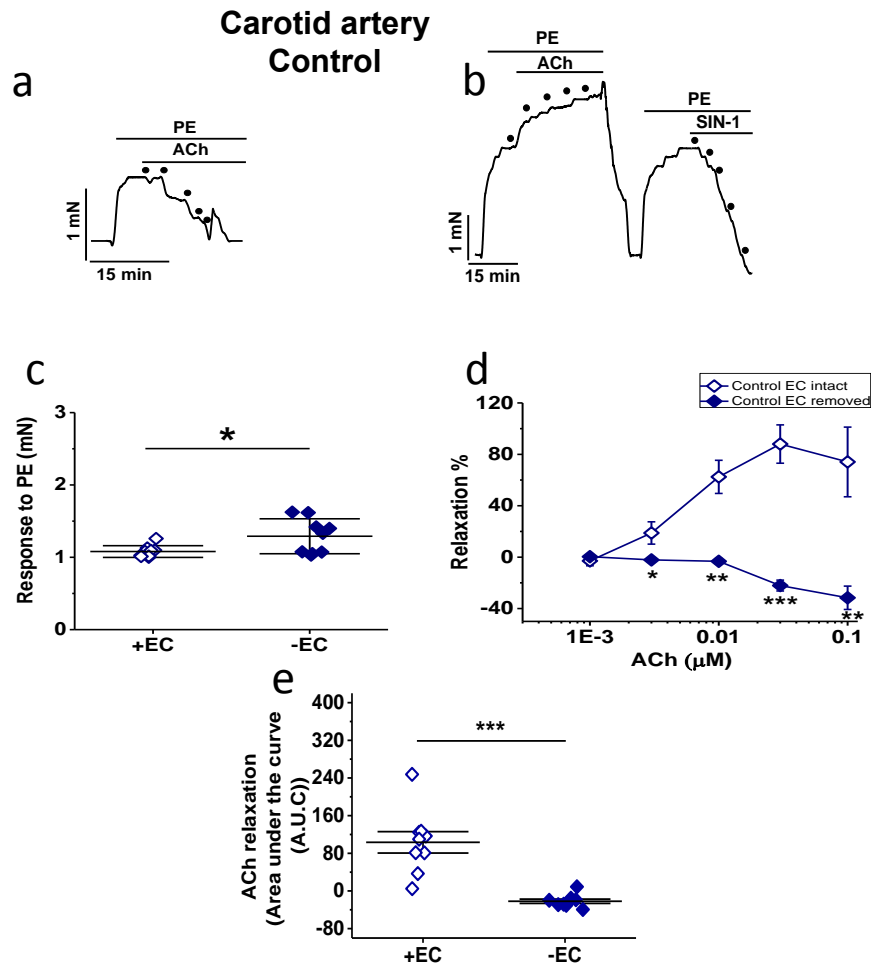


Figure 5-19: The effect of removal of endothelial cells on ACh induced-relaxation in control mice carotid arteries.

(a) Typical trace showing a concentration-dependent dilatory response to acetylcholine (ACh) as indicated by the dots (0.001, 0.003, 0.01, 0.03 and 0.1 μM) before removing the endothelial cells. (b) Typical trace showing a concentration-dependent dilatory response to ACh after removing the endothelial cells (-EC) and the application of (concentration) amino-3-morpholinyl-1,2,3-oxadiazolium (SIN-1) as indicated by the dots (0.001, 0.003, 0.01, 0.03 and 0.1 μM) (c) Quantification of the effects of removing the endothelial cells on phenylephrine (PE)-induced constriction in control carotid arteries of mice ($n=8$). (d) Concentration response curves to ACh in carotid arteries of control mice before and after endothelial cells removing ($n=8$). (e) The area under the curve (AUC) of the response to ACh before and after removing the endothelial cells of carotid arteries isolated from control mice ($n=8$). Responses are expressed as percent constriction and as the area under the curve (AUC) of the response to ACh. Mean \pm SEM values are depicted. Asterisks indicate statistically significant difference (* $p < 0.05$, ** $p < 0.01$ and *** $p < 0.001$).

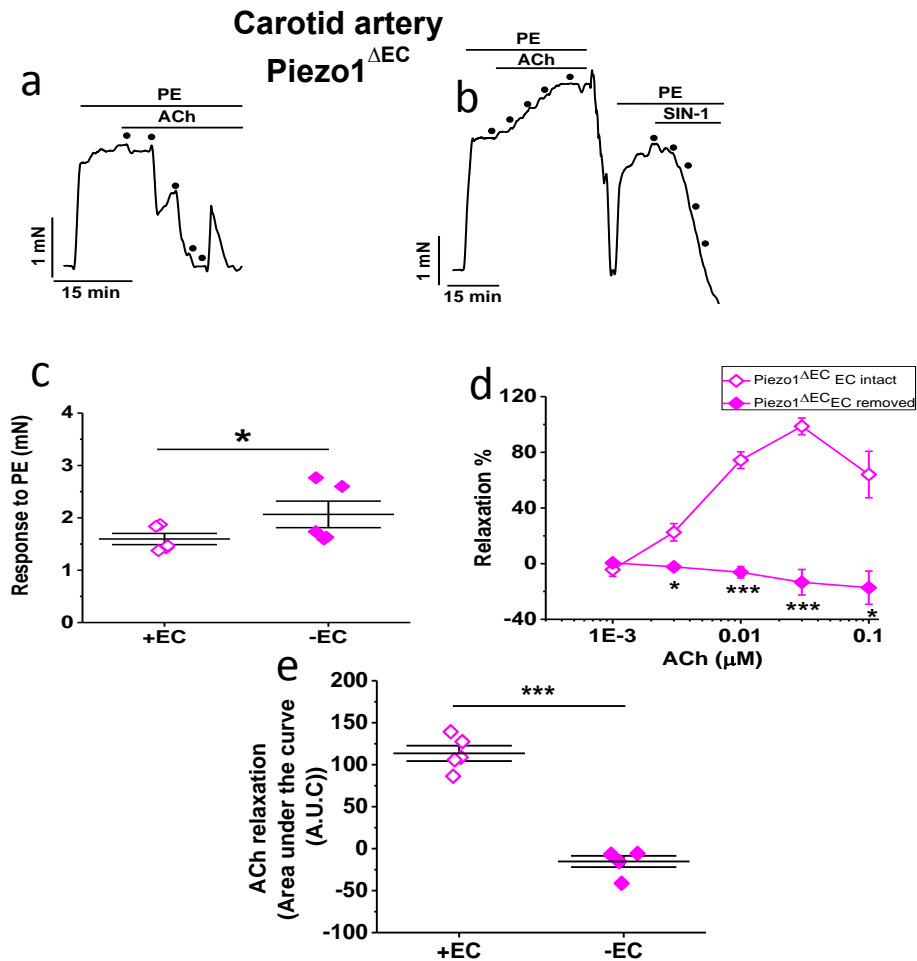


Figure 5-20: The effect of removal of endothelial cells on ACh induced-relaxation in Piezo1^{ΔEC} mice carotid arteries

(a) Typical trace showing a concentration-dependent dilatory response to acetylcholine (ACh) as indicated by the dots (0.001, 0.003, 0.01, 0.03 and 0.1 μM) before removing the endothelial cells. (b) Typical trace showing a concentration-dependent dilatory response to ACh after removing the endothelial cells (-EC) and the application of (concentration) amino-3-morpholinyl-1,2,3-oxadiazolium (SIN-1) as indicated by the dots (0.001, 0.003, 0.01, 0.03 and 0.1 μM) (c) Quantification of the effects of removing the endothelial cells on phenylephrine (PE)-induced constriction in Piezo1^{ΔEC} carotid arteries of mice ($n=8$). (d) Concentration response curves to ACh in carotid arteries of Piezo1^{ΔEC} mice before and after endothelial cells removing ($n=8$). (e) The area under the curve (AUC) of the response to ACh before and after removing the endothelial cells of carotid arteries isolated from Piezo1^{ΔEC} mice ($n=8$). Responses are expressed as percent constriction and as the area under the curve (AUC) of the response to ACh. Mean \pm SEM values are depicted. Asterisks indicate statistically significant difference (* $p < 0.05$ and *** $p < 0.001$).

Saphenous artery

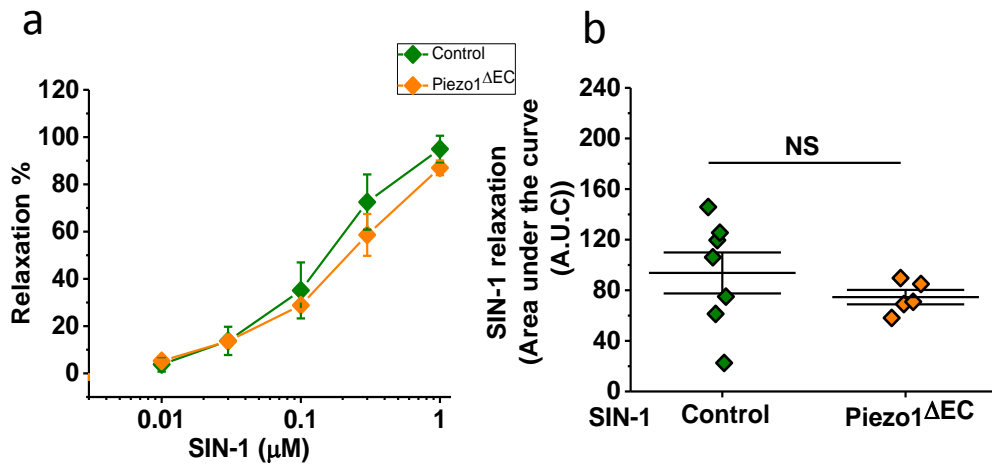


Figure 5-21: Comparison of effects of removing the endothelial cells in control and endothelial *Piezo1*^{ΔEC} mice saphenous arteries.

(a) Concentration response curves to NO-donor, Linsidomine (SIN-1) in saphenous arteries from control and *Piezo1*^{ΔEC} mice ($n=7$ and 5 , respectively). (b) The area under the curve (AUC) of the response to SIN-1 in saphenous arteries isolated from control *Piezo1*^{ΔEC} mice ($n=7$ and 5 , respectively). Data are expressed as percent constriction and the AUC of the response to ACh. Mean \pm SEM values are depicted. NS=not significant.

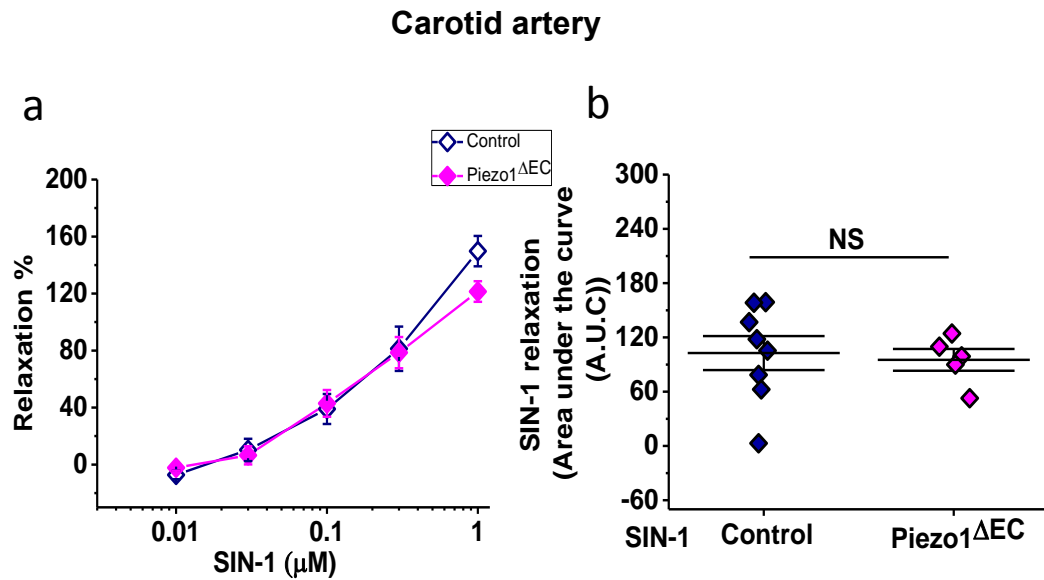


Figure 5-22: Comparison of effects of removing the endothelial cells in control and endothelial Piezo1 ΔEC mice carotid arteries.

(a) Concentration response curves to NO-donor, Linsidomine (SIN-1) in carotid arteries from control and Piezo1 ΔEC mice ($n=8$ and 5 , respectively). (b) The area under the curve (AUC) of the response to SIN-1 in carotid arteries isolated from control and Piezo1 ΔEC mice ($n=8$ and 5 , respectively). Data are expressed as percent constriction and the AUC of the response to ACh. Mean \pm SEM values are depicted. NS=not significant.

5.2.7 Yoda1 induced relaxation in the saphenous and carotid arteries of control and Piezo1^{ΔEC} mice

The aim was to determine if activation of Piezo1 by Yoda1, a synthetic small-molecule activator of Piezo1 (Syeda et al., 2015), results in contraction/relaxation of arteries.

Endothelium-intact saphenous arteries from control and Piezo1^{ΔEC} mice were pre-contracted with PE (0.3 μM) then Yoda1 (0.1–10 μM) was applied as shown in Fig. 5.23a, and 5.23b respectively. Only a small concentration-dependent relaxation response of Yoda1 was seen in saphenous arteries from control and Piezo1^{ΔEC} mice. The concentration range (0.01 - 10 μM) of activation of Piezo1 channels by Yoda-1 and the concentration-response curve in control and Piezo1^{ΔEC} mice matched the concentration-response curve for Yoda1 in HUVECs and HEK-Piezo1 cells (performed by Dr. Melanie Ludlow) confirming that the responses are mediated by Piezo1. Furthermore, the relaxation was not different between both saphenous arteries from control and Piezo1^{ΔEC} mice (Fig. 5.23c). No significant difference was found in the AUC of the response to Yoda1 for each individual curve in both groups (Fig. 5.23d). These data suggest that relaxation induced by Yoda1 might be promoted through other cell types such as VSMCs.

Interestingly Yoda1 caused contraction in carotid arteries with intact endothelium from control and Piezo1^{ΔEC} mice which were pre-contracted with PE (0.3 μM). When stable pre-constrictions were obtained the Yoda1 (0.1–10 μM) response was assessed as shown in Fig. 5.24a, and 5.24b respectively, no evidence was found for such an effect of Yoda1 in these arteries, where Yoda1 does not have any relaxation effect and caused a small contraction in control and Piezo1^{ΔEC} mice carotid arteries (Fig. 5.24c). Furthermore, no significant difference was observed in the AUC of the response to Yoda1 for each individual curve in control and Piezo1^{ΔEC} mice carotid arteries (Fig. 5.24d). Overall, this suggests a lack of role of endothelial Piezo1 in mouse saphenous and carotid arteries of mice. Further experiments are needed with Yoda1 in the absence of PE pre-constriction.

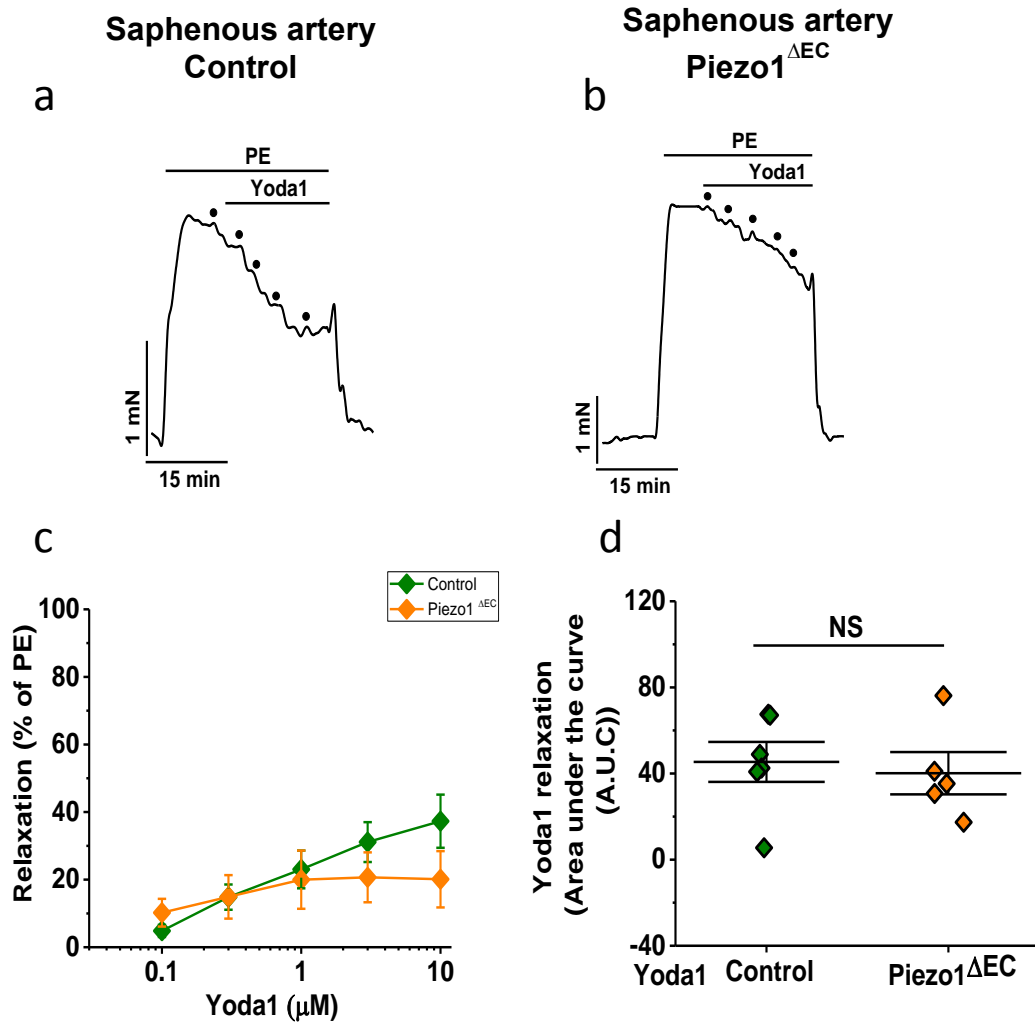


Figure 5-23: Endothelial-dependent relaxation induced by Yoda1 in control compared with endothelial Piezo1^{ΔEC} saphenous arteries

(a) Typical trace showing a concentration-dependent dilatory response to Yoda1 as indicated by the dots (0.1, 0.3, 1, 3 and 10 μM) in saphenous arteries isolated from control mice. (b) As for (a) except in saphenous arteries isolated from Piezo1^{ΔEC} mice. (c) Concentration response curves to Yoda1 in control ($n=5$) and Piezo1^{ΔEC} ($n=5$) mice. (d) The area under the curve (AUC) of the response to Yoda1 of saphenous arteries isolated from control ($n=5$) and Piezo1^{ΔEC} mice ($n=5$). Responses are expressed as percent relaxation, and as the AUC of the response to Yoda1. Mean \pm SEM values are depicted. NS=not significant.

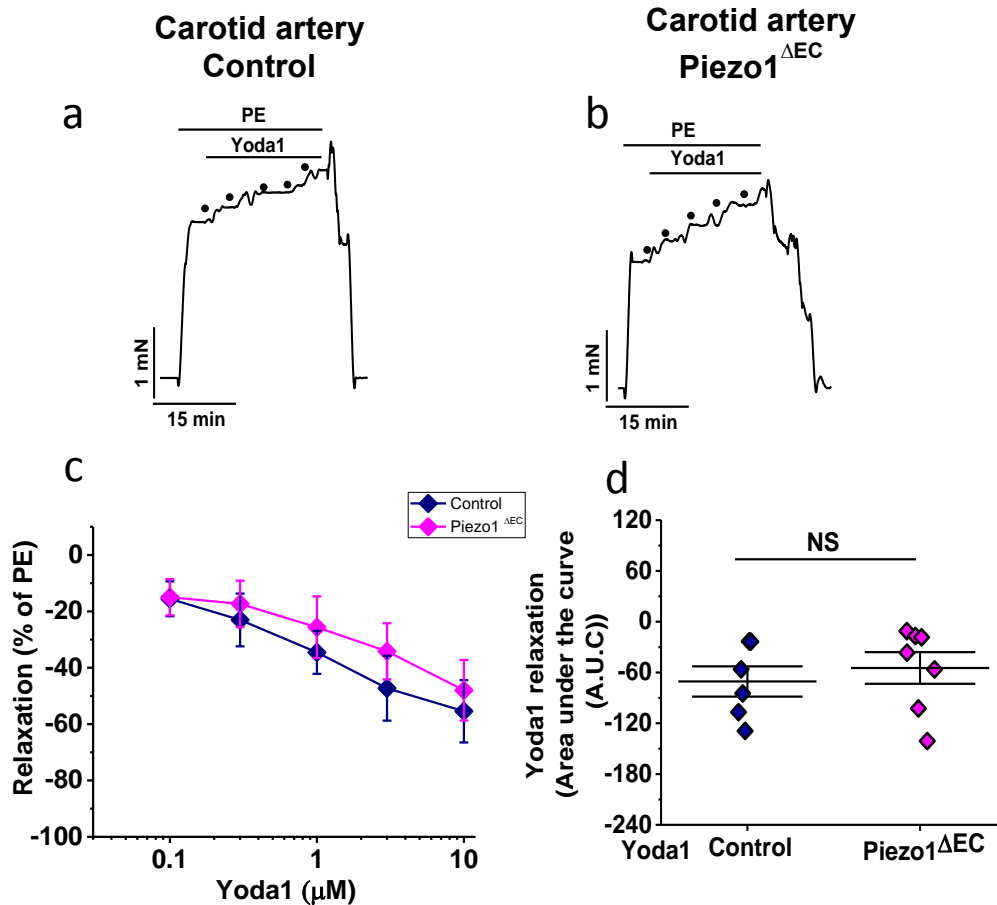


Figure 5-24: Endothelial-dependent relaxation induced by Yoda1 in control compared with endothelial Piezo1^{ΔEC} carotid arteries

(a) Typical trace showing a concentration-dependent dilatory response to Yoda1 as indicated by the dots (0.1, 0.3, 1, 3 and 10 μM) in carotid arteries isolated from control mice. (b) As for (a) except in carotid arteries isolated from Piezo1^{ΔEC} mice. (c) Concentration response curves to Yoda1 in control ($n=6$) and Piezo1^{ΔEC} ($n=7$) mice. (d) The area under the curve (AUC) of the response to Yoda1 of carotid arteries isolated from control ($n=6$) and Piezo1^{ΔEC} mice ($n=7$). Responses are expressed as percent relaxation, and as the AUC of the response to Yoda1. Mean \pm SEM values are depicted. NS=not significant.

5.2.8 The effect of removal of endothelial cells on Yoda1-induced relaxation in saphenous and carotid arteries from control and Piezo1^{ΔEC} mice

Given that the deletion of Piezo1 in ECs had no effect on the responses to Yoda-1 in these vessels, it would suggest that the Yoda-1 induced effects were endothelial-independent. To confirm this, Yoda-1 was applied to vessels from which the endothelium had been removed by gently rubbing the lumen of the arteries with a wire and the failure of 1 μM ACh to relax saphenous and carotid arteries was considered as endothelium-denuded.

A typical trace for relaxation to Yoda1 was obtained in a concentration dependent manner with and without ECs in both control and Piezo1^{ΔEC} mice saphenous and carotid arteries (Fig. 5.25a and 5.26a for saphenous arteries and 5.27a and 5.28a for carotid arteries, respectively). No difference in either vessel confirms endothelial-independence, where after removal of the endothelium, Yoda1-induced relaxation remained in control and Piezo1^{ΔEC} mice saphenous arteries and did not alter this small relaxation response in either control or Piezo1^{ΔEC} mice saphenous arteries (Fig. 5.25b and 5.26b). The control and Piezo1^{ΔEC} mice carotid arteries had no difference in their responses to Yoda1 and the effect of Yoda1 was not noticeably altered following removal of the ECs in control or Piezo1^{ΔEC} mice carotid arteries (Fig. 5.27b and 5.28b). Similarly, saphenous arteries from Piezo1^{ΔEC} mice without functional endothelium have been shown to produce a constriction of similar magnitude to PE (Fig. 5.25c and 5.26c, respectively). However, in carotid arteries, a significant increase in contraction to PE was seen when endothelium was removed (Fig. 5.27c and 5.28c, respectively). Furthermore, no significant difference was found in the AUC of the response to Yoda1 before and after removing the ECs in control and Piezo1^{ΔEC} mice saphenous and carotid arteries (Fig. 5.25d and 5.26d for saphenous arteries and 5.27d and 5.28d for carotid arteries, respectively). Therefore, these results suggest that Piezo1 might be involved in the small relaxation mediated by vascular SMCs in saphenous arteries and without consequence with removing the endothelium in carotid arteries.

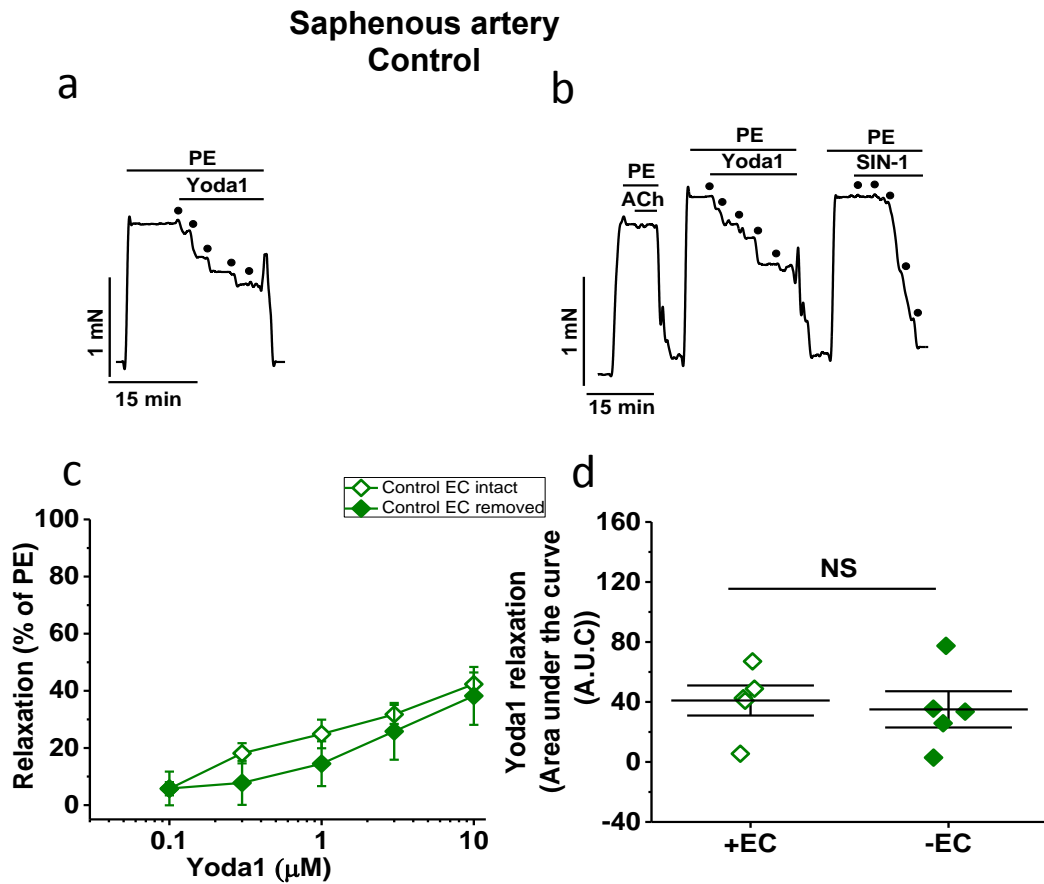


Figure 5-25: The effect of the endothelium removal on Yoda1-induced relaxation in saphenous arteries from control mice

(a) Typical trace showing a concentration-dependent response to Yoda1 as indicated by the dots (0.1, 0.3, 1, 3 and 10 μM) in the saphenous arteries isolated from control mice before and (b) after EC removing (-EC). (c) Concentration response curves to Yoda1 in the saphenous arteries from control mice before and after -EC ($n=5$). (d) The area under the curve (AUC) of the response to Yoda1 before and after EC removal in the saphenous arteries isolated from control mice ($n=5$). Responses are expressed as percent constriction and as the AUC of the response to Yoda1. Mean \pm SEM values are depicted. NS=not significant.

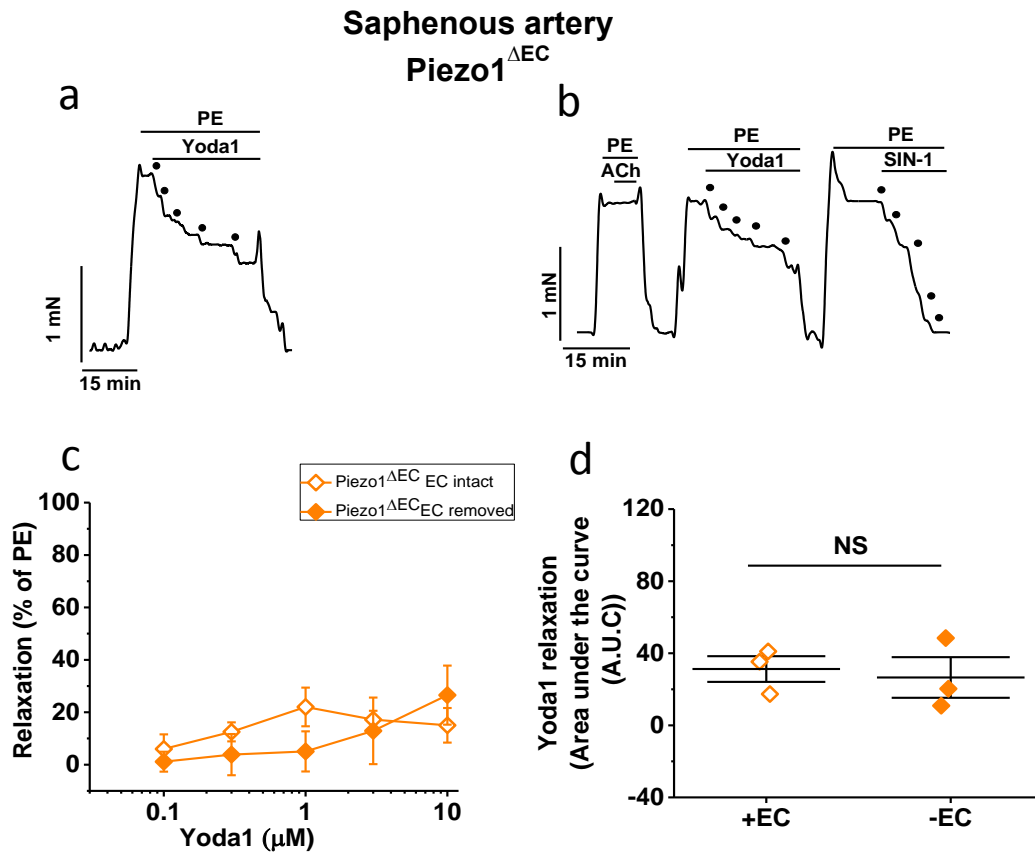


Figure 5-26 The effect of the endothelium removal on Yoda1-induced relaxation in saphenous arteries from Piezo1^{ΔEC} mice

(a) Typical trace showing a concentration-dependent response to Yoda1 as indicated by the dots (0.1, 0.3, 1, 3 and 10 μM) in the saphenous arteries isolated from Piezo1^{ΔEC} mice before and (b) after EC removing (-EC). (c) Concentration response curves to Yoda1 in the saphenous arteries from Piezo1^{ΔEC} mice before and after -EC ($n=3$). (d) The area under the curve (AUC) of the response to Yoda1 before and after -EC in the saphenous arteries isolated from Piezo1^{ΔEC} mice ($n=3$). Responses are expressed as percent constriction and as the AUC of the response to Yoda1. Mean \pm SEM values are depicted. NS=not significant.

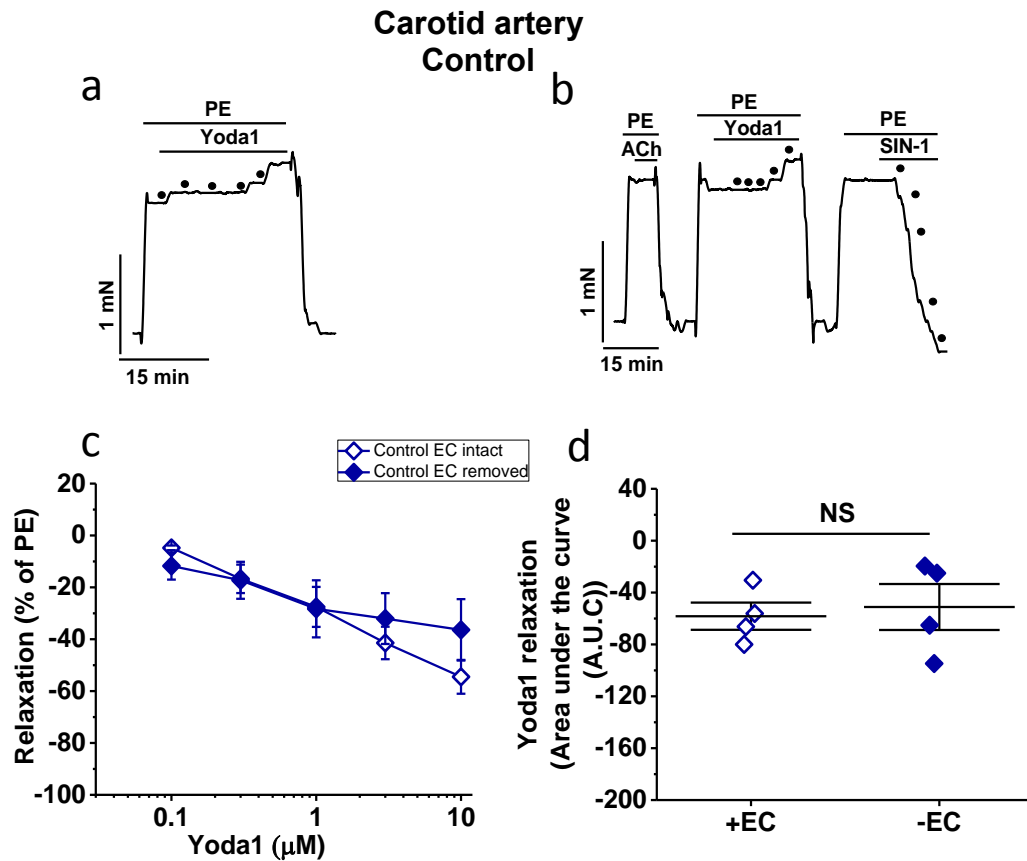


Figure 5-27: The effect of the endothelium removal on Yoda1-induced relaxation in carotid arteries from control mice

(a) Typical trace showing a concentration-dependent response to Yoda1 as indicated by the dots (0.1, 0.3, 1, 3 and 10 μM) in the carotid arteries isolated from control mice before and (b) after EC removing (-EC). (c) Concentration response curves to Yoda1 in the carotid arteries from control mice before and after -EC ($n=4$). (d) The area under the curve (AUC) of the response to Yoda1 before and after -EC in the carotid arteries isolated from control mice ($n=4$). Responses are expressed as percent constriction and as the AUC of the response to Yoda1. Mean \pm SEM values are depicted. NS=not significant.

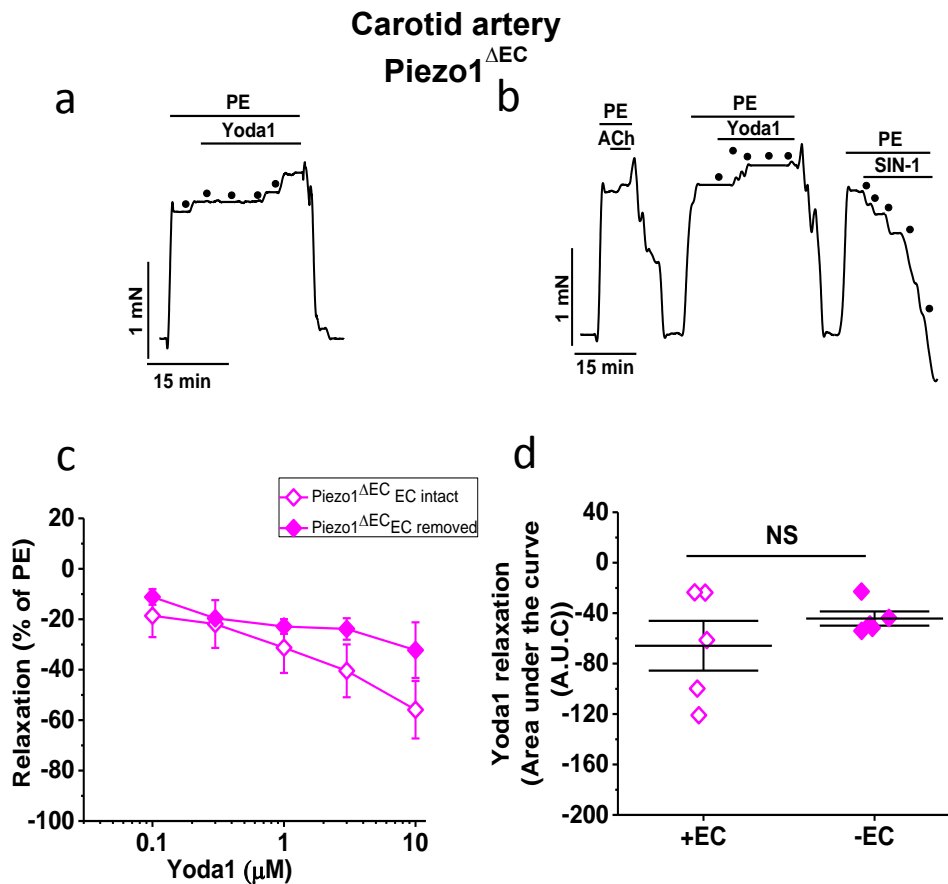


Figure 5-28: The effect of the endothelium removal on Yoda1-induced relaxation in carotid arteries from Piezo1^{ΔEC} mice

(a) Typical trace showing a concentration-dependent response to Yoda1 as indicated by the dots (0.1, 0.3, 1, 3 and 10 μM) in the carotid arteries isolated from Piezo1^{ΔEC} mice before and (b) after EC removing (-EC). (c) Concentration response curves to Yoda1 in the carotid arteries from Piezo1^{ΔEC} mice before and after -EC ($n=3$). (d) The area under the curve (AUC) of the response to Yoda1 before and after -EC in the carotid arteries isolated from Piezo1^{ΔEC} mice ($n=5$). Responses are expressed as percent constriction and as the AUC of the response to Yoda1. Mean \pm SEM values are depicted. NS=not significant.

5.3 Discussion

Surprisingly, these data provide no evidence for the presence of functional Piezo1 channels and no anti-EDH effect of Piezo1 in the endothelium of saphenous or carotid arteries. Furthermore, the data do show endothelial-independent responses to Yoda-1.

5.3.1 Deletion of endothelial cell Piezo1 does not affect high potassium or phenylephrine-induced contraction in saphenous or carotid arteries from control and Piezo1^{ΔEC} mice.

Contractile responses induced by either K⁺ or PE, were initially studied. The saphenous artery developed more force in response to high K⁺ as compared to the carotid artery. The same phenomenon was observed with PE at high concentrations, indicating that it is indeed a difference in contractile machinery. The smaller response in the carotid artery can be explained via a bigger influence of spontaneously released NO. Furthermore, the carotid artery is an elastic artery, and the saphenous artery is a muscular artery, where the muscular arteries ability to contract is promoted by the formation of the structural elements of the arterial wall and the lower volume of elastic tissue. This phenotypic heterogeneity may have outcomes for the vessel contractile capacity (Levický and Dolezel, 1979).

Moreover, there was no difference in the sensitivity to K⁺ or PE between any of the groups of saphenous and carotid arteries from control and Piezo1^{ΔEC} mice. These contractile responses were not influenced by endothelial Piezo1 deletion in either type of arteries.

5.3.2 Deletion of endothelial cell Piezo1 does not affect ACh-induced vasorelaxation in saphenous or carotid arteries from control and Piezo1^{ΔEC} mice.

ACh-induced relaxation was similar in both groups of saphenous and carotid arteries from control and Piezo1^{ΔEC} mice. Piezo1 deletion does not alter the responses to ACh,

implying that endothelial Piezo1 played no role in the relaxation response to ACh in these arteries.

Endothelium-dependent contractions, found in various types of mouse arteries (aorta, carotid, and femoral arteries) (Liu et al., 2012, Golubinskaya et al., 2014, Zhou et al., 2005), were also observed in carotid but not in saphenous arteries from control and Piezo1^{ΔEC} mice. These contractions are a secondary contraction to ACh that was observed after a high concentration had been applied. It was presumed to be an endothelium-derived contraction and not a direct effect of ACh on the SMCs since this secondary contractile response to ACh was abolished by removing the ECs. Therefore, this latter contraction at higher concentrations of ACh appears to be due to the release of EDCF in particular the cyclooxygenase enzyme that is involved in the production of EDCF (Vanhoutte and Tang, 2008). In contrast to carotid arteries, in saphenous arteries from control and Piezo1^{ΔEC} mice, ACh-induced relaxations were not affected and cyclooxygenase products do not contribute to endothelium-dependent relaxation at the concentrations of ACh used in this study.

5.3.3 Deletion of endothelial cell Piezo1 does not affect EDHF or NO-mediated vasorelaxation in saphenous or carotid arteries from control and Piezo1^{ΔEC} mice.

In the elastic arteries, the basal NO formation inhibition through endothelial NOS with L-NAME constantly raised the tension but not in the muscular arteries (Leloup et al., 2015). The tension in saphenous artery from control and Piezo1^{ΔEC} mice was unaffected after the incubation with L-NAME or combination of apamin plus charybdotoxin. However, the tension in carotid artery from control and Piezo1^{ΔEC} mice significantly increased after the incubation with L-NAME but not with the combination of apamin plus charybdotoxin. This indicates that the basal NO release is not essential in saphenous arteries isolated from control and Piezo1^{ΔEC} mice, but basal NO secretion is greater in carotid arteries from control and Piezo1^{ΔEC} mice. Interestingly, in saphenous or carotid arteries isolated from control and Piezo1^{ΔEC} mice the contractile response of PE was significantly affected by the presence of L-NAME but not with the presence of both apamin and charybdotoxin.

The important contribution of NO and EDHF to endothelium-dependent relaxation presents a significant heterogeneity between species and types of vessels (Triggle et al., 1999). Treatment of saphenous arteries from control and Piezo1^{ΔEC} mice with L-NAME resulted in a significant shift of about 80-fold of the endothelium-dependent concentration-relaxation curve to ACh, showing that under conditions where NOS activity is absent, an endothelium-dependent relaxation can still be produced by ACh and this relaxation has the properties of being mediated by an EDHF. Furthermore, the relaxation to ACh following incubation with the combination of apamin and charybdotoxin produced a significant rightward shift of about 20-fold of ACh-induced relaxation in any of the groups tested. However, the relaxation to ACh was not completely abolished. This raised the possibility of the remaining relaxation being due to NO.

In small muscular resistance arteries, marked endothelium-dependent vasodilatation can continue during pharmacological NOS inhibition or NOS deficiency (Huang et al., 2000). This has been attributed to EDHF (Feletou and Vanhoutte, 1999, Busse et al., 2002). This mechanism involves SK_{ca}²⁺ and IK_{ca}²⁺ channels which are located in the plasmalemma of the ECs (Edwards et al., 1998, Stankevičius et al., 2006, Grgic et al., 2009). Activation of these channels can cause endothelium-dependent vasodilatation by conduction of the ECs hyperpolarisation to the underlying SMCs by gap junctions (Félétou and Vanhoutte, 2009).

These results are consistent with previous findings in which the EDHF was the dominant mechanism in rat mesenteric artery but not in femoral artery due to the presence of efficient gap junction communication between ECs and SMCs in mesenteric artery but not femoral artery. Furthermore, EDHF contributes to ACh-induced relaxation and the endothelium-dependent vasodilator EDHF changes during development in the saphenous artery of the rat (Sandow et al., 2004, Sandow et al., 2002). Chennupati et al 2013 also showed that EDHF contributed to endothelium-dependent relaxations but it decreased with age and the contribution of endothelium-derived NO increased in adult male mouse saphenous arteries (Chennupati et al., 2013).

In carotid arteries from control and Piezo1^{ΔEC} mice, ACh elicited almost no response following incubation with L-NAME and the ACh response seemed completely dependent on NO (fully blocked by L-NAME), indicating that EDHF was not the prevalent relaxing

factor in these arteries. This was in contrast to the EDHF, in response to ACh following apamin plus charybdotoxin incubation which showed that the arteries were still capable of a full relaxation in the presence of these agents which block EDHF. Therefore, it can be concluded that there is no contribution of non-NO factors to ACh-induced relaxation in the carotid artery and that if any relaxation by hyperpolarisation, could be mediated through NO. These data do not necessarily mean that the full relaxation to ACh is mediated by NO rather than EDHF in the carotid arteries, but they do show that when EDHF production was blocked NO was capable of fully compensating. This is in agreement with previous findings in mouse and rabbit carotid vessels (Golubinskaya et al., 2014, Cohen et al., 1997). Furthermore, the contribution of EDHF factor to the relaxation of the saphenous, but not the carotid artery, this is again in agreement with previous study that showed the relevant role of EDHF reduced as the size of the vessel increased (Shimokawa et al., 1996).

Furthermore, it was shown that no anti-EDHF effect of Piezo1 occurred in saphenous (similar in diameter to second-order mesenteric artery) or carotid artery and that Piezo1 activity did not interfere with the relaxation as ACh responses were similar in saphenous and carotid arteries from control and Piezo1^{ΔEC} mice. No anti-EDH effect of Piezo1 in these arteries as seen in the mesenteric artery confirmed that there is vascular bed specificity of the Piezo1 vasoconstrictor mechanism. Vascular bed specificity was also found in response to exercise to promote blood flow redistribution, vasoconstriction in intestines and vasodilatation in skeletal muscle (Joyner and Casey, 2015). Thus, Piezo1 plays an essential role in redistribution of blood flow during the periods of physical activity by restriction blood flow.

5.3.4 The effect of removal of endothelial cells on ACh-induced relaxation in saphenous or carotid arteries from control and Piezo1^{ΔEC} mice.

Removing the endothelium totally abolished ACh-induced relaxation, indicating that the ability of ACh to induce relaxation was lost in endothelium-denuded saphenous and carotid arteries isolated from control and Piezo1^{ΔEC} mice, which is consistent with previous studies. Removal of the endothelium significantly increased the response to PE in carotid arteries from control and Piezo1^{ΔEC} mice but not in saphenous arteries from

control and Piezo1^{ΔEC} mice, suggesting that PE caused the contraction through direct activation of SMCs. SIN-1, a NO donor, causes relaxation by direct activation of sGC, resulting in a rise in cGMP levels in SMC (Plane, Sampson et al. 2001). Here, data showed that there was no difference in the levels of SIN-1-induced relaxation in saphenous or carotid arteries isolated from control and Piezo1^{ΔEC} mice, suggesting that the responses mediated by SIN-1 were not affected by Piezo1 deletion in saphenous or carotid arteries isolated from control and Piezo1^{ΔEC} mice.

5.3.5 Endothelial-dependent relaxation induced by Yoda1 in saphenous or carotid arteries from control and Piezo1^{ΔEC} mice.

Yoda1, a chemical activator of Piezo1 (Syeda et al., 2015) induced a small relaxation in saphenous arteries from control and Piezo1^{ΔEC} mice compared to mesenteric artery. However, the relaxation induced by Yoda1 was not significantly reduced in Piezo1^{ΔEC} mice. Therefore, the ability of Yoda1 to induce relaxation is not affected by the endothelial Piezo1 deletion showing that an endothelium-independent pathway is also involved in the vasorelaxation similar to the mesenteric artery. In contrast to the saphenous artery, Yoda1 in carotid arteries from control and Piezo1^{ΔEC} mice induced contraction rather than relaxation which might reflect a Piezo1 role or some other unidentified mechanism associated with Piezo1.

5.3.6 The effect of removal of endothelial cells on Yoda1-induced relaxation in saphenous or carotid arteries from control and Piezo1^{ΔEC} mice.

Removal of ECs did not alter the effects of Yoda1 in either group. In saphenous artery, as mentioned before, it can be concluded that the ability of Yoda1 to provide relaxation is largely endothelial independent, and that Piezo1 present in SMC ((Retailleau et al., 2015) might be involved in this relaxation. Furthermore, in carotid arteries, the contraction seen with Yoda1 did not change by removing the ECs. This can be related to the different expression or function of Piezo1 in different types of arteries.

5.4 Conclusion

Studies with mouse saphenous arteries and carotid arteries indicate that the function of endothelial Piezo1 may not be the same from vessel to vessel.

Chapter 6 Final summary and Future Directions

This study was focussed on investigating and understanding the role of the mechanosensitive cation channel Piezo1 in arteries. Disruption of the Piezo1 gene in mice has demonstrated that this channel has a critical role in vascular development in embryogenesis (Li et al., 2014) and in adult vascular regulation (Wang et al., 2016(Wang et al., 2016)), however, the mechanism(s) by which Piezo1 contributes to these processes largely remains to be determined. Therefore, within this work the function of Piezo1 has been examined using wire myography, assessing its contribution to the contractility of intact blood vessels.

Four structurally and functionally distinct arteries, the thoracic aorta, mesenteric, saphenous and carotid arteries, were selected. Their physiological differences are evident just by comparing their responses to PE and ACh. The lowest concentration of PE to constrict mesenteric, saphenous and carotid arteries was fairly similar, between 0.03 and 0.1 μM , however, the EC_{50} concentrations and the magnitude of the constrictive effect varied considerably (Table 6. 1). Carotid arteries showed greater sensitivity to ACh than mesenteric or saphenous arteries, although the extent of relaxation at a 1 μM concentration was relatively similar (Table 6. 1). It is well known that elastic and muscular arteries differ in function and in the magnitude of their response to vasoconstrictor effects (Bevan et al., 1972). Carotid and renal arteries, which are pathways to BP sensors, have a higher ratio of collagen to elastin than the femoral and mesenteric arteries, which are pathways to regulated beds (Fischer and Llaurodo, 1966). Thus the various patterns of structure and content in collagen to elastin ratio through these four types of arteries would result in various vessel wall mechanical properties. Therefore, it was unlikely that the contribution, if any, of Piezo1 to these arteries would be equivalent and a comparison of the four vessels types should provide a more rounded understanding of the role(s) and importance of this channel. This proved to be the case, Piezo1 having a prominent role in mesenteric arteries that was not mirrored in the thoracic aorta, saphenous or carotid arteries.

Mice in which the Piezo1 gene had been disrupted in EC displayed no obvious phenotype. Their resting BP was normal (Fig 3. 18) and isolated mesenteric, saphenous and carotid arteries constricted and relaxed in response to the PE and ACh respectively in the same manner as control vessels (Figs 4. 3 and 5, 5. 4, 5, 7 and 8). However,

multiple pieces of data point to a functional role of Piezo1 in blood vessels. Yoda-1, a Piezo1 agonist, had effects on all tested arteries, though the nature of these effects was not consistent. Mesenteric and saphenous arteries from control mice both respond with vasorelaxation, though the magnitude of this response was almost two fold greater in the former (Table 6. 2). In contrast carotid arteries from control mice respond with vasoconstriction. For the thoracic aorta relaxation was seen in vessels from wild mice, however, constriction was seen in vessels from control mice, the reason for this difference most probably relating to mouse genotype, as discussed in chapter 3. Overall this suggests that the role for Piezo1 is multifaceted and non-uniform between vessels. Slightly unexpectedly, only in thoracic aorta was the Yoda-1 response (relaxation) dependent upon ECs. It was also sensitive to L-NAME, fitting with the finding the Yoda-1 leads to phosphorylation and so activation of eNOS (Fig 3. 9) (Wang et al., 2016). For the other vessels the response to Yoda-1 is most likely explained by the presence of Piezo1 in VSMC ((Retailleau et al., 2015). It is obvious that influx of Ca^{2+} into these cells could lead to contraction, however, how Piezo1 activation could result in contraction, as in the case in thoracic aorta and carotid arteries from control mice, is less clear and requires further exploration. It would be interesting to repeat these experiments on arteries isolated from mice globally heterozygous for Piezo1 (Li et al., 2014).

Consistent with the absence of an endothelial based effect of Yoda-1 essentially no difference was found between control and Piezo1^{ΔEC} mice in carotid or saphenous arteries. However, a significant difference was identified in mesenteric arteries. There was no effect on the sensitivity or magnitude of the response to ACh alone, but when production of EDHF was inhibited by the combination of apamin and charybdotoxin, inhibitors of two K^+ channels which are important for EDHF, the relaxation to ACh was clearly impaired. Thus, deletion of endothelial Piezo1 enhances the EDHF response in mesenteric arteries. The fact that the EDHF effect was not amplified by Piezo1 disruption in saphenous or carotid arteries indicates that nature of the EDHF component may not be the same from artery to artery, thus is in agreement with the theory that EDHF is more critical in small resistance arteries compared with conduit arteries (Berman et al., 2002), and also that Piezo1 might not be expressed in endothelium of all vessels.

While wire myography allows the Piezo1 channel to be assessed in the context of an intact vessel, it does have limitations. Vascular contractility is evaluated in the absence of circulating factors, sympathetic activity and importantly blood flow, when compared

with *in vivo*. The solution bathing the vessels is static, thus the experiments primarily consider the contribution of the constitutive activity of Piezo1, not its activation by shear stress. Therefore, a functional role for endothelial Piezo1 in saphenous and carotid arteries cannot be discounted. Equally, the possible impact of the absence of continuous exposure to pulsatile shear stress on Piezo1 stability and trafficking cannot be overlooked. Wang and colleagues, using pressure myography, reported Yoda-1 stimulated relaxation in mesenteric arteries that is reduced in their Piezo1^{ΔEC} mouse. Given that within the work presented here Yoda-1 induced relaxation was equivalent in mesenteric vessels from control and Piezo1^{ΔEC} mice it would be interesting to study saphenous and carotid arteries using the pressure myograph.

Regardless of these limitations, an important anti-EDHF role for Piezo1 activity was identified in mesenteric arteries, providing insight into our finding that BP in active Piezo1^{ΔEC} mice was increased to a lesser extent than control mice. Mesenteric arteries are crucial to BP control, consequently require the additional EDHF mechanism to back up the NO. The saphenous and the carotid arteries, in contrast, are capable of relaxation via the release of NO, but its relaxation effect does not impact upon BP. Thus, the lack of a role for endothelial Piezo1 in saphenous and carotid arteries is consistent with prior knowledge that whole body physical activity involves reduced blood flow to the gastrointestinal tract but increased or sustained blood flow to skeletal muscle and the brain (Qamar and Read, 1987, Perko et al., 1998, Joyner and Casey, 2015).

Exercise can protect against or reduce the risk of high BP, but the hypertension experienced during exercise has been shown to be an essential predecessor of continuous hypertension (Sabbahi et al., 2016, Miyai et al., 2002). Given that hypertension remains one of the major health issues of the 21st century, promoting new methodologies and tools for studying Piezo1 channels are involved in the regulation of BP in a manner which allows it to enhance physical performance.

In summary, this study has demonstrated a functional role for Piezo1 in arterial vessels. In ECs there a dichotomy exists, Piezo1 channels being linked to both NO-dependent vasorelaxant and anti-EDHF based vasoconstrictant effects. Add to this the further endothelial-independent vasoactive effects of Yoda-1 and it appears that Piezo1 has a complex role in the cardiovascular system. An influence of endothelial Piezo1 on EDHF

function in second order mesenteric arteries was revealed by comparing Piezo1^{ΔEC} mice with control mice. This effect was vascular bed-specific, not being observed in either saphenous or carotid arteries, which, unlike mesenteric vessels, do not undergo vasoconstriction during exercise. Thus, implying that in mouse vasculature, Piezo1 channels are involved in the regulation of BP in a way which allows it to enhance physical performance.

		Mesenteric arteries		Saphenous arteries		Carotid arteries	
		Control	Piezo1 ^{AEC}	Control	Piezo1 ^{AEC}	Control	Piezo1 ^{AEC}
high K ⁺	effect	contraction	34.4% decrease in contraction vs control	contraction	no difference to control	contraction	no difference to control
PE	effect	contraction	no difference to control	contraction	no difference to control	contraction	no difference to control
	EC ₅₀	~0.2 μM		(plateau not reached by 1 μM)		(plateau not reached by 1 μM)	
	+ L-NAME	50% increase	35% increase	30% increase	36% increase	65% increase	35% increase
ACh	effect	relaxation	Decrease only at one ACh concentration	relaxation	no difference to control	relaxation	no difference to control
	EC ₅₀	~0.1 μM		(plateau not reached by 1 μM)		~0.01 μM	
	+ Apa + Ch	Decrease only at some ACh concentrations	90% decrease (AUC)	33% decrease (AUC)	25% decrease (AUC)	no effect	no difference to control
	+ L-NAME	72% decrease (AUC)	no difference to control	60% decrease (AUC)	64% decrease (AUC)	96% decrease (AUC)	90% decrease (AUC)
SIN-1	effect	relaxation	no difference to control	relaxation	no difference to control	relaxation	no difference to control
	EC ₅₀	~0.1 μM		(plateau not reached by 1 μM)		(plateau not reached by 1 μM)	

Table 6-1: Summarised data for effects of vasoconstriction and vasodilation agonists on mouse mesenteric, saphenous and carotid arteries

		Aorta (WT mice)	Aorta (Cre- mice)	Mesenteric arteries (Cre- mice)	Saphenous arteries (Cre- mice)	Carotid arteries (Cre- mice)
Yoda-1	basal arteries	no effect				
	effect	relaxation	contraction	relaxation	relaxation	contraction
	EC ₅₀	2.3 μ M	plateau not reached by 10 μ M	1.8 μ M	plateau not reached by 10 μ M	plateau not reached by 10 μ M
	10 μ M Yoda-1 response magnitude vs PE			~60%	~38%	
	endothelial cell dependent?	yes		no	no	no
	+ L-NAME	relaxation inhibited by 99%		relaxation inhibited by 30%	contraction unaffected	contraction unaffected
	Piezo1 ^{ΔEC} (Cre+)	-	no difference to control (cre-)	no difference to control (cre-)	no difference to control (cre-)	no difference to control (cre-)

Table 6-2: Summarised data for effects induced by Yoda1 on mouse aorta, mesenteric, saphenous and carotid arteries from control and Piezo1 ^{Δ EC} mouse

List of References

- AGMON, Y., KHANDHERIA, B. K., MEISSNER, I., SCHWARTZ, G. L., SICKS, J. D., FOUGHT, A. J., O'FALLON, W. M., WIEBERS, D. O. & TAJIK, A. J. 2003. Is aortic dilatation an atherosclerosis-related process?: Clinical, laboratory, and transesophageal echocardiographic correlates of thoracic aortic dimensions in the population with implications for thoracic aortic aneurysm formation. *Journal of the American College of Cardiology*, 42, 1076-1083.
- AHN, S. J., FANCHER, I. S., BIAN, J. T., ZHANG, C. X., SCHWAB, S., GAFFIN, R., PHILLIPS, S. A. & LEVITAN, I. 2017. Inwardly rectifying K⁺ channels are major contributors to flow-induced vasodilatation in resistance arteries. *J Physiol*, 595, 2339-2364.
- AIELLO, E. A., MALCOLM, A. T., WALSH, M. P. & COLE, W. C. 1998. β -Adrenoceptor activation and PKA regulate delayed rectifier K⁺ channels of vascular smooth muscle cells. *American Journal of Physiology-Heart and Circulatory Physiology*, 275, H448-H459.
- AKATA, T., KANNA, T., YOSHINO, J. & TAKAHASHI, S. 2003. Mechanisms of direct inhibitory action of isoflurane on vascular smooth muscle of mesenteric resistance arteries. *The Journal of the American Society of Anesthesiologists*, 99, 666-677.
- ALBUISSON, J., MURTHY, S. E., BANDELL, M., COSTE, B., LOUIS-DIT-PICARD, H., MATHUR, J., FÉNEANT-THIBAUT, M., TERTIAN, G., DE JAUREGUIBERRY, J.-P. & SYFUSS, P.-Y. 2013. Dehydrated hereditary stomatocytosis linked to gain-of-function mutations in mechanically activated PIEZO1 ion channels. *Nature communications*, 4.
- ANDOLFO, I., ALPER, S. L., DE FRANCESCHI, L., AURIEMMA, C., RUSSO, R., DE FALCO, L., VALLEFUOCO, F., ESPOSITO, M. R., VANDORPE, D. H. & SHMUKLER, B. E. 2013. Multiple clinical forms of dehydrated hereditary stomatocytosis arise from mutations in PIEZO1. *Blood*, 121, 3925-3935.
- BAE, C., GNANASAMBANDAM, R., NICOLAI, C., SACHS, F. & GOTTLIEB, P. A. 2013. Xerocytosis is caused by mutations that alter the kinetics of the mechanosensitive channel PIEZO1. *Proceedings of the National Academy of Sciences*, 110, E1162-E1168.
- BALLIGAND, J.-L., FERON, O. & DESSY, C. 2009. eNOS activation by physical forces: from short-term regulation of contraction to chronic remodeling of cardiovascular tissues. *Physiological Reviews*, 89, 481-534.
- BARRETT, K., BARMAN, S., BOITANO, S. & BROOKS, H. 2010. Blood as a circulatory fluid & the dynamics of blood & lymph flow. *Ganong's review of medical physiology*, 521-554.
- BARYSHNIKOV, S. G., PULINA, M. V., ZULIAN, A., LINDE, C. I. & GOLOVINA, V. A. 2009. Orai1, a critical component of store-operated Ca²⁺ entry, is functionally associated with Na⁺/Ca²⁺ exchanger and plasma membrane Ca²⁺ pump in proliferating human arterial myocytes. *American Journal of Physiology-Cell Physiology*, 297, C1103-C1112.
- BAYLISS, W. M. 1902. On the local reactions of the arterial wall to changes of internal pressure. *The Journal of physiology*, 28, 220-231.
- BEECH, D., MURAKI, K. & FLEMMING, R. 2004. Non-selective cationic channels of smooth muscle and the mammalian homologues of Drosophila TRP. *The Journal of physiology*, 559, 685-706.

- BENETOS, A., ADAMOPOULOS, C., BUREAU, J.-M., TEMMAR, M., LABAT, C., BEAN, K., THOMAS, F., PANNIER, B., ASMAR, R. & ZUREIK, M. 2002. Determinants of accelerated progression of arterial stiffness in normotensive subjects and in treated hypertensive subjects over a 6-year period. *Circulation*, 105, 1202-1207.
- BERDEAUX, A. & GIUDICELLI, J. 1987. Antihypertensive drugs and baroreceptor reflex control of heart rate and blood pressure. *Fundamental & clinical pharmacology*, 1, 257-282.
- BERK, B. C., ABE, J. I., MIN, W., SURAPISITCHAT, J. & YAN, C. 2001. Endothelial atheroprotective and anti-inflammatory mechanisms. *Annals of the New York Academy of Sciences*, 947, 93-111.
- BERMAN, R. S., MARTIN, P. E., EVANS, W. H. & GRIFFITH, T. M. 2002. Relative contributions of NO and gap junctional communication to endothelium-dependent relaxations of rabbit resistance arteries vary with vessel size. *Microvascular research*, 63, 115-128.
- BERRA-ROMANI, R., RAQEEB, A., GUZMAN-SILVA, A., TORRES-JÁCOME, J., TANZI, F. & MOCCIA, F. 2010. Na⁺-Ca²⁺ exchanger contributes to Ca²⁺ extrusion in ATP-stimulated endothelium of intact rat aorta. *Biochemical and biophysical research communications*, 395, 126-130.
- BERRIDGE, M. J. 1995. Capacitative calcium entry. *Biochemical Journal*, 312, 1.
- BERRIDGE, M. J. & IRVINE, R. F. 1989. Inositol phosphates and cell signalling.
- BEURG, M. & FETTIPLACE, R. 2017. PIEZO2 as the anomalous mechanotransducer channel in auditory hair cells. *The Journal of physiology*.
- BEVAN, J., BEVAN, R., PURDY, R., ROBINSON, C., SU, C. & WATERSON, J. 1972. Comparison of adrenergic mechanisms in an elastic and a muscular artery of the rabbit. *Circulation research*, 30, 541-548.
- BILLINGTON, C. K. & PENN, R. B. 2003. Signaling and regulation of G protein-coupled receptors in airway smooth muscle. *Respiratory research*, 4, 4.
- BLUMENTHAL, J. A., SHERWOOD, A., GULLETTE, E. C., BABYAK, M., WAUGH, R., GEORGIADES, A., CRAIGHEAD, L. W., TWEEDY, D., FEINGLOS, M. & APPELBAUM, M. 2000. Exercise and weight loss reduce blood pressure in men and women with mild hypertension: effects on cardiovascular, metabolic, and hemodynamic functioning. *Archives of internal medicine*, 160, 1947-1958.
- BOITTIN, F.-X., MACREZ, N., HALET, G. & MIRONNEAU, J. 1999. Norepinephrine-induced Ca²⁺ waves depend on InsP₃ and ryanodine receptor activation in vascular myocytes. *American Journal of Physiology-Cell Physiology*, 277, C139-C151.
- BOLTON, T., LANG, R. & TAKEWAKI, T. 1984. Mechanisms of action of noradrenaline and carbachol on smooth muscle of guinea-pig anterior mesenteric artery. *The Journal of Physiology*, 351, 549-572.
- BONEV, A. D., JAGGAR, J. H., RUBART, M. & NELSON, M. T. 1997. Activators of protein kinase C decrease Ca²⁺ spark frequency in smooth muscle cells from cerebral arteries. *American Journal of Physiology-Cell Physiology*, 273, C2090-C2095.
- BOS, J. L. 2003. Epac: a new cAMP target and new avenues in cAMP research. *Nature Reviews Molecular Cell Biology*, 4, 733-738.
- BOS, J. L. 2006. Epac proteins: multi-purpose cAMP targets. *Trends in biochemical sciences*, 31, 680-686.
- BRADLEY, A. & MORGAN, K. 1987. Alterations in cytoplasmic calcium sensitivity during porcine coronary artery contractions as detected by aequorin. *The Journal of physiology*, 385, 437.
- BRYAN, R. M., YOU, J., GOLDING, E. M. & MARRELLI, S. P. 2005. Endothelium-derived Hyperpolarizing Factor A Cousin to Nitric Oxide and Prostacyclin. *The Journal of the American Society of Anesthesiologists*, 102, 1261-1277.

- BUDZYN, K., PAULL, M., MARLEY, P. D. & SOBEY, C. G. 2006. Segmental differences in the roles of rho-kinase and protein kinase C in mediating vasoconstriction. *Journal of Pharmacology and Experimental Therapeutics*, 317, 791-796.
- BUSSE, R., EDWARDS, G., FÉLÉTOU, M., FLEMING, I., VANHOUTTE, P. M. & WESTON, A. H. 2002. EDHF: bringing the concepts together. *Trends in pharmacological sciences*, 23, 374-380.
- BUSSE, R. & MÜLSCH, A. 1990. Calcium-dependent nitric oxide synthesis in endothelial cytosol is mediated by calmodulin. *FEBS letters*, 265, 133-136.
- CAHALAN, S. M., LUKACS, V., RANADE, S. S., CHIEN, S., BANDELL, M. & PATAPOUTIAN, A. 2015. Piezo1 links mechanical forces to red blood cell volume. *Elife*, 4, e07370.
- CARVAJAL, J. A., GERMAIN, A. M., HUIDOBRO-TORO, J. P. & WEINER, C. P. 2000. Molecular mechanism of cGMP-mediated smooth muscle relaxation. *Journal of cellular physiology*, 184, 409-420.
- CATTERALL, W. A., PEREZ-REYES, E., SNUTCH, T. P. & STRIESSNIG, J. 2005. International Union of Pharmacology. XLVIII. Nomenclature and structure-function relationships of voltage-gated calcium channels. *Pharmacological reviews*, 57, 411-425.
- CHADHA, P. S., LIU, L., RIKARD-BELL, M., SENADHEERA, S., HOWITT, L., BERTRAND, R. L., GRAYSON, T. H., MURPHY, T. V. & SANDOW, S. L. 2011. Endothelium-dependent vasodilation in human mesenteric artery is primarily mediated by myoendothelial gap junctions intermediate conductance calcium-activated K⁺ channel and nitric oxide. *Journal of Pharmacology and Experimental Therapeutics*, 336, 701-708.
- CHATAIGNEAU, T., FÉLÉTOU, M., HUANG, P. L., FISHMAN, M. C., DUHAULT, J. & VANHOUTTE, P. M. 1999. Acetylcholine-induced relaxation in blood vessels from endothelial nitric oxide synthase knockout mice. *British journal of pharmacology*, 126, 219-226.
- CHAYTOR, A., EVANS, W. H. & GRIFFITH, T. 1998. Central role of heterocellular gap junctional communication in endothelium-dependent relaxations of rabbit arteries. *The Journal of Physiology*, 508, 561-573.
- CHEN, G. & CHEUNG, D. W. 1997. Effect of K⁽⁺⁾-channel blockers on ACh-induced hyperpolarization and relaxation in mesenteric arteries. *American Journal of Physiology-Heart and Circulatory Physiology*, 272, H2306-H2312.
- CHEN, G., SUZUKI, H. & WESTON, A. H. 1988. Acetylcholine releases endothelium-derived hyperpolarizing factor and EDRF from rat blood vessels. *British journal of pharmacology*, 95, 1165-1174.
- CHENNUPATI, R., LAMERS, W. H., KOEHLER, S. E. & DE MEY, J. G. 2013. Endothelium-dependent hyperpolarization-related relaxations diminish with age in murine saphenous arteries of both sexes. *British journal of pharmacology*, 169, 1486-1499.
- CHIU, J.-J. & CHIEN, S. 2011. Effects of disturbed flow on vascular endothelium: pathophysiological basis and clinical perspectives. *Physiological reviews*, 91, 327-387.
- CHOBANIAN, A. V., BAKRIS, G. L., BLACK, H. R., CUSHMAN, W. C., GREEN, L. A., IZZO, J. L., JONES, D. W., MATERSON, B. J., OPARIL, S. & WRIGHT, J. T. 2003. Seventh report of the joint national committee on prevention, detection, evaluation, and treatment of high blood pressure. *hypertension*, 42, 1206-1252.
- CHRISTENSEN, K. L. & MULVANY, M. J. 2001. Location of resistance arteries. *Journal of vascular research*, 38, 1-12.
- CINAR, E., ZHOU, S., DECOURCEY, J., WANG, Y., WAUGH, R. E. & WAN, J. 2015. Piezo1 regulates mechanotransductive release of ATP from human RBCs. *Proceedings of the National Academy of Sciences*, 112, 11783-11788.

- CINES, D. B., POLLAK, E. S., BUCK, C. A., LOSCALZO, J., ZIMMERMAN, G. A., MCEVER, R. P., POBER, J. S., WICK, T. M., KONKLE, B. A. & SCHWARTZ, B. S. 1998. Endothelial cells in physiology and in the pathophysiology of vascular disorders. *Blood*, 91, 3527-3561.
- CLAPHAM, D. E. & NEER, E. J. 1997. G protein $\beta\gamma$ subunits. *Annual review of pharmacology and toxicology*, 37, 167-203.
- COATS, P. & HILLIER, C. 1999. Determination of an optimal axial-length tension for the study of isolated resistance arteries on a pressure myograph. *Experimental physiology*, 84, 1085-1094.
- COHEN, R. A., PLANE, F., NAJIBI, S., HUK, I., MALINSKI, T. & GARLAND, C. J. 1997. Nitric oxide is the mediator of both endothelium-dependent relaxation and hyperpolarization of the rabbit carotid artery. *Proceedings of the National Academy of Sciences*, 94, 4193-4198.
- CONTI, M. & ADELSTEIN, R. 1981. The relationship between calmodulin binding and phosphorylation of smooth muscle myosin kinase by the catalytic subunit of 3': 5'-cAMP-dependent protein kinase. *Journal of Biological Chemistry*, 256, 3178-3181.
- COOKE, C.-L. M. & DAVIDGE, S. T. 2003. Endothelial-dependent vasodilation is reduced in mesenteric arteries from superoxide dismutase knockout mice. *Cardiovascular research*, 60, 635-642.
- CORNELISSEN, V. A. & SMART, N. A. 2013. Exercise training for blood pressure: a systematic review and meta-analysis. *Journal of the American Heart Association*, 2, e004473.
- COSTE, B., HOUGE, G., MURRAY, M. F., STITZIEL, N., BANDELL, M., GIOVANNI, M. A., PHILIPPAKIS, A., HOISCHEN, A., RIEMER, G. & STEEN, U. 2013. Gain-of-function mutations in the mechanically activated ion channel PIEZO2 cause a subtype of Distal Arthrogyrosis. *Proceedings of the National Academy of Sciences*, 110, 4667-4672.
- COSTE, B., MATHUR, J., SCHMIDT, M., EARLEY, T. J., RANADE, S., PETRUS, M. J., DUBIN, A. E. & PATAPOUTIAN, A. 2010. Piezo1 and Piezo2 are essential components of distinct mechanically activated cation channels. *Science*, 330, 55-60.
- COSTE, B., MURTHY, S. E., MATHUR, J., SCHMIDT, M., MECHIOUKHI, Y., DELMAS, P. & PATAPOUTIAN, A. 2015. Piezo1 ion channel pore properties are dictated by C-terminal region. *Nat Commun*, 6, 7223.
- COSTE, B., XIAO, B., SANTOS, J. S., SYEDA, R., GRANDL, J., SPENCER, K. S., KIM, S. E., SCHMIDT, M., MATHUR, J. & DUBIN, A. E. 2012. Piezo proteins are pore-forming subunits of mechanically activated channels. *Nature*, 483, 176-181.
- DAVIES, P. F. 1995. Flow-mediated endothelial mechanotransduction. *Physiological reviews*, 75, 519-560.
- DAVIES, P. F. 2009. Hemodynamic shear stress and the endothelium in cardiovascular pathophysiology. *Nature clinical practice Cardiovascular medicine*, 6, 16-26.
- DAVIS, K. A., SAMSON, S. E., HAMMEL, K. E., KISS, L., FULOP, F. & GROVER, A. K. 2009. Functional linkage of Na⁺-Ca²⁺-exchanger to sarco/endoplasmic reticulum Ca²⁺ pump in coronary artery: comparison of smooth muscle and endothelial cells. *Journal of cellular and molecular medicine*, 13, 1775-1783.
- DAVIS, M. J. 1993. Myogenic response gradient in an arteriolar network. *American Journal of Physiology-Heart and Circulatory Physiology*, 264, H2168-H2179.
- DAVIS, M. J. & HILL, M. A. 1999. Signaling mechanisms underlying the vascular myogenic response. *Physiological Reviews*, 79, 387-423.
- DE MEY, J. & VANHOUTTE, P. 1982. Heterogeneous behavior of the canine arterial and venous wall. Importance of the endothelium. *Circulation Research*, 51, 439-447.

- DEANFIELD, J., DONALD, A., FERRI, C., GIANNATTASIO, C., HALCOX, J., HALLIGAN, S., LERMAN, A., MANCIA, G., OLIVER, J. J. & PESSINA, A. C. 2005. Endothelial function and dysfunction. Part I: Methodological issues for assessment in the different vascular beds: a statement by the Working Group on Endothelin and Endothelial Factors of the European Society of Hypertension. *Journal of hypertension*, 23, 7-17.
- DERNELIS, J. & PANARETOU, M. 2005. Aortic stiffness is an independent predictor of progression to hypertension in nonhypertensive subjects. *Hypertension*, 45, 426-431.
- DILLON, P. F., AKSOY, M. O., DRISKA, S. P. & MURPHY, R. A. 1981. Myosin phosphorylation and the cross-bridge cycle in arterial smooth muscle. *Science*, 211, 495-497.
- DINGEMANS, K. P., TEELING, P., LAGENDIJK, J. H. & BECKER, A. E. 2000. Extracellular matrix of the human aortic media: an ultrastructural histochemical and immunohistochemical study of the adult aortic media. *The Anatomical Record*, 258, 1-14.
- DORA, K., HINTON, J., WALKER, S. & GARLAND, C. 2000. An indirect influence of phenylephrine on the release of endothelium-derived vasodilators in rat small mesenteric artery. *British journal of pharmacology*, 129, 381-387.
- DORA, K. A., GALLAGHER, N. T., MCNEISH, A. & GARLAND, C. J. 2008. Modulation of endothelial cell KCa3.1 channels during endothelium-derived hyperpolarizing factor signaling in mesenteric resistance arteries. *Circulation research*, 102, 1247-1255.
- DROUIN, A. & THORIN, E. 2009. Flow-induced dilation is mediated by Akt-dependent activation of endothelial nitric oxide synthase-derived hydrogen peroxide in mouse cerebral arteries. *Stroke*, 40, 1827-1833.
- DULING, B., GORE, R., DACEY JR, R. & DAMON, D. 1981. Methods for isolation, cannulation, and 878 in vitro study of single microvessels. *American Journal of Physiology (Heart and Circulatory Physiology)*, 879, H108-H116.
- DULING, B. R. & BERNE, R. M. 1970. Propagated vasodilation in the microcirculation of the hamster cheek pouch. *Circulation Research*, 26, 163-170.
- EDWARDS, G., DORA, K., GARDENER, M., GARLAND, C. & WESTON, A. 1998. K⁺ is an endothelium-derived hyperpolarizing factor in rat arteries. *Nature*, 396, 269-272.
- ENDO, K., ABIRU, T., MACHIDA, H., KASUYA, Y. & KAMATA, K. 1995. Endothelium-derived hyperpolarizing factor does not contribute to the decrease in endothelium-dependent relaxation in the aorta of streptozotocin-induced diabetic rats. *General Pharmacology: The Vascular System*, 26, 149-153.
- ENOURI, S., MONTEITH, G. & JOHNSON, R. 2011. Characteristics of myogenic reactivity in isolated rat mesenteric veins. *American Journal of Physiology-Regulatory, Integrative and Comparative Physiology*, 300, R470-R478.
- ERMAKOV, Y. A., KAMARAJU, K., SENGUPTA, K. & SUKHAREV, S. 2010. Gadolinium ions block mechanosensitive channels by altering the packing and lateral pressure of anionic lipids. *Biophysical journal*, 98, 1018-1027.
- EVANS, E. L., CUTHBERTSON, K., ENDESH, N., RODE, B., BLYTHE, N. M., HYMAN, A. J., HALL, S. J., GAUNT, H. J., LUDLOW, M. J. & FOSTER, R. 2018. Yoda1 analogue (Dooku1) which antagonises Yoda1-evoked activation of Piezo1 and aortic relaxation. *British journal of pharmacology*.
- FÉLÉTOU, M. The endothelium, Part I: Multiple functions of the endothelial cells--focus on endothelium-derived vasoactive mediators. Colloquium Series on Integrated Systems Physiology: From Molecule to Function, 2011. Morgan & Claypool Life Sciences, 1-306.
- FELETOU, M. & VANHOUTTE, P. 1999. The third pathway: endothelium-dependent hyperpolarization. *Journal of physiology and pharmacology: an official journal of the Polish Physiological Society*, 50, 525-534.

- FÉLÉTOU, M. & VANHOUTTE, P. M. 2006. Endothelium-derived hyperpolarizing factor. *Arteriosclerosis, thrombosis, and vascular biology*, 26, 1215-1225.
- FÉLÉTOU, M. & VANHOUTTE, P. M. 2009. EDHF: an update. *Clinical science*, 117, 139-155.
- FELMEDEN, D. C. & LIP, G. Y. 2005. Endothelial function and its assessment. *Expert opinion on investigational drugs*, 14, 1319-1336.
- FISCHER, G. M. & LLAURADO, J. G. 1966. Collagen and elastin content in canine arteries selected from functionally different vascular beds. *Circulation research*, 19, 394-399.
- FLEMING, I. 2001. Cytochrome p450 and vascular homeostasis. *Circulation research*, 89, 753-762.
- FLEMING, I. 2010. Molecular mechanisms underlying the activation of eNOS. *Pflügers Archiv-European Journal of Physiology*, 459, 793-806.
- FLEMING, I., FISSALTHALER, B., DIXIT, M. & BUSSE, R. 2005. Role of PECAM-1 in the shear-stress-induced activation of Akt and the endothelial nitric oxide synthase (eNOS) in endothelial cells. *Journal of cell science*, 118, 4103-4111.
- FRANCIS, S. H., BUSCH, J. L. & CORBIN, J. D. 2010. cGMP-dependent protein kinases and cGMP phosphodiesterases in nitric oxide and cGMP action. *Pharmacological reviews*, 62, 525-563.
- FRANKLIN, S. S. 2005. Arterial stiffness and hypertension. *Hypertension*, 45, 349-351.
- FRANTZ, C., STEWART, K. M. & WEAVER, V. M. 2010. The extracellular matrix at a glance. *J Cell Sci*, 123, 4195-4200.
- FUKAO, M., HATTORI, Y., KANNO, M., SAKUMA, I. & KITABATAKE, A. 1997. Sources of Ca²⁺ in relation to generation of acetylcholine-induced endothelium-dependent hyperpolarization in rat mesenteric artery. *British journal of pharmacology*, 120, 1328-1334.
- FURCHGOTT, R. F. & ZAWADZKI, J. V. 1980. The obligatory role of endothelial cells in the relaxation of arterial smooth muscle by acetylcholine. *Nature*, 288, 373-376.
- GARLAND, C., YAROVA, P. L., JIMÉNEZ-ALTAYÓ, F. & DORA, K. 2011. Vascular hyperpolarization to β -adrenoceptor agonists evokes spreading dilatation in rat isolated mesenteric arteries. *British journal of pharmacology*, 164, 913-921.
- GARLAND, C. J. & DORA, K. A. 2016. EDH: endothelium-dependent hyperpolarization and microvascular signalling. *Acta Physiologica*.
- GARLAND, C. J. & MCPHERSON, G. A. 1992. Evidence that nitric oxide does not mediate the hyperpolarization and relaxation to acetylcholine in the rat small mesenteric artery. *British journal of pharmacology*, 105, 429-435.
- GIBBONS, G. H. & DZAU, V. J. 1994. The emerging concept of vascular remodeling. *New England Journal of Medicine*, 330, 1431-1438.
- GLOERICH, M. & BOS, J. L. 2010. Epac: defining a new mechanism for cAMP action. *Annual review of pharmacology and toxicology*, 50, 355-375.
- GOKINA, N. I., KNOT, H. J., NELSON, M. T. & OSOL, G. 1999. Increased Ca²⁺ sensitivity as a key mechanism of PKC-induced constriction in pressurized cerebral arteries. *American Journal of Physiology-Heart and Circulatory Physiology*, 277, H1178-H1188.
- GOLAN, D. E., TASHJIAN, A. H. & ARMSTRONG, E. J. 2011. *Principles of pharmacology: the pathophysiologic basis of drug therapy*, Lippincott Williams & Wilkins.
- GOLUBINSKAYA, V., BRANDT-ELIASSON, U., GAN, L.-M., KJERRULF, M. & NILSSON, H. 2014. Endothelial function in a mouse model of myeloperoxidase deficiency. *BioMed research international*, 2014.
- GORDAN, R., GWATHMEY, J. K. & XIE, L.-H. 2015. Autonomic and endocrine control of cardiovascular function. *World journal of cardiology*, 7, 204.

- GOTO, K., FUJII, K., ONAKA, U., ABE, I. & FUJISHIMA, M. 2000. Renin-angiotensin system blockade improves endothelial dysfunction in hypertension. *Hypertension*, 36, 575-580.
- GRAYSON, T. H., HADDOCK, R. E., MURRAY, T. P., WOJCIKIEWICZ, R. J. & HILL, C. E. 2004. Inositol 1, 4, 5-trisphosphate receptor subtypes are differentially distributed between smooth muscle and endothelial layers of rat arteries. *Cell calcium*, 36, 447-458.
- GRGIC, I., KAISTHA, B. P., HOYER, J. & KÖHLER, R. 2009. Endothelial Ca²⁺-activated K⁺ channels in normal and impaired EDHF-dilator responses—relevance to cardiovascular pathologies and drug discovery. *British journal of pharmacology*, 157, 509-526.
- GUDERMANN, T., HOFMANN, T., Y SCHNITZLER, M. M. & DIETRICH, A. Activation, subunit composition and physiological relevance of DAG-sensitive TRPC proteins. Novartis Foundation symposium, 2004. Chichester; New York; John Wiley; 1999, 103-117.
- GÜNTNER, T., JANKOWSKI, V., KRETSCHMER, A., NIERHAUS, M., VAN DER GIET, M., ZIDEK, W. & JANKOWSKI, J. PROGRESS IN UREMIC TOXIN RESEARCH: Endothelium and Vascular Smooth Muscle Cells in the Context of Uremia. Seminars in dialysis, 2009. Wiley Online Library, 428-432.
- GUO, Y. R. & MACKINNON, R. 2017. Structure-based membrane dome mechanism for Piezo mechanosensitivity. *Elife*, 6, e33660.
- GUYTON, A. C., COLEMAN, T. G., COWLEY, A. W., SCHEEL, K. W., MANNING, R. D. & NORMAN, R. A. 1972. Arterial pressure regulation: overriding dominance of the kidneys in long-term regulation and in hypertension. *The American journal of medicine*, 52, 584-594.
- HAI, C. & MURPHY, R. A. 1989. Ca²⁺ crossbridge phosphorylation, and contraction. *Annual review of physiology*, 51, 285-298.
- HALL, J., JONES, T. H., CHANNER, K. S. & JONES, R. D. 2006. Mechanisms of agonist-induced constriction in isolated human mesenteric arteries. *Vascular pharmacology*, 44, 427-433.
- HALL, J. E. 2015. *Guyton and Hall Textbook of Medical Physiology E-Book*, Elsevier Health Sciences.
- HALPERN, W. & OSOL, G. 1985. Blood Vessel Diameter Measurement¹. *Resistance Vessels: Physiology, Pharmacology and Hypertensive Pathology*. Karger Publishers.
- HARDIE, R. C. 2007. TRP channels and lipids: from Drosophila to mammalian physiology. *The Journal of physiology*, 578, 9-24.
- HAYASHI, K. & NAIKI, T. 2009. Adaptation and remodeling of vascular wall; biomechanical response to hypertension. *Journal of the mechanical behavior of biomedical materials*, 2, 3-19.
- HE, F. J. & MACGREGOR, G. A. 2004. Effect of longer-term modest salt reduction on blood pressure. *The Cochrane Library*.
- HEBBES, C. P. 2016. Pharmacological modulation of cardiac function and blood vessel calibre. *Anaesthesia & Intensive Care Medicine*, 17, 48-54.
- HEITZER, T., SCHLINZIG, T., KROHN, K., MEINERTZ, T. & MÜNZEL, T. 2001. Endothelial dysfunction, oxidative stress, and risk of cardiovascular events in patients with coronary artery disease. *Circulation*, 104, 2673-2678.
- HERRERA, G. M., HEPPNER, T. J. & NELSON, M. T. 2001. Voltage dependence of the coupling of Ca²⁺ sparks to BKCa channels in urinary bladder smooth muscle. *American Journal of Physiology-Cell Physiology*, 280, C481-C490.
- HILL, A. J., HINTON, J. M., CHENG, H., GAO, Z., BATES, D. O., HANCOX, J. C., LANGTON, P. D. & JAMES, A. F. 2006a. A TRPC-like non-selective cation current activated by α 1-adrenoceptors in rat mesenteric artery smooth muscle cells. *Cell calcium*, 40, 29-40.

- HILL, M. A. & DAVIS, M. J. 2007. Coupling a change in intraluminal pressure to vascular smooth muscle depolarization: still stretching for an explanation. *American Journal of Physiology-Heart and Circulatory Physiology*, 292, H2570-H2572.
- HILL, M. A., DAVIS, M. J., MEININGER, G. A., POTOČNIK, S. J. & MURPHY, T. V. 2006b. Arteriolar myogenic signalling mechanisms: Implications for local vascular function. *Clinical hemorheology and microcirculation*, 34, 67-79.
- HILL, M. A., MEININGER, G. A., DAVIS, M. J. & LAHER, I. 2009. Therapeutic potential of pharmacologically targeting arteriolar myogenic tone. *Trends in pharmacological sciences*, 30, 363-374.
- HOFMANN, F., FEIL, R., KLEPPISCH, T. & SCHLOSSMANN, J. 2006. Function of cGMP-dependent protein kinases as revealed by gene deletion. *Physiological reviews*, 86, 1-23.
- HOLLMANN, M. W., STRUMPER, D., HERROEDER, S. & DURIEUX, M. E. 2005. Receptors, G proteins, and their interactions. *The Journal of the American Society of Anesthesiologists*, 103, 1066-1078.
- HORIGUCHI, S., WATANABE, J., KATO, H., BABA, S., SHINOZAKI, T., MIURA, M., FUKUCHI, M., KAGAYA, Y. & SHIRATO, K. 2001. Contribution of Na⁺/Ca²⁺ exchanger to the regulation of myogenic tone in isolated rat small arteries. *Acta physiologica scandinavica*, 173, 167-173.
- HUANG, A., SUN, D., CARROLL, M. A., JIANG, H., SMITH, C. J., CONNETTA, J. A., FALCK, J. R., SHESELY, E. G., KOLLER, A. & KALEY, G. 2001. EDHF mediates flow-induced dilation in skeletal muscle arterioles of female eNOS-KO mice. *American Journal of Physiology-Heart and Circulatory Physiology*, 280, H2462-H2469.
- HUANG, A., SUN, D., SMITH, C. J., CONNETTA, J. A., SHESELY, E. G., KOLLER, A. & KALEY, G. 2000. In eNOS knockout mice skeletal muscle arteriolar dilation to acetylcholine is mediated by EDHF. *American Journal of Physiology-Heart and Circulatory Physiology*, 278, H762-H768.
- HUANG, P. L., HUANG, Z., MASHIMO, H. & BLOCH, K. D. 1995. Hypertension in mice lacking the gene for endothelial nitric oxide synthase. *Nature*, 377, 239.
- HUGHES, J. M. & BUND, S. J. 2002. Arterial myogenic properties of the spontaneously hypertensive rat. *Experimental physiology*, 87, 527-534.
- HULL JR, S., KAISER, L., JAFFE, M. & SPARKS JR, H. 1986. Endothelium-dependent flow-induced dilation of canine femoral and saphenous arteries. *Journal of Vascular Research*, 23, 183-198.
- HUMPHREY, J. 2008. Vascular adaptation and mechanical homeostasis at tissue, cellular, and sub-cellular levels. *Cell biochemistry and biophysics*, 50, 53-78.
- HUMPHREY, J., EBERTH, J., DYE, W. & GLEASON, R. 2009. Fundamental role of axial stress in compensatory adaptations by arteries. *Journal of biomechanics*, 42, 1-8.
- IKEDA, R., CHA, M., LING, J., JIA, Z., COYLE, D. & GU, J. G. 2014. Merkel cells transduce and encode tactile stimuli to drive A β -afferent impulses. *Cell*, 157, 664-675.
- INOUE, K., NISHIMURA, H., KUBOTA, J. & KITaura, Y. 2000. Nitric oxide mediates inhibitory effect of losartan on angiotensin-induced contractions in hamster but not rat aorta. *Journal of the Renin-Angiotensin-Aldosterone System*, 1, 180-183.
- JACOBS, M. 1984. Mechanism of action of hydralazine on vascular smooth muscle. *Biochemical pharmacology*, 33, 2915-2919.
- JAGGAR, J., WELLMAN, G., HEPPNER, T., PORTER, V., PEREZ, G., GOLLASCH, M., KLEPPISCH, T., RUBART, M., STEVENSON, A. & LEDERER, W. 1998. Ca²⁺ channels, ryanodine receptors and Ca²⁺-activated K⁺ channels: a functional unit for regulating arterial tone. *Acta Physiol Scand*, 164, 577-87.
- JOANNIDES, R., HAEFELI, W. E., LINDER, L., RICHARD, V., BAKKALI, E. H., THUILLEZ, C. & LÜSCHER, T. F. 1995. Nitric oxide is responsible for flow-

- dependent dilatation of human peripheral conduit arteries in vivo. *Circulation*, 91, 1314-1319.
- JOHNSON, P. C. 1991. The myogenic response. *Physiology*, 6, 41-42.
- JOYNER, M. J. & CASEY, D. P. 2015. Regulation of increased blood flow (hyperemia) to muscles during exercise: a hierarchy of competing physiological needs. *Physiological reviews*, 95, 549-601.
- KAESS, B. M., RONG, J., LARSON, M. G., HAMBURG, N. M., VITA, J. A., LEVY, D., BENJAMIN, E. J., VASAN, R. S. & MITCHELL, G. F. 2012. Aortic stiffness, blood pressure progression, and incident hypertension. *Jama*, 308, 875-881.
- KAGAN, H. M. & SULLIVAN, K. A. 1982. [35] Lysyl oxidase: Preparation and role in elastin biosynthesis. *Methods in enzymology*, 82, 637-650.
- KANG, K.-T. 2014. Endothelium-derived relaxing factors of small resistance arteries in hypertension. *Toxicological research*, 30, 141-148.
- KANG, L. S., REYES, R. A. & MULLER-DELP, J. M. 2009. Aging impairs flow-induced dilation in coronary arterioles: role of NO and H₂O₂. *American Journal of Physiology-Heart and Circulatory Physiology*, 297, H1087-H1095.
- KANSUI, Y., GARLAND, C. J. & DORA, K. A. 2008. Enhanced spontaneous Ca²⁺ events in endothelial cells reflect signalling through myoendothelial gap junctions in pressurized mesenteric arteries. *Cell calcium*, 44, 135-146.
- KARAKI, H., OZAKI, H., HORI, M., MITSUI-SAITO, M., AMANO, K.-I., HARADA, K.-I., MIYAMOTO, S., NAKAZAWA, H., WON, K.-J. & SATO, K. 1997. Calcium movements, distribution, and functions in smooth muscle. *Pharmacological reviews*, 49, 157-230.
- KATAKAM, P. V., HOENIG, M., UJHELYI, M. R. & MILLER, A. W. 2000. Cytochrome P450 activity and endothelial dysfunction in insulin resistance. *Journal of vascular research*, 37, 426-434.
- KAUPP, U. B. & SEIFERT, R. 2002. Cyclic nucleotide-gated ion channels. *Physiological reviews*, 82, 769-824.
- KAUSER, K., CLARK, J. E., MASTERS, B. S., DE MONTELLANO, P. O., MA, Y.-H., HARDER, D. R. & ROMAN, R. J. 1991. Inhibitors of cytochrome P-450 attenuate the myogenic response of dog renal arcuate arteries. *Circulation Research*, 68, 1154-1163.
- KHAVANDI, K., GREENSTEIN, A. S., SONOYAMA, K., WITHERS, S., PRICE, A., MALIK, R. A. & HEAGERTY, A. M. 2008. Myogenic tone and small artery remodelling: insight into diabetic nephropathy. Oxford University Press.
- KHAVANDI, K., GREENSTEIN, A. S., SONOYAMA, K., WITHERS, S., PRICE, A., MALIK, R. A. & HEAGERTY, A. M. 2009. Myogenic tone and small artery remodelling: insight into diabetic nephropathy. *Nephrology Dialysis Transplantation*, 24, 361-369.
- KLABUNDE, R. 2011. *Cardiovascular physiology concepts*, Lippincott Williams & Wilkins.
- KO, E. A., HAN, J., JUNG, I. D. & PARK, W. S. 2008. Physiological roles of K⁺ channels in vascular smooth muscle cells. *Journal of Smooth Muscle Research*, 44, 65-81.
- KO, E. A., PARK, W. S., FIRTH, A. L., KIM, N., YUAN, J. X.-J. & HAN, J. 2010. Pathophysiology of voltage-gated K⁺ channels in vascular smooth muscle cells: modulation by protein kinases. *Progress in biophysics and molecular biology*, 103, 95-101.
- KOLLER, A., HUANG, A., SUN, D. & KALEY, G. 1995. Exercise Training Augments Flow-Dependent Dilation in Rat Skeletal Muscle Arterioles Role of Endothelial Nitric Oxide and Prostaglandins. *Circulation Research*, 76, 544-550.
- KRAMER, S., LAW, I., TOBE, S. & BIOTHEM, A. 1989. Fluid flow stimulates tissue plasminogen activator secretion by cultured human endothelial cells.

- KRUSE, L. S., SANDHOLDT, N. T., GAMMELTOFT, S., OLESEN, J. & KRUSE, C. 2006. Phosphodiesterase 3 and 5 and cyclic nucleotide-gated ion channel expression in rat trigeminovascular system. *Neuroscience letters*, 404, 202-207.
- KUBO, M., QUAYLE, J. & STANDEN, N. 1997. Angiotensin II Inhibition of ATP-Sensitive K⁺ Currents in Rat Arterial Smooth Muscle Cells Through Protein Kinase C. *The Journal of Physiology*, 503, 489-496.
- KUNG, C., MARTINAC, B. & SUKHAREV, S. 2010. Mechanosensitive channels in microbes. *Annual review of microbiology*, 64, 313-329.
- KWON, S. C., PYUN, W. B., PARK, G. Y., CHOI, H. K., PAIK, K. S. & KANG, B. S. 1999. The Involvement of K⁺ Channels and the Possible Pathway of EDHF in the Rabbit Femoral Artery. *Yonsei Medical Journal*, 40, 331-338.
- LAGAUD, G., RANDRIAMBOAVONJY, V., ROUL, G., STOCLET, J. & ANDRIANTSITOHAINA, R. 1999. Mechanism of Ca²⁺ release and entry during contraction elicited by norepinephrine in rat resistance arteries. *American Journal of Physiology-Heart and Circulatory Physiology*, 276, H300-H308.
- LAHIRI, M. K., KANNANKERIL, P. J. & GOLDBERGER, J. J. 2008. Assessment of autonomic function in cardiovascular disease: physiological basis and prognostic implications. *Journal of the American College of Cardiology*, 51, 1725-1733.
- LAMPING, K. G., NUNO, D. W., SHESELY, E. G., MAEDA, N. & FARACI, F. M. 2000. Vasodilator mechanisms in the coronary circulation of endothelial nitric oxide synthase-deficient mice. *American Journal of Physiology-Heart and Circulatory Physiology*, 279, H1906-H1912.
- LANNER, J. T., GEORGIU, D. K., JOSHI, A. D. & HAMILTON, S. L. 2010. Ryanodine receptors: structure, expression, molecular details, and function in calcium release. *Cold Spring Harbor perspectives in biology*, 2, a003996.
- LARGE, W. A., SALEH, S. N. & ALBERT, A. P. 2009. Role of phosphoinositol 4, 5-bisphosphate and diacylglycerol in regulating native TRPC channel proteins in vascular smooth muscle. *Cell calcium*, 45, 574-582.
- LAVIADES, C., VARO, N., FERNÁNDEZ, J., MAYOR, G., GIL, M. J., MONREAL, I. & DíEZ, J. 1998. Abnormalities of the extracellular degradation of collagen type I in essential hypertension. *Circulation*, 98, 535-540.
- LEBLANC, N., LEDOUX, J., SALEH, S., SANGUINETTI, A., ANGERMANN, J., O'DRISCOLL, K., BRITTON, F., PERRINO, B. A. & GREENWOOD, I. A. 2005. Regulation of calcium-activated chloride channels in smooth muscle cells: a complex picture is emerging. *Canadian journal of physiology and pharmacology*, 83, 541-556.
- LEHOUX, S., CASTIER, Y. & TEDGUI, A. 2006. Molecular mechanisms of the vascular responses to haemodynamic forces. *Journal of internal medicine*, 259, 381-392.
- LELOUP, A. J., VAN HOVE, C. E., HEYKERS, A., SCHRIJVERS, D. M., DE MEYER, G. R. & FRANSEN, P. 2015. Elastic and muscular arteries differ in structure, basal NO production and voltage-gated Ca²⁺-channels. *Frontiers in physiology*, 6, 375.
- LEO, C. H., JELINIC, M., GOOI, J. H., TARE, M. & PARRY, L. J. 2014. A vasoactive role for endogenous relaxin in mesenteric arteries of male mice. *PloS one*, 9, e107382.
- LEUNG, Y. K., DU, J., HUANG, Y. & YAO, X. 2010. Cyclic Nucleotide-Gated Channels Contribute to Thromboxane A₂-Induced Contraction of Rat Small Mesenteric Arteries. *PloS one*, 5, e11098.
- LEVICKÝ, V. & DOLEZEL, S. 1979. Elastic tissue and smooth muscle volume in elastic and muscular type arteries in the dog. *Physiologia Bohemoslovaca*, 29, 351-360.
- LI, J., HOU, B., TUMOVA, S., MURAKI, K., BRUNS, A., LUDLOW, M. J., SEDO, A., HYMAN, A. J., MCKEOWN, L., YOUNG, R. S., YULDASHEVA, N. Y., MAJEED, Y., WILSON, L. A., RODE, B., BAILEY, M. A., KIM, H. R., FU, Z.,

- CARTER, D. A., BILTON, J., IMRIE, H., AJUH, P., DEAR, T. N., CUBBON, R. M., KEARNEY, M. T., PRASAD, K. R., EVANS, P. C., AINSCOUGH, J. F. & BEECH, D. J. 2014. Piezo1 integration of vascular architecture with physiological force. *Nature*, 515, 279-82.
- LI, Y.-S. J., HAGA, J. H. & CHIEN, S. 2005. Molecular basis of the effects of shear stress on vascular endothelial cells. *Journal of biomechanics*, 38, 1949-1971.
- LI, Z., FROEHLICH, J., GALIS, Z. S. & LAKATTA, E. G. 1999. Increased expression of matrix metalloproteinase-2 in the thickened intima of aged rats. *Hypertension*, 33, 116-123.
- LIAO, D., ARNETT, D. K., TYROLER, H. A., RILEY, W. A., CHAMBLESS, L. E., SZKLO, M. & HEISS, G. 1999. Arterial stiffness and the development of hypertension. *Hypertension*, 34, 201-206.
- LIAO, J. C. & KUO, L. 1997. Interaction between adenosine and flow-induced dilation in coronary microvascular network. *The American journal of physiology*, 272, H1571-81.
- LIU, B., LUO, W., ZHANG, Y., LI, H., ZHU, N., HUANG, D. & ZHOU, Y. 2012. Involvement of cyclo-oxygenase-1-mediated prostacyclin synthesis in the vasoconstrictor activity evoked by ACh in mouse arteries. *Experimental physiology*, 97, 277-289.
- LIU, H., XIONG, Z. & SPERELAKIS, N. 1997. Cyclic Nucleotides Regulate the Activity of L-type Calcium Channels in Smooth Muscle Cells from Rat Portal Vein. *Journal of molecular and cellular cardiology*, 29, 1411-1421.
- LIU, M., LARGE, W. & ALBERT, A. 2005. Stimulation of β -adrenoceptors inhibits store-operated channel currents via a cAMP-dependent protein kinase mechanism in rabbit portal vein myocytes. *The Journal of physiology*, 562, 395-406.
- LÓPEZ, B., QUEREJETA, R., GONZÁLEZ, A., BEAUMONT, J., LARMAN, M. & DÍEZ, J. 2009. Impact of treatment on myocardial lysyl oxidase expression and collagen cross-linking in patients with heart failure. *Hypertension*, 53, 236-242.
- LUKACS, V., MATHUR, J., MAO, R., BAYRAK-TOYDEMIR, P., PROCTER, M., CAHALAN, S. M., KIM, H. J., BANDELL, M., LONGO, N. & DAY, R. W. 2015. Impaired PIEZO1 function in patients with a novel autosomal recessive congenital lymphatic dysplasia. *Nature communications*, 6.
- LÜSCHER, T. & VANHOUTTE, P. M. 1986. Endothelium-dependent contractions to acetylcholine in the aorta of the spontaneously hypertensive rat. *Hypertension*, 8, 344-348.
- LÜSCHER, T. F., RICHARD, V., TSCHUDI, M., YANG, Z. & BOULANGER, C. 1990. Endothelial control of vascular tone in large and small coronary arteries. *Journal of the American College of Cardiology*, 15, 519-527.
- MAKSIMOVIC, S., NAKATANI, M., BABA, Y., NELSON, A. M., MARSHALL, K. L., WELLNITZ, S. A., FIROZI, P., WOO, S.-H., RANADE, S. & PATAPOUTIAN, A. 2014. Epidermal Merkel cells are mechanosensory cells that tune mammalian touch receptors. *Nature*, 509, 617-621.
- MARIEB, E. N. & HOEHN, K. 2007. *Human anatomy & physiology*, Pearson Education.
- MARTIN, W., FURCHGOTT, R. F., VILLANI, G. M. & JOTHIANANDAN, D. 1986. Depression of contractile responses in rat aorta by spontaneously released endothelium-derived relaxing factor. *Journal of Pharmacology and Experimental Therapeutics*, 237, 529-538.
- MARTINI, F. & NATH, J. 2012. Bartholomew. Fundamentals anatomy & physiology Ninth edition. USA: Benjamin Cummings.
- MCMILLIN, M. J., BECK, A. E., CHONG, J. X., SHIVELY, K. M., BUCKINGHAM, K. J., GILDERSLEEVE, H. I., ARACENA, M. I., AYLSWORTH, A. S., BITOUN, P. & CAREY, J. C. 2014. Mutations in PIEZO2 cause Gordon syndrome, Marden-Walker syndrome, and distal arthrogyriposis type 5. *The American Journal of Human Genetics*, 94, 734-744.

- MCSHERRY, I. N., SPITALER, M. M., TAKANO, H. & DORA, K. A. 2005. Endothelial cell Ca²⁺ increases are independent of membrane potential in pressurized rat mesenteric arteries. *Cell calcium*, 38, 23-33.
- MIAN, K. B. & MARTIN, W. 1995. Differential sensitivity of basal and acetylcholine-stimulated activity of nitric oxide to destruction by superoxide anion in rat aorta. *British journal of pharmacology*, 115, 993-1000.
- MILLER, F., DELLSPERGER, K. C. & GUTTERMAN, D. D. 1997. Myogenic constriction of human coronary arterioles. *American Journal of Physiology-Heart and Circulatory Physiology*, 273, H257-H264.
- MIURA, H., WACHTEL, R. E., LIU, Y., LOBERIZA, F. R., SAITO, T., MIURA, M. & GUTTERMAN, D. D. 2001. Flow-induced dilation of human coronary arterioles important role of Ca²⁺-activated K⁺ channels. *Circulation*, 103, 1992-1998.
- MIYAI, N., ARITA, M., MIYASHITA, K., MORIOKA, I., SHIRAISHI, T. & NISHIO, I. 2002. Blood pressure response to heart rate during exercise test and risk of future hypertension. *Hypertension*, 39, 761-6.
- MOHANTA, S., YIN, C., WEBER, C., HU, D. & HABENICHT, A. J. 2016. Aorta atherosclerosis lesion analysis in hyperlipidemic mice. *Bio-protocol*, 6.
- MONCADA, S., GRYGLEWSKI, R., BUNTING, S. & VANE, J. 1976. An enzyme isolated from arteries transforms prostaglandin endoperoxides to an unstable substance that inhibits platelet aggregation. *Nature*, 263, 663-665.
- MONVOISIN, A., ALVA, J. A., HOFMANN, J. J., ZOVEIN, A. C., LANE, T. F. & IRUELA-ARISPE, M. L. 2006. VE-cadherin-CreERT2 transgenic mouse: A model for inducible recombination in the endothelium. *Developmental Dynamics*, 235, 3413-3422.
- MOORE, P., AL-SWAYEH, O., CHONG, N., EVANS, R. & GIBSON, A. 1990. L-NG-nitro arginine (L-NOARG), a novel, L-arginine-reversible inhibitor of endothelium-dependent vasodilatation in vitro. *British journal of pharmacology*, 99, 408-412.
- MOOSMANG, S., SCHULLA, V., WELLING, A., FEIL, R., FEIL, S., WEGENER, J. W., HOFMANN, F. & KLUGBAUER, N. 2003. Dominant role of smooth muscle L-type calcium channel Cav1. 2 for blood pressure regulation. *The EMBO Journal*, 22, 6027-6034.
- MORTON, J. S., RUEDA-CLAUSEN, C. F. & DAVIDGE, S. T. 2011. Flow-mediated vasodilation is impaired in adult rat offspring exposed to prenatal hypoxia. *Journal of applied physiology*, 110, 1073-1082.
- MOYES, A. J., STANFORD, S. C., HOSFORD, P. S., HOBBS, A. J. & RAMAGE, A. G. 2016. Raised arterial blood pressure in neurokinin-1 receptor-deficient mice (NK1R^{-/-}): evidence for a neural rather than a vascular mechanism. *Experimental physiology*, 101, 588-598.
- MULVANY, M. 1994. Resistance vessels in hypertension. *Textbook of Hypertension. Oxford, United Kingdom: Blackwell Scientific Publications*, 103-119.
- MULVANY, M. & AALKJAER, C. 1990. Structure and function of small arteries. *Physiological reviews*, 70, 921-961.
- MULVANY, M., NILSSON, H. & FLATMAN, J. 1982. Role of membrane potential in the response of rat small mesenteric arteries to exogenous noradrenaline stimulation. *The Journal of physiology*, 332, 363.
- MULVANY, M. J. 2012. Small artery remodelling in hypertension. *Basic & clinical pharmacology & toxicology*, 110, 49-55.
- MUMTAZ, S., BURDYGA, G., BORISOVA, L., WRAY, S. & BURDYGA, T. 2011. The mechanism of agonist induced Ca²⁺ signalling in intact endothelial cells studied confocally in in situ arteries. *Cell calcium*, 49, 66-77.
- MURTADA, S. C., ARNER, A. & HOLZAPFEL, G. A. 2012. Experiments and mechanochemical modeling of smooth muscle contraction: significance of filament overlap. *Journal of theoretical biology*, 297, 176-186.

- NELSON, M., PATLAK, J., WORLEY, J. & STANDEN, N. 1990. Calcium channels, potassium channels, and voltage dependence of arterial smooth muscle tone. *American Journal of Physiology-Cell Physiology*, 259, C3-C18.
- NELSON, M. T. & QUAYLE, J. M. 1995. Physiological roles and properties of potassium channels in arterial smooth muscle. *American Journal of Physiology-Cell Physiology*, 268, C799-C822.
- NONOMURA, K., WOO, S.-H., CHANG, R. B., GILLICH, A., QIU, Z., FRANCISCO, A. G., RANADE, S. S., LIBERLES, S. D. & PATAPOUTIAN, A. 2017. Piezo2 senses airway stretch and mediates lung inflation-induced apnoea. *Nature*, 541, 176-181.
- O'ROURKE, S. T. 2007. Antianginal actions of beta-adrenoceptor antagonists. *American journal of pharmaceutical education*, 71, 95.
- O'SULLIVAN, S. E., KENDALL, D. A. & RANDALL, M. D. 2004. Heterogeneity in the mechanisms of vasorelaxation to anandamide in resistance and conduit rat mesenteric arteries. *British journal of pharmacology*, 142, 435-442.
- OHTA, Y., TSUCHIHASHI, T. & KIYOHARA, K. 2011. Relationship between blood pressure control status and lifestyle in hypertensive outpatients. *Internal Medicine*, 50, 2107-2112.
- OISHI, H., BUDEL, S., SCHUSTER, A., STERGIOPULOS, N., MEISTER, J.-J. & BÉNY, J.-L. 2001. Cytosolic-free calcium in smooth-muscle and endothelial cells in an intact arterial wall from rat mesenteric artery in vitro. *Cell calcium*, 30, 261-267.
- ORLOV, S. N., TREMBLAY, J. & HAMET, P. 1996. cAMP signaling inhibits dihydropyridine-sensitive Ca²⁺ influx in vascular smooth muscle cells. *Hypertension*, 27, 774-780.
- OSOL, G., BREKKE, J. F., MCELROY-YAGGY, K. & GOKINA, N. I. 2002. Myogenic tone, reactivity, and forced dilatation: a three-phase model of in vitro arterial myogenic behavior. *American Journal of Physiology-Heart and Circulatory Physiology*, 283, H2260-H2267.
- OSOL, G., LAHER, I. & CIPOLLA, M. 1991. Protein kinase C modulates basal myogenic tone in resistance arteries from the cerebral circulation. *Circulation Research*, 68, 359-367.
- PALMER, R. M., FERRIGE, A. & MONCADA, S. 1987. Nitric oxide release accounts for the biological activity of endothelium-derived relaxing factor. *Nature*, 327, 524-526.
- PALTAUF-DOBURZYNSKA, J., FRIEDEN, M., SPITALER, M. & GRAIER, W. F. 2000. Histamine-induced Ca²⁺ oscillations in a human endothelial cell line depend on transmembrane ion flux, ryanodine receptors and endoplasmic reticulum Ca²⁺-ATPase. *The Journal of physiology*, 524, 701-713.
- PEACH, M. J., SINGER, H. A., IZZO, N. J. & LOEB, A. L. 1987. Role of calcium in endothelium-dependent relaxation of arterial smooth muscle. *The American journal of cardiology*, 59, A35-A43.
- PERKO, M. J., NIELSEN, H. B., SKAK, C., CLEMMESSEN, J. O., SCHROEDER, T. V. & SECHER, N. H. 1998. Mesenteric, coeliac and splanchnic blood flow in humans during exercise. *J Physiol*, 513 (Pt 3), 907-13.
- PINTEROVA, M., KAREN, P., KUNEŠ, J. & ZICHA, J. 2010. Role of nifedipine-sensitive sympathetic vasoconstriction in maintenance of high blood pressure in spontaneously hypertensive rats: effect of Gi-protein inactivation by pertussis toxin. *Journal of hypertension*, 28, 969-978.
- PIPER, A. & LARGE, W. 2004. Direct effect of Ca²⁺-calmodulin on cGMP-activated Ca²⁺-dependent Cl⁻ channels in rat mesenteric artery myocytes. *The Journal of physiology*, 559, 449-457.
- POHL, J., WINDER, S. J., ALLEN, B. G., WALSH, M. P., SELLERS, J. R. & GERTHOFFER, W. T. 1997. Phosphorylation of calponin in airway smooth

- muscle. *American Journal of Physiology-Lung Cellular and Molecular Physiology*, 272, L115-L123.
- PREWITT, R. L., RICE, D. C. & DOBRIAN, A. D. 2002. Adaptation of resistance arteries to increases in pressure. *Microcirculation*, 9, 295-304.
- PURVES, G. I., KAMISHIMA, T., DAVIES, L. M., QUAYLE, J. M. & DART, C. 2009. Exchange protein activated by cAMP (Epac) mediates cAMP-dependent but protein kinase A-insensitive modulation of vascular ATP-sensitive potassium channels. *The Journal of physiology*, 587, 3639-3650.
- QAMAR, M. I. & READ, A. E. 1987. Effects of exercise on mesenteric blood flow in man. *Gut*, 28, 583-7.
- QUAYLE, J. M., NELSON, M. & STANDEN, N. 1997. ATP-sensitive and inwardly rectifying potassium channels in smooth muscle. *Physiological reviews*, 77, 1165-1232.
- QUINN, K. V., GIBLIN, J. P. & TINKER, A. 2004. Multisite phosphorylation mechanism for protein kinase A activation of the smooth muscle ATP-sensitive K⁺ channel. *Circulation research*, 94, 1359-1366.
- RACHEV, A., KANE, T. & MEISTER, J. 1997. Experimental investigation of the distribution of residual strains in the artery wall.
- RAFFETTO, J. D., YU, P., RESLAN, O. M., XIA, Y. & KHALIL, R. A. 2012. Endothelium-dependent nitric oxide and hyperpolarization-mediated venous relaxation pathways in rat inferior vena cava. *Journal of vascular surgery*, 55, 1716-1725.
- RANADE, S. S., QIU, Z., WOO, S.-H., HUR, S. S., MURTHY, S. E., CAHALAN, S. M., XU, J., MATHUR, J., BANDELL, M. & COSTE, B. 2014. Piezo1, a mechanically activated ion channel, is required for vascular development in mice. *Proceedings of the National Academy of Sciences*, 111, 10347-10352.
- RAPOPORT, R. M. & MURAD, F. 1983. Agonist-induced endothelium-dependent relaxation in rat thoracic aorta may be mediated through cGMP. *Circulation Research*, 52, 352-357.
- RATH, G., DESSY, C. & FERON, O. 2009. Caveolae, caveolin and control of vascular tone: nitric oxide (NO) and endothelium derived hyperpolarizing factor (EDHF) regulation. *Journal of physiology and pharmacology: an official journal of the Polish Physiological Society*, 60, 105-9.
- RATZ, P. H., BERG, K. M., URBAN, N. H. & MINER, A. S. 2005. Regulation of smooth muscle calcium sensitivity: KCl as a calcium-sensitizing stimulus. *American Journal of Physiology-Cell Physiology*, 288, C769-C783.
- RELAIX, F. & ZAMMIT, P. S. 2012. Satellite cells are essential for skeletal muscle regeneration: the cell on the edge returns centre stage. *Development*, 139, 2845-2856.
- RETAILLEAU, K., DUPRAT, F., ARHATTE, M., RANADE, S. S., PEYRONNET, R., MARTINS, J. R., JODAR, M., MORO, C., OFFERMANN, S., FENG, Y., DEMOLOMBE, S., PATEL, A. & HONORÉ, E. 2015. Piezo1 in Smooth Muscle Cells Is Involved in Hypertension-Dependent Arterial Remodeling. *Cell Reports*, 13, 1161-1171.
- ROACH, M. R. & BURTON, A. C. 1957. The reason for the shape of the distensibility curves of arteries. *Canadian journal of biochemistry and physiology*, 35, 681-690.
- ROBERTSON, D., JOHNSON, G. A., ROBERTSON, R. M., NIES, A. S., SHAND, D. G. & OATES, J. A. 1979. Comparative assessment of stimuli that release neuronal and adrenomedullary catecholamines in man. *Circulation*, 59, 637-643.
- ROBINSON, B. F., EPSTEIN, S. E., BEISER, G. D. & BRAUNWALD, E. 1966. Control of heart rate by the autonomic nervous system: studies in man on the interrelation between baroreceptor mechanisms and exercise. *Circulation Research*, 19, 400-411.

- RODE, B., SHI, J., ENDESH, N., DRINKHILL, M. J., WEBSTER, P. J., LOTTEAU, S. J., BAILEY, M. A., YULDASHEVA, N. Y., LUDLOW, M. J. & CUBBON, R. M. 2017. Piezo1 channels sense whole body physical activity to reset cardiovascular homeostasis and enhance performance. *Nature Communications*, 8.
- RODRÍGUEZ-RODRÍGUEZ, R., YAROVA, P., WINTER, P. & DORA, K. 2009. Desensitization of endothelial P2Y1 receptors by PKC-dependent mechanisms in pressurized rat small mesenteric arteries. *British journal of pharmacology*, 158, 1609-1620.
- SABBAHI, A., ARENA, R., ELOKDA, A. & PHILLIPS, S. A. 2016. Exercise and Hypertension: Uncovering the Mechanisms of Vascular Control. *Prog Cardiovasc Dis*, 59, 226-234.
- SAMPSON, L. J., DAVIES, L. M., BARRETT-JOLLEY, R., STANDEN, N. B. & DART, C. 2007. Angiotensin II-activated protein kinase C targets caveolae to inhibit aortic ATP-sensitive potassium channels. *Cardiovascular research*, 76, 61-70.
- SANDOO, A., VAN ZANTEN, J. J. V., METSIOS, G. S., CARROLL, D. & KITAS, G. D. 2010. The endothelium and its role in regulating vascular tone. *The open cardiovascular medicine journal*, 4, 302.
- SANDOW, S. L., GOTO, K., RUMMERY, N. M. & HILL, C. E. 2004. Developmental changes in myoendothelial gap junction mediated vasodilator activity in the rat saphenous artery. *The Journal of physiology*, 556, 875-886.
- SANDOW, S. L., TARE, M., COLEMAN, H. A., HILL, C. E. & PARKINGTON, H. C. 2002. Involvement of myoendothelial gap junctions in the actions of endothelium-derived hyperpolarizing factor. *Circulation research*, 90, 1108-1113.
- SCHMIDT, H. H., HOFMANN, H., SCHINDLER, U., SHUTENKO, Z. S., CUNNINGHAM, D. D. & FEELISCH, M. 1996. No· NO from NO synthase. *Proceedings of the National Academy of Sciences*, 93, 14492-14497.
- SHADWICK, R. E. 1999. Mechanical design in arteries. *Journal of Experimental Biology*, 202, 3305-3313.
- SHEN, B., CHENG, K.-T., LEUNG, Y.-K., KWOK, Y.-C., KWAN, H.-Y., WONG, C.-O., CHEN, Z.-Y., HUANG, Y. & YAO, X. 2008. Epinephrine-induced Ca²⁺ influx in vascular endothelial cells is mediated by CNGA2 channels. *Journal of molecular and cellular cardiology*, 45, 437-445.
- SHI, Y., WU, Z., CUI, N., SHI, W., YANG, Y., ZHANG, X., ROJAS, A., HA, B. T. & JIANG, C. 2007. PKA phosphorylation of SUR2B subunit underscores vascular KATP channel activation by beta-adrenergic receptors. *American Journal of Physiology-Regulatory, Integrative and Comparative Physiology*, 293, R1205-R1214.
- SHIMOKAWA, H., YASUTAKE, H., FUJII, K., OWADA, M. K., NAKAIKE, R., FUKUMOTO, Y., TAKAYANAGI, T., NAGAO, T., EGASHIRA, K. & FUJISHIMA, M. 1996. The importance of the hyperpolarizing mechanism increases as the vessel size decreases in endothelium-dependent relaxations in rat mesenteric circulation. *Journal of cardiovascular pharmacology*, 28, 703-711.
- SHIODE, N., MORISHIMA, N., NAKAYAMA, K., YAMAGATA, T., MATSUURA, H. & KAJIYAMA, G. 1996. Flow-mediated vasodilation of human epicardial coronary arteries: effect of inhibition of nitric oxide synthesis. *Journal of the American College of Cardiology*, 27, 304-310.
- SI, H., HEYKEN, W.-T., WÖLFLE, S. E., TYSIAC, M., SCHUBERT, R., GRGIC, I., VILIANOVICH, L., GIEBING, G., MAIER, T. & GROSS, V. 2006. Impaired endothelium-derived hyperpolarizing factor-mediated dilations and increased blood pressure in mice deficient of the intermediate-conductance Ca²⁺-activated K⁺ channel. *Circulation research*, 99, 537-544.
- SIMONDS, W. F. 1999. G protein regulation of adenylate cyclase. *Trends in pharmacological sciences*, 20, 66-73.

- SMIRNOV, S. V. & AARONSON, P. I. 1992. Ca²⁺ currents in single myocytes from human mesenteric arteries: evidence for a physiological role of L-type channels. *The Journal of Physiology*, 457, 455.
- SMYTH, J. T., HWANG, S. Y., TOMITA, T., DEHAVEN, W. I., MERCER, J. C. & PUTNEY, J. W. 2010. Activation and regulation of store-operated calcium entry. *Journal of cellular and molecular medicine*, 14, 2337-2349.
- SNEDEKER, J. G. & GAUTIERI, A. 2014. The role of collagen crosslinks in ageing and diabetes-the good, the bad, and the ugly. *Muscles, ligaments and tendons journal*, 4, 303.
- SOKOYA, E. M., BURNS, A. R., SETIAWAN, C. T., COLEMAN, H. A., PARKINGTON, H. C. & TARE, M. 2006. Evidence for the involvement of myoendothelial gap junctions in EDHF-mediated relaxation in the rat middle cerebral artery. *American Journal of Physiology-Heart and Circulatory Physiology*, 291, H385-H393.
- SOMLYO, A. P. & SOMLYO, A. V. 2003. Ca²⁺ sensitivity of smooth muscle and nonmuscle myosin II: modulated by G proteins, kinases, and myosin phosphatase. *Physiological reviews*, 83, 1325-1358.
- STANKEVIČIUS, E., LOPEZ-VALVERDE, V., RIVERA, L., HUGHES, A. D., MULVANY, M. J. & SIMONSEN, U. 2006. Combination of Ca²⁺-activated K⁺ channel blockers inhibits acetylcholine-evoked nitric oxide release in rat superior mesenteric artery. *British journal of pharmacology*, 149, 560-572.
- SUN, D., YAN, C., JACOBSON, A., JIANG, H., CARROLL, M. A. & HUANG, A. 2007. Contribution of epoxyeicosatrienoic acids to flow-induced dilation in arteries of male ER α knockout mice: role of aromatase. *American Journal of Physiology-Regulatory, Integrative and Comparative Physiology*, 293, R1239-R1246.
- SYEDA, R., XU, J., DUBIN, A. E., COSTE, B., MATHUR, J., HUYNH, T., MATZEN, J., LAO, J., TULLY, D. C. & ENGELS, I. H. 2015. Chemical activation of the mechanotransduction channel Piezo1. *Elife*, 4, e07369.
- TAMMARO, P., SMITH, A. L., CROWLEY, B. L. & SMIRNOV, S. V. 2005. Modulation of the voltage-dependent K⁺ current by intracellular Mg²⁺ in rat aortic smooth muscle cells. *Cardiovascular research*, 65, 387-396.
- TAYLOR, M. S., BONEV, A. D., GROSS, T. P., ECKMAN, D. M., BRAYDEN, J. E., BOND, C. T., ADELMAN, J. P. & NELSON, M. T. 2003. Altered expression of small-conductance Ca²⁺-activated K⁺ (SK3) channels modulates arterial tone and blood pressure. *Circulation research*, 93, 124-131.
- TAYLOR, S. G. & WESTON, A. H. 1988. Endothelium-derived hyperpolarizing a new endogenous inhibitor from the vascular endothelium. *Trends in pharmacological sciences*, 9, 272-274.
- TIAN, L., COGHILL, L. S., MCCLAFFERTY, H., MACDONALD, S. H.-F., ANTONI, F. A., RUTH, P., KNAUS, H.-G. & SHIPSTON, M. J. 2004. Distinct stoichiometry of BKCa channel tetramer phosphorylation specifies channel activation and inhibition by cAMP-dependent protein kinase. *Proceedings of the National Academy of Sciences of the United States of America*, 101, 11897-11902.
- TIRUPPATHI, C., AHMED, G. U., VOGEL, S. M. & MALIK, A. B. 2006. Ca²⁺ signaling, TRP channels, and endothelial permeability. *Microcirculation*, 13, 693-708.
- TRIGGLE, C., WALDRON, H. D. & COLE, W. 1999. ENDOTHELIUM-DERIVED HYPERPOLARIZING FACTOR (S): SPECIES AND TISSUE HETEROGENEITY. *Clinical and Experimental Pharmacology and Physiology*, 26, 176-179.
- UCHIDA, E., BOHR, D. F. & HOBLER, S. W. 1967. A method for studying isolated resistance vessels from rabbit mesentery and brain and their responses to drugs. *Circulation research*, 21, 525-536.
- ULLRICH, T., OBERLE, S., ABATE, A. & SCHRÖDER, H. 1997. Photoactivation of the nitric oxide donor SIN-1. *FEBS letters*, 406, 66-68.

- VALLANCE, P. & CHAN, N. 2001. Endothelial function and nitric oxide: clinical relevance. *Heart*, 85, 342-350.
- VAN DER SLOT, A. J., VAN DURA, E. A., DE WIT, E. C., DEGROOT, J., HUIZINGA, T. W., BANK, R. A. & ZUURMOND, A.-M. 2005. Elevated formation of pyridinoline cross-links by profibrotic cytokines is associated with enhanced lysyl hydroxylase 2b levels. *Biochimica et Biophysica Acta (BBA)-Molecular Basis of Disease*, 1741, 95-102.
- VAN DER SLOT, A. J., ZUURMOND, A.-M., VAN DEN BOGAERDT, A. J., ULRICH, M. M., MIDDELKOOP, E., BOERS, W., RONDAY, H. K., DEGROOT, J., HUIZINGA, T. W. & BANK, R. A. 2004. Increased formation of pyridinoline cross-links due to higher telopeptide lysyl hydroxylase levels is a general fibrotic phenomenon. *Matrix biology*, 23, 251-257.
- VAN VARIK, B., RENNENBERG, R., REUTELINGSPERGER, C., KROON, A., DE LEEUW, P. & SCHURGERS, L. J. 2012. Mechanisms of arterial remodeling: lessons from genetic diseases. *Frontiers in genetics*, 3, 290.
- VANBAVEL, E., MEULEN, E. T. & SPAAN, J. A. 2001. Role of Rho-Associated Protein Kinase in Tone and Calcium Sensitivity of Cannulated Rat Mesenteric Small Arteries. *Experimental Physiology*, 86, 585-592.
- VANBAVEL, E., MOOIJ, T., GIEZEMAN, M. J. & SPAAN, J. A. 1990. Cannulation and continuous cross-sectional area measurement of small blood vessels. *Journal of pharmacological methods*, 24, 219-227.
- VANBAVEL, E. & MULVANY, M. J. 1994. Role of wall tension in the vasoconstrictor response of cannulated rat mesenteric small arteries. *The Journal of Physiology*, 477, 103-115.
- VANHOUTTE, P. M., FELETOU, M. & TADDEI, S. 2005. Endothelium-dependent contractions in hypertension. *British journal of pharmacology*, 144, 449-458.
- VANHOUTTE, P. M. & TANG, E. H. 2008. Endothelium-dependent contractions: when a good guy turns bad! *The Journal of physiology*, 586, 5295-5304.
- WAGENSEIL, J. E. & MECHAM, R. P. 2009. Vascular extracellular matrix and arterial mechanics. *Physiological reviews*, 89, 957-989.
- WALDRON, G. & COLE, W. 1999. ACTIVATION OF VASCULAR SMOOTH MUSCLE K⁺ CHANNELS BY ENDOTHELIUM-DERIVED RELAXING FACTORS. *Clinical and experimental pharmacology and physiology*, 26, 180-184.
- WANG, F., KNUTSON, K., ALCAINO, C., LINDEN, D. R., GIBBONS, S. J., KASHYAP, P., GROVER, M., OECKLER, R., GOTTLIEB, P. A. & LI, H. J. 2017. Mechanosensitive ion channel Piezo2 is important for enterochromaffin cell response to mechanical forces. *The Journal of physiology*, 595, 79-91.
- WANG, S., CHENNUPATI, R., KAUR, H., IRING, A., WETTSCHURECK, N. & OFFERMANN, S. 2016. Endothelial cation channel PIEZO1 controls blood pressure by mediating flow-induced ATP release. *The Journal of clinical investigation*, 126, 4527.
- WATANABE, J., KARIBE, A., HORIGUCHI, S., KEITOKU, M., SATOH, S., TAKISHIMA, T. & SHIRATO, K. 1993. Modification of myogenic intrinsic tone and [Ca²⁺]_i of rat isolated arterioles by ryanodine and cyclopiazonic acid. *Circulation Research*, 73, 465-472.
- WATTS, S. W., RONDELLI, C., THAKALI, K., LI, X., UHAL, B., PERVAIZ, M. H., WATSON, R. E. & FINK, G. D. 2007. Morphological and biochemical characterization of remodeling in aorta and vena cava of DOCA-salt hypertensive rats. *American Journal of Physiology-Heart and Circulatory Physiology*, 292, H2438-H2448.
- WEBB, R. C. 2003. Smooth muscle contraction and relaxation. *Advances in physiology education*, 27, 201-206.
- WEISS, D. N., PODBERESKY, D. J., HEIDRICH, J. & BLAUSTEIN, M. P. 1993. Nanomolar ouabain augments caffeine-evoked contractions in rat arteries. *American Journal of Physiology-Cell Physiology*, 265, C1443-C1448.

- WHITE, R., BOTTRILL, F. E., SIAU, D. & HILEY, C. R. 2001. Protein kinase A-dependent and-independent effects of isoproterenol in rat isolated mesenteric artery: interactions with levromakalim. *Journal of Pharmacology and Experimental Therapeutics*, 298, 917-924.
- WON, J., VANG, H., LEE, P., KIM, Y., KIM, H., KANG, Y. & OH, S. 2017. Piezo2 Expression in Mechanosensitive Dental Primary Afferent Neurons. *Journal of Dental Research*, 0022034517702342.
- WOOTEN, M. W., SEIBENHENER, M. L., MATTHEWS, L. H., ZHOU, G. & COLEMAN, E. S. 1996. Modulation of ζ -Protein Kinase C by Cyclic AMP in PC12 Cells Occurs Through Phosphorylation by Protein Kinase A. *Journal of neurochemistry*, 67, 1023-1031.
- WU, J., LEWIS, A. H. & GRANDL, J. 2017a. Touch, Tension, and Transduction—The Function and Regulation of Piezo Ion Channels. *Trends in biochemical sciences*, 42, 57-71.
- WU, Z., GRILLET, N., ZHAO, B., CUNNINGHAM, C., HARKINS-PERRY, S., COSTE, B., RANADE, S., ZEBARJADI, N., BEURG, M. & FETTIPLACE, R. 2017b. Mechanosensory hair cells express two molecularly distinct mechanotransduction channels. *Nature neuroscience*, 20, 24.
- XIA, X.-M., ZENG, X. & LINGLE, C. J. 2002. Multiple regulatory sites in large-conductance calcium-activated potassium channels. *Nature*, 418, 880-884.
- XIN, X., HE, J., FRONTINI, M. G., OGDEN, L. G., MOTSAMAI, O. I. & WHELTON, P. K. 2001. Effects of alcohol reduction on blood pressure. *Hypertension*, 38, 1112-1117.
- XIONG, Z., SPERELAKIS, N. & FENOGLIO-PREISER, C. 1994. Regulation of L-type calcium channels by cyclic nucleotides and phosphorylation in smooth muscle cells from rabbit portal vein. *Journal of vascular research*, 31, 271-279.
- XU, S.-Z. & BEECH, D. J. 2001. TrpC1 is a membrane-spanning subunit of store-operated Ca^{2+} channels in native vascular smooth muscle cells. *Circulation Research*, 88, 84-87.
- XU, S.-Z., BOULAY, G., FLEMMING, R. & BEECH, D. J. 2006. E3-targeted anti-TRPC5 antibody inhibits store-operated calcium entry in freshly isolated pial arterioles. *American Journal of Physiology-Heart and Circulatory Physiology*, 291, H2653-H2659.
- YANG, C., KWAN, Y.-W., CHAN, S.-W., LEE, S. M.-Y. & LEUNG, G. P.-H. 2010. Potentiation of EDHF-mediated relaxation by chloride channel blockers. *Acta pharmacologica Sinica*, 31, 1303-1311.
- YAO, X. & GARLAND, C. J. 2005. Recent developments in vascular endothelial cell transient receptor potential channels. *Circulation research*, 97, 853-863.
- YAP, F. C., TAYLOR, M. S. & LIN, M. T. 2014. Ovariectomy-induced reductions in endothelial SK3 channel activity and endothelium-dependent vasorelaxation in murine mesenteric arteries. *PLoS one*, 9, e104686.
- ZHANG, S. L., YU, Y., ROOS, J., KOZAK, J. A., DEERINCK, T. J., ELLISMAN, M. H., STAUDERMAN, K. A. & CAHALAN, M. D. 2005. STIM1 is a Ca^{2+} sensor that activates CRAC channels and migrates from the Ca^{2+} store to the plasma membrane. *Nature*, 437, 902-905.
- ZHOLOS, A., JOHNSON, C., BURDYGA, T. & MELANAPHY, D. 2011. TRPM channels in the vasculature. *Transient Receptor Potential Channels*. Springer.
- ZHOU, Y., VARADHARAJ, S., ZHAO, X., PARINANDI, N., FLAVAHAN, N. A. & ZWEIER, J. L. 2005. Acetylcholine causes endothelium-dependent contraction of mouse arteries. *American Journal of Physiology-Heart and Circulatory Physiology*, 289, H1027-H1032.
- ZIEMAN, S. J., MELENOVSKY, V. & KASS, D. A. 2005. Mechanisms, pathophysiology, and therapy of arterial stiffness. *Arteriosclerosis, thrombosis, and vascular biology*, 25, 932-943.

- ZOU, H., RATZ, P. H. & HILL, M. A. 2001. Temporal aspects of Ca²⁺ and myosin phosphorylation during myogenic and norepinephrine-induced arteriolar constriction. *Journal of vascular research*, 37, 556-567.
- ZYGMUNT, P. M. & HÖGESTÄTT, E. D. 1996. Role of potassium channels in endothelium-dependent relaxation resistant to nitroarginine in the rat hepatic artery. *British journal of pharmacology*, 117, 1600-1606.